ISSN : 2277 - 548X (Online)
2320 - 8430 (Print)

IJCI

International Journal On Cybernetics & Informatics (IJCI)

February 2016, Volume 5, Number 1

AIRCC Publishing Corporation

Preface

I am pleased to introduce the proceedings of the IDES joint International Conferences **on Dec 26, 2015, in Cochin, India.** Research in engineering has a long history. Today it has become the core backbone of industrial economy. **This unique conference** aims at bringing together the researchers, scientists, and engineers in all areas of Engineering and Technology. It provides an international platform for sharing of original research, new ideas and practical experiences in the different technical fields. This conference has focused on the frontier topics related to Computer Science, Civil, Mechanical, Electrical and Electronics Engineering subjects.

Altogether there are 61 papers included in the proceedings registered for various tracks and there are 21 papers registered for the AIRCC journal track. These, serve to demonstrate the popularity of the IDES conferences for sharing ideas and findings with a truly international engineering community. Thank you to all those who have contributed to producing such a comprehensive conference and proceedings and thus contributed to the improvement of the teaching and research. Various new design techniques are applied in different fields. It is no doubt that the relation between academic research and industrial activity must match continuously. The relevance of this joint conference theme, towards overall technological development to a wide variety of disciplines is reflected in the diverse range of papers that have been submitted for publication.

I would like to thank all the reviewers for their time and effort in reviewing the papers. The quality of these papers is a tribute to the authors and also to the reviewers who have guided any necessary improvement. I would like to express my special thanks to all the Associate Editors for their tremendous efforts.

I would like to express my deep appreciation to all the honorable members who agreed to be the chair and co-chair for this conference. It is my pleasant duty to acknowledge the support from the organizers of the conference **IDES, ACEECom, AMAE and ACEE.**

It has been an honor for me to have the chance to be the editor in chief of the proceedings. I have enjoyed considerably working in cooperation with the different committees. The IDES 2015 conferences and proceedings are a credit to a large group of people and everyone should be proud of the outcome.

Dr. Naveed S A
Jawaharlal Nehru Engineering College, India

Editorial Board

Editorial Board

Table of Contents

COLOCATION MINING IN UNCERTAIN DATA SETS: A PROBABILISTIC APPROACH

M.Sheshikala[1], D. Rajeswara Rao[2], and Md. Ali Kadampur[3]

[1,3]S.R Engineering College
[2]Kl University

ABSTRACT

In this paper we investigate colocation mining problem in the context of uncertain data. Uncertain data is a partially complete data. Many of the real world data is Uncertain, for example, Demographic data, Sensor networks data, GIS data etc.,. Handling such data is a challenge for knowledge discovery particularly in colocation mining. One straightforward method is to find the Probabilistic Prevalent colocations (PPCs). This method tries to find all colocations that are to be generated from a random world. For this we first apply an approximation error to find all the PPCs which reduce the computations. Next find all the possible worlds and split them into two different worlds and compute the prevalence probability. These worlds are used to compare with a minimum probability threshold to decide whether it is Probabilistic Prevalent colocation (PPCs) or not. The experimental results on the selected data set show the significant improvement in computational time in comparison to some of the existing methods used in colocation mining.

KEYWORDS

Probabilistic Approach, Colocation Mining, Un-certain Data Sets

1. INTRODUCTION

Basically colocation mining is the sub-domain of data mining. The research in colocation mining has advanced in the recent past addressing the issues with applications, utility and methods of knowledge discovery. Many techniques inspired by data base methods (Join based, Join-less, Space Partitioning, etc.,) have been attempted to find the prevalent colocation patterns in spatial data. Fusion and fuzzy based methods have been in use. However due to growing size of the data and computational time requirements highly scalable and computationally time efficient framework for colocation mining is still desired. This paper presents a computational time efficient algorithm based on Probabilistic approach in the uncertain data.

Consider a spatial data set collected from a geographic space which consists of features like birds (of different types), rocks, different kinds of trees, houses, which is shown in Fig: 4. From this the frequent patterns on a spatial dimension can be identified, for example, < *bird, house* > and < *tree, rocks*>, the patterns are said to be colocated and they help infer a specific eco-system. This paper presents a computationally efficient method to identify such prevalent patterns from spatial data sets.

Since the object data is scattered in space (spatial coordinates) extracting information from it is quite difficult due to complexity of spatial features, spatial data types, and spatial relationships.
For example, a cable service provider may be interested in services frequently requested by geographical neighbours, and thus gain sales promotion data. The subscriber of the channel is

DOI: 10.5121/ijci.2016.5101

located on a wide geographical positions and has wide ranging interest/preferences. Further in the process of collecting data there may be some missing links giving rise to uncertainty in the data. From the data mining point of view all this adds to complexity of analysis and needs to be handled properly. The paper addresses the uncertainty and data complexity issues in finding prevalent colocations.

The paper includes 1.The methods for finding the exact Probabilistic Prevalent colocations (PPCs). 2. Developing a dynamic programming algorithm to find Probabilistic Prevalent colocations (PPCs) which dramatically reduces the computation time. 3. Results of application of the proposed method on different data sets.

The remaining paper is organized as follows: In Section-1, we discuss the introduction, and related work is discussed in Section-2. In section-3 we discuss the definitions, and a block diagram to show the complete flow to find PPCs are discussed in section-4, In section-5 we discuss dynamic- programming algorithm for finding all Probabilistic Prevalent Colocations. We show the experiment results in Section-6. Finally, in section-7 we suggest future work.

2. RELATED WORK

Many methods have been extensively explored in order to find the Prevalent colocations in spatially Precise data. Some of these methods are:

2.1 Space Partitioning Method:

This approach finds the neigh-boring objects of a subset of features. It finds the partition centre points with base objects and decomposes the space from partitioning points using a geometric approach and then finds a feature within a distance threshold from the partitioning point in each area. This approach may generate incorrect colocation patterns, because it may miss some of the colocation instances across partition areas which can be identified from the below Fig:1.

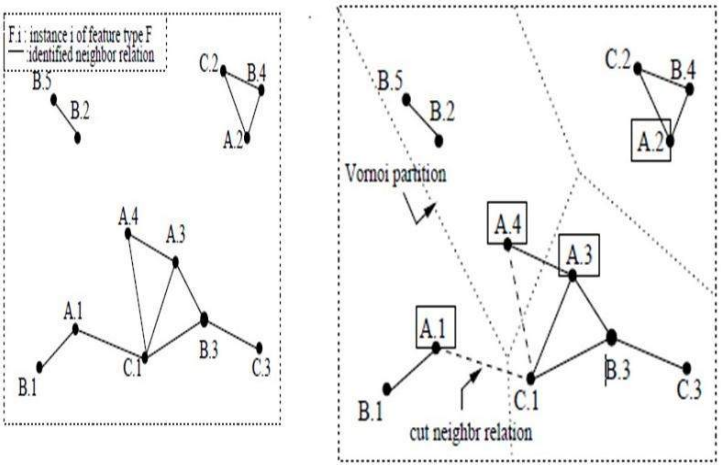

Fig. 1. Space Partitioning Approach

2.2. Join-Based Approach

This approach finds the correct and complete colocation instances, first it finds all neighboring pair objects (of size 2) using a geometric method, the method finds the instance of size k(> 2)

colocations by joining the instances of its size k-1 subset colocation where the first k-2 objects are common. This approach is computationally expensive with the increase of colocation patterns and their instances as in Fig:2.

This approach finds the correct and complete colocation instances, first it finds all neighbouring pair objects (of size 2) using a geometric method, the method finds the instance of size k(> 2) colocations by joining the instances of its size k-1 subset colocation where the first k-2 objects are common. This approach is computationally expensive with the increase of colocation patterns and their instances as in Fig:2.

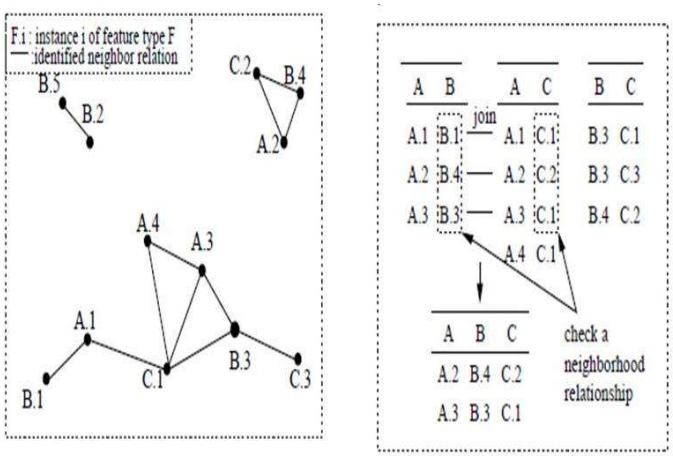

Fig. 2. Join-Based Approach

2.3. Join-Less Approach

The join-less approach puts the spatial neighbor relationship between instances into a compressed star neighborhood. All the possible table instances for every colocation pattern were generated by scanning the star neighbourhood, and by 3-time filtering operation. This join-less colocation mining algorithm is efficient since it uses an instance look-up schema instead of an expensive spatial or instance join operation for identifying colocation table instances, but the computation time of generating colocation table instances will increase with the growing length of colocation pattern as in Fig:3.

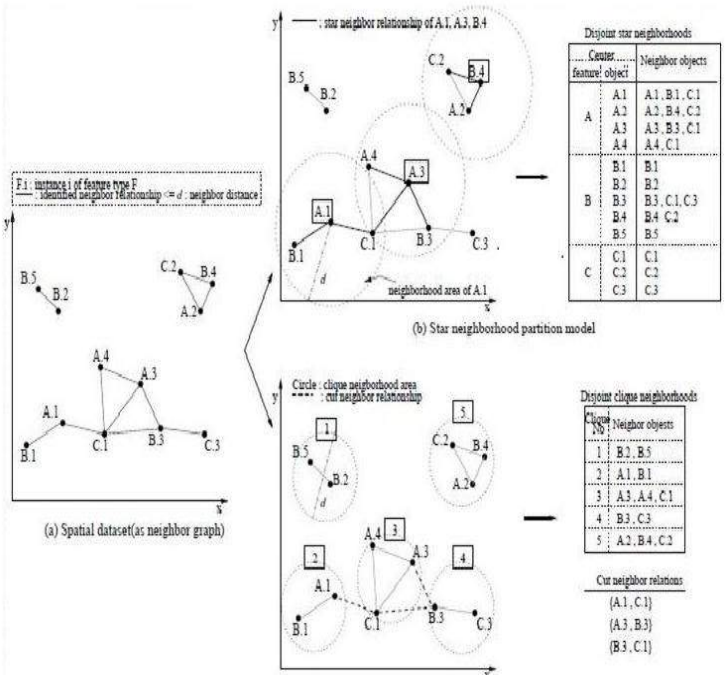

Fig: 3 Join-Less Approach

2.4. CPI-tree Algorithm

This algorithm proposed by Wnag et al in[11] developed in new structure called CPI-tree(colocation pattern instance tree) which could materialize the neighbor relationships of spatial data sets, and find all the table instances recursively from it. This method gives up Apriori like model, (i.e.) to generate size-k prevalence colocations after size(k-1) prevalence colocations, but Apriori candidate generate-test method reduces the number of candidate sets significantly and leads to performance gain.

2.5. Morimoto[8]

It was the first to define the problem in finding frequent neighbouring colocations in spatial databases based on number of instances of colocation, to measure the prevalence colocation but with a drawback not possessing the anti-monotone property.

2.6. Huang et al.[6]

In this paper a general framework was proposed for a prior-gen based colocation mining, in which minimum-participation ratio measure was taken instead of support, in which anti-monotone property which increases the computational efficiency. Later a paper[14],[16] was published which proposed a join-based algorithm to find prevalent colocation patterns, but as the size of the data set grows the number of joins increases. Later Huang et al. extended the problem to mining confident colocation patterns in which maximum participation ratio was taken instead of minimum participation ratio which is used to measure the prevalence of confident colocation.

2.7. Yoo etal.[9],[10]

Proposed two algorithms, one among these is partial-join algorithm and the other is join-less algorithm. These two algorithms discusses the information in which joins are used to identify k-

size colocation table instances which were substituted by scanning the materialized neighborhood tables and looking-up size k-1 instances, but in this approach there are some repeated scanning of materialized neighborhoods.

2.8. Wang et al. [11]

A CPI-tree-based approach was developed by storing star-neighbourhoods in a more compact format and a prefix tree instead of a table, which reduces the repeated scans of materialized neighbourhoods as in[9]. In this paper [12] discovered colocation patterns from interval data. As different applications are growing the researchers are more devoted to extend the traditional frequent pattern mining to uncertain data sets. [1], [2], [3].

2.9. Chui et al.[3]

Proposed a method which accurately mine the frequent patterns maintaining the efficiency, later in paper [4], methods were used for finding the frequent items in very large uncertain data sets Besides the above representative colocation mining problem, in this paper we are closely related to finding the prevalent colocations using the Probabilistic approximation approach[13].

3. THE BASIC DEFINITIONS

3.1. Uncertain Data Sets

Uncertain data set is defined as the data that may contain errors or may only be partially complete. Many advanced technologies have been developed to store and record large quantities of data continuously. In many cases, For Example:

1. Demographic data sets, Provides only partially aggregated data sets because of privacy concerns.
2. The output of sensor networks is uncertain because of the noise in sensor inputs or errors in wireless transmission.
3. Geographic information systems may contain partial data because of privacy Concern.
4. Data collected from satellites.

Thus each aggregated record can be represented by a probability distribution. Many uncertain reasoning methods, such as fuzzy set theory, evidence theory, and neural networks, are powerful computational tools for data analysis and have good potential for data mining as well. But traditional spatial data mining and knowledge discovery did not pay attention to these characteristics. In this paper, on the basis of analysis of uncertainty in spatial data is analyzed briefly.

3.2. Probabilistic Approach

Probabilistic approaches enable variation and uncertainty to be quantified, mainly by using distributions instead of fixed values in risk assessment. A distribution describes the range of possible values and shows which values within the range are most likely. Probabilistic approach is used in the context of uncertain data as data is collected from a wider range of data sources.

Table . 1. A Sample Example Of Spatial Uncertain Data Set

Id if Instance w	Spatial Feature	Location	Probability
1	A1	in Fig.1	0.1
2	A2	in Fig.1	0.4
3	A3	in Fig.1	0.7
4	B1	in Fig.1	0.1
5	B2	in Fig.1	1
6	C1	in Fig.1	1
7	C2	in Fig.1	0.1
8	D1	in Fig.1	0.4
9	D2	in Fig.1	0.1

3.3. Spatial Data

Spatial data also known as geo-spatial data is the information which identifies the geographic location of features and boundaries on Earth, such as Forests, Oceans etc., Usually Spatial data is stored in terms of numeric values.

3.4. Colocation Mining

It is the process of finding patterns that are colocated in nearby regions. Co-location rule process finds the subsets of features whose instances are frequently located together in geographic space. Many important applications use colocation mining. For example:

1. NASA (studying the climatologically effects, land use classification),
2. National Institute of Health (predicting the spread of disease),
3. National Institute of Justice (finding crime hot spots),
4. Transportation agencies (detecting local instability in traffic).

It is found that classical data mining techniques are often inadequate for spatial data mining and different techniques need to be developed. For this we discuss the co-location pattern mining over spatial data sets.

3.5. Spatial Colocation Mining

It is a group of spatial features whose instances are frequently located around the geographic space. Let F= $\{f_1, f_2, \ldots\ldots\ldots f_n\}$ be the set of features and Z= $\{P_1, P_2, \ldots\ldots\ldots\ldots, P_n\}$ where $\{P_1, P_2, \ldots\ldots\ldots\ldots, P_n\}$ are the subsets of features $\{f_1, f_2, \ldots\ldots\ldots f_n\}$ Let T be the threshold set {d, min_ *prev*, P_m} then C ∈ Z such that for C, T is valid. For example from the Fig:1 we can identify the features and instances related in a spatial data set

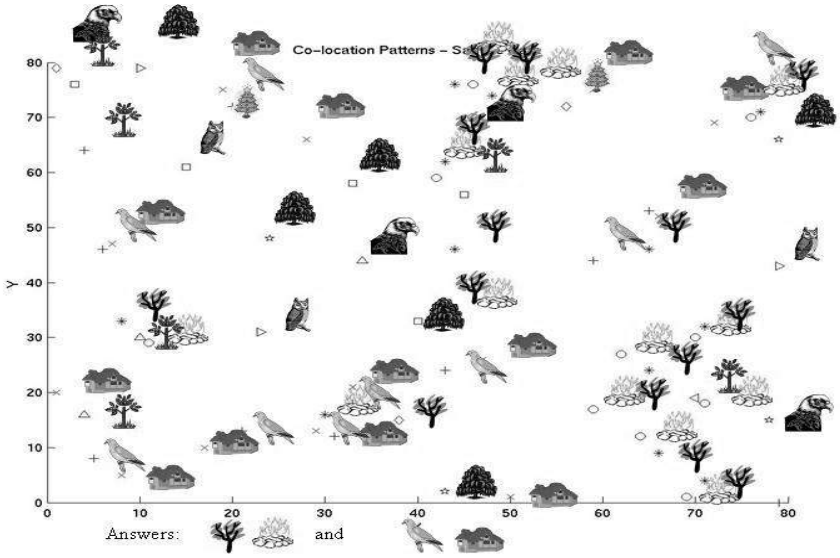

Fig: 4 Example of Spatial Colocation data

From the Fig:4 we can identify that there are different types of features like tree, Bird, Rocks and House and we have instances for the features like trees which are of various types of trees, and Birds which are like Eagle, Sparrow, Owl, and the Features like rock and house are having only one kind of instance. From the figure we can conclude that rocks and a type of tree is colocated, Sparrow and house are colocated.

From the Fig:4 we can identify that there are different types of features like tree, Bird, Rocks and House and we have instances for the features like trees which are of various types of trees, and Birds which are like Eagle, Sparrow, Owl, and the Features like rock and house are having only one kind of instance. From the figure we can conclude that rocks and a type of tree is colocated, Sparrow and house are colocated.

3.6. Instance of a Feature

The instances of a feature are the existential probability of the instance in the place location. If F is a feature then $F.i$ is an instance.

3.7. Spatially Uncertain Feature

A spatial feature contains the spatial instances, and a data set Z containing spatially uncertain features is called spatially Uncertain data set. If Z is a data set then set of features are A, B, C,...

3.8. Probability of Possible Worlds

For each colocation of k-size, c=$\{f_1, f_2, \ldots\ldots\ldots\ldots f_n$ of each instance $F.i$ there are two different possible worlds (i) one among them is that the instance is present (ii) and the other is absent.

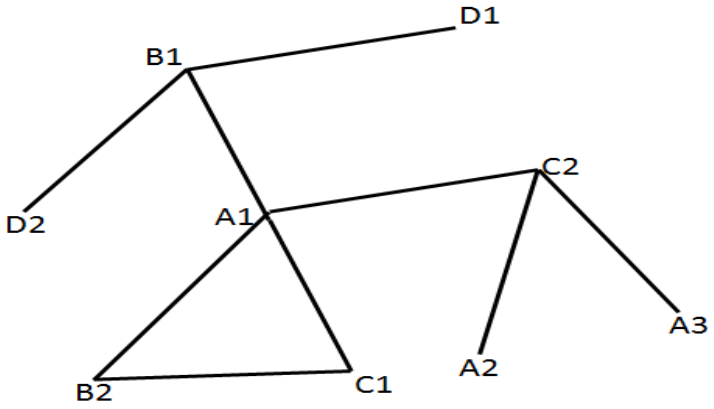

Fig: 5 Distribution of example spatial Instance

Take the set of features F=$\{f_1, f_2, \ldots\ldots\ldots f_n\}$ and the set of instances S= $\{S_{f_1}, S_{f_2}, \ldots\ldots\ldots, S_{f_n}\}$, where S_{f_i} $(1 <= i <= k)$ is the set of instances in S and there are $2^{|S|}$= $2^{\left|s_{f_1}, s_{f_2}, \ldots\ldots\ldots\ldots, s_{fn}\right|}$ possible worlds at most. Each Possible world w is associated with a probability P (w) that is the true world, where P (w) > 0.

3.9. Neib_tree

The Neib_tree is constructed for the Table-I which indicates the existence of the path from one feature to the other. If there is a path it indicates that a table instance is existing. This Neighbouring tree eliminates the duplicates can be seen in Fig:6.

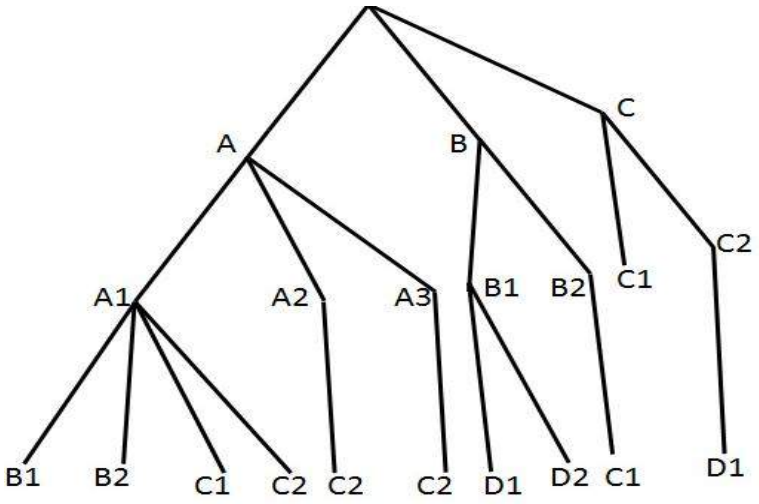

Fig: 6 Neib_tree for Fig:5

4. BLOCK DIAGRAM

Basic flow of co-location pattern mining: In this section, we present a flow diagram which describes the flow of identifying the Probabilistic Prevalent colocations. Given a Spatial data set, a neighbour relationship, and interest measure thresholds the basic colocation pattern mining involves 4 steps as in Fig: 3

Table 2. Computational Process Of Colocation (A,C)

A1	A2	A3	C1	C2
0	0	0	0	0
0	0	0	0	1
0	0	0	1	0
0	0	0	1	1
0	0	1	0	0
0	0	1	0	1
0	0	1	1	0
0	0	1	1	1
0	1	0	0	0
0	1	0	0	1
0	1	0	1	0
0	1	0	1	1
0	1	1	0	0
0	1	1	0	1
0	1	1	1	0
0	1	1	1	1
1	0	0	0	0
1	0	0	0	1
1	0	0	1	0
1	0	0	1	1
1	0	1	0	0
1	0	1	0	1
1	0	1	1	0
1	0	1	1	1
1	1	0	0	0
1	1	0	0	1
1	1	0	1	0
1	1	0	1	1
1	1	1	0	0
1	1	1	0	1
1	1	1	1	0
1	1	1	1	1

First candidate colocation patterns are generated and the colocation instances and spitted into two worlds from the spatial data set. Next, find the probabilities using minimum prevalence and compute summation of table instances of each colocation, Next find prevalent colocation using minimum probability.

5. THE BASIC ALGORITHM

The algorithm (Algorithm-1) is designed to find all PPCs with (min_prev, min_prob) pairing. The algorithm uses dynamic approach where in it prunes out the candidates which are not prevalent and works on the reduced search space to find the PPCs. It uses an approximation

Table 3. Computational Process Of Colocation(A,C)

Possible World$_w$	P(w_i)
w_1={C1}	0:1458
w_2={C1,C2}	0:0162
w_3={A3,C1}	0:3402
w_4={A3,C1,C2}	0:0378
w_5={A2,C1}	0:0972
w_6={A2,C1,C2}	0:0108
w_7={A2,A3,C1}	0:2268
w_8={A2,A3,C1,C2}	0:0252
w_9={A1,C1}	0:0162
w_{10}={A1,C1,C2}	0:0018
w_{11}={A1,A3,C1}	0:0378
w_{12}={A1,A3,C1,C2}	0:0042
w_{13}={A1,A2,C1}	0:0108
w_{14}={A1,A2,C1,C2}	0:0012
w_{15}={A1,A2,A3,C1}	0:0252
w_{16}={A1,A2,A3,C1,C2}	0:0028

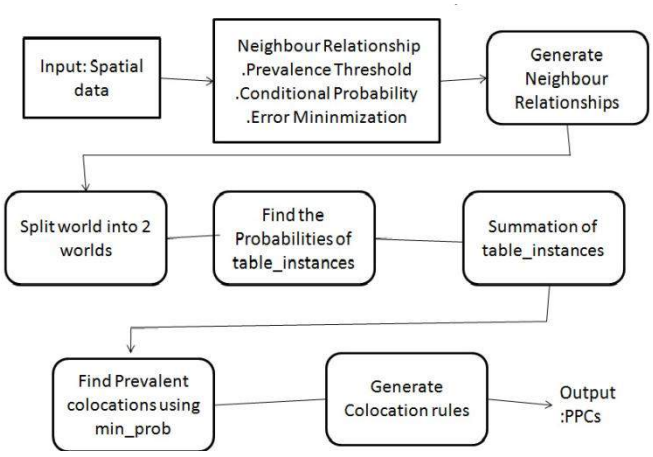

Fig:7 Block diagram to find the PPCs

approach by accepting an initial error that would be tolerated in finding the PPCs and thereby speeds up the process of finding the PPCs. The algorithm is presented below:

Algorithm-1

Input:

$F = (f_1, f_2, \ldots\ldots\ldots, f_n)$ a set of Spatial Features;

S: A spatially uncertain data set;

min_prev: A minimum prevalence threshold;

min_prob: A minimum Probability Threshold;

e: An Approximation error;

Probability of table instances:

$$P_r^{(c,f_1)}[0,0]_w = 1;$$
$$P_r^{(c,f_1)}[0,0]_w = 1;$$
$$P_r^{(c,f_1)}[0,0]_w = 0\ (1 < i < 1);$$

$P_r^{(c,f_1)}[0,0]_w = 0\ (1 < i < 1);$

Output:-

(min_prev, min_prob) PPCs.

Begin

1) Read approximation error **e**.
2) if e=1 STOP
3) else
4) Call Neib_tree_gen(F, S, NHR); // to identify table instances.
5) Assign $P1 = F$, $k = 2$;
6) While (not empty P_{k-1} and $k \leq n$) do
   (i) for each colocation $"W"$ of size $'k'$ compute Probabilities of worlds from equation-3:
   (ii) Split W into W_1 and W_2 where $W_1 = f_1.j >$ $(f_2.j, f_3.j \ldots\ldots, f_n.j)$ $W_2 =$ $f_2, f_3 \ldots\ldots\ldots\ldots, f_n,$ and $W_2 \subseteq$ w;
   (iii) for each set w=$(f_1.l, \ldots\ldots\ldots, f_n.l)$ compute Probability of table _instances as equation-4:.
   (iv) for each w compute Prevalence Probability $P(PR^R(c) \geq min\ prev)_{w_{1+w}}$ as equation-5:
   (v) Compute the summation of all Prevalence Probabilities $PPs = PPs + (P1 + P2 + \ldots\ldots\ldots + Pn)$
   (vi) if $(PPs \leq min\_prob)$ then c=c-C_k;
   (vii) P_k=sel_prev_colocation(C_k, min_prev, min_prob);
   (viii) $k = k + 1$;
   (ix) $end\ while$;
7) STOP;
8) Return $(P2 \cup P3 \ldots\ldots\ldots \cup Pn)$

End.

$$P(W) = \prod_{i=1}^{n}\left(\prod_{(e \in s_{f_i}) \in w} P(e) * \prod_{(e \in s_{f_i}) \ni w} (1 - P(e))\right) \quad (3)$$

$$P^{(c,f_1)}[i,j]_w = \begin{cases} P^{(c,f_1)}[i,j]_w \ if,\ f_1.j \in table_{instance_{w \cup f_1^j}}(c) \\ P^{(c,f_1)}[i,j-1]_w \cdot (1-p_j) + P^{(c,f_1)}[i-1,j-1]_w \cdot p_j \\ \qquad if, f_1.j \in table_{instance_{w \cup f_1^j}}(c) \\ \qquad and \geq j.min\_previstrue \\ 0 \qquad otherwise, \end{cases}$$

$$P^{(c,f_1)}[i,j]_w = \begin{cases} P^{(c,f_1)}[i,j-1]_w \quad if,\ f_1.j \notin table_{instance_{w \cup f_1^j}}(c) \\ P^{(c,f_1)}[i,j-1]_w \cdot (1-p_j) + P^{(c,f_1)}[i-1,j-1]_w \cdot p_j \quad (4) \\ \qquad otherwise, \end{cases}$$

$$\left(\sum_{i=1}^{l_1} P^{(c,f_1)}[i,j]_w \left(\sum_{j=0}^{\frac{|1-\min\_prev|}{\min\_prev} * i} P^{(c,\bar{f_1})}[j,\ l_1]_w \right) \right) \quad (5)$$

6. TRACING THE ALGORITHM

6.1 Step 1,2,3. Reading the value of e

if the value of e is 1 then the algorithm stops and prints that all colocations are Prevalent. Otherwise if the value is in between 0<e<1 then execute steps from 4 to 14.

6.2. Step 4, 5: The Initializing Steps

After finding all neighbouring instance pairs, a Neib_tree can be generated using the method [5]. For example fig:2 are a Neib_tree generate from Fig:1 These Neib_tree consist of a set of features which are organized in ordered and branched form.

6.3. Step (i): Generating Coarse Combination instances from each collocation

This step computes the coarse combinations of different colocation of k-size. For example for colocation (A,C) we get a set of 24 combination instances out of 25 combinations whose probability is greater than zero.

6.4. Step (ii): Splitting of Colocation instances

Splitting of a colocation into two different worlds (i.e.)., colocation based on the set of features which has largest number of instances. W_1 is the set of possible worlds of ff1g and W_2 is that of possible set of worlds of $\{f_1, f_2, \ldots\ldots\ldots\ldots, f_n\}$. For example in this paper the Colocation (A, C) are divided into 2 worlds out of which W_1 in consisting of all instances of {A} & {A, C} and W_2 consisting alone {C} instances (i.e.), {C1} & {C1, C2}.

6.5. Step (iii): Computing the Probability of table instances in world W_2

Computing the Probability of table instances W_2 where W_2 is consisting of ({C1},{C1,C2}) using the equations-(4) (i,e)., *for* $Pr(c, f_1)[i,j]\{C2\}$ and $Pr(c, \bar{f_1})[i,j]\{C2\}$. After finding the Probabilities the values can be seen in TABLE IV and V :

Table 4. The Computation Of The $P(c, f_1)[i,j]\{C1\}$ And $P(c, \bar{f_1})[i,j]\{C1\}$

	j =0	j =1	j =2	j =3
i=0	(1,1)	(0.7,1)	(0.7,0.6)	(0.7,0.24)
i =1	(0,0)	(0.3,0)	(0.3,0.4)	(0.3,0.52)
i =2	(0,0)	(0,0)	(0,0)	(0,0.24)
i =3	(0,0)	(0,0)	(0,0)	(0,0)

Table 5. The Computation Of The $P(c, f_1)[i, j]\{C1, C2\}$ And $P(c, \bar{f}_1)[i, j]\{C1, C2\}$

	j=0	j =1	j =3	j =4
i =0	(1,1)	(0.7,1)	(0.42,1)	(0.42,0.4)
i =1	(0,0)	(0.3,0)	(0.46,0)	(0.46,0.6)
i =2	(0,0)	(0,0)	(0.12,0)	(0.12,0)
i =4	(0,0)	(0,0)	(0,0)	(0,0)

6.6. Step (iv): Computing the Prevalence Probability of world W_2

After computing step-9 for each set colocation of k-size, now compute the prevalence probability from equation: 5 For example for colocation (A,C) if the min_prev is 0.5 then for the table_ instances { C1} the value is 0.205 and for{ C1, C2 } the value is 0.058.

6.7. Step (v): Summation of Prevalence Probabilities

After computing the prevalence Probability of all colocation then we make the summation of all Prevalence Probability. For example for colocation (A, C) the value of {C1} is 0.2052 and {C1, C2} is 0.058 and the summation of both { C1 } & {C1, C2} is 0.2632

6.8. Step (vi), (vii) : Checking with Minimum Probability

if the summation is less than the minimum probability then it is removed from Probabilistic Prevalent Colocations, Otherwise added to prevalent Colocation. From the above example if the min_prob is 0.3 then colocation (A, C) is filtered and if it is 0.2 then colocation is selected.

6.9. Step (ix)

The colocation size is increased and Steps from 6 to 13 are executed.

6.10. Step 7

Once all the Probabilistic Prevalent Colocations are identified the algorithm stops.

6.11. Step 8

A Union of all Probabilistic Prevalent Colocations are written from a set of features.

7. RESULTS

The results are compared against a data set given in the following Table-VI which consists of 7 features with an average of 2 instances.

Table 6. A Synthetic Sample Data Set

Features	X-Coordinates	Y-Coordinates	Probability
0	328	1362	0.5
0	190	1140	0.4
0	392	1220	0.9
1	290	1264	0.1
1	330	1480	1
2	260	1278	0.1
3	185	1440	0.1
3	320	1500	0.4
3	330	1500	0.7
4	150	1580	0.1
4	150	1300	1
5	225	1300	1
5	260	1530	0.1
6	220	1650	0.4
6	60	1590	1

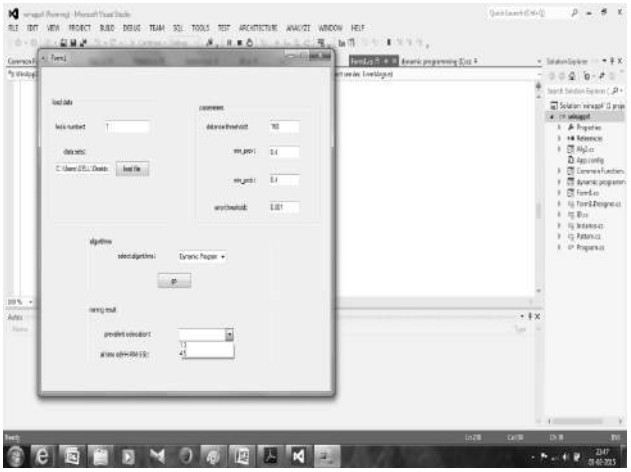

Fig:8 PPCs for Table-VI with $min\_prev = 0.4$ and $min\_prob = 0.4$, d=150,and $\varepsilon = 0.001$

Likewise when the comparisons are made against the complete data set from Table-VI we get the following Prevalent and non-Prevalent colocations, varying the min_prev and min_prob for the distance threshold=150 which are shown in Fig:9.

<min_prev,min_prob>	Prevalent Colocations	Non Prevalent Colocations
<0.2,0.2>	(0,1)(0,3)(0,5)(1,3)(4,5)(0,1,3)	(0,2)(0,4)(1,2)(1,4)(1,5)(2,3)(2,4)(2,5)(3,4)(3,5)(0,1,2)
<0.2,0.4>	(0,1)(0,3)(0,5)(1,3)(4,5)(0,1,3)	(0,2)(0,4)(1,2)(1,4)(1,5)(2,3)(2,4)(2,5)(3,4)(3,5)(0,1,2)
<0.2,0.6>	(1,3)(4,5)	(0,2)(0,3)(0,4)(0,5)(1,2)(1,4)(1,5)(2,3)(2,4)(2,5)(3,4)(3,5)(0,1,2)(0,1,3)
<0.2,0.8>	(1,3)(4,5)	(0,2)(0,3)(0,4)(0,5)(1,2)(1,4)(1,5)(2,3)(2,4)(2,5)(3,4)(3,5)(0,1,2)(0,1,3)
<0.4,0.2>	(0,1)(0,3)(0,5)(1,3)(4,5)(0,1,3)	(0,2)(0,4)(1,2)(1,4)(1,5)(2,3)(2,4)(2,5)(3,4)(3,5)(0,1,2)
<0.4,0.4>	(1,3)(4,5)	(0,2)(0,3)(0,4)(0,5)(1,2)(1,4)(1,5)(2,3)(2,4)(2,5)(3,4)(3,5)(0,1,2)(0,1,3)
<0.4,0.6>	(1,3)(4,5)	(0,2)(0,3)(0,4)(0,5)(1,2)(1,4)(1,5)(2,3)(2,4)(2,5)(3,4)(3,5)(0,1,2)(0,1,3)
<0.4,0.8>	(1,3)(4,5)	(0,2)(0,3)(0,4)(0,5)(1,2)(1,4)(1,5)(2,3)(2,4)(2,5)(3,4)(3,5)(0,1,2)(0,1,3)
<0.6,0.2>	(1,3)(4,5)	(0,2)(0,3)(0,4)(0,5)(1,2)(1,4)(1,5)(2,3)(2,4)(2,5)(3,4)(3,5)(0,1,2)(0,1,3)
<0.6,0.4>	(1,3)(4,5)	(0,2)(0,3)(0,4)(0,5)(1,2)(1,4)(1,5)(2,3)(2,4)(2,5)(3,4)(3,5)(0,1,2)(0,1,3)
<0.6,0.6>	(1,3)(4,5)	(0,2)(0,3)(0,4)(0,5)(1,2)(1,4)(1,5)(2,3)(2,4)(2,5)(3,4)(3,5)(0,1,2)(0,1,3)
<0.6,0.8>	(4,5)	(0,2)(0,3)(0,4)(0,5)(1,2)(1,3)(1,4)(1,5)(2,3)(2,4)(2,5)(3,4)(3,5)(0,1,2)(0,1,3)

Fig: 9 PPCs for Table-VI with varying min_prev and min_prob, and d=150,and ε = 0.001

As expected, the smaller the min_prev and min_prob values lead to an increase in number of PPCs which increases the computation time as shown in Fig:10.

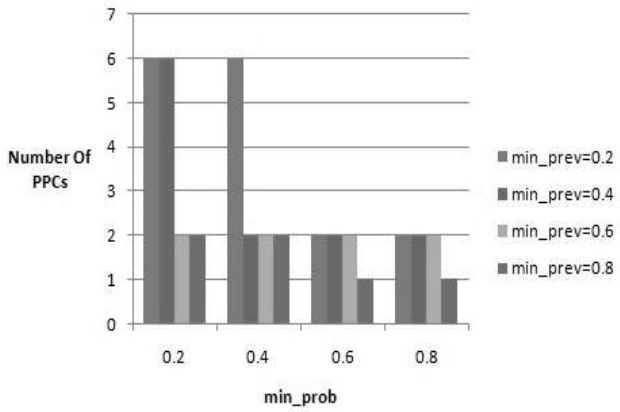

Fig: 10 Varying min_prev and min_prob and d=150, and ε = 0.001

From the graph below it is proved that the computation time for the improved Approximation algorithm works well when compared to dynamic algorithm: as shown in Fig: 11.

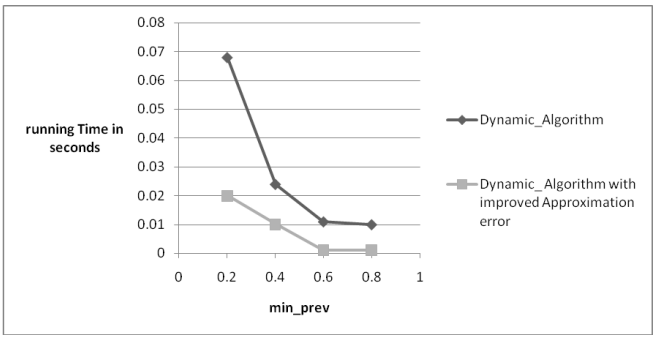

Fig.11: Varying min_prev and min_prob, d=150, and ε= 0.001

8. CONCLUSION

We have proposed a method for finding Probabilistic Prevalent Colocation in Spatially Uncertain data sets which are likely to be prevalent. We have given an approach in which the computation time is drastically reduced. Future Work can include the parallel computation for finding the Prevalent Colocation which are evaluated independently and this work can also be expanded to find the Probabilistic Prevalent colocations in other Spatially Uncertain data models, for example fuzzy data models and graphical spatial data. Further keeping in view the work can be extended to find the important sub functionalities in colocation mining to formulate colocation mining specific primitives for the next generation programmer which we can expect to evolve as a scripting language. In essence the scope of the work can cover data base technologies, parallel programming domain, graphical graph methods, programming language paradigms and software architectures.

REFERENCES

[1] C.C. Aggarwal et al, ”Frequent Pattern Mining with Uncertain Data,” Proc. 15th ACM SIGKDD Int’l Conf. Knowledge Discovery and Data Mining(KDD), pp. 29-37, 2009.

[2] T. Bernecker, H-P Kriegel, M. Renz, F. Verhein, and A. Zuefle, ”Proba-bilistic Frequent Itemset Mining in Uncertain Databases,” Proc. 15th ACM SIGKDD Conf. Knowledge Discovery and Data Mining(KDD ‘09), pp. 119-127, 2009. [05]

[3] C.-K. Chui, B. Kao, and E. Hung, ”Mining Frequent Item sets from Uncertain Data,” Proc. 11th Pacific-Asia Conf. Knowledge Discovery and Data Mining(PAKDD), pp. 47-58, 2007.

[4] C.-K. Chui, B. Kao, ”A Decremental Approach for Mining Frequent Item sets from Uncertain Data,” Proc. 12th Pacific-Asia Conf. Knowledge Discovery and Data Mining(PAKDD), pp. 64-75, 2008.

[5] Y. Huang, H. Xiong, and S. Shekar, ”Mining Confident Co-Location Rules Without a Support Threshold,” Proc. ACM Symp. Applied Com-puting, pp. 497-501, 2003.

[6] Y. Huang, S. Shekar, and H. Xiong, ”Discovering Co-Location Patterns from Spatial Data Sets: A General Approach,” IEEE Trans. knowledge and Data Eng., vol. 16, no. 12, pp. 1472-1485, Dec. 2004.

[7] Y. Huang, J. Pei, and H. Xiong, ”Mining Co-Location Patterns with Rare Events from Spatial Data Sets,” Geoinformatics, vol. 10, no. 3, pp. 239-260, Dec. 2006.

[8] Y. Morimoto, ”Mining Frequent Neighbouring Class Sets in Spatial Databases,” Proc. Seventh ACM SIGKDD Int’l Conf. Knowledge Discovery and Data Mining(KDD), pp. 353-358, 2001.

[9] J.S. Yoo, S. Shekar,J. Smith, and J.P. Kumquat, ”A Partial Join Approach for Mining Co-Location Patterns,” Proc. 12th Ann. ACM Int’l Workshop Geographic Information Systems (GIS), pp. 241-249, 2004.

[10] J.S. Yoo and S. Shekar, ”A Join less Approach for Mining Spatial Co-Location Patterns,” IEEE Trans. knowledge and Data Eng.(TKDE), vol. 18, no. 10, pp. 1323-1337, Dec. 2006.

[11] L. Wang, Y. Bao, J. Lu and J. Yip, ”A New Join-less Approach for Co-Location Pattern Mining,” Proc. IEEE Eighth ACM Int’l Conf. Computer and Information Technology (CIT), pp. 197-202, 2008.

[12] L. Wang, H. Chen, L. Zhao and L. Zhou, ”Efficiently Mining Co-Location Rules of Interval Data,” Proc. Sixth Int’l Conf. Advanced Data Mining and Applications, pp. 477-488, 2010.

[13] Q. Zhang, F. Li, and K. Yi, ”Finding Frequent Items in Probabilistic Data,” Proc. ACM SIGMOD Int’l Conf. Management of Data, pp. 819-832, 2008.

[14] L. Wang, P. Wu, and H. Chen, ”Finding Probabilistic Prevalent Colocations in Spatially Uncertain Data Sets,” IEEE Trans. knowledge and Data Eng.(TKDE), vol. 25, no. 4, pp. 790-804, Apr. 2013.

REAL TIME ERROR DETECTION IN METAL ARC WELDING PROCESS USING ARTIFICIAL NEURAL NETWORKS

Prashant Sharma[1], Dr. Shaju K. Albert[2] and S. Rajeswari[3]

[1]Computer Division, Indira Gandhi Centre For Atomic Research, Kalpakkam
[2]Material Technology Division, Indira Gandhi centre for Atomic Research, Kalpakkam
[3]Computer Division, Indira Gandhi Centre for Atomic Research, Kalpakkam

ABSTRACT

Quality assurance in production line demands reliable weld joints. Human made errors is a major cause of faulty production. Promptly Identifying errors in the weld while welding is in progress will decrease the post inspection cost spent on the welding process. Electrical parameters generated during welding, could able to characterize the process efficiently. Parameter values are collected using high speed data acquisition system. Time series analysis tasks such as filtering, pattern recognition etc. are performed over the collected data. Filtering removes the unwanted noisy signal components and pattern recognition task segregate error patterns in the time series based upon similarity, which is performed by Self Organized mapping clustering algorithm. Welder's quality is thus compared by detecting and counting number of error patterns appeared in his parametric time series. Moreover, Self Organized mapping algorithm provides the database in which patterns are segregated into two classes either desirable or undesirable. Database thus generated is used to train the classification algorithms, and thereby automating the real time error detection task. Multi Layer Perceptron and Radial basis function are the two classification algorithms used, and their performance has been compared based on metrics such as specificity, sensitivity, accuracy and time required in training.

KEYWORDS

Manual Metal Arc welding Process, Neural networks, Self Organized Mapping, Multi Layer Perceptron, Radial Basis Functions

1. INTRODUCTION

Manual Arc welding process, though carried out using specifically designed power sources, is a dynamic and stochastic process due to random behavior of the electric arc and the metal transfer that takes place during welding. Fluctuations in voltage and current are so rapid and random that a high speed data acquisition system is required to capture these variations. Data thus, acquired can be analyzed to derive characteristic feature of the welding process. Data collected is huge and contain features corresponding to the performance of welding power source, welding consumables and the welder. As far as power source and welding consumables are concerned, their qualities can be improved by using better technology and better composition respectively. But process is greatly affected by human made errors. Number of errors as well as uniformity of the weld greatly depends upon the experience of welder. Presently existing techniques declare quality of welder by inspecting the weld done by him, through various NDT techniques, which are time consuming and resource intensive. Amit kumar et al. has done a detailed study on

utilization of ANN in welding technology[1] and suggest ANN can be used to greatly optimize welding techniques.

T. Polte and D. Rehfeldt [2] suggest better alternative for declaring weld quality. Electrical parameters (current and voltage) obtained from power supply terminal are of random character and varies over wide range. Consequently statistical behavior of these parameters is used to characterize process, which can thereafter be used to detect the type of errors in the process. PDD transformation of voltage time series is fed to the ANN to classify the type of errors. On the other hand, J. Mirapeix and P.B. Garcia-Allende[3] used spectroscopic analysis of plasma spectra produced during welding to monitor quality of resulting weld seams. Plasma spectra captured during welding process goes through PCA technique, thereby reducing spectral dimensions and consequently they are fed to ANN for fault detection task. ANN is also used by Hakan Ates[4] for prediction of welding parameters such as hardness, tensile strength, elongation and impact strength. A. Sanchez Roca obtained a model using ANN for estimating stability of gas metal arc welding [5]. Application of ANNs for prediction of the weld bead geometry using features derived from the infrared thermal video of a welding process has also been done [6].

A novel and less computation intensive method of error detection is presented in this paper. Since the electrical parameters are clear description of the process in real time, so rather than using their PDD transformations we can directly use these waveforms to promptly recognize the process errors. Artificial neural networks (ANN) are employed to analyze the processed data. Self organized mapping (SOM) [9] algorithm clusters the input voltage data based upon waveform similarity. Database thus prepared is used to rank welders as well as it also trains classification algorithms. Multi Layer Perceptron (MLP) and Radial Basis function (RBF) are two type of ANN classifiers used to perform classification task on database obtained from SOM algorithm. Gradient descent algorithm trains MLP model. In RBF, transformation to higher dimension is performed using K means clustering algorithm [8], thereafter learning of separation boundary is done using gradient descent algorithm. Both the ANN classifiers are able to perform classification task fairly accurately. Performance of both has been compared.

2. EXPERIMENTAL

Aim of the experiment is to acquire voltage and current values from terminals of power supply. Fig shows block diagram of the setup deployed to perform data acquisition task.

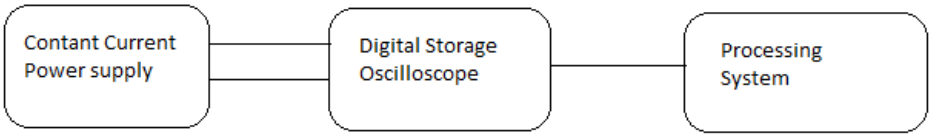

Figure 1. Experimental Setup

Online monitoring of the welding process is done and measured signals are transferred to process computer via Digital Signal Oscilloscope. Hall Effect current sensor measures current though power cord and voltage differential probe measures voltage values across power supply terminals. Voltage and Current signals thus acquired can be considered as time series and they can be subjected to various time series analysis.

Constant current power supply subside the process variations in current signal thus only voltage time series is selected for further processing. Data processing steps such as filtering, down sampling and segmentation was applied to voltage time series and Figure 2 depicts every processing step.

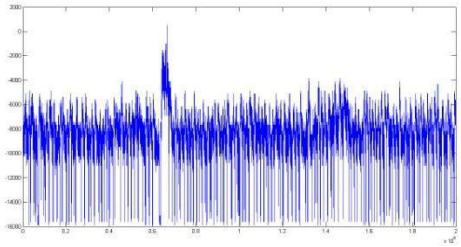

2.1. Raw voltage time series

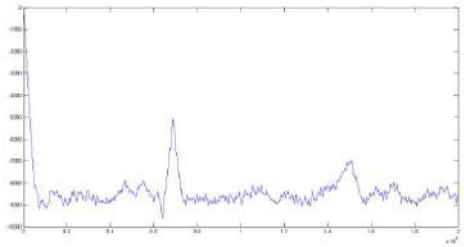

2. 2. Filtered voltage time series

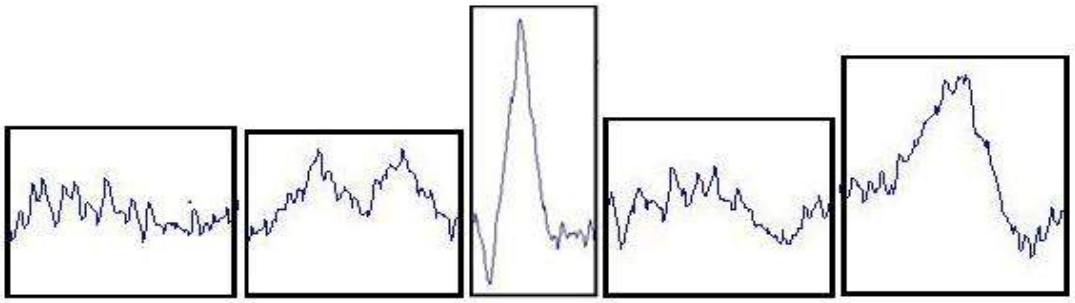

2.3. Segments of Filtered waveform

Figure 2. figure 2.1 shows raw voltage waveform 2.2 shows filtered waveform and 2.3 shows segments of filtered waveform

In Figure 2.3 third and fifth segments are most unsteady and these patterns correspond to error in weld at that particular time. Detecting these patterns with data mining algorithm will help us to pinpoint error in the weld in real time.

Every welder undergoes 3 trails, thus for 30 welders we are having 90 voltage time series. After applying proper filtering technique, every voltage time series is segmented into 17 segments, each of 100000 data points (thus each welder is having total of 51 segments from his three voltage time series).This procedure give us total of 1530 segments, each of 1,00,000 data points. Thereafter applying downsampling reduces data point in each segment from 100000 to just 50. As signal has only low frequency contents, thus this much downsampling doesn't affect overall shape of segment.

3. RESULTS AND DISCUSSIONS

Database of segment is not classified i.e. it is not known that which pattern belong to which class, thus an unsupervised clustering algorithm is required to group together the patterns based on similarity. Therefore, using Self Organized Mapping unsupervised clustering algorithm similar patterns are grouped together to form 9 different groups. Groups that are clustering steady patterns are identified and all the patterns clustered under it are marked as desirable patterns. And patterns under other groups are marked as undesirable. As we already know that each welder has 51 patterns, counting is done for number of undesirable pattern. Welder which has most number of undesirable patterns is ranked the lowest and that is how the ranking is performed.

Weights of the cluster 4 and 5 came out to have least standard deviation. Thus all the patterns under it are marked as desirable. And patterns under other clusters are marked as undesirable and these are error patters. Now, the pattern database is classified and is suitable for supervised learning of classification algorithm. This step will help in automating the task of error detection.

Table 1. Parameters of SOM algorithm

Parameter	Value
Number of training iteration	Until no considerable change in weight of clusters occurs
Number of training patterns	1530
Dimension of each pattern	50
Initial learning rate	0.3
Current radius	5.0
Rate of decreasing in radius	0.1
Number of clusters	9

Table 2. Number of patterns clustered by each clusters

Cluster index	No. of Patterns clustered
1	101
2	135
3	232
4	243
5	533
6	81
7	46
8	101
9	58

Database is now modified by marking 1 against the pattern which is belonging to desirable class and marking 0 against the patterns that belongs to undesirable class. This modified database is used for supervised learning of Multilayer Perceptron and radial basis function type neural networks. 70% of database is used for learning and 30% is used for testing. Comparative study of performance of both networks on same database is done.

Table 3. Parameter values for MLP

Parameter	Values
Number of training iteration	10000
Number of hidden layer	1 and 2
Initial learning rate	0.3
Rate of decreasing learning rate	0.001

Table 4. Parameter values for RBF

Parameter	Values
Number of training iteration	10000
Number of hidden layer	1
Initial learning rate	0.3
Regularization parameter	0.3

3.1. Simulation results

Training of classification algorithms is done using 1021 entries and last 509 entries are used for testing purpose. Selection of number of hidden nodes in single layer and double layer MLP was done based on study done by Wanas [7].

Table 6. Topology of MLP and RBF networks

MLP	Topology	True classification	misclassification	%correct evaluation
	50-25-25-2	477	32	93.71
	50-35-2	458	51	89.99
RBF	50-95-2	455	54	89.31
	50-80-2	452	57	88.80

Table 7. Comparison between RBF and MLP

	MULTILAYER PERCEPTRON		RADIAL BASIS NETWORK	
No of nodes	35 nodes	25 nodes Layer1 25 nodes Layer2	80 nodes	95 nodes
Sensitivity	0.8755	0.9572	0.8055	0.8288
Specificity	0.9246	0.9365	0.9762	0.9603
Accuracy%	89.9804	94.6955	88.8016	89.391
Time required	9mins 23secs	16 mins 10 secs	1min 52secs	2 mins 9 sec

Table 6 suggest that 2 layer MLP network gave least % test error among the three types of networks. % test error shown by RBF network was indeed highest, but time required for training the RBF network was 5 times less as compared to that required by MLP network as shown in Table 7. It is also seen that, specificity, which is the fraction of true negative classifications, was highest for RBF network and sensitivity, which is the fraction of true positive classification, was highest for two layer network. Comparison results between MLP and RBF are complying with the study done by Santos et al. [10].

Choosing any of the two trained neural network (based upon the accuracy needed) we could able to detect number of error patterns in the incoming voltage time series in real time, thereby detecting the errors in weld in real time.

4. CONCLUSIONS

Technique is developed to detect number of error patterns in a time series using Artificial Neural Networks. Self Organized mapping algorithm could successfully segregate the steady patterns and patterns that are in error. Reference database is generated using clustering process done by SOM. Both MLP and RBF network can easily be trained with reference database and thereby be used to classify an unknown pattern. Two layered MLP gave better error performance than RBF but training time required by MLP was almost 5 times as that required by RBF.

REFERENCES

[1] Amit Kumar, Vikas Chauhan , Ankur Singh Bist, "Role of Artificial Neural Network in Welding Technology: A Survey", 2013, IJCA, vol 67, No. 1.

[2] T. Plote and D. Rehfeldt, "Gas metal arc welding process monitoring and quality evaluation using neural networks", IOM, 2000, Vol 5, No. 5.

[3] J. Mirapeix, Realtime "Real-time Arc-welding defect detection and classification with principal component analysis using artificial neural networks", Elsevier, 2007, vol 40, Issue 4, 315-323.

[4] Hakan Ates, "Prediction of gas metal arc welding parameters based on artificial neural networks", Elsevier, 2006, vol 8, Issue 7, 2015-2023.

[5] A. Sanchez Roca et.al," Artificial Neural Networks and acoustic emission applied to stability analysis in gas metal arc welding", STWJ, 2009, vol 14, 117-124.

[6] P. Ghanty et al.,"Artificial neural network approach for estimating weld bead width and depth of penetration from infrared thermal image of weld pool", STWJ, 2008, vol 13, 395-401

[7] Wanas N, "On optimal hidden nodes in neural network", IEEE, 1998, vol 2, 918-921.

[8] N Benoudjit and M Verleysen, "On the Kernel-Widths in Radial Basis Function Networks", IEEE,2003, 18, 139-154.

[9] Teuvo Kohonen, "The Self Organising Map", 1998.

[10] Santos, Tupp, Bonzi, Fileti, "Comparison Between Multilayer Feedforward Neural Networks and a Radial Basis Function Network to Detect and Locate Leaks in Pipelines Transporting.2013, AIDIC, vol 32.

RELIABLE SOFTWARE FRAMEWORK FOR VEHICULAR SAFETY APPLICATIONS ON CLOUD

Ms. Deepa. D. Saibannavar[1] and Dr. S. A. Kulkarni[2]

[1]Lecturer, K.L.S Institute of Management and Research, Belgaum, India
[2]Professor and Head, Dept. of ISE, K.L.S Gogte Institute of Technology, Belgaum, India

ABSTRACT

Vehicular Ad-hoc Networks (VANET'S) have become viable and valuable for their wide variety of novel applications to improve driver's experience. The topology of network is highly time varying due to high mobility of vehicular nodes. This makes challenging to detect and diagnose errors in software applications used in the vehicles. Software reliability in vehicles is critical factor and significant challenge to be met. Misbehaving and faulty software applications in vehicle have to be detected and diagnosed from disrupting operation as it is hard to address in life critical vehicular network environment. The work proposes an advanced diagnostics system to be loaded in Road Side Units (RSU's) so that operating software is periodically transmits the codes generated by the vehicle configured with OBD to the RSU for test. The software is diagnosed at the RSU accessing the data from cloud servers for reliability. Later, a fixed patch is transmitted back to the vehicle via RSU's. The result in this paper shows the analysis of different temperature variables used in vehicles and are efficiently measured.

KEYWORDS

VANET's, Road Side Units, On-Board Units, On-Board Diagnostics, Diagnosis;

1. INTRODUCTION

Vehicular Ad-hoc Network (VANET) is an important component part of Intelligent Transportation Systems (ITS). As an open wireless network, VANETs is an application of Ad-Hoc Network for vehicle communication. It mainly consists of the vehicles with on-board units (OBDs), and the roadside units (RSUs). To provide and share information, there are two kinds of communications types one is vehicle-to-vehicle (V-2-V) communication; the other is vehicle-to-roadside communications (V-2-R). By V-2-V communication, people can obtain more information and use the shared information to improve road safety. By V-2-R communication, people can communicate with RSU to access internet for downloading and updating files or inquire neighborhood location information [1]. Thus, compared with the traditional pure infrastructure-based network, the hybrid of V-2-V and V-2-R communications is promising since it can not only overcome the disadvantages of infrastructure-based network, but also overcome the disadvantage of non-infrastructure-based network.

In Cloud Computing stores information permanently on the internet servers and it allows users to cache it temporarily [2]. The only concern is that the data sending and receiving from cloud must be done reliably. The basic hardware and software are still the integral part but the high level service capabilities are available to build the application. In the background of these services are the data and the resources.

DOI: 10.5121/ijci.2016.5103

In recent few years, Vehicular Ad-hoc Networks (VANETs) have gained much interest within the automobile and research worlds. One reason is the consideration in a increasing number of applications designed for passenger safety and comfort– such as emergency braking, traffic jam detection, scope for entertainment and cooperative driving – as well as in applications aiming at the comfort of passengers, such as chat-rooms, games and data-sharing with neighboring vehicles (e.g., CarTorrent[1]) The increased use of software has not only affected car warranty costs but has also made cars harder to repair.

Therefore, this work proposes the remote diagnosis system to detect the errors in software applications to improve reliability of the target vehicle using cloud. The RSU takes the control of the vehicle retrieve log information generated by the OBD device fixed in vehicle and cloud server, testing is performed by comparing the log information retrieved from cloud and vehicle. In this work we make use of "TORQUE Android application" which allows using the codes generated by the OBD. Test results are analyzed, if errors are detected, the results is updated to next RSU to fix the errors and reinstall the correct application software to the vehicle via RSU considering the speed and direction of the vehicle.

Vehicle mobility is usually constrained by road layout, speed limits, traffic and vehicle destination. If the vehicle is travelling within the speed limit the RSU will be able to dynamically reconfigure the correct software or else if it is exceeding the speed limit then warning messages is sent to the driver indicating the error and providing him location of next nearest RSU where he can reconfigure the correct software application. Therefore, this work proposes the diagnosis of the software and software up gradation of software's used by the vehicles on fly.

2. PREVIOUS WORK

Safety, comfort driving and infotainment applications for passengers are some of the main services proposed for VANETs. Some services are critical, such as collision warning; other services need bandwidth, such as video-streaming services. QoS (Quality of Service) provisioning and providing highly reliable applications are a challenge in VANETs due to their special features which result in frequent routing path disruptions. In this section, we discuss the related work that has been accomplished in the field of vehicular adhoc networks and also discuss various limitations that were observed.

The authors S. M. Mahmud, S. Shanker, and I. Hossain[3] proposed a protocol by means of which software download is performed using an Intelligent Transportation Systems (ITS) infrastructure. The automotive company issues symmetric keys to encrypt the software transmitted between the software supplier and the vehicle. To increase the security in the transmission, they propose that the software should be sent twice and possibly also in random order to avoid attackers from predicting the message order. To authenticate the vehicle, a set of authentication keys are installed in the vehicle and also stored in a central server and transmitted to the appropriate AP within the ITS during authentication.

The authors I. Hossain and S. M. Mahmud[4] introduced a special device denoted Network Device Monitor (NDM) which is installed in the AP within an ITS infrastructure. The purpose of the NDM is to authenticate vehicles, manage the session keys for the multicast group, and to send software to the vehicles therein. A set of authentication keys are installed in the vehicle and also stored in a central server. These keys are transmitted and used by the NDM to authenticate the vehicle. Furthermore, digital certificates were used as authentication keys for authentication between the automotive company, the software supplier, and the NDM. Nilsson and Larson propose a firmware update process [5] where the firmware is split into smaller fragments and transmitted to the vehicle. Each fragment is hashed and the hash is concatenated to the previous

fragment. Thus all fragments needs to be hashed before any of them can be transmitted The hash of the first fragment is used as an initial fragment containing a digital signature over the first hash, thereby ensuring that all following hashes cannot be modified without detection. Encryption is also applied to the transmission. This protocol ensures data integrity, data authentication, data confidentiality, and data freshness. Munir Sayyad, Sanjay Nalbalwar, Jagdish Bakal, Shomik Dasgupta [6] proposed Advanced Intelligent Vehicular Analytics records all the vehicular diagnostic data using OBD scan tool program and then wirelessly transmit the data to a central server thereby creating a database of the vehicular data. The database created will be used from the business point of view to generate applications using Web 3.0 architecture. An Interactive Graphical Interface (IGUI) for a cellular phone will be developed so that the owner of a particular vehicle will get real time live update of the vehicle's health. A semantic web of data would be generated to facilitate further progress in this field. This way the owner will know the fault in the vehicle and when to take the vehicle to the service station. The authors in [7] gave the first understanding of the impact of the vehicle's speed, transmission rate, 802.11 bit-rate, and packet size on throughput and delay of vehicle-roadside communication and illustrated a basic picture of how running vehicles contact with roadside hot spots through a "drive-thru" data access.

3. PROBLEM FORMATION

To develop a remote diagnosis system to upgrade, test and fix the software application used in vehicles using V-2-I communication model of vehicular ad-hoc networks on cloud. The software in the vehicles (i.e. OBD) can be remotely updated with a bug-fixed software release over the wireless connection and also makes it possible to diagnose many vehicles at the same time via RSU. Reprogramming software in the traditional way is a time consuming procedure that requires test equipment to be connected physically to each vehicle. This increases the driver safety and comfort and allows him to use reliable and updated version of software.

3.1 Necessity of the proposed system

Vehicles of today have become gradually more dependent on software to handle their operations and functionalities. For automotive industry maintaining, updating and diagnosing the software in vehicles has therefore become a challenging and costly process. By introducing wireless communications to vehicles, it has greatly improved vehicular maintenance and has brought many other new applications to the vehicles. The following benefits of this system are listed below:

- To provide a new and improved wireless vehicle diagnostic and software upgrade system with a relatively fast response time and improved accuracy.
- To supports Remote software download that will give the customers the opportunity to get the latest software versions installed without having to take the car to an authorized repair shop.
- To support a wide range of applications and services targeting to improve the utilization and the quality of the transportation infrastructure, safety and facilitates driver assistance.
- To help the automotive industry to understand the flaws and problems frequently arising in the vehicles which help them to take appropriate decisions to increase the customer satisfaction that benefits the business.

3.2 Work process

This system works as follows:

- Vehicle on road probes the RSU-1 by sending the version number, vehicle ID and hello

packet. RSU-1(waiting for the hello packet) receives the hello packet and performs the version check accessing its own database.

After the version check performed by the RSU-1 in zone-1 it will reply back with the status (up to date or update required) of the version check to the incoming vehicle (position-2) with OBD as shown in Figure 1. If the received version number of the vehicle matches with version stored on RSU then the RSU will reply the vehicle stating "version up to date". If the received version number of the vehicle does not match with version stored on RSU then the RSU will reply the vehicle stating "Warning: Old version is use Updating is required".

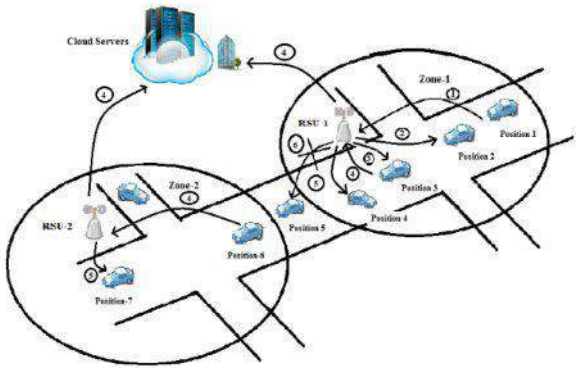

Figure 1. System Infrastructure

- The RSU-1 requests the log information from vehicle (position-3) if the version number is up to date if it not RSU-1 starts updating the application in vehicle (position-3) on successful completion of update a flag is set.
- Vehicle (position-3) will reply back by sending the log information to the RSU-1. At the same the RSU-1 will also access the log details from the cloud server by sending the vehicle ID. The RSU-1 will perform a test by comparing the log details fetched from the vehicle and cloud server.
- If application check is passed in the RSU-1, it will reply back to vehicle (position-4) application working correctly or if it fails the RSU-1 will fix and sends the patch to the vehicle.
- Due to high speed the vehicle (position-5) moves outside the range of Zone-1 link breaks and reliability check is suspended.
- Step 4 is repeated until all the applications are tested. The RSU-2 of Zone-2 resumes testing the reliability of the software of the vehicle once the vehicle enters the Zone-2 (position-6).
- If OBD in vehicle (position-7) successfully receives the file then vehicle responds back to the RSU-2 of Zone-2 by sending the positive Acknowledgement (ACK) and sets the flag bit on successfully completion.

3.3 Challenges

To develop this system we come across some of the difficulties

- Vehicles move at higher speeds and consequently lifetimes of communication links are shorter; thus, links must cope with the rapid changes in the network topology.
- Due to the limited factors in OBD such as buffer size, transmission capacity of a RSU and the frequency of data recording. This may led to non-reliable data transfer and also may fail in receiving appropriate data required for diagnosis.

- Vehicle mobility is usually constrained by road layout, speed limits, traffic and vehicle destination. If the vehicle is in exceeding the speed limit then it results in receiving an incomplete patch. This requires the intelligent file transfer.
- Using of cloud storage is biggest concern due to data integrity and unauthorized Access.

4. RESULTS

4.1 On-Board Diagnostics (OBD)

In this work the vehicle is fixed with OBD-II device[8]. The OBD-II device provides an access to various subparts of the vehicle. OBD-II collects the data from the various ECU (Engine Control Unit) and sends the data to TORQUE[9] application which will be in form of HEX values. So the TORQUE application takes the responsibility of converting this HEX values to user understandable values which is then used by RSU's for testing and comparing with the details stored on cloud. OBD-II works on Request/Reply basis. The below given figure 2(a) shows how the OBD-II device is connected to vehicle and figure 2(b) is the snapshot of TORQUE application.

Figure 2 (a) OBD-II (b) TORQUE Application Interface

4.2 Establishing the communication between vehicles (client) RSU (server) and cloud (backend server):

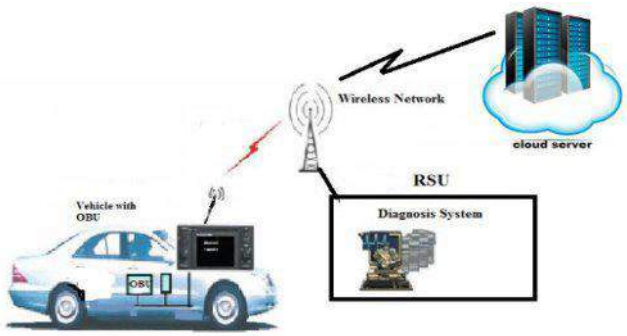

Figure 3. Vehicles with OBD

Wireless connection should be established between the vehicle and RSU and RSU and cloud server. This is done by configuring Ad-hoc network and 802.11d interface cards which allows communicating between the OBD devices installed in the vehicle with the RSU and sending the log details/codes generated by the application to RSU for testing. Communication between the RSU and the cloud server is through internet as shown in figure 3. Cloud servers update the RSU with the latest applications available, correct threshold values corresponding to different vehicles and so on.

4.3 Applications Tested

Temperature measurement in today's industrial environment encompasses a wide variety of needs and applications. To meet this wide array of needs the process controls industry has developed a large number of sensors and devices to handle this demand. Temperature is a very critical and widely measured variable in all vehicles. Many applications are developed to monitor or control the temperature and warn the drivers regarding the status of devices [10]. In this paper we take an example of application measuring various temperature variables like engine coolant temperature, Air intake temperature and Catalyst temperature. Each of these temperature variables have standard threshold values as shown in Table 1 which defines the status of the engine which can be classified has working in normal condition (operating efficiently or not working as expected (Inefficient operation).

1. **Engine Coolant Temperature:** The coolant temperature sensor is used to measure the temperature of the engine coolant of an internal combustion engine. The readings from this sensor are then fed back to the Engine control unit (ECU), which uses this data to adjust the fuel injection and ignition timing [11].
2. **Air Intake Temperature:** The Intake Air Temperature (IAT) monitors the temperature of the air entering the engine [12].

Catalyst Temperature: Catalytic converters are one of the greatest emission add-ons ever to be installed on vehicles [12]. They help in cleaning up the pollutants left over from combustion, they reduce hydrocarbons (HC) and carbon monoxide (CO) emissions to extremely low levels, when everything is operating normally if not the vehicles fail to pass the emission test [12].

Table 1. Temperature measures

Temperature variables	**Threshold temperature Values**	
	Operating Effiecintly	**Inefficient operation**
Engine Coolant Temperature	Range 200◦ F -225◦ F	225◦ F Above
Intake Air Temperature	+ 40◦ F/-40◦ F Ambient Temperature	+ 40◦ F/-40◦ F Above Ambient Temperature
Catalyst Temperature	Range 400◦ F -1600◦ F	1900◦ F Above

The graph in Figure 4 performs the analysis of Engine Coolant temperature against the speed of the vehicle for low temperature, high temperature and required temperature. The Graphs shown in figure 4(a)(b)(c) is generated in Java[13] by feeding the real time data obtained by TORQUE application. The graph in Figure 4 performs the analysis of Intake Air Temperature vs. speed also considering constant ambient temperature. The graph in Figure 5 performs the analysis of Catalyst Temperature vs. speed also considering constant ambient temperature.

4.4 Log Section

Log section of the application running displays the current status of application test as well as it also displays the connection status with RSU. It gives the following details

1. Connection establishment with the nearest RSU.
2. Version check performed by the RSU.
3. Updation process scheduled by the RSU if current version in use is old.
4. Status of working of application i.e the application is displaying appropriate messages or no if yes then working is fine else it displays application is faulty.

Therefore it should schedule the updation.

5. Finally it also displays which all applications have successfully updated so that it can schedule the application only which has not been updated. Snapshot of log section is shown in figure 5.

4.5 Cloud Server

Cloud server stores all the details of the applications running in the vehicles like the latest version release of applications, which are the suitable application available to vehicles based on the OBD model so that it can update the RSU's frequently as soon as the new version is available. It runs in background and uses PHP scripts to fetch the data of the vehicle.

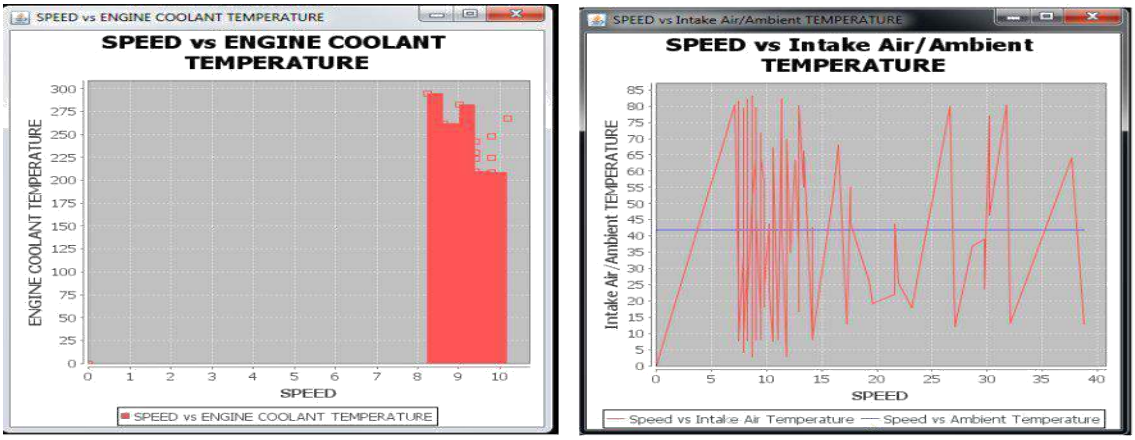

Figure 4 (a) Engine coolant temperature vs. Speed (b) Intake air temperature vs Speed

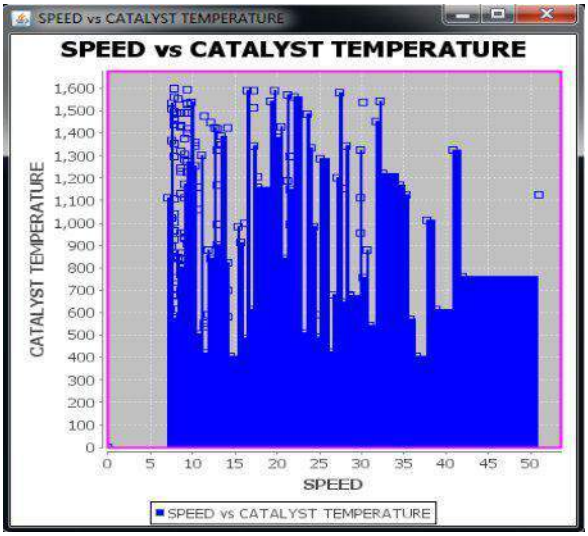

Figure 4 (c) Intake air temperature vs Speed

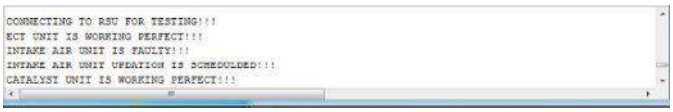

Figure 5. Log section

In this paper, the proposed system checks whether the application developed to give the warning or alert messages to driver when the temperature is exceeding the threshold value is operating or

is displaying appropriate warning/alert messages. It also checks the application installed is a latest version or require the application updating. If the application is not displaying appropriate messages then the bug in the application has to be detected by using the values generated by the vehicle which is sent to RSU and the RSU performs the testing by requesting the application details from the cloud server and fix the bug by reinstalling a bug free patch to the vehicle.

5. CONCLUSION

The convergence of wireless telecommunications and various kinds of services are enabling the deployment of different kinds of application software's in vehicles to improve the driver comfort and safety. Reliability of software applications in vehicles is very critical so these have to be periodically tested and diagnosed. This paper presents a new software diagnosis system which also updates the software applications installed in stationary vehicles on fly. The results in this paper are performed by simulating the temperature testing application which warns the driver about faulty behavior of engine by checking the temperature variables and helps to test and diagnose software applications in vehicles to improve the reliability and update them if required with the help of the cloud servers. In future this approach can be used for testing few more applications to provide bug free applications to improve driver safety and comfort.

REFERENCES

[1] Zhang Jianhong, Xu Min, and Liu Liying, "On the security of a secure batch verification with Group Testing for VANET", International Journal of Network Security, Vol.16, No.5, PP.351–358, Sept. 2014

[2] "Privacy-Preserving public auditing for Data Storage security in Cloud ComputingCong" Wang, Qian Wang, and Kui Ren Wenjing Lou "Technical Program at IEEE INFOCOM 2010

[3] Mathias Johanson Alkit Communications AB Sweden "Information and communication support for Automotive testing and validation" New Trends and Developments in Automotive System Engineering

[4] S. M. Mahmud, S. Shanker, and I. Hossain. "Secure software upload in an intelligent Vehicle via wireless communication links". Proceedings of the IEEE Intelligent Vehicles Symposium. 2005, pp. 588–593. doi: 10.1109/IVS.2005.1505167

[5] I. Hossain and S. M. Mahmud. "Secure multicast protocol for remote software upload in intelligent Vehicles". Proc. of the 5th Ann. Intel. Vehicle Systems Symp. of National Defense Industries Association (NDIA). National Automotive Center and Vectronics Technology. Traverse City, Michigan, June 2005, pp. 145–155

[6] D. K. Nilsson and U. E. Larson. "Secure Firmware Updates over the Air in Intelligent Vehicles". Proceedings IEEE International Conference on Communications Workshops (ICC Workshops '08). May 2008, pp. 380–384. doi: 10.1109/ICCW.2008.78

[7] Munir Sayyad1*, Sanjay Nalbalwar2, Jagdish Bakal3, Shomik Dasgupta "Advanced intelligent Vehicular analytics (AIVA) using IMS Architecture", International Journal of Smart Home Vol. 5, No. 2, April, 2011.

[8] OBD-II Background http://www.obdii.com/background.html

[9] TORQUE Engine Performance and Diagnostic Tool http://torque-bhp.com/

[10] MVFRI reasearch Summary Kennerly H. Digges, Edmund Fournier Underhood Temperature Measurements Based on a contract with: Biokinetics and Associates, Ltd.

[11] Engine coolant temperature ECT sensor engine codecom.] http://carrelease.info/view/engine-coolant-temperature-ect-sensor-engine-codescom.

[12] catalytic converter-Auto diagnosis repair help http://www.aa1car.com/library/converter.htm

[13] Socket Communications http://www.oracle.com/technetwork/java/socket-140484.html

A VARIABLE SPEED PFC CONVERTER FOR BRUSHLESS SRM DRIVE

Mrs. M. Rama Subbamma[1], Dr. V. Madhusudhan[2], Dr. K. S. R. Anjaneyulu [3] and Dr. P. Sujatha[4]

[1]Professor, Department of E.E.E, G.C.E.T, Y.S.R Kadapa, A.P
[2] Principal, K.O.R.M.C.E, Y.S.R Kadapa, A.P
[3]Professor, Department of E.E.E, JNTUCE, Anantapur, A.P
[4]Professor, Department of E.E.E, JNTUCE, Anantapur, A.P

ABSTRACT

In many industrial applications Switched Reluctance Motor (SRM) is mainly used because of its high efficiency and low maintenance. Its mechanical structure is so simple to construct because it has salient poles, stator and rotor. Stator has concentrated winding and there is no winding on rotor. So therefore no need of commutator and brushes. The SRM drive has another advantage of fast dynamic response and fault tolerant capability. However since this drive requires DC excitation so we need to convert AC-DC, this AC-DC conversion imposes low power factor on grid side and this leads to high losses. Here we have consider air-compressor used for household applications. In this paper we are proposing PWM rectifier on AC side for Power factor correction the same rectifier is used for control of DC-link voltage. Also SRM motor is Driven by Asymmetrical converter, the speed of the Motor is changed by changing the DC-link voltage of Asymmetrical converter. A MATLAB/SIMULINK based model is developed for various loading conditions and simulation results are presented.

KEYWORDS

Switched Reluctance Motor (SRM), PWM (Pulse Width Modulation) Rectifier, Power Factor Correction

1. INTRODUCTION

In any machine torque can be produced by two ways, (i) Electromagnetic principle (ii) Reluctance principle. The example for the electromagnetic torque produced motor is Induction Motor. But it has disadvantage of low efficiency, high maintenance and no fault tolerant capability. These problems can addressed by using a Reluctance motor. In SRM we have only one winding placed on the stator, no winding on the rotor, so rotor can run at high speeds. But it has a disadvantage of low power factor when it is applied in air- conditioner applications[1]. This drawback is addressed in this paper. In previous literature Brushless DC motor(BLDC) is used in air-conditioners, but it has disadvantage of high cost and lifetime of permanent magnets. In this research work we are proposing SRM in place of BLDC motor. Just like BLDC motor SRM requires converter for switching the phases. The input of the converter is DC supply, but in household applications the input is AC and we need to convert AC-DC[2-5]. One simple way to convert AC-DC is use of a Diode bridge rectifier but it has disadvantage of low power factor on AC side and pulsating DC on DC side. This problem is overcome by using many techniques in literature [7-10]. In this work we are proposing simplified PWM rectifier for power factor correction and DC voltage control. The proposed control strategy maintains almost unity power factor on AC side and constant DC on DC side.

DOI: 10.5121/ijci.2016.5104

2. OPERATION OF SRM

The operation principle of the SRM is so simple; as current is flowing through one of the stator windings, the rotor pole try to align with the excited stator pole this will generates the torque. The direction of rotation is based on the order of the excited stator windings. Continuous torque can be obtained by synchronizing the each phase's excitation with rotor position. In order to get the reluctance torque the number of stator and rotor poles must be different. In this work we considered 6/4 pole SRM as shown in figure 1.

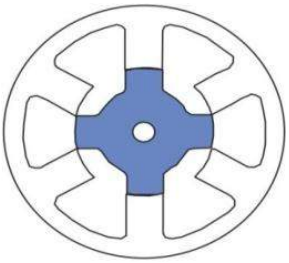

Fig.1. SRM with 6/4 pole.

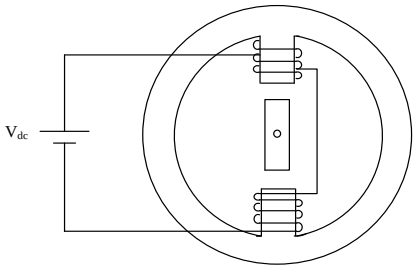

Fig.2. Aligned position

The SRM operation can be explained based on two positions (i)Aligned position (ii) unaligned position. Aligned position is position where the rotor pole is under the same axis of stator pole at this position flux is maximum and inductance is maximum as shown in figure 2.

Unaligned position is a position where rotor pole axis is in between stator pole axis as shown in figure 3. For motoring operation SRM phase winding is excited in unaligned position and de-energizes in aligned position.

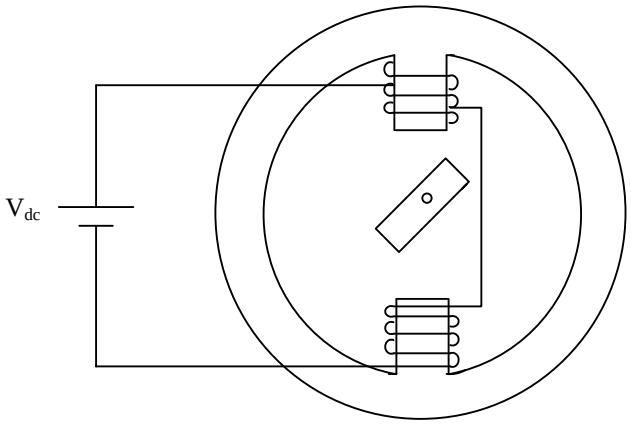

Fig.3. Unaligned position

3. SRM CONVERTER

For continuous rotation of rotor, we need to switch the phases based on rotor position for this we need a converter. There are various converters proposed in literature for simplicity we have considered asymmetrical converter as shown in figure 4. By turning on any two power switches in one winding circulates a current in that phase of SRM. Once the rotor reaches unaligned position the switches are turned off. In figure 4 by switching S_1 & S_2 we can excite phase A winding for current control we will turn S_2 continuously and switching the switch S_1. when the rotor reaches aligned position we will turnoff S_1 & S_2 then current is passing through D_1 and D_2 in the reverse direction to source.

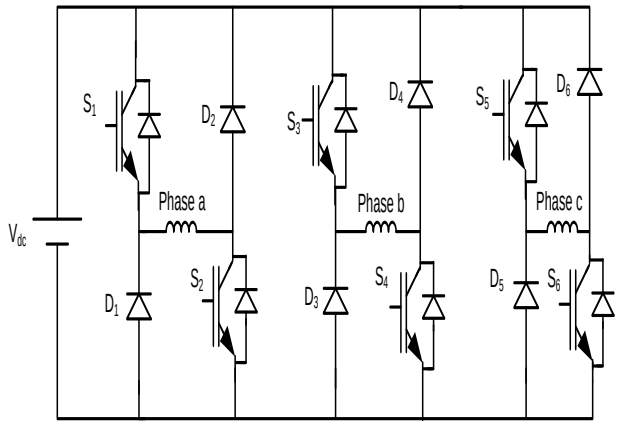

Fig.4. Asymmetrical converter for 6/4 SRM Drive

4. RECTIFIER FED SRM DRIVE

The conventional SRM fed with diode bridge rectifier shown in figure 5, on AC side it has diode bridge rectifier on motor side it has asymmetrical converter. This circuit has disadvantage of low power factor and low efficiency.

The proposed PWM rectifier fed SRM drive shown in figure 6. The frontend converter consist of four IGBT's controlled by power factor correction control strategy. The motor side asymmetrical converter is same as in figure 5. By varying the DC-Link voltage we are controlling the speed of the SRM.

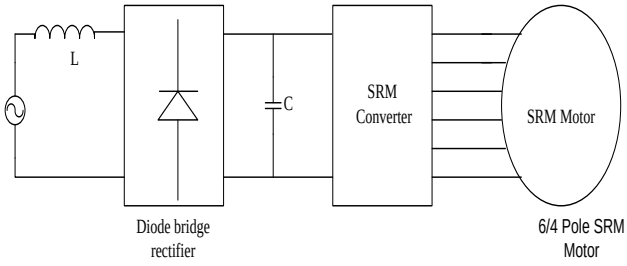

Fig.5. Conventional SRM drive

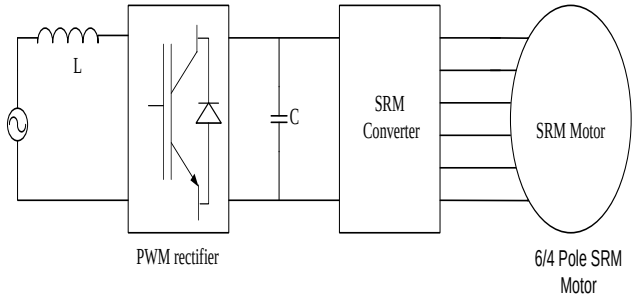

Fig.6. Proposed SRM drive

5. DESIGN OF SRM DRIVE

Here we consider 2KW SRM drive, the various components designed based on following equations

5.1. Selection of DC Link Voltage and Intermediate DC link Capacitor

The VSC is supplied by a single-phase 220 V AC supply. The selection of minimum DC link voltage depends on amplitude of AC voltage and desired rated DC link voltage of a SRM Drive. T_t must be greater than or equal to the peak value of supply voltage and equal to desired rated DC link voltage of the SRM Drive.

$$V_{dc} \geq V_m = V_{rated} \qquad (1)$$

Where V_m is peak value of single-phase supply voltage and V_{rated} is desired rated DC link voltage of a power of the SRM Drive.

A 200V DC link is selected and for maintaining the constant DC link voltage, an intermediate DC link capacitor is used. The selection of a DC link capacitor is given as,

$$C_{dc} = I_{dc}/2\omega V_{dcripple} \qquad (2)$$

where I_{dc} is the DC link current which is obtained as,

$$I_{dc} = \frac{P_{dc}}{V_{dc}} = 10A \qquad (3)$$

w is the angular frequency in rad/s and V_{dc} ripple is the I% of rated DC link voltage. The DC link capacitor is obtained as 1900 µF, using Eq. (2).

5.2. Selection of Interface Inductor

An interface inductor is used between AC supply and AC terminals of a single-phase VSC. The inductor is used to absorb PWM voltages. The fundamental rms voltage V_c at VSC terminal is given as,

$$V_c = (mV_{dc})/\sqrt{2} \qquad (4)$$

Where m is modulation index, and it is considered I. V_{dc} is the reference DC link voltage (200V). The fundamental ms voltage at VSC terminals obtained as 282.88V using Eq. (4). The relation between fundamental voltages at VSC terminals is given as,

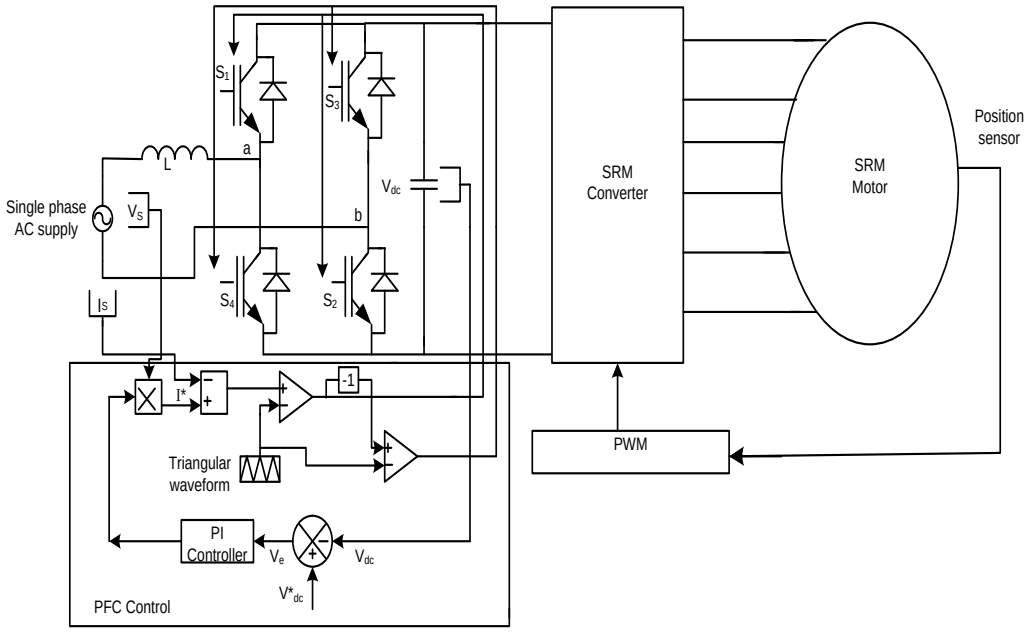

Fig.7.Control Scheme for PWM rectifier fed SRM Drive

$$V_c = \sqrt{[V_s^2 + (I_s^2 X_1^2)} \qquad (5)$$

Where Vs is rms value of input supply voltage which is taken as 220V and Is is rms value of supply current as,

$$I_s = \frac{P_{in}}{V_s} = 9.09amp \qquad (6)$$

Therefore, interface inductor is obtained using Eq. (5) is 17 mH.

5.3. Design of Voltage Source converter (VSC)

The voltage source converter (VSC) is designed on the basis of apparent power through the VSC. The rms current through each leg of VSC is obtained 9.09A using Eq. (6). Where P_{in} the input power at VSC terminals. The maximum current through IGBTs is calculated as [18],

$$I_{max} = 1.25\{I_{p-p} + \sqrt{2}I_{vsc}\} \qquad (7)$$

Considered 10 % peak-peak ripple current, the maximum current through IGBT is obtained 17 Amp. Therefore 25A, 600V IGBT's are used for the VSC.

5.4. Design of SRM converter

The SRM converter consists of six IGBTs switches. The selection of IGBTs is based on rated current of a SRM. The stall current of SRM is 8.45A, as obtained from manufacturer data sheet and maximum current through IGBT in each phase is obtained as,

$$I_{max} = 1.25\{I_{pp} + \sqrt{2}I_{vsi}\} \qquad (8)$$

Considered 10% peak-peak ripple in stall current, maximum current through IGBTs is obtained as 15A. Therefore 15A, 600V IGBT's are selected for a three-phase converter.

6. MATHEMATICAL MODELLING OF SRM DRIVE

The equivalent switched reluctance motor drive is shown in figure 8. Here we have consider linear approximation it means we have neglected saturation effect. The induced emf across any phase is directly proportional to flux linked by the phase. The flux linked will depends on two parameters (i) rotor position and (ii)current.

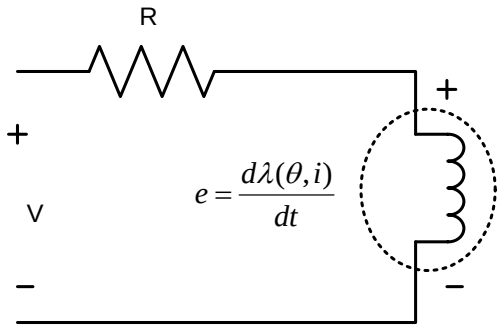

Fig.8. Equivalent circuit of switched reluctance motor

$$V = Ri + \frac{d\lambda(\theta,i)}{dt} \qquad (9)$$

Where V is the applied phase voltage to phase, R is the phase resistance, and e is back EMF. Ordinarily, e is the function of phase current and rotor position, and flux λ can be expressed as the product of inductance and winding current:

$$\lambda(\theta,i) = iL(\theta,i) \qquad (10)$$

And from (8) the function can be rewritten as: $V = Ri + \frac{d\lambda(\theta,i)}{di}\frac{di}{dt} + \frac{d\lambda(\theta,i)}{d\theta}\frac{d\theta}{dt}$ (11)

The general torque expression is: $T(\theta,i) = \frac{\partial \int_0^i \lambda(\theta,i)}{\partial\theta}$ (12)

In general, the dynamical model of a SRM is characterized by the rotor angular speed and angular position relationship:

$$\omega = \frac{d\theta}{dt} \qquad (13)$$

$$T\text{-}T_{load} = J\frac{d\omega}{dt} + F\omega \qquad (14)$$

$$V = Ri + L(\theta,i)\frac{di}{dt} + i_{\omega}\frac{dL(\theta,i)}{d\theta} \qquad (15)$$

The average torque can be written depending on the number of phases of the SRM as:

$$T = \sum_{phase=1}^{n} T_{phase} \qquad (16)$$

7. SIMULATION ANALYSIS

Case I: Diode Bridge based Switched Reluctance Motor.

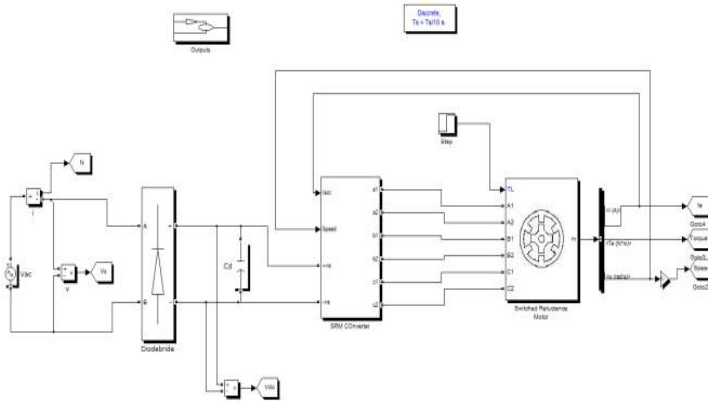

Fig.9. Simulation model of proposed SRM with Diode Bridge Rectifier

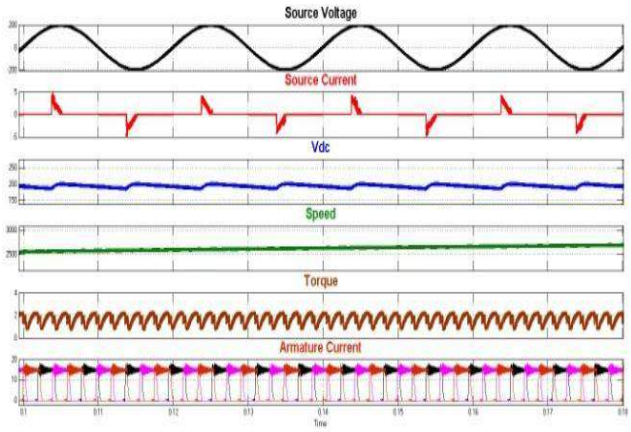

Fig.10. Simulation output waveforms of Source voltage, source current, rectifier output voltage, speed, torque and armature current of SRM

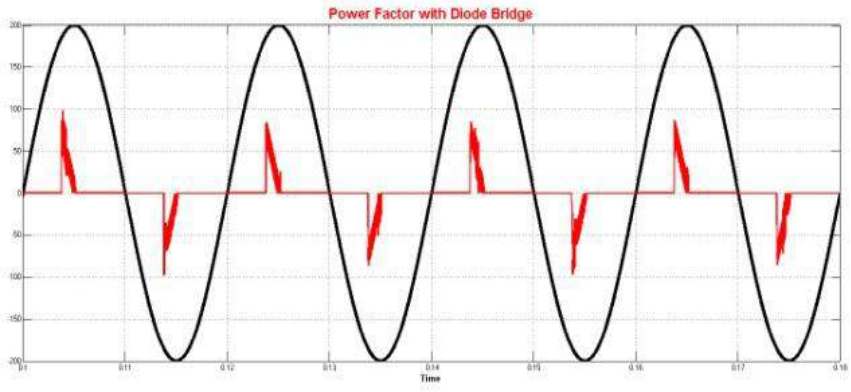

Fig.11. Simulation output wave form of Power factor with Diode Bridge Rectifier based SRM

Because of using Diode Bridge rectifier the load draws pulsating current from input side shown in fig.11, then voltage and current are not in a phase. So we achieve low power factor.

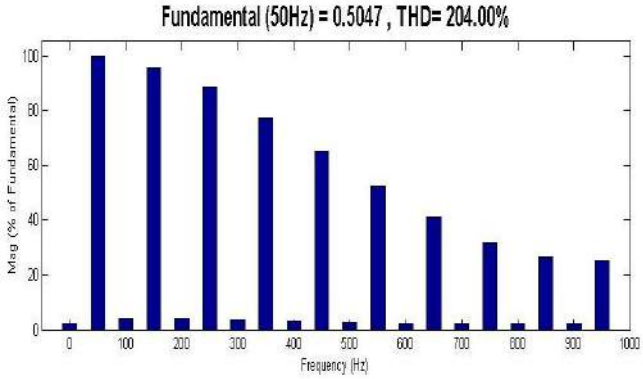

Fig.12. Total Harmonic Distortion of Source Current with Diode Bridge Rectifier based SRM

Fig.12 shows the total harmonic distortion profile of input current, it is high because diode bridge rectifier is used at front end.

Case II: PFC Rectifier based Switched Reluctance Motor at starting condition.

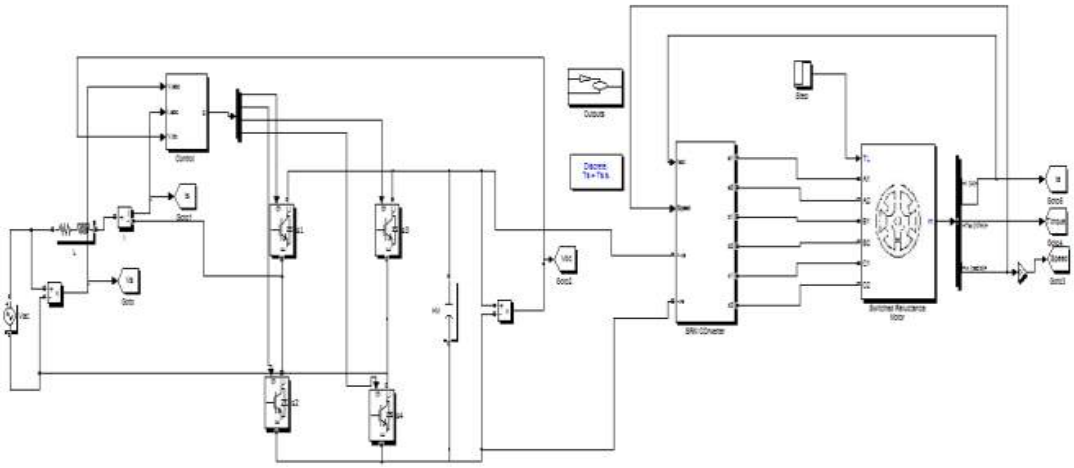

Fig.13. Simulation model of proposed SRM at starting condition with PFC Rectifier

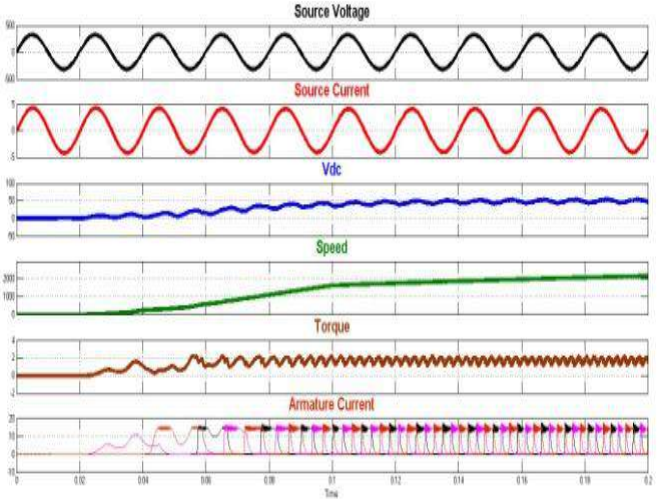

Fig.14. Simulation output waveforms of Source voltage, source current, rectifier output voltage, speed, torque and armature current of SRM

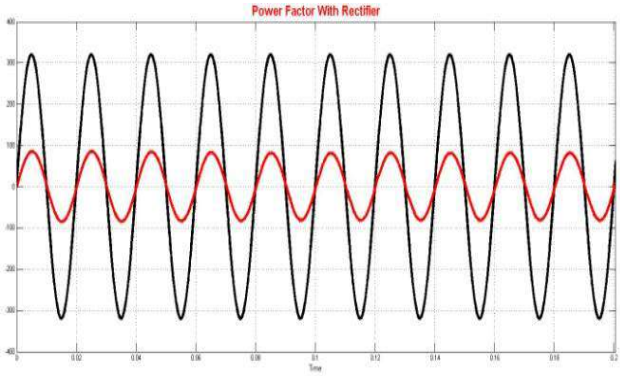

Fig.15. Simulation output wave form of Power factor with PFC Rectifier based SRM

Fig.15 shows the input voltage and current of PFC converter. These are in phase, then power factor is near to unity.

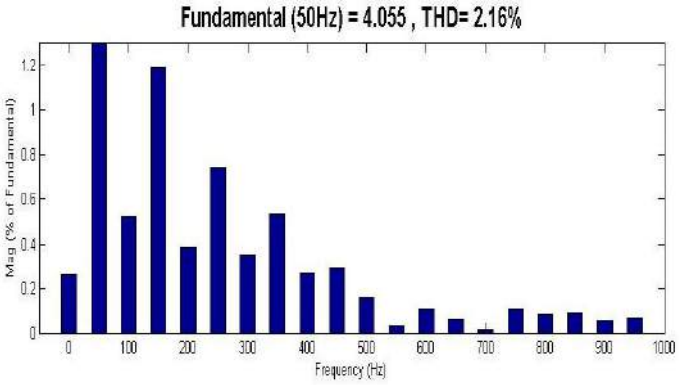

Fig.16. Total Harmonic Distortion of Source Current with PFC Rectifier based SRM

Fig.16 shows the total harmonic distortion profile for input current. It is lower value after using pfc converter at front end.

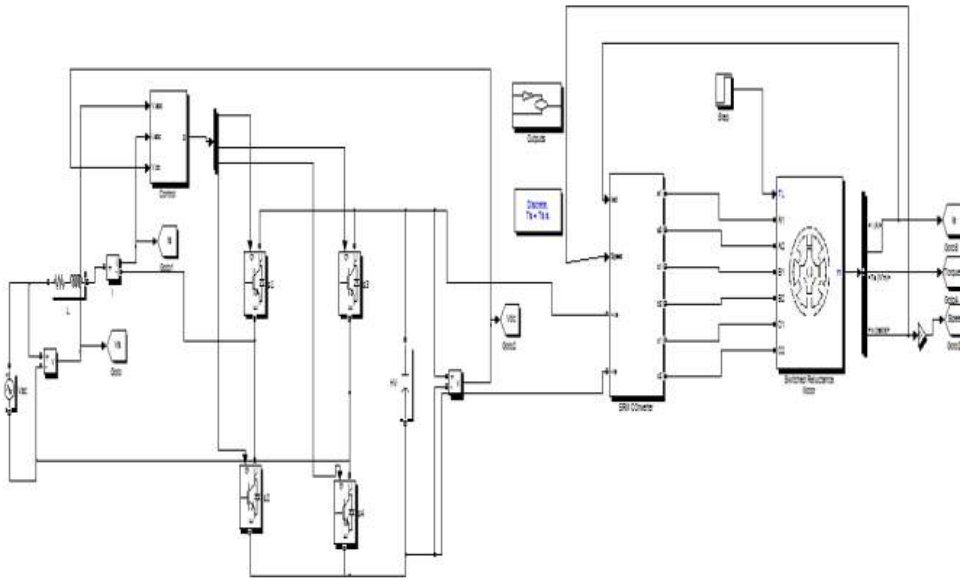

Fig.17. Simulation model of proposed SRM with PFC Rectifier at step variation of Voltage from 100V to 150V

Case III: PFC Rectifier based Switched Reluctance Motor with step variation of Voltage from 100V to 150V.

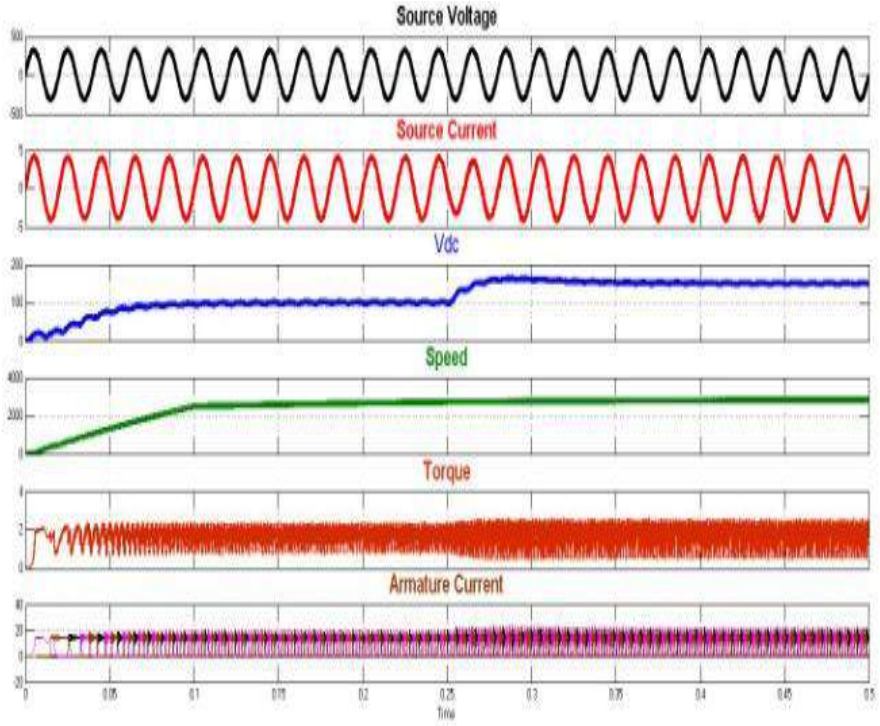

Fig .18. Simulation output waveforms of Source voltage, source current, rectifier output voltage, speed, torque and armature current of SRM at step variation of Voltage from 100V to 150V

From fig.18 we can show that if dc link voltage is varying from 100 to 150V, machine speed is does not change, speed is constant.

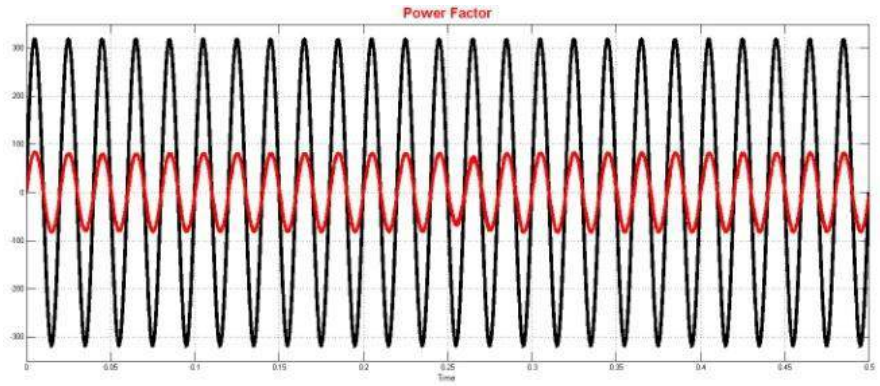

Fig.19. Simulation output wave form of Power factor with PFC Rectifier based SRM at step variation of Voltage from 100V to 150V

From fig.19. We can show that if changing the dc link voltage, but power factor maintained constant, it is near unity.

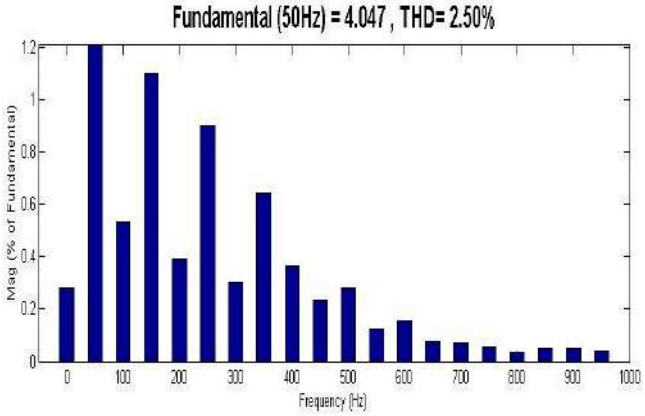

Fig.20.. Total Harmonic Distortion of Source Current with PFC Rectifier based SRM

Case IV: PFC Rectifier based Switched Reluctance Motor with 200 input Voltage.

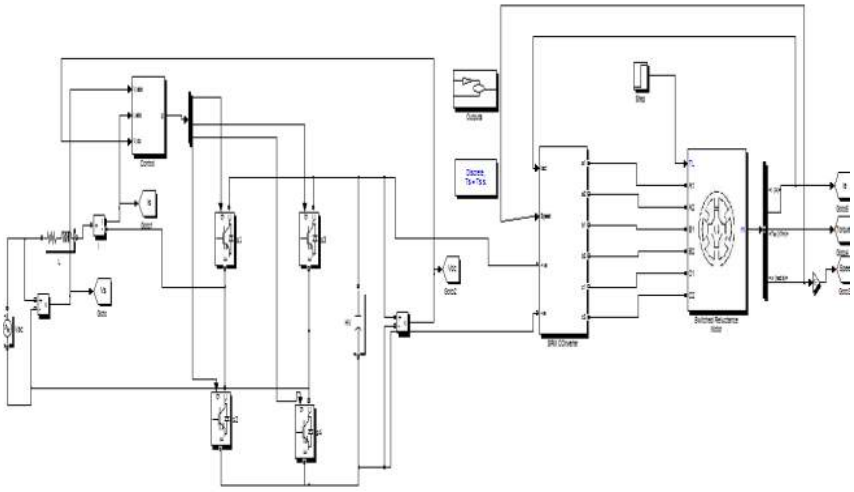

Fig.20. Simulation model of proposed SRM with PFC Rectifier with 200 input Voltage

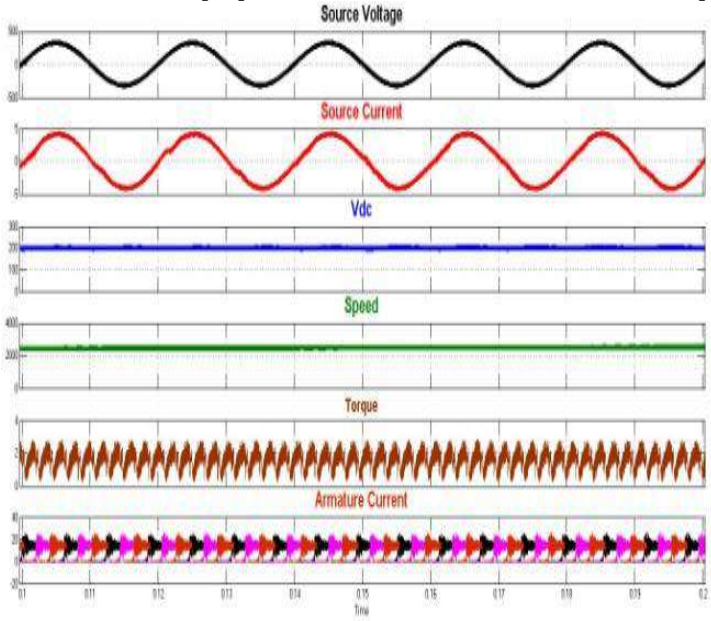

Fig.21. Simulation output waveforms of Source voltage, source current, rectifier output voltage, speed, torque and armature current of SRM with 200 input Voltage

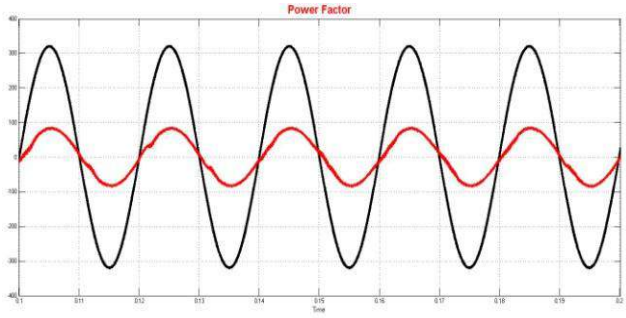

Fig.22. Simulation output wave form of Power factor with PFC Rectifier based SRM with 200 input Voltage

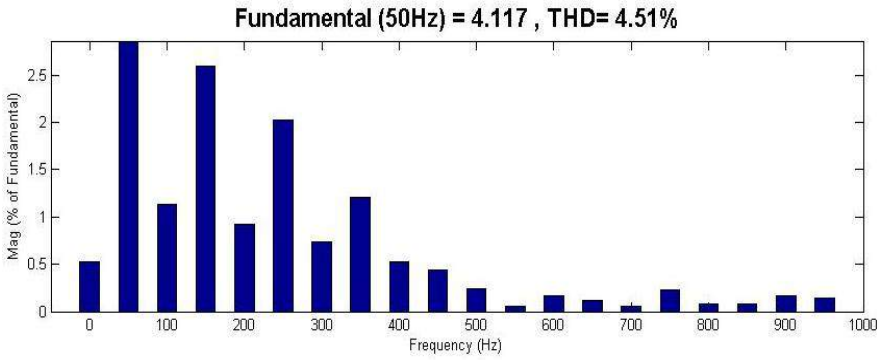

Fig.23. Total Harmonic Distortion of Source Current with PFC Rectifier based SRM

Fig.21 shows that switched reluctance motor characteristics like speed, torque and armature current in steady state. Fig.22 shows that input power factor and fig.23 shows THD profile.

Case V: PFC Rectifier based Switched Reluctance Motor with step variation of Voltage from 320V to 220V.

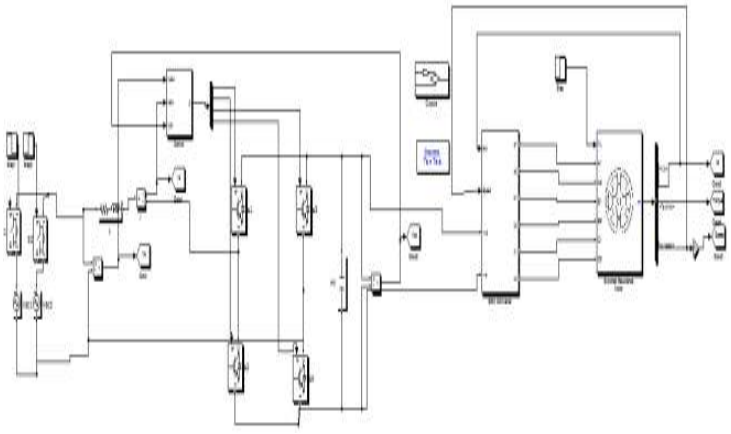

Fig.24. Simulation model of proposed SRM with PFC Rectifier at step variation of Voltage from 320V to 220V

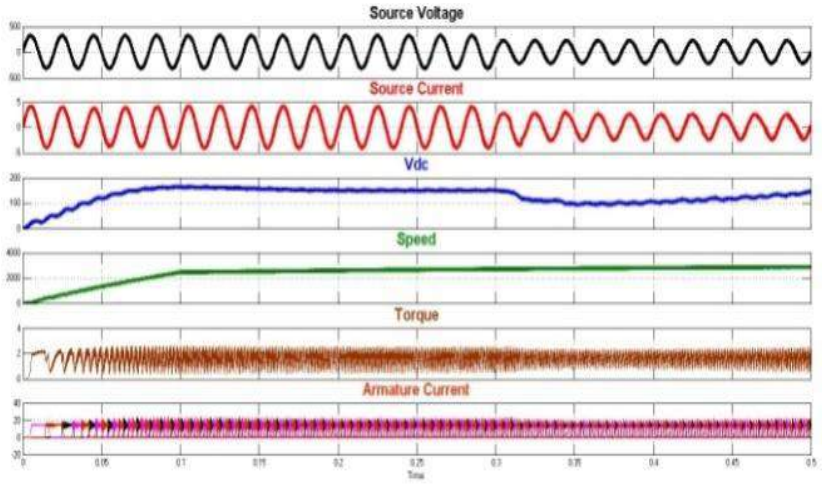

Fig.25. Simulation output waveforms of Source voltage, source current, rectifier output voltage, speed, torque and armature current of SRM at step variation of Voltage from 320V to 220V

Fig.25 Shows that SRM characteristics, after changing the input voltage of PFC rectifier. If voltage is changed then speed does not change.

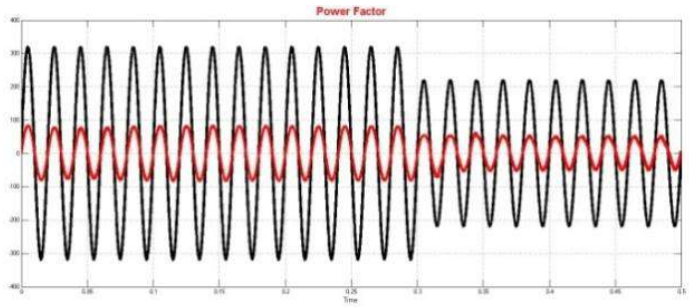

Fig.26. Simulation output wave form of Power factor with PFC Rectifier based SRM at step variation of Voltage from 320V to 220V

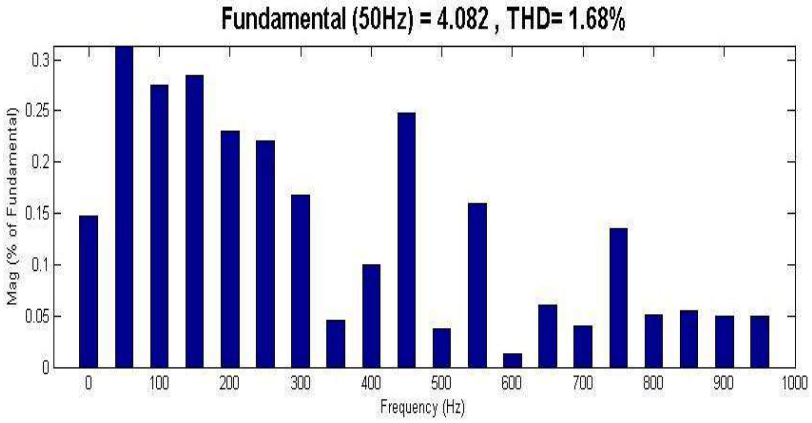

Fig.27. Total Harmonic Distortion of Source Current with PFC Rectifier based SRM.

Fig.26 shows that input power factor and fig.27 shows that THD profile of input current.

8. CONCLUSION

Optimizing the switch angles in switched reluctance motor drives with PWM controller have been planned and successes with simulation implementation. The principle of operation, with parameters and PWM rectifier concerns and simulation results has been conferred. The switch on and switch off angles are used in PWM is optimized so as to get considered a high power factor SRM drives and to take care of the desired speed. To increase the ability issue of SRM drives is consummated by variable the switch on and turns off angles along with adjusting the typical voltage applied to the stator. The switch on and switch off angles is definitely enforced exploitation the PWM controller. The planned strategy is appropriate for both lower ratings and higher ratings of SRM drives. From the simulation analysis it's a good strategy to enhance the power factor for considered SRM drives.

REFERENCES

[1] Rashidi, M. M. Namazi, A. Bayat and S.M. Saghaiannejad "Power Factor Improvement Using Current Source Rectifier with Battery Charging Capability in Regenerative Mode of Switched Reluctance Motor Drives", in proc. 2013 IEEE conference.

[2] R. Krishnan, Switched Reluctance Motor Drives, Boca Raton, FL: CRC Press, 2001.

[3] M. Cacciato, A. Consoli, G. Scarcella and G. Scelba, "A switched reluctance motor drive for home appliances with high power factor capability," in Power Electronics Specialists Conference - PESC 2008, Jun 15-19, 2008, pp. 1235 – 1241.

[4] W. K. Thong and C. Pollock, "Low-Cost Battery-Powered Switched Reluctance Drives with Integral Battery-Charging Capability," IEEE Trans. Industry Applications, Vol. 36, No. 6, pp 1676-1681, Nov./Dec. 2000.

[5] R. Krisinan, G. H. Rim, Modeling, "Simulation An Analysis Of Variable Speed Constant Frequency Power Conversion Scheme with A Permanent Magnet Brushless DC Generator," in Proc. 1988 IEEE Industrial Electronics Society Conf, IECON, pp. 332 – 337.

[6] H.R. Karshenas, J. Mousavi, "A new direct sinusoidal input/output acac converter with unidirectional switches", in Proc. 2008 IEEE Electrical Machines and Systems Conf, pp. 1885–1890.

[7] Power Factor Improvement Using Current Source Rectifier with Battery Charging Capability in Regenerative Mode of Switched Reluctance Motor Drives.

[8] N. Mohan, M. Undeland, and W. P. Robbins, Power Electronics: Converters, Applications and Design. Hoboken, NJ: Wiley, 1995.

[9] J. Tseng and C. L. Chen, "A novel ZVT PWM Cuk power factor corrector," IEEE Trans. Ind. Electron., vol. 46, no. 4, pp. 780–787, Aug. 1999.

[10] Singh and G. D. Chaturvedi, "Analysis, design and development of single switch Cuk ac–dc converter for low power battery charging application," in Proc. IEEE PEDES, 2006, pp. 16.

[11] L. Puttaswamy, B. Singh, and B. P. Singh, "Investigations on dynamic behavior of permanent magnet brushless dc motor drive," Elect. Power Compon. Syst., vol. 23, no. 6, pp. 689–701, Nov. 1995.

REDUCING SOURCE CURRENT HARMONICS DUE TO BALANCED AND UN-BALANCED VOLTAGE VARIATION WITH FUZZY CONTROLLED D-STATCOM

Mr. K. Ravi Sankar[1], Mr. Dr.V. Kamaraju[2] and Mr. Dr. R. Srinivasa Rao[3]

[1]Assoc. Professor, Department of EEE, Coastal Institute of Technology and Management,Vizag, Andhra Pradesh, India.
[2]Professor, Department of EEE, Mahaveer Institute of Science and Technology, Bandlaguda, Hyderabad, Telangana, India
[3]Professor, Department of EEE, University College of Engineering, JNTUK, Kakinada, Andhra Pradesh

ABSTRACT

Electricity demand has been increasing due to the increase of population and industries. Hence it is very important to feed the demand with quality of generation. Improvement of power quality is the greater concern in advanced power system element, it is essential to congregate the need of energy by employ the renewable energy generating sources like pv, fuel cell, biomass, wind, etc and utilizing many more applications like grid interconnected systems, power quality improvement. The situations like harmonic, reactive power exchanging, power factor correction, balanced and un-balanced voltage variations & so on, due to greater effect on highly susceptible loads are to be encouraged in power distribution system. To enhance these circumstances, custom power appliances are used to achieve high grid voltage stability. In this paper, a voltage distortions controlled D-STATCOM based on fuzzy controller is a meticulous power appliance for enhancing harmonic distortions from high power semiconductor switching device, exchanging the both active & reactive power, defend the gird stability by implementing DG technology, to regulate the power quality issues in power distribution network. This paper implements the comparative analysis of PI and Fuzzy controlled DSTATCOM with energy backup scheme, controlled by pwm control technique and founded that fuzzy based IPQ theory for generation of reference current signals improves the power quality than PI based IPQ theory and this analysis is dynamically evaluated with Matlab/Simulink.

KEYWORDS

D-STATCOM, balanced-un-balanced voltage variations, fuzzy controller and Harmonics.

1. INTRODUCTION

Renewable generation from wind and sun has enlarged considerably throughout past few years and forms a significance proportion of the whole generation within the grid. This renewable generation is focused in a very few states, to the extent that it can't be known as marginal generation and high thought must run to balance the variability of such generation. There's a formidable programme for increase of such Renewable Generation and so, it's imperative to figure out how forward for facilitating massive scale integration of such variable Renewable Energy Sources (RES), keeping the protection of the grid. Moreover, as we tend to move towards a tighter frequency band, it becomes even more difficult to balance this variable RES. Generation

from RE Sources depends on nature, i.e. wind rate and sunshine. The variability of RES power will be self-addressed through improved statement techniques that are still evolving. Once the proportion of RES becomes important, special attention must be paid to accurately forecast their output. The changes in RES might affect the electrical network. There has been excessive traction of non-sinusoidal current and voltage in electrical network, due to excessive usage of non-linear masses. Power quality could also be marked in synchronous and non- synchronized phenomena and this will result into visiting synchrononised with ac wave at power frequency.

A group of controllers along known as Custom Power Devices (CPD), that embody the DSTATCOM (distribution static compensator), The DSTATCOM, a shunt connected device will take care of the quality issues in the current it contains a de electrical condenser. Three phase electrical converter module ac filter ,coupling electrical device and an impression strategy the electronic block of D-STATCOM is the voltage sourced electrical converter, which converters an input dc voltage into three phase output voltage in harmonic. The D-STATCOM puts electrical convert, convert the dc-link voltage Vdc on electrical condenser. It can be presumed D-STATCOM may be treated as voltage control supply.

The proposed fuzzy based instant power theory is valid for pure sin or non-sinusoidal and balanced or unbalanced power systems and were later planned [4-8].The part of the output voltage of the thyristor-based electrical converter, Vi, is controlled within the same approach because the distribution system voltage, Vs. The proposed DSTATCOM relies on the fuzzy based instant power theory; it provides smart compensation characteristics in steady state furthermore as transient states compared to Proportional Integral (PI) based IPT Controller [9]. The FUZZY based instant power theory generates the reference currents needed to compensate the distorted line current harmonics and reactive power accurately when compared to the PI controller since it reduces both error and change in error and also large variation in errors. Hence the proposed concept has been analyzed with FUZZY controlled IPT and compared its advantages with the PI controlled IPT.

2. PRINCIPAL OF THE D-STATCOM

The D-STATCOM is that the solid-state-based power device version of the SVC. The construct of the D-STATCOM was planned by Gyugyi in 1976. In operation as a shunt-connected SVC, its electrical phenomenon or inductive output currents is controlled severally from its connected AC bus voltage. Attributable to the fast-switching characteristic of power converters, the D-STATCOM provides a lot of quicker response as compared to the SVC.

The shunt compensator will live the PCC voltages and within reference current generations algorithms with none drawback as these voltages area unit pure sinusoids. This may not be attainable in actual systems where the masses area with at top of the feeder.

The PCC voltage is distorted by the switch frequency harmonics generated by D-STATCOM. There will be switch and resistive loss within the D-STACOM circuit. These losses should be proved by the system. We have a tendency to should so fitly modify the reference current generation rule to accommodate of these factors. Finally, to supply a path for the harmonic current generated by the CMLI primarily based VSI realizing the D-STATCOM to flow; we have a tendency to should place further filters within the circuit.

In addition, within the event of a fast amendment in system voltage, the electrical condenser voltage doesn't amendment instantaneously; thus, the D-STATCOM effectively reacts for the specified responses. As an example, if the system voltage drops for any reason, there's an inclination for the D-STATCOM to inject electrical phenomenon power to support the unfit

voltages. On paper, the ability device used within the D-STATCOM is either a VSC or a current-source device (CSC). In observe, however, the VSC is most popular owing to the bidirectional voltage-blocking capability needed by the ability semiconductor devices utilized in CSCs. to realize this type switch characteristic, an extra diode should be connected nonparallel with a standard semiconductor switch, instead the organic structure of the semiconductor should be changed. Each of those alternatives increase the physical phenomenon losses and total system value. In general, a CSC derives its terminal power from a current supply, i.e., a reactor. As compared, a charged reactor is way lousier than a charged electrical condenser. Moreover, the VSC needs a current-source filter at its AC terminals that is of course provided by the coupling electrical device outpouring inductance, whereas extra electrical condenser banks square measure required at the AC terminals of the CSC. Finally, the VSCs will operate with higher potency than the CSCs waste high-energy applications.

A suitable VSC is chosen supported the subsequent considerations: the voltage rating of the facility network, this harmonic demand, the system complexness, etc. Basically, the D-STATCOM system is comprised of 3 main parts: a VSC, a group of coupling reactors or a transformer, and a controller. The inductances of the increased power transformers will act as coupling reactors, while at a very high voltage system. The very purpose of the coupling inductors is to strain these elements, that square measure generated primarily by the output voltage facility. The voltage quality downside may be a concern, wherever the D-STASTCOM is connected to the facility at PCC. Voltages, currents and square measure fed into controller to compare with commands.

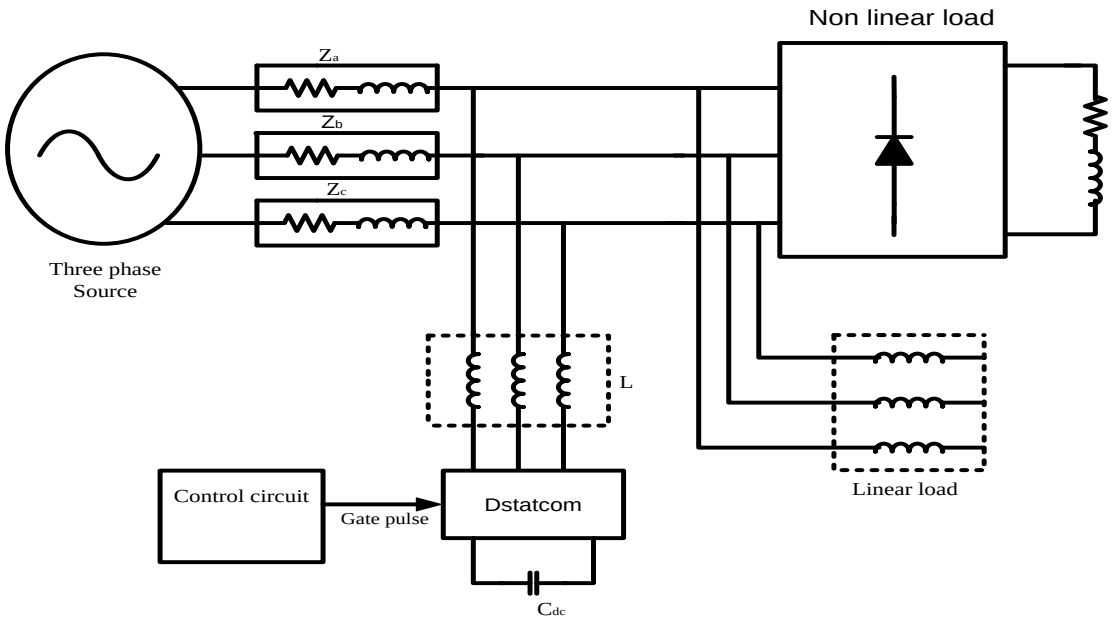

Fig.1.Basic Block Diagram of IPT Controlled DSTATCOM with Reactive and Harmonic Loads

The control performs as feedback control and brings a collection of changes consequently. The diagram illustration of the D-STATCOM system with non-linear load is illustrated in Fig.1. The VSC is described as a perfect supply related to internal loss that connected to the ac power via coupling reactors. The exchange of the real power and reactive power between d-statcom and additional able area unit typically controlled by the amplitude sections of the output voltage. Within the case of a perfect lossless power convertor, the output voltage of the convertor is controlled to be in section thereupon of the ability system. During this case, there's no real power circulated within the D-STATCOM; so, a true power supply isn't required. To work the D-STATCOM in electrical phenomenon mode or volt-ampere generation, +Q, the magnitude of the

convertor output voltage is controlled to be larger than the voltage at the PCC. In distinction, the magnitude of the output voltage of the convertor is controlled to be but that of the ability system at the PCC on order to soak up reactive power or to work the D-STATCOM in inductive mode, -Q. However, in observe, the convertor is related to internal losses caused by non-ideal power semiconductor devices and passive elements. As a result, with none correct controls, the condenser voltage are going to be discharged to compensate these losses, and can constantly decrease in magnitude. To regulate the condenser voltage, very low phase shift δ is introduced between the device voltage and therefore the installation voltage.

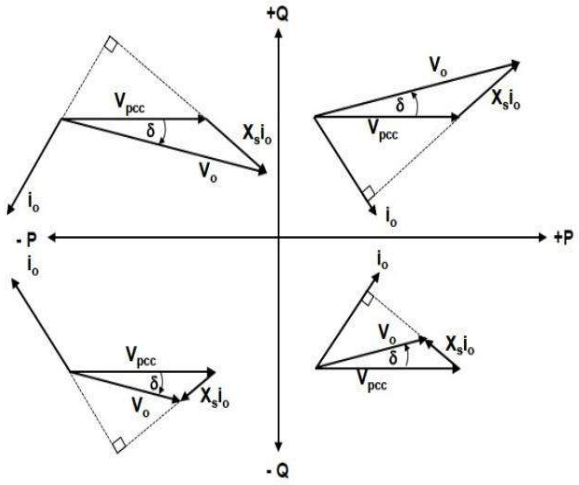

Fig .2. Phasor Diagram for Power Exchanges in Four Quadrants of DSTATCOM

A small lag of the device voltage with relevance the voltage at the PCC causes real power to ensue the ability system to the D-STATCOM, whereas the active power is transferred from the D-STATCOM to the ability system by dominant the device voltage in order that it leads the voltage at the PCC. Fig .2. illustrates phasor diagrams of the voltage at the PCC, device output current and voltage all told four quadrants of the PQ plane.

3. CONTROL STRATEGY

From the very beginning of the electrical distribution system, voltage regulation, reactive power burden and unbalanced loading of the phases are major problems faced by the power engineers. With the advent of custom power devices and FACTS technology, the concept of DSTATCOM has appeared which has served the purpose of dynamic reactive power compensation. With a few modifications, DSATACOM can also be used for neutral current compensation, load balancing and voltage regulation.

For reactive power compensation, DSTATCOM provides reactive power as required by the load and thus the supply current remains at unity power issue (UPF). Since solely real power is being provided by the supply, load equalization is achieved by creating the supply reference current balanced.

Control strategy plays an important role in overall performance of the compensating device. The management of a compensating device is completed in 3 stages. Within the 1st stage, the essential voltage and current signals area unit detected power transformers (PT's), CT's, Hall-effect sensors, and isolation amplifiers to assemble correct system info. Within the second stage, compensating commands in terms of current or voltage levels area unit derived supported completely different management ways and device configurations. Within the third stage of management, the gating signals for the solid-state devices of the compensating devices area unit

generated either in open loop or closed-loop system. Among the foremost in style schemes area unit PWM, whereas for closed-loop system, unipolar pulse breadth modulation management technique is that the most typical kind of pursuit management for CMLI based mostly shunt compensators.

There are unit several management approaches offered for the generation of reference supply currents for the management of VSC of DSTATCOM for three-phase, three-wire system within the literature viz.

1. Instantaneous Power Theory (IP Theory),
2. Synchronous Reference Frame (SRF) Theory,
3. Id-Iq Theory,
4. Modified Id-Iq Theory.
5.

Among the different control techniques applied to three-phase three-wire compensators, the SRF based technique is found to be suitable for different topologies of DSTATCOM. The IRP theory is simple and proven to be one of the best performances under various operating conditions and hence this theory is used for the control of proposed H-bridge DSTATCOM.

3.1. Proposed Instantaneous Power Theory (IPT)

IP theory was primarily planned by Akagi. This theory relies on the transformation of 3 section quantities to 2 section quantities in α-β frame and also the calculation of instant active and reactive power during this frame. A basic diagram of this theory is shown in fig.3. detected inputs $Vsa, Vsb, Vsc \text{ and } iLa, iLb, iLc$ are fed to the controller, and these quantities ar processed to come up with reference current commands $(i_{Sa}^{*}, i_{Sb}^{*}, i_{Sc}^{*})$, that are fed to a pulse dimension modulation (PWM) signal generator to come up with final shift signals fed to the D-STATCOM; Hence this block control the D-Statcom.

The source voltages can be given as:

$$\begin{aligned} va &= Vm \sin(\omega t) \\ vb &= Vm \sin(\omega t - 2\pi/3) \\ vc &= Vm \sin(\omega t - 4\pi/3) \end{aligned} \quad (1)$$

Load currents of the system given as:

$$\begin{aligned} i_{La} &= \sum I_{Lan} sin\{n(\omega t) - \theta_{an}\} \\ i_{Lb} &= \sum I_{Lbn} sin\{n(\omega t - 2\pi/3) - \theta_{bn}\} \\ i_{Lc} &= \sum I_{Lcn} sin\{n(\omega t - 2\pi/3) - \theta_{cn}\} \end{aligned} \quad (2)$$

In 3 phase coordinates, a, b, and c axes are fixed on the same plane, with the phase difference by 2π/3. The instantaneous space vectors *va* and *iLa* are set on the "*a*" axis, and their amplitude varies in positive and negative directions with time. This is true for the other two phases also. By using Park's transformation can be transformed to these phases.

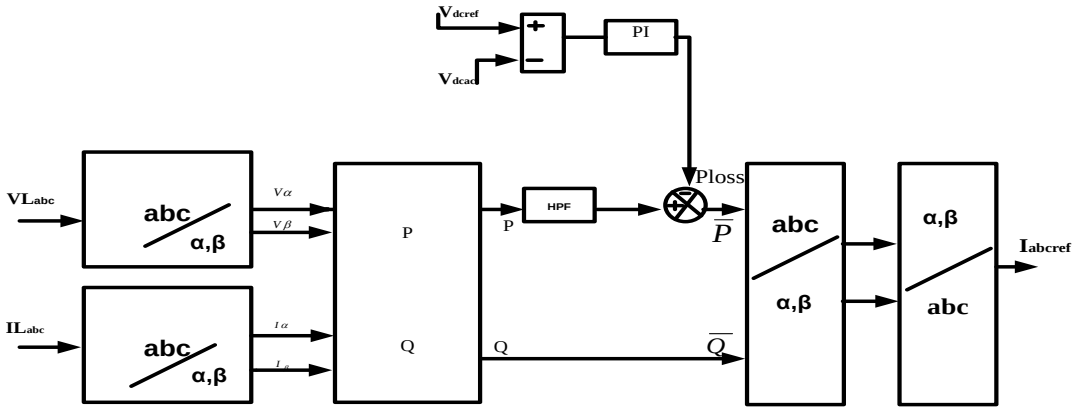

Fig .3. Block Diagram of Proposed Control Strategy- Instantaneous Power Theory

$$\begin{bmatrix} v_\alpha \\ v_\beta \end{bmatrix} = \sqrt{\frac{2}{3}} \begin{bmatrix} 1 & -1/2 & -1/2 \\ 0 & \sqrt{3}/2 & -\sqrt{3}/2 \end{bmatrix} \begin{bmatrix} v_a \\ v_b \\ v_c \end{bmatrix} \quad (3)$$

$$\begin{bmatrix} i_\alpha \\ i_\beta \end{bmatrix} = \sqrt{\frac{2}{3}} \begin{bmatrix} 1 & -1/2 & -1/2 \\ 0 & \sqrt{3}/2 & -\sqrt{3}/2 \end{bmatrix} \begin{bmatrix} i_a \\ i_b \\ i_c \end{bmatrix} \quad (4)$$

Where α and β axes are the orthogonal coordinates. Conventional instantaneous power for three-phase circuit can be defined as

$$p = v_\alpha i_\alpha + v_\beta v_\beta \quad (5)$$

Where p is equal to conventional equation

$$p = v_a i_a + v_b i_b + v_c i_c \quad (6)$$

Hence the IRP can be given as

$$q = -v_\beta i_\alpha + v_\alpha i_\beta \quad (7)$$

Therefore, in matrix form, instantaneous real and reactive power are given as

$$\begin{bmatrix} p \\ q \end{bmatrix} = \begin{bmatrix} v_\alpha & v_\beta \\ -v_\beta & v_\alpha \end{bmatrix} \begin{bmatrix} i_\alpha \\ i_\beta \end{bmatrix} \quad (8)$$

The α-β currents can be obtained as

$$\begin{bmatrix} i_\alpha \\ i_\beta \end{bmatrix} = \frac{1}{\Delta} \begin{bmatrix} v_\alpha & v_\beta \\ -v_\beta & v_\alpha \end{bmatrix} \begin{bmatrix} p \\ q \end{bmatrix} \quad (9)$$

Where

$$\Delta = v_\alpha^2 + v_\beta^2 \quad (10)$$

Instantaneous active and reactive powers p and q can be decomposed into an average (dc) and an oscillatory component.

$$p = \bar{p} + \tilde{p}$$
$$q = \bar{q} + \tilde{q} \quad (11)$$

Where $\bar{p}$ and $\bar{q}$ are the average (dc) part and $\tilde{p}$ and $\tilde{q}$ are the oscillatory (ac) part of these real and reactive instantaneous powers. Reference source currents are calculated to compensate the

reactive power and the oscillatory component of the instantaneous active power. Therefore, the reference source currents $i_{s\alpha}^{*}$ and $i_{s\beta}^{*}$ in α-β coordinate are expressed as

$$\begin{bmatrix} i_{s\alpha}^{*} \\ i_{s\beta}^{*} \end{bmatrix} = \frac{1}{\Delta} \begin{bmatrix} v_{\alpha} & -v_{\beta} \\ v_{\beta} & v_{\alpha} \end{bmatrix} \begin{bmatrix} \bar{p} \\ 0 \end{bmatrix} \qquad (12)$$

Theses currents can be transformed in a-b-c quantities to find the reference currents in a-b-c coordinates using inverse transformation.

$$\begin{bmatrix} i_{sa}^{*} \\ i_{sb}^{*} \\ i_{sc}^{*} \end{bmatrix} = \sqrt{\frac{2}{3}} \begin{bmatrix} 1/\sqrt{2} & 1 & 0 \\ 1/\sqrt{2} & -1/2 & \sqrt{3}/2 \\ 1/\sqrt{2} & -1/2 & -\sqrt{3}/2 \end{bmatrix} \begin{bmatrix} i_{0}^{*} \\ i_{s\alpha}^{*} \\ i_{s\beta}^{*} \end{bmatrix} \qquad (13)$$

Where i_{0}^{*} is the zero sequence components, which is zero in three- phase three wire system.
The generated reference currents are compared with actual currents by using Hysteresis current controller for generation of pulses.

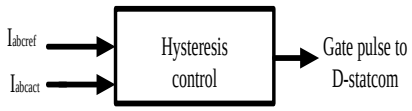

Fig .4. Generation of Gating pulses

4. FLC CONTROLLER

The identified power quality and harmonics problems can be effectively reduced by controlling D-STATCOM. Fuzzy logic is wide employed in controlling technique. The word "fuzzy" maintain fact that the logic concerned will wear down ideas that can't be expressed as "true" or "false" however rather as "partially true". Though various approaches like genetic algorithms and ANN will perform even as well as formal logic in several cases, formal logic has the advantage that the answer to the matter is forged in terms that human operators will perceive, so their expertise is employed in the look of the managementler of prognosticative current control. The linguistic variables area unit outlined as (NB, NM, NS, Z, PS, PM, PB) that means negative big, negative medium, negative small, zero, positive small, positive medium and positive big. The membership functions area unit shown in Fig.5.

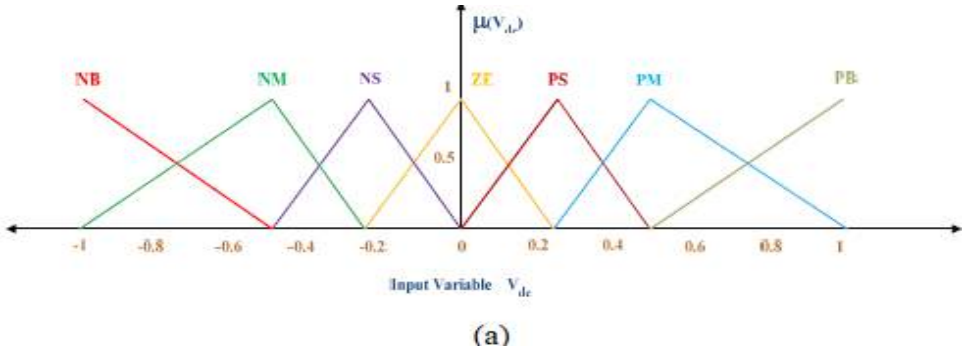

(a)

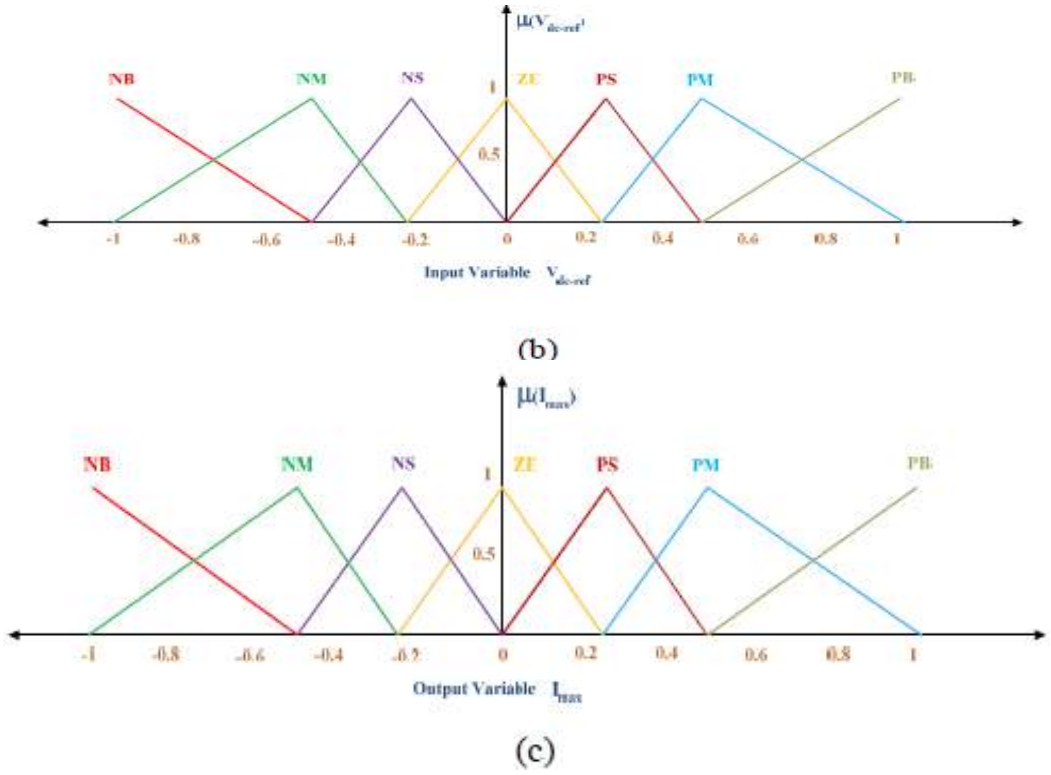

Fig.5. (a) Input ANF normalized membership function; (b) Input Vdc-ref Normalized Membership Function; (c) Output Imax Normalized Membership Function.

Table 1. The Membership functions for FLC

E / CE	NB	NM	NS	Z	PS	PM	PB
PB	Z	PS	PM	PB	PB	PB	PB
PM	NS	Z	PS	PM	PB	PB	PB
PS	NM	NS	Z	PS	PM	PB	PB
Z	NB	NM	NS	Z	PS	PM	PB
NS	NB	NB	NM	NS	Z	PS	PM
NM	NB	NB	NM	NM	NS	Z	PS
NB	NB	NB	NB	NB	NM	NS	Z

From the table I, each error and its change in error is divided into 7 X 7 membership functions as:

Negative Big (*NB*), Negative Medium (*NM*), Negative Small (*NS*), Zero (*Z*), Positive Small (*PS*), Positive Medium (*PM*) and Positive Big (*PB*).

5. MATLAB/SIMULINK ANALYSIS

Here simulation is carried out in different cases.

1). Performance of D-Statcom at Balanced Sinusoidal Source Voltage.
2). Performance of D-Statcom at Balanced Non-Sinusoidal Source Voltage.
3). Performance of D-Statcom at Un-Balanced Sinusoidal Source Voltage.

4). Performance of PI Controlled D-Statcom at Un-Balanced Non-Sinusoidal Source Voltage.
5). Performance of FUZZY Controlled D-Statcom at Un-Balanced Non-Sinusoidal Source Voltage.

Case I: Performance of D-Statcom at Balanced Sinusoidal Source Voltage.

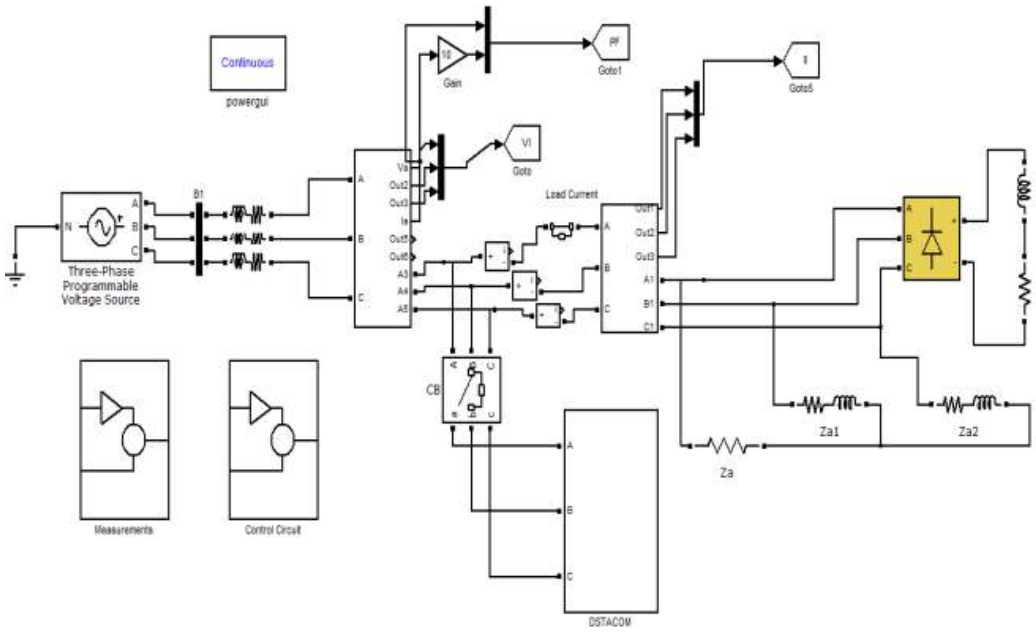

Fig.6. Simulink model of D-Statcom at Balanced Sinusoidal Source Voltage

Fig.6. Shows The Matlab/Simulink Model Of Power System Network With D-Statcom At Balanced Sinusoidal Source Voltage.

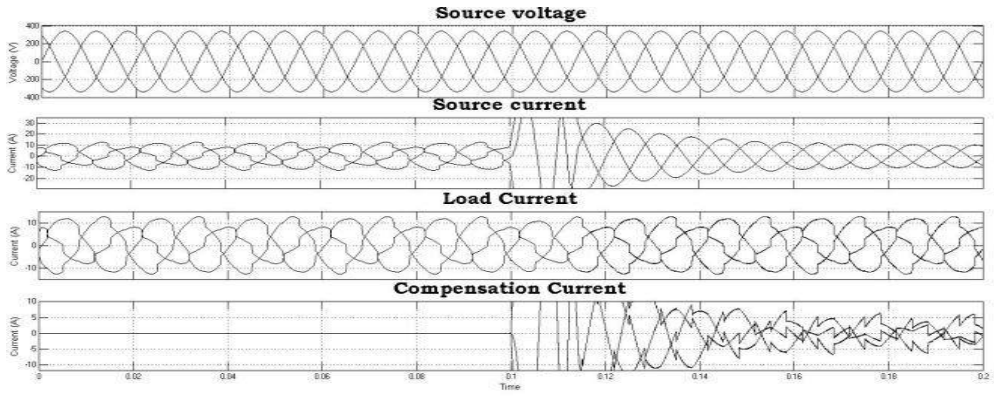

Fig.7. Simulated output wave forms of Source voltage, Source, Load and Compensation Current.

Fig.7. Shows The Simulated Output Wave Forms Of The Source Voltage And Source Current, Load Current And Compensation Current At Balanced Sinusoidal Source Voltage.

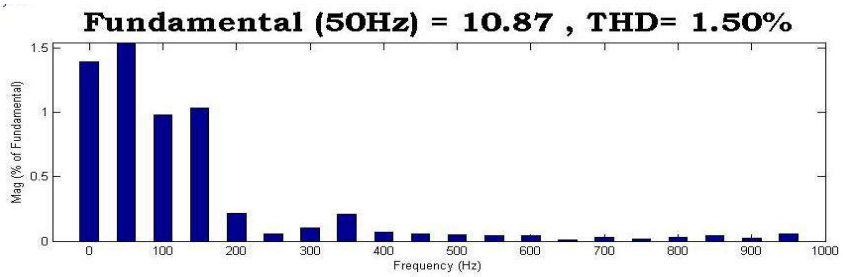

Fig.8. THD of Source Current.

Fig.8.Shows the Total Harmonic Distortion of Source Current at Balanced Sinusoidal Source Voltage.

Case II: Performance of D-Statcom at Balanced Non-Sinusoidal Source Voltage.

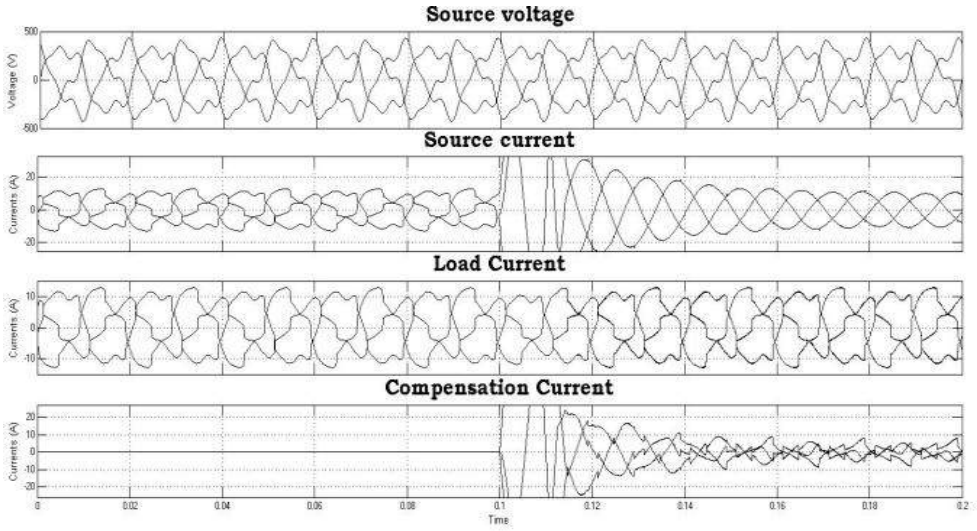

Fig.9. Simulated output wave forms of Source voltage, Source current, Load current and Compensation Current

Fig.9. shows the simulated output wave forms of source voltage and current load current and compensation current at balanced non-sinusoidal source voltage.

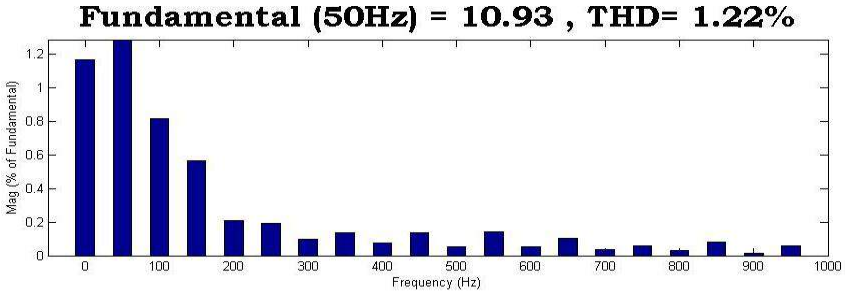

Fig.10. THD of Source Current

Fig.10. shows the total harmonic distortion of source current at balanced non- sinusoidal source voltage.

Case III: Performance of D-Statcom at Un-Balanced Sinusoidal Source Voltage.

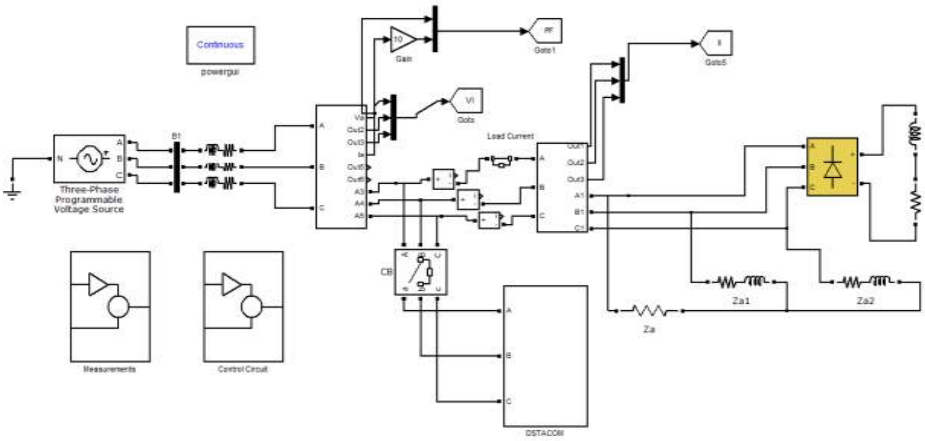

Fig.11. Simulink model of D-Statcom at Un-Balanced Sinusoidal Source Voltage

Fig.11. shows the Matlab/Simulink model of power system network with D-STATCOM at un-balanced sinusoidal source voltage.

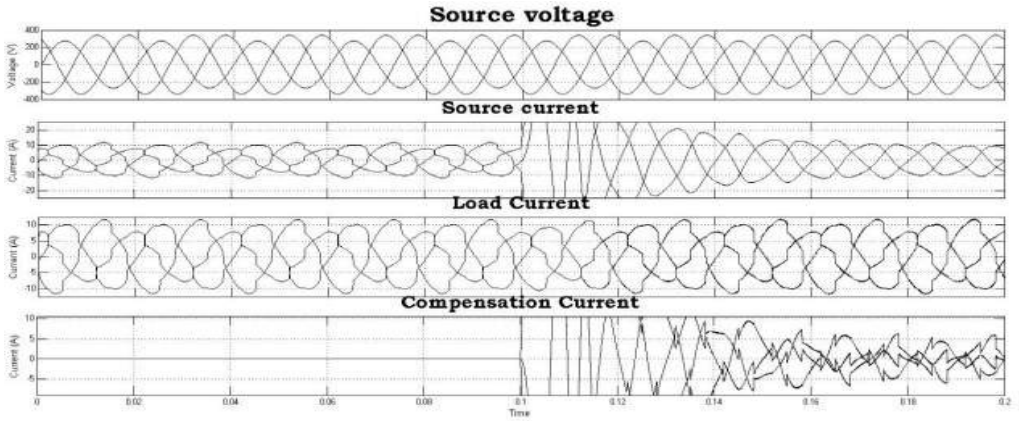

Fig.12. Simulated output wave forms of Source voltage, Source current, Load current and Compensation Current

Fig.12. shows the output wave forms of source voltage and current, load current and compensation current at un-balanced sinusoidal source voltage.

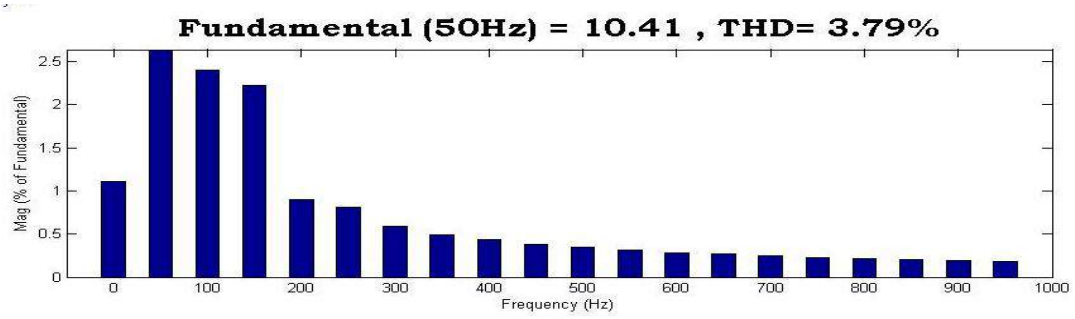

Fig.13.THD of Source Current

Fig.13. shows the total harmonic distortion of source current at un-balanced sinusoidal source voltage shows 3.79%.

Case IV: Performance of PI Controlled D-Statcom at Un-Balanced Non-Sinusoidal Source Voltage.

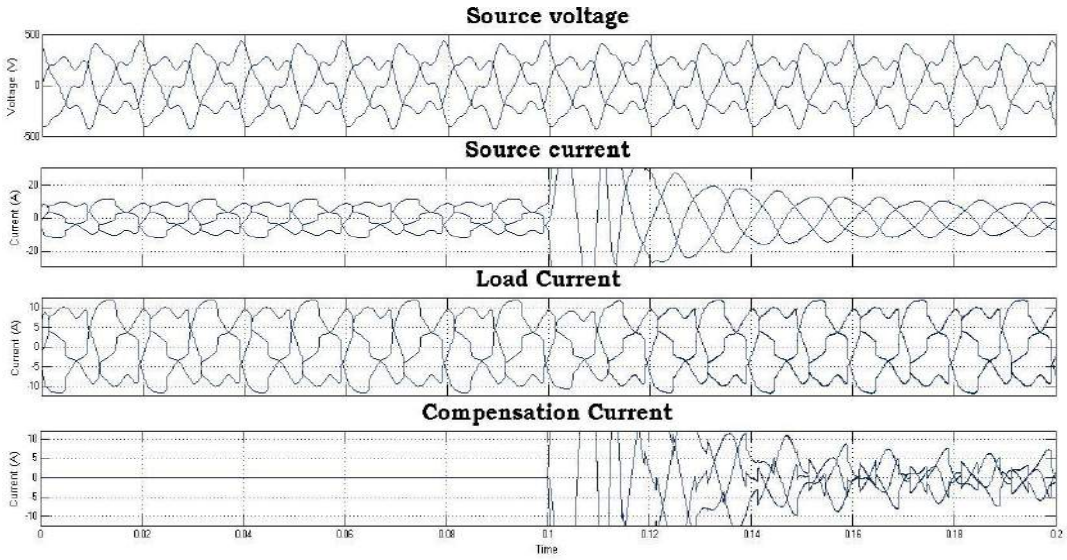

Fig.14. Simulated output wave forms of Source voltage, Source current, Load current and Compensation Current

Fig.14. shows the output wave form of source voltage and current, load current and compensation current at un-balanced non-sinusoidal source voltage with PI Controller.

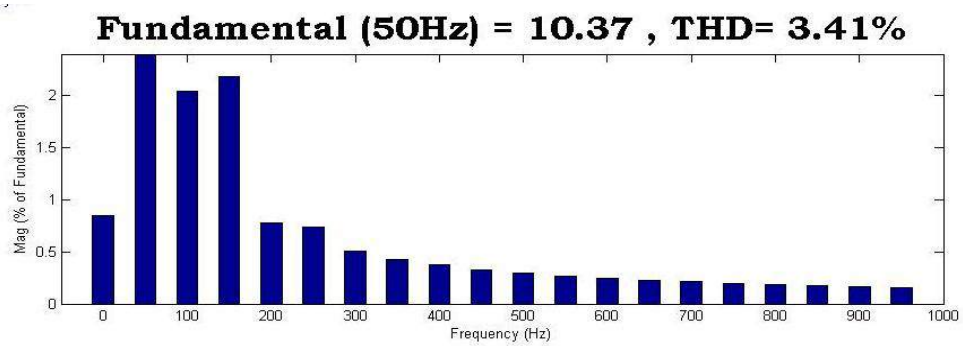

Fig.15. THD of Source Current

Fig.15.shows the total harmonic distortions of source current at un-balanced non-sinusoidal source voltage with PI Controller

Case V: Performance of FUZZY controlled D-Statcom at Un-Balanced Non-Sinusoidal Source Voltage.

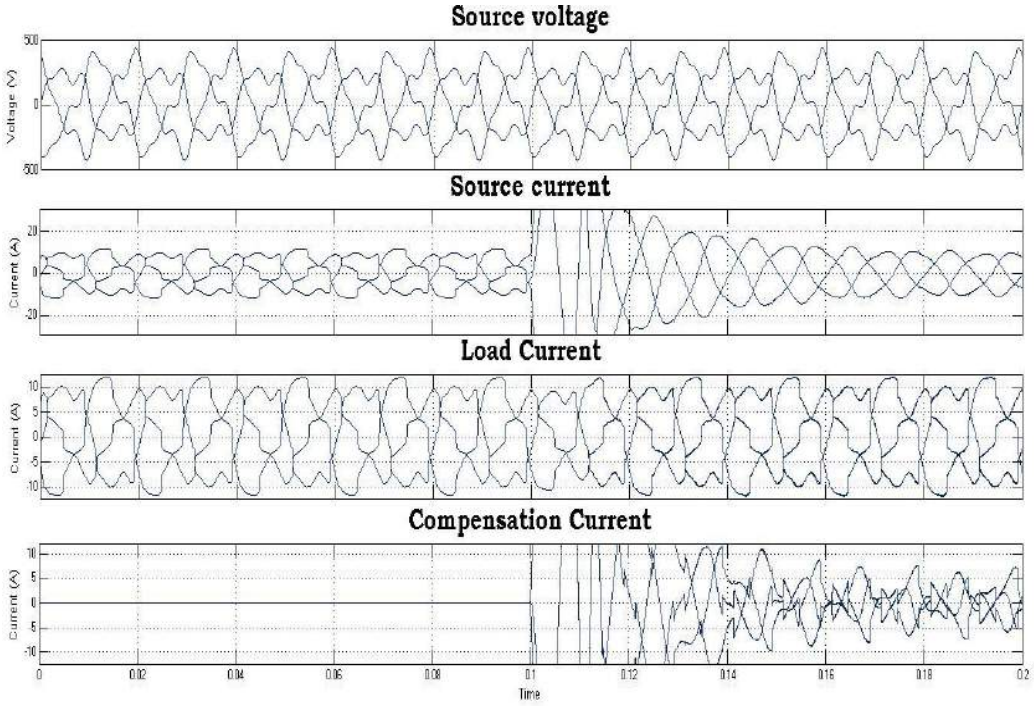

Fig.16. Simulated output wave forms of Source voltage, Source current, Load current and Compensation

Fig.16. shows the output wave form of source voltage and current, load current and compensation current at un-balanced non-sinusoidal source voltage under FUZZY controlled D-Statcom.

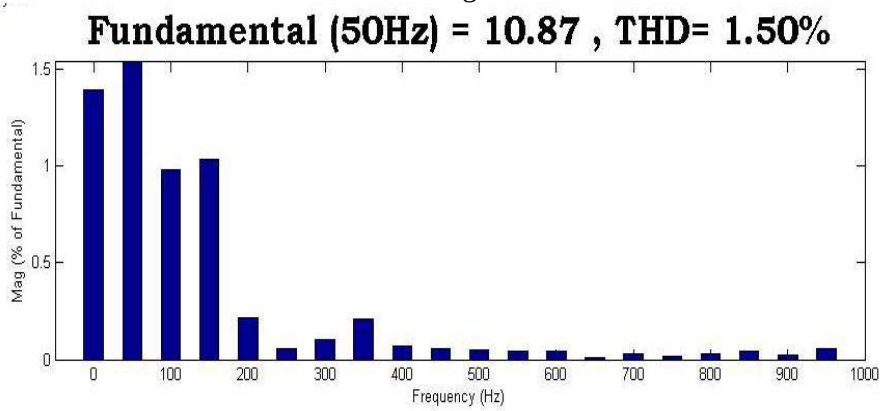

Fig.17. THD of Source Current

Fig.17.Shows the Total Harmonic Distortion of Source Current at Un-Balanced Non-Sinusoidal Source Voltage with Fuzzy Controlled D-Statcom.

6. CONCLUSION

In this paper, the renewable sources interconnection with the main supply can influence the power quality at the point of common coupling and can pollute the electrical network with Balanced Sinusoidal and Un-Balanced Non-Sinusoidal voltage distortions and harmonic components which

exceed the stipulated limits. The proposed fuzzy based D-Statcom is employed to compensate the harmonics and reactive current caused due to the Balanced Sinusoidal and Un-Balanced Non-Sinusoidal voltage distortions and non-linear load in distribution system. From the simulation analysis the source current harmonics has been reduced to 1.5% with FUZZY based IPT controlled DSTATCOM but the PI based IPT controlled DSTATCOM only reduces up to 3.41%. Hence it has been proven that fuzzy based IPT controller is suitable for enhancing the power quality at Balanced and Un-Balanced Voltage Variations.

REFERENCES

[1] A.E. Hammad, Comparing the Voltage source capability of Present and future Var Compensation Techniques in Transmission System, IEEE Trans, on Power Delivery. Volume 1. No.1 Jan 1995.

[2] G.Yalienkaya, M.H.J Bollen, P.A. Crossley, "Characterization of Voltage Sags in Industrial Distribution System", IEEE transactions on industry applications, volume 34, No. 4, July/August, PP.682-688, 1999.

[3] Haque, M.H., "Compensation of Distribution Systems Voltage sags by DVR and D-STATCOM", Power Tech Proceedings, 2001 IEEE Porto, Volume 1, PP.10-13, September 2001.

[4] Anaya-Lara O, Acha E., "Modeling and Analysis Of Custom Power Systems by PSCAD/EMTDC", IEEE Transactions on Power Delivery, Volume 17, Issue: 2002, Pages: 266-272.

[5] Bollen, M.H.J.,"Voltage sags in Three Phase Systems", Power Engineering Review, IEEE, Volume 21, Issue: 9, September 2001, PP: 11-15.

[6] M.Madrigal, E.Acha. "Modeling of Custom Power Equipment Using Harmonics Domain Techniques", IEEE 2000.

[7] R.Meinski, R.Pawelek and I.Wasiak, "Shunt Compensation For Power Quality Improvement Using a D-STATCOM controller Modelling and Simulation", IEEE Proce, Volume 151, No. 2, March 2004.

[8] J.Nastran , R. Cajhen, M. Seliger, and P.Jereb,"Active Power Filters for Nonlinear AC loads, IEEE Trans.on Power Electronics Volume 9, No.1, PP: 92-96, Jan 2004.

[9] L.A.Moran, J.W. Dixon, and R.Wallace, A Three Phase Active Power Filter with fixed Switching Frequency For Reactive Power and Current Harmonics Compensation, IEEE Trans. On Industrial Electronics. Volume 42, PP:402-8, August 1995.

DG FED MULTILEVEL INVERTER BASED D-STATCOM FOR VARIOUS LOADING CONDITIONS

Naarisetti Srinivasa Rao[1] and R. Kalyani[2]

[1]Associate Professor, Department of Electrical & Computer Engineering
College of Engineering and Technology, Dilla University, Dilla, Ethiopia
[2]Assistant Professor, Department of Electrical & Electronics Engineering, Mahaveer Institute of Engineering and Technology, Bandlaguda, Telangana, India.

ABSTRACT

During the past few decades, power industries have proved that the adverse impacts on the PQ can be mitigated or avoided by conventional means, and that technique using fast controlled force commutated power electronics (PE) are even more effective. PQ compensators can be categorized into two main types. One is shunt connected compensation device that effectively eliminates harmonics. The other is the series connected device, which has an edge over the shunt type for correcting the distorted system side voltages and voltage sags caused by power transmission system faults. The STATCOM used in distribution systems is called DSTACOM (Distribution-STACOM) and its configuration is the same, but with small modifications. Recent advances in the power-handling capabilities of static switch devices such as 3.3kV, 4.5kV, and 6.5kV Insulated Gate Bipolar Transistors (IGBTs) with voltage rating commercially available, have made the use of the voltage source inverters (VSI) feasible for high-power applications. High power and high-voltage conversion systems have become very important issues for the power electronic industry handling the large ac drive and electrical power applications at both the transmission and distribution levels. For these reasons, new families of multilevel inverters have emerged as the solution for working with higher voltage levels. Multilevel inverters (MLI) include an array of power semiconductors and capacitor voltage sources, the output of which generate voltages with stepped waveforms. These converter topologies can generate high-quality voltage waveforms with power semiconductor switches operating at a frequency near the fundamental. It significantly reduces the harmonics problem with reduced voltage stress across the switch. This research work is mainly focusing on application of multilevel DSTATCOM for power quality improvement in distribution system with integration of RES. Matlab/Simulink based model is developed and simulation results are presented.

KEYWORDS

DSTATCOM, Cascaded H- Bridge Multilevel Inverter, Pulse Width Modulation, renewable energy sources

1. INTRODUCTION

"A power electronic based system and other static equipment that provide control of one or more AC transmission system parameters to enhance controllability and increase power transfer capability [3]." Among FACTS controllers, the shunt controllers have shown feasibility in term of cost effectiveness in a wide range of problem-solving from transmission to distribution levels [1, 2]. For decades, it has been recognized that the transmittable power through transmission/distribution lines could be increased, and the voltage profile along the transmission/distribution line could be controlled by an appropriate amount of compensated reactive current or power. Moreover, the shunt controller can improve transient stability and can

DOI: 10.5121/ijci.2016.5106

damp out power oscillation. Using a high-speed power converter, the shunt controller can further alleviate or even cancel the flicker problem caused by electrical arc furnaces and regulate the voltage levels within certain criteria [7].

In principle, all shunt-type controllers inject additional current into the system at the point of common coupling (PCC). An impedance of the shunt controller, which is connected to the line voltage, causes a variable current flow, and hence represents an injection of current into the line. As long as the injected current is in phase quadrature with the line voltage, the shunt controller only supplies or consumes variable reactive power. Among recently developed power converter topologies, multilevel converters have become an important technology, and have been utilized in high-power applications, particularly FACTS controllers [5, 6]. Several multilevel converter topologies have been developed to demonstrate their superiority in such applications. With converter modules in series, and with balanced voltage-sharing among them, lower-voltage switches can possibly be used in high-voltage systems. Thus, the low-voltage-oriented insulated gate bipolar transistor (IGBT) devices can be stacked for medium-voltage systems [3, 4]. For higher-voltage applications, however, efforts have been made to use GTO-based devices for multilevel converters.

In harmonic elimination, reactive power compensation, cascaded-multilevel VSCs with separated DC capacitors are somewhat the most feasible topology for many reasons. The cascaded-multilevel converter (CMC) is constructed with a number of identical H-bridge converters. This modular feature makes the cascaded converter very attractive and simple in structure. The cascaded converter topology not only simplifies hardware manufacturability, but also makes the entire system flexible in terms of power capability. In addition, for the same power capability, the cascaded converter requires fewer total components. Auxiliary components, such as the clamped diodes and capacitors, are not required in the CMC topology [7, 8]. The CMC-based D-STATCOM, however, challenges researchers to improve its dynamic responses and to balance its excessive number of DC capacitor voltages. To date, several papers have discussed the configurations and control strategies for the reactive power compensation systems that utilize CMCs based on these previous works, an accurate model and an effective control technique associated with the simple DC capacitor balancing strategy are elements important to achieving a high-performance, stable, cost-effective CMC-based D-STATCOM [6, 8]. Finally the proposed DSTATCOM is used for integrating the PV system.

2. CASCADED MULTILEVEL BASED VOLTAGE-SOURCE CONVERTERS FOR D-STATCOM APPLICATION

An attractive to the seven-level converter is a multilevel VSC. Without semiconductor devices connected in series, the multilevel converters show feasible capability of clamping the voltages across individual devices below their limitations. This allows the recent semiconductor devices to be utilized in higher-voltage applications without incurring voltage sharing problems. Another significant advantage of the multilevel configuration is the harmonic reduction in the output waveform with very low switching frequency, line frequency for example. Besides the high-voltage capability, multilevel converters also provide other advantages over the seven-level converters. The multilevel converter in the four following aspects: output voltage quality, DC capacitance requirement, losses and power capacity. The schematics of the cascaded multilevel-converter are shown in Fig.1. Respectively.

With its modularity and flexibility, the CMC shows superiority in high-power applications, especially shunt and series connected FACTS controllers. The CMC synthesizes its output near sinusoidal voltage waveforms by combining many isolated voltage levels. With a sufficiently high number of voltage levels, a premium-quality output waveform with fast system response can

be achieved by switching the main power semiconductor devices only at the line frequency. This naturally minimizes the entire system losses and the output filter requirement. In addition, by adding more H-bridge converters, the amount of Var can simply increased without redesign

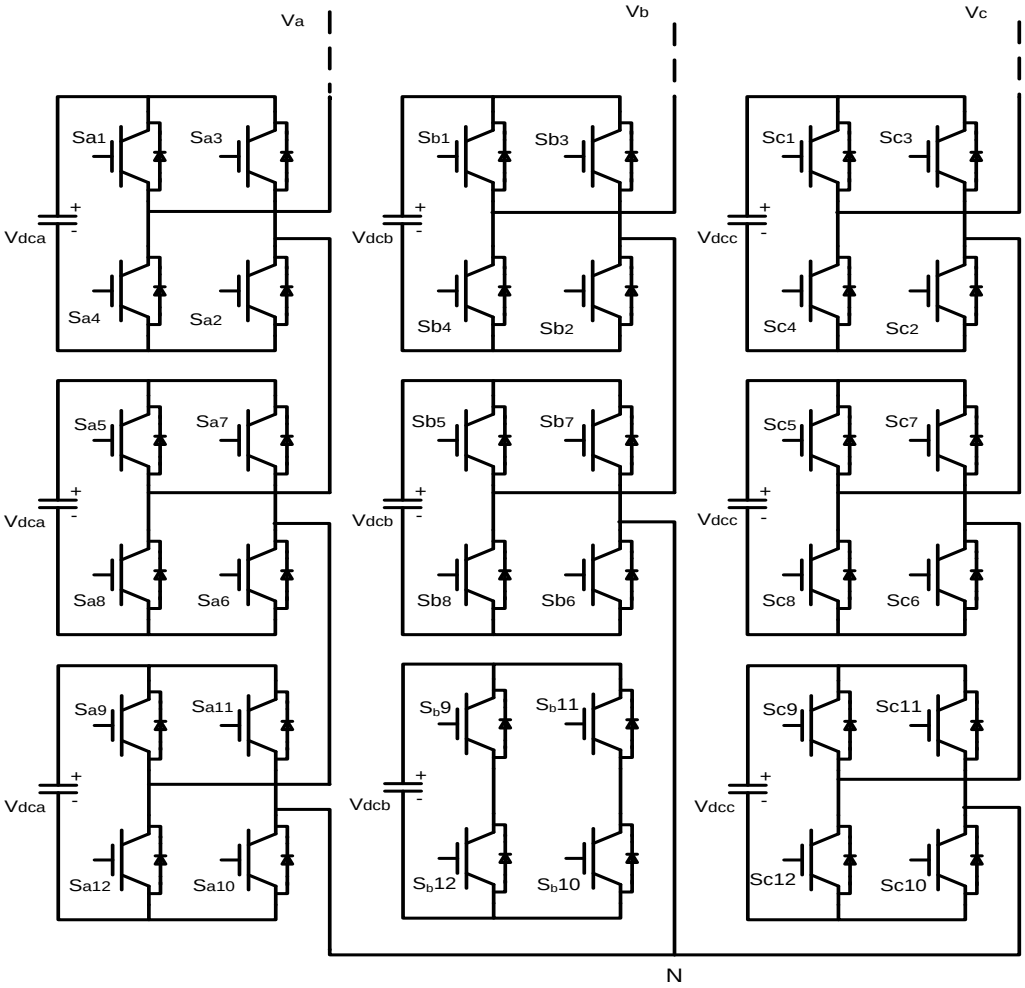

Fig.1. Schematic Diagram of 7-Level Cascaded Multilevel Converter

the power stage, and build-in redundancy against individual H-bridge converter failure can be realized. Moreover, a three-phase CMC topology is essentially composed of three identical phase legs of the series-chain of H-bridge converters, which can possibly generate different output voltage waveforms and offers the potential for AC system phase-balancing. This feature is impossible in other VSC topologies utilizing a common DC link. By nature of this topology, however, the CMC is impossible to apply in intertie or back-to back applications, such as universal power flow controllers (UPFC). Fortunately, with energy storage systems, the CMC can now successfully overcome this limitation. This combination also enhances recent low-voltage energy-storage system technology for high-voltage applications. A great combination of the D-STATCOM concept and the CMC topology is a promising controller in the modern FACTS technology.

3. CONTROL STRATEGY

IRP theory was initially proposed by Akagi. This theory is based on the transformation of three phase quantities to two phase quantities in α-β frame and the calculation of instantaneous active

and reactive power in this frame. A basic block diagram of this theory is shown in fig.2. Sensed inputs Vsa, Vsb, Vsc and iLa, iLb, iLc are fed to the controller, and these quantities are processed to generate reference current commands $(i^*_{Sa}, i^*_{Sb}, i^*_{Sc})$, which are fed to a pulse width modulation (PWM) signal generator to generate final switching signals fed to the D-STATCOM; therefore this block works as controller for D-STATCOM.

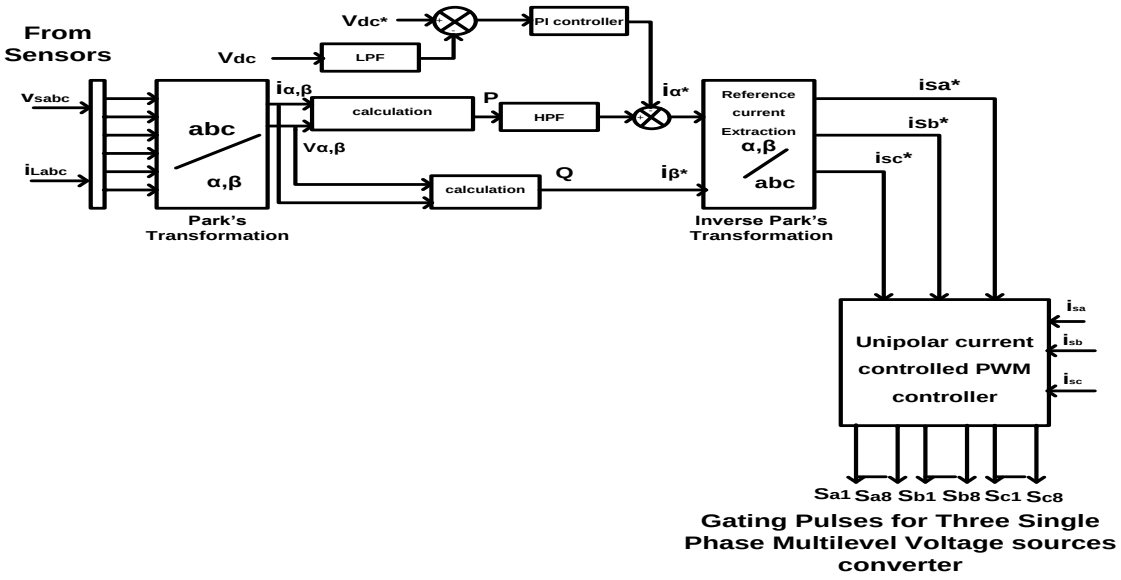

Fig.2. Block Diagram of Proposed Control Strategy- Instantaneous Real & Reactive Power Theory

The system terminal voltages are given as

$$va = Vm\sin(\omega t)$$
$$vb = Vm\sin(\omega t - 2\pi/3)$$
$$vc = Vm\sin(\omega t - 4\pi/3) \quad (1)$$

And the respective load currents are given as

$$i_{La} = \sum I_{Lan} sin\{n(\omega t) - \theta_{an}\}$$
$$i_{Lb} = \sum I_{Lbn} sin\{n(\omega t - 2\pi/3) - \theta_{bn}\}$$
$$i_{Lc} = \sum I_{Lcn} sin\{n(\omega t - 2\pi/3) - \theta_{cn}\} \quad (2)$$

In a-b-c coordinates, a, b, and c axes are fixed on the same plane, apart from each other by 2π/3. The instantaneous space vectors va and iLa are set on the "a" axis, and their amplitude varies in positive and negative directions with time. This is true for the other two phases also. These phasors can be transformed into α–β coordinates using Park's transformation as follows:

$$\begin{bmatrix} v_\alpha \\ v_\beta \end{bmatrix} = \sqrt{\frac{2}{3}} \begin{bmatrix} 1 & -1/2 & -1/2 \\ 0 & \sqrt{3}/2 & -\sqrt{3}/2 \end{bmatrix} \begin{bmatrix} v_a \\ v_b \\ v_c \end{bmatrix} \quad (3)$$

$$\begin{bmatrix} i_\alpha \\ i_\beta \end{bmatrix} = \sqrt{\frac{2}{3}} \begin{bmatrix} 1 & -1/2 & -1/2 \\ 0 & \sqrt{3}/2 & -\sqrt{3}/2 \end{bmatrix} \begin{bmatrix} i_a \\ i_b \\ i_c \end{bmatrix} \quad (4)$$

Where α and β axes are the orthogonal coordinates. Conventional instantaneous power for three-phase circuit can be defined as

$$p = v_\alpha i_\alpha + v_\beta v_\beta \quad (5)$$

Where p is equal to conventional equation

$$p = v_a i_a + v_b i_b + v_c i_c \quad (6)$$

Similarly, the IRP is defined as

$$q = -v_\beta i_\alpha + v_\alpha i_\beta \quad (7)$$

Therefore, in matrix form, instantaneous real and reactive power are given as

$$\begin{bmatrix} p \\ q \end{bmatrix} = \begin{bmatrix} v_\alpha & v_\beta \\ -v_\beta & v_\alpha \end{bmatrix} \begin{bmatrix} i_\alpha \\ i_\beta \end{bmatrix} \quad (8)$$

The α-β currents can be obtained as

$$\begin{bmatrix} i_\alpha \\ i_\beta \end{bmatrix} = \frac{1}{\Delta} \begin{bmatrix} v_\alpha & v_\beta \\ -v_\beta & v_\alpha \end{bmatrix} \begin{bmatrix} p \\ q \end{bmatrix} \quad (9)$$

Where

$$\Delta = v_\alpha^2 + v_\beta^2 \quad (10)$$

Instantaneous active and reactive powers p and q can be decomposed into an average (dc) and an oscillatory component.

$$p = \bar{p} + \tilde{p}$$
$$q = \bar{q} + \tilde{q} \quad (11)$$

Where $\bar{p}$ and $\bar{q}$ are the average (dc) part and $\tilde{p}$ and $\tilde{q}$ are the oscillatory (ac) part of these real and reactive instantaneous powers. Reference source currents are calculated to compensate the IRP and the oscillatory component of the instantaneous active power. Therefore, the reference source currents $i_{s\alpha}^*$ and $i_{s\beta}^*$ in α-β coordinate are expressed as

$$\begin{bmatrix} i_{s\alpha}^* \\ i_{s\beta}^* \end{bmatrix} = \frac{1}{\Delta} \begin{bmatrix} v_\alpha & -v_\beta \\ v_\beta & v_\alpha \end{bmatrix} \begin{bmatrix} \bar{p} \\ 0 \end{bmatrix} \quad (12)$$

Theses currents can be transformed in a-b-c quantities to find the reference currents in a-b-c coordinates using inverse transformation.

$$\begin{bmatrix} i_{sa}^* \\ i_{sb}^* \\ i_{sc}^* \end{bmatrix} = \sqrt{\frac{2}{3}} \begin{bmatrix} 1/\sqrt{2} & 1 & 0 \\ 1/\sqrt{2} & -1/2 & \sqrt{3}/2 \\ 1/\sqrt{2} & -1/2 & -\sqrt{3}/2 \end{bmatrix} \begin{bmatrix} i_0^* \\ i_{s\alpha}^* \\ i_{s\beta}^* \end{bmatrix} \quad (13)$$

Where i_0^* is the zero sequence components, which is zero in three- phase three wire system.

4. PHOTOVOLTAIC SYSTEM

In the crystalline silicon PV module, the complex physics of the PV cell can be represented by the equivalent electrical circuit shown in Fig. 4. For that equivalent circuit, a set of equations have been derived, based on standard theory, which allows the operation of a single solar cell to be simulated using data from manufacturers or field experiments.

The series resistance RS represents the internal losses due to the current flow. Shunt resistance Rsh, in parallel with diode, this corresponds to the leakage current to the ground. The single exponential equation which models a PV cell is extracted from the physics of the PN junction and is widely agreed as echoing the behavior of the PV cell

$$I = I_L - I_{sc}\left(exp\frac{(V+R_sI)}{V_L} - 1\right) - \frac{(V+R_sI)}{R_{sh}} \quad (14)$$

The number of PV modules connected in parallel and series in PV array are used in expression. The Vt is also defined in terms of the ideality factor of PN junction (n), Boltzmann's constant (KB), temperature of photovoltaic array (T), and the electron charge (q). Applied a dynamical electrical array reconfiguration (EAR) strategy on the photovoltaic (PV) generator of a grid-connected PV system based on a plant-oriented configuration, in order to improve its energy production when the operating conditions of the solar panels are different. The EAR strategy is carried out by inserting a controllable switching matrix between the PV generator and the central inverter, which allows the electrical reconnection of the available PV modules.

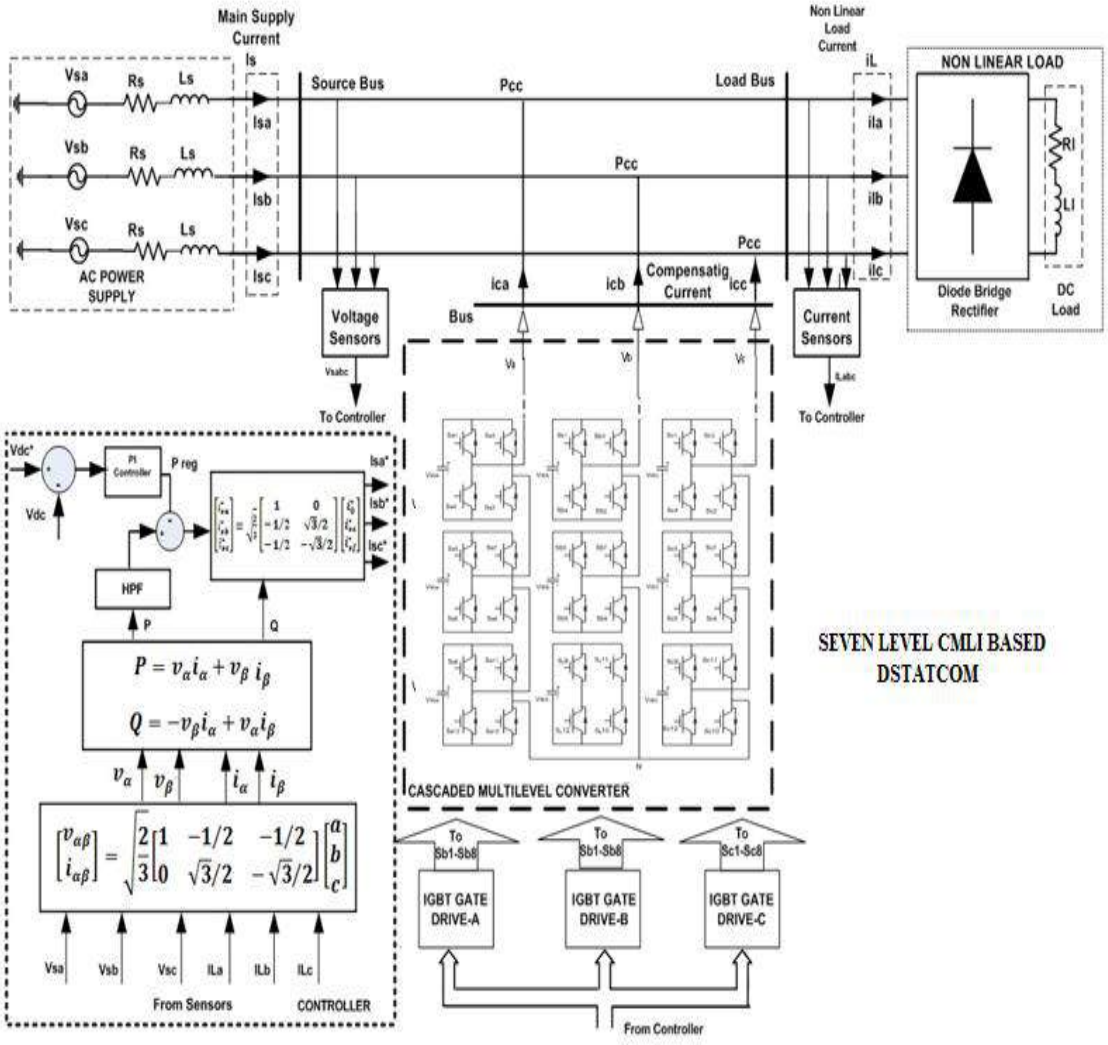

Fig.3.Schematic diagram of non-linear load with cascaded seven level inverter D-STATCOM

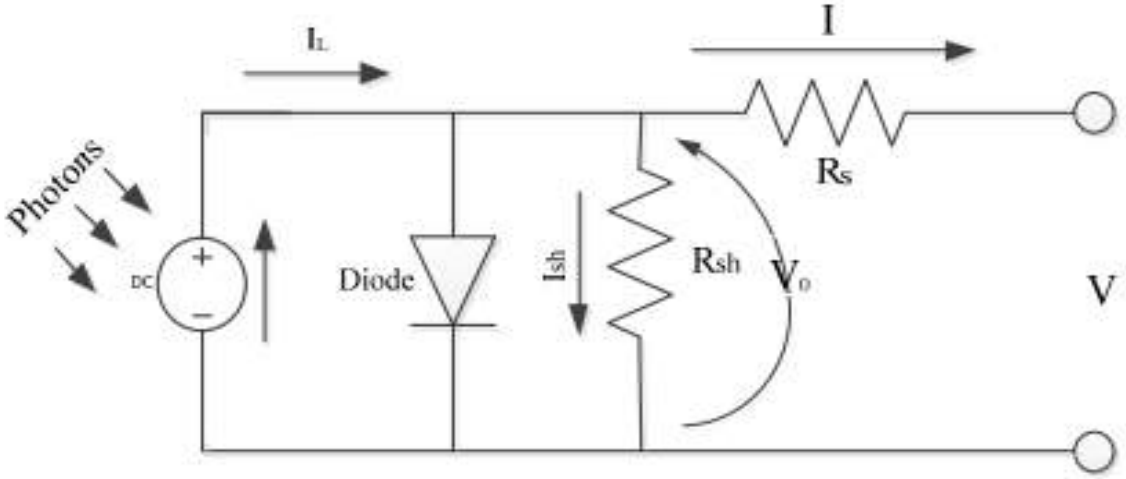

Fig.4 Equivalent electrical circuit of a PV module

5. DG INTEGRATION WITH DSTATCOM

Distributed generation (or DG) generally refers to small scale electric power generators that produce electricity at a site close to customers or that are tied to an electric distribution system. Distributed generators include, but are not limited to synchronous generators, induction generators, reciprocating engines, micro turbines (combustion turbines that run on high energy fossil fuels such as oil, propane, natural gas, gasoline or diesel), combustion gas turbines, fuel cells, solar photovoltaic's, and wind turbines. Globally, the long-term technical potential of wind energy is believed to be five times total current global energy production, or 40 times current electricity demand. This could require wind turbines to be installed over large areas, particularly in areas of higher wind resources. Offshore resources experience average wind speeds of ~90% greater than that of land, so offshore resources could contribute substantially more energy.

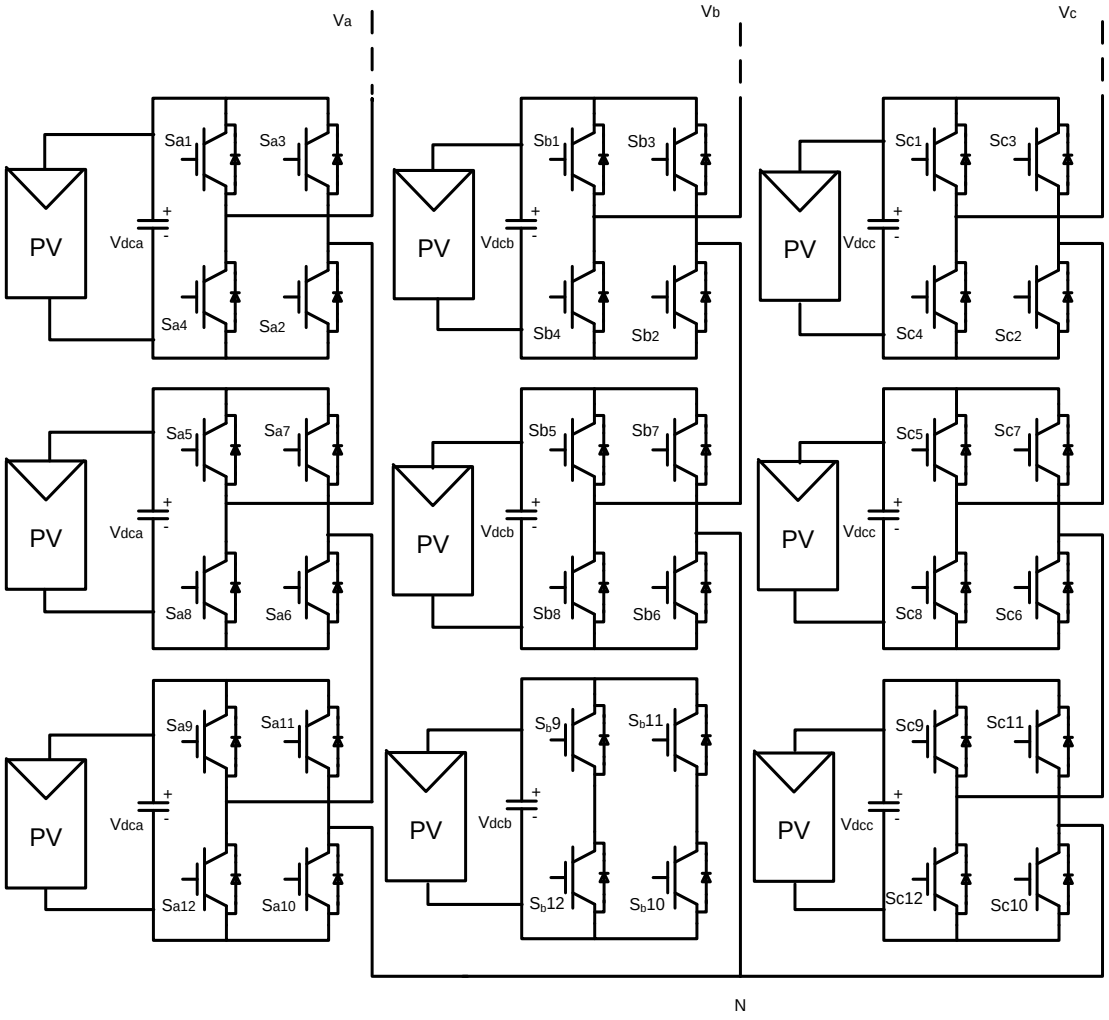

Fig.5.schematic diagram of DG integration with seven level inverter

6. MATLAB/SIMULATION RESULTS

Here the simulation is carried out by two cases

Case.1. Balanced Non-linear load with seven level cascaded multilevel D-STATCOM.
Case.2. Un-balanced Non-linear load with seven level Cascaded multilevel D-STATCOM.
Case1. Balanced Non-linear load with seven level cascaded multilevel *D-STATCOM.*

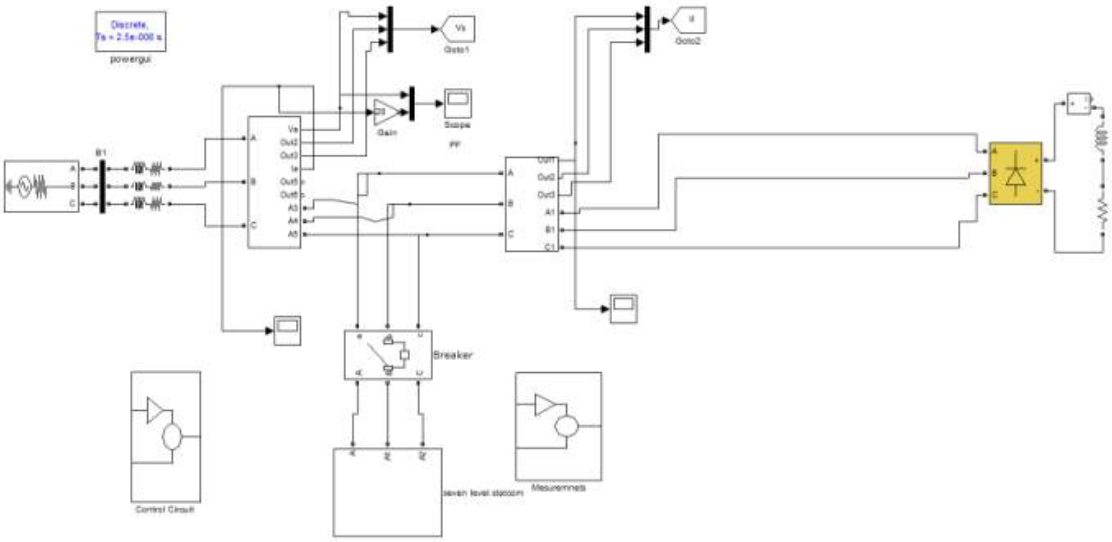

Fig.6.Matlab/Simulink model of balanced non-linear load with seven level cascaded multilevel D-STATCOM

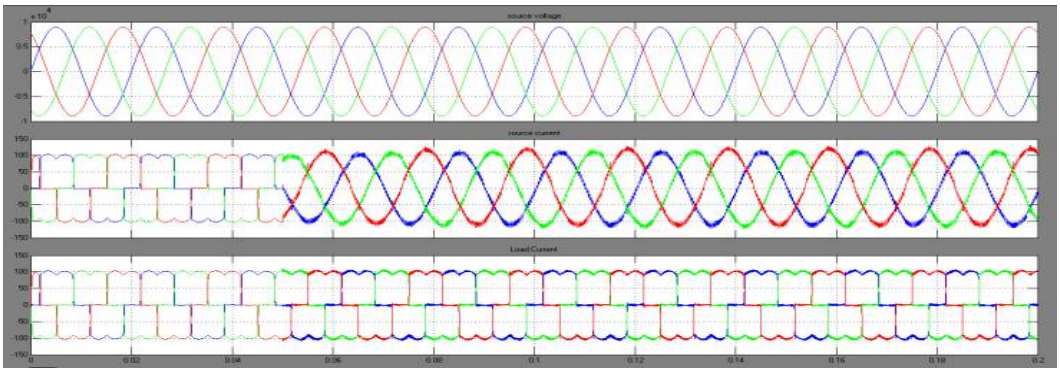

Figure 7: Source voltage, Source current, Load current

Figure 7 shows the source voltages, source currents and load currents respectively with balanced non-linear load and Cascaded Multilevel Seven level.

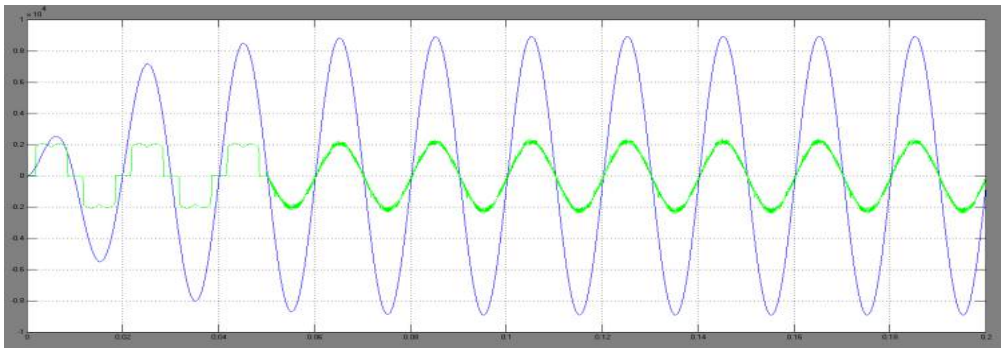

Figure 8: Power Factor with balanced non-linear load

Figure 8 shows the power factor waveforms of the designed system with balanced non-liner load seven level cascaded multilevel D-STATCOM .The waveform clearly shows that there is no unity power factor.

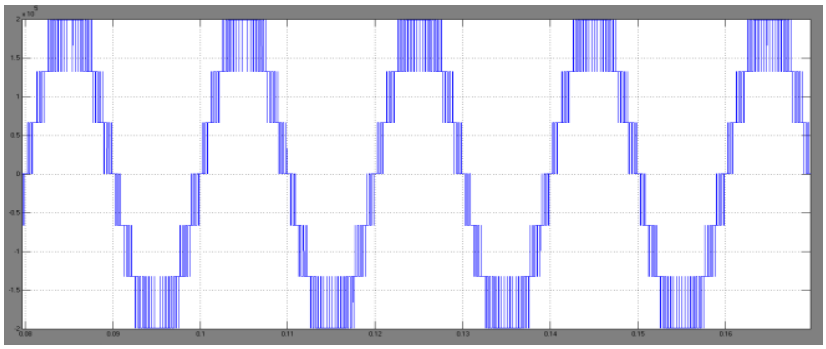

Fig.9.Seven Level output voltage

Figure.9.Shows the Seven level output voltage, when system is connected to cascade seven level multilevel D-STATCOM.

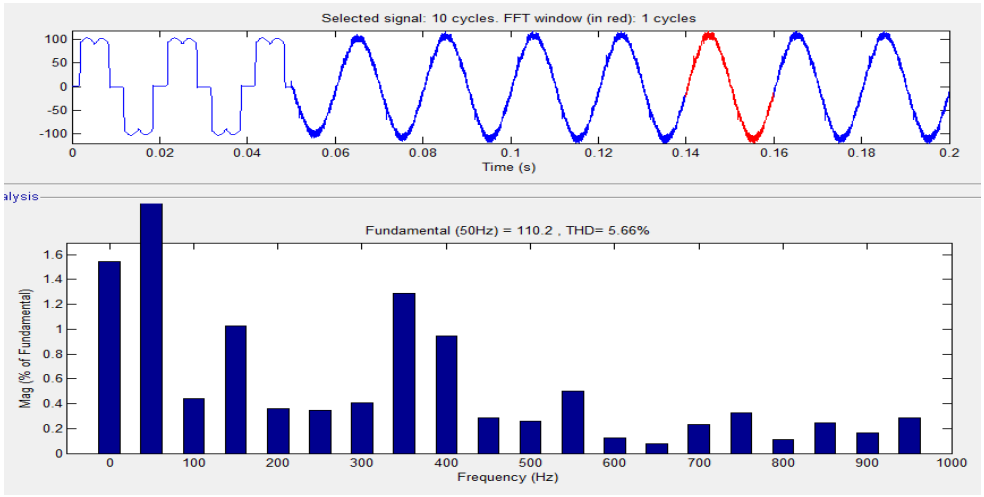

Figure 10: Harmonic spectrum of Phase-A Source current for seven level D-STATCOM

Figure10 shows the harmonic spectrum of Phase –A Source current for balanced non-linear load with cascaded Multilevel Seven level D-STATCOM. The THD of source current is 5.66%.

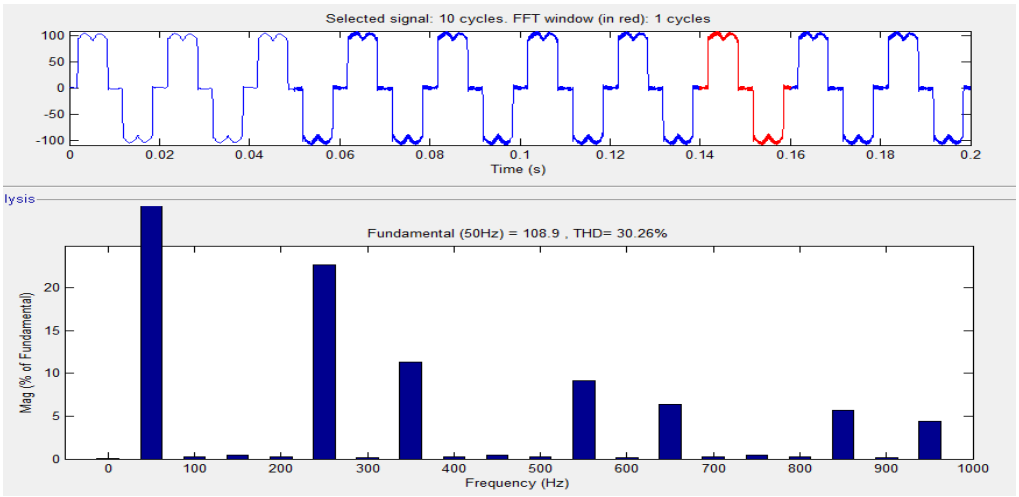

Figure 11: Harmonic spectrum of Phase-A load current for seven level D-STATCOM

Figure11 shows the harmonic spectrum of Phase –A Load current for balanced non-linear load with cascaded Multilevel Seven level D-STATCOM. The THD of source current is 30.26%.

Case2. Un-balanced Non-linear load with seven level Cascaded multilevel D-STATCOM.

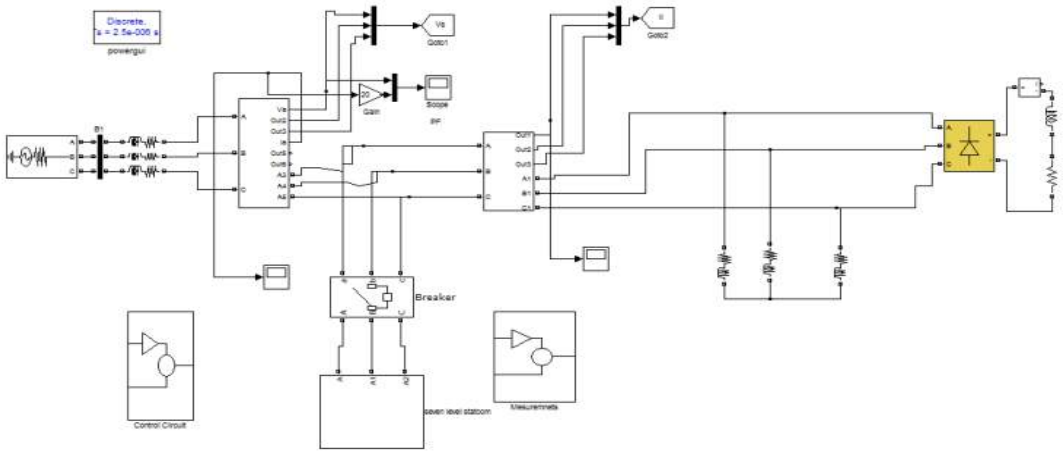

Figure.12.Matlab/Simulink model of unbalanced non-linear load with seven level cascaded multilevel D-STATCOM

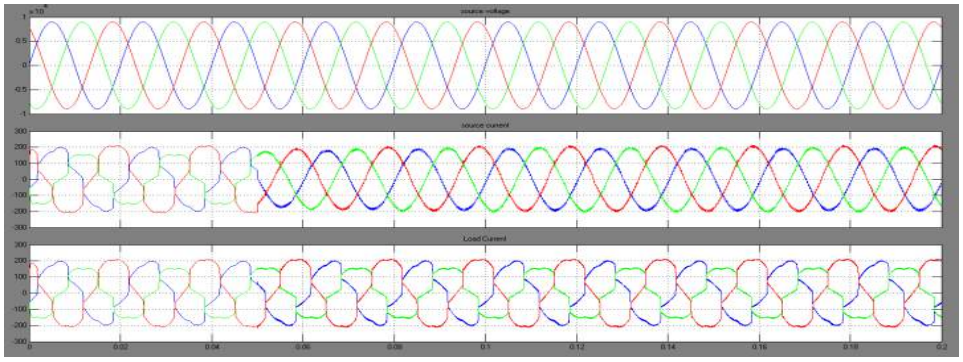

Figure 13: Source voltage, Source current, Load current

Figure-13 shows the source voltages, source currents and load currents for unbalanced non-linear load with Cascaded Multilevel Seven level.

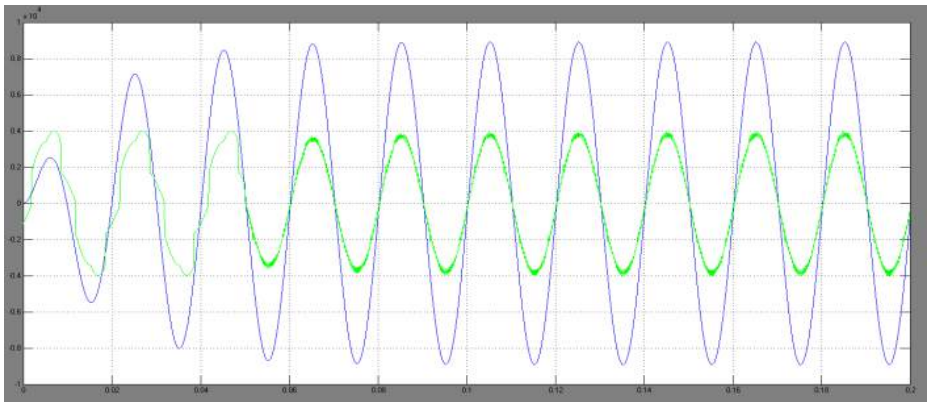

Figure 14: Power Factor with unbalanced non-linear load

Figure 14 shows the power factor waveforms of the designed system with unbalanced non-liner load seven level cascaded multilevel D-STATCOM.

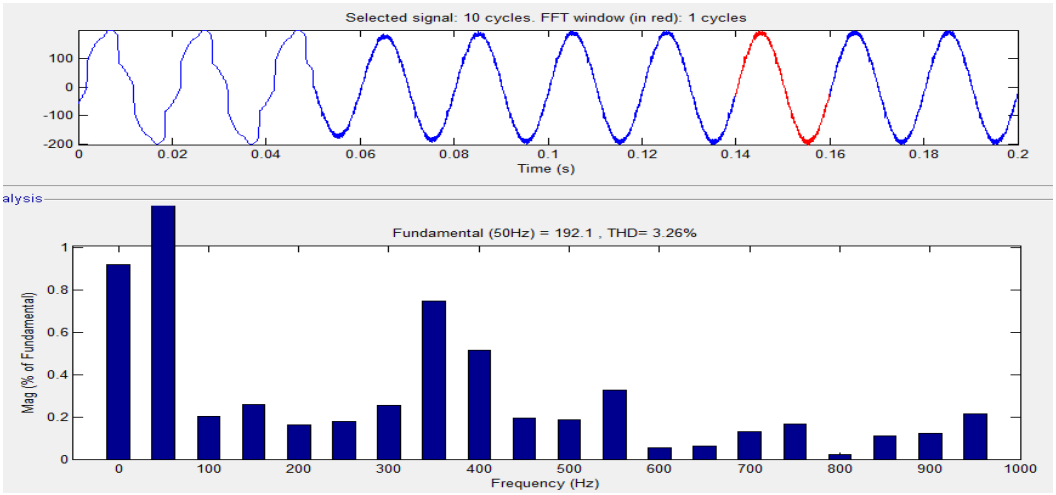

Figure 15: Harmonic spectrum of Phase-A Source current for seven level D-STATCOM

Figure15 shows the harmonic spectrum of Phase –A Source current for unbalanced non- linear load with cascaded Multilevel Seven level D-STATCOM. The THD of source current is 3.26%.

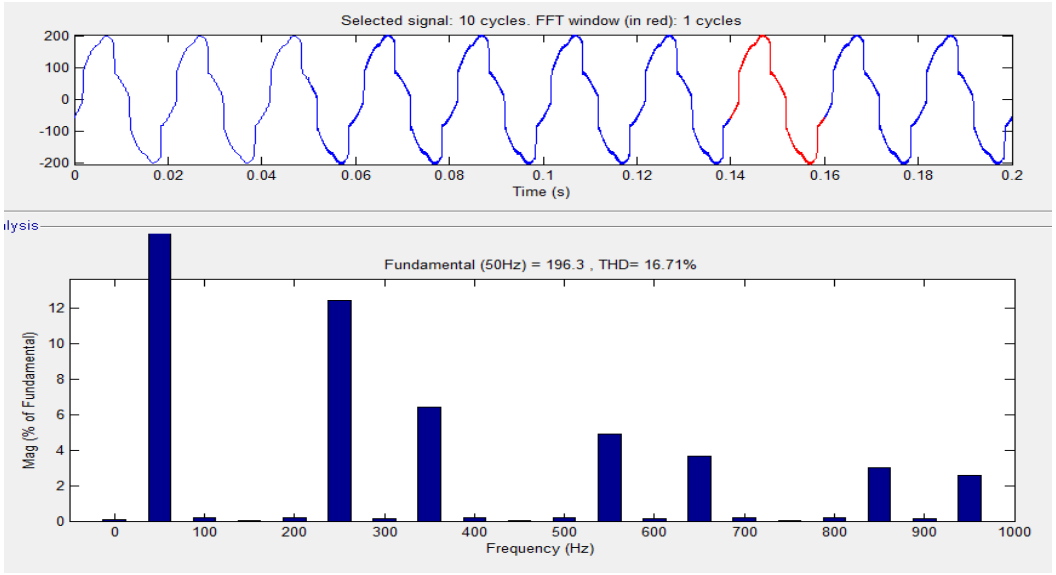

Figure 16: Harmonic spectrum of Phase-A Load current for seven level D-STATCOM

Figure16 shows the harmonic spectrum of Phase –A Load current for unbalanced non- linear load with cascaded Multilevel Seven level D-STATCOM. The THD of load current is 16.71%.

7. CONCLUSION

Seven level cascaded multilevel voltage source inverter based D-STATCOM using instantaneous real-power controller is found to be an effective solution for power line conditioning. D-STATCOM with the proposed controller reduces harmonics and provides reactive power compensation due to balanced non-linear and unbalanced non-linear load currents; as a result

source current(s) become sinusoidal and unity power factor is also achieved under both transient and steady state conditions. The proposed instantaneous real-power controller uses reduced computation for reference current calculations compared to conventional approach. The cascaded inverter switching signals are generated using triangular-sampling current controller; it provides a dynamic performance under transient and steady state conditions.

REFERENCES

[1] Ghosh and G. Ledwich, Power Quality Enhancement using Custom Power Devices, Kluwer Academic Publisher, Boston, MA, 2002.

[2] Ghosh and G. Ledwich, "Load Compensating DSTATCOM in weak AC systems," IEEE Trans. Power Delivery, vol.18, No. 4, pp. 1302-1309, Oct. 2003.

[3] J. S Lai and F. Z. Peng, "Multilevel converters A new breed of power converters," IEEE Trans. Industry Applications, vol.32, no.3,

[4] F. Z. Peng., J. W. McKeever and, D .J. Adams, "A power line conditioner using cascade multilevel inverters for distribution system," IEEE Trans. Industry Applications, vol.34, no.6, pp. 1293-1298, Nov.-Dec.1998.

[5] W. Liqiao, L. Ping, L. Jianlin and Z. Zhongchao, "Study on shunt active power filter based on cascaded multilevel converters," 35th IEEE Power Electr. Spec. Conf. (APEC), vol.5, pp. 3512-3516, 20-25 June 2004.

[6] H. Gruning,"Power Electronics Circuit Arrangement having Plural Power Converters", U.S. Patent No. 5,805,487, 1998.

[7] G. Carrara, S. Gardelta, M. Marchesoni,"A new multilevel PWM method: theoretical analysis", IEEE Trans. On power electronics Vol. 7. No. 3 , July, pp.497-505, 1992.

[8] V. Agelidis, M. Calais," Application specific harmonic performance evaluation of multicarrier PWM techniques", IEEE-PESC'98 Conference Record, pp. 172-178, 1998.

INTENTIONAL BLANK

OPENING RANGE BREAKOUT STOCK TRADING ALGORITHMIC MODEL

Mrs.S.Mahalakshmi[1] and Mr.Vignesh P[2]

[1] Assistant Professor, Department of ISE, BMSIT&M, Bengaluru, India
[2] Student,Department of ISE, BMSIT&M, Bengaluru, India

ABSTRACT

Stock Trading Algorithmic Model is an important research problem that is dealt with knowledge in fundamental and technical analysis, combined with the knowledge expertise in programming and computer science. There have been numerous attempts in predicting stock trends, we aim to predict it with least amount of computation and to decrease the space complexity. The goal of this paper is to create a hybrid recommendation system that will inform the trader about the future of a stock trend in order to improve the profitability of a short term investment. We make use of technical analysis tools to incorporate this recommendation into our system. In order to understand the results, we implemented a prototype in R programming language.

KEYWORDS

Stock Trading Algorithmic Model, Breakout Trading, R Programming, Short term trading.

1. INTRODUCTION

Stock Trading Algorithms have gained a significant place in research due to its profitable benefits. A lot of researches are focused to find solutions on how to make a good investment. From the survey we have concluded that there are multiple solutions in order to acquire results. Some of these solutions are: By using fundamental analysis and technical analysis [1], Arbitrage analysis [1], Time series model [1], Temporal Data mining or by combining them to have more precise prediction [10].

The main problems are that it is not easy to predict the Stock Market trend because of its non linear, dynamic and chaotic identity, combined with macroeconomic factors and noisy time series. To forecast, technical analysis uses factors such as charts, market indicators, and the relationship between volume and price indicators. In Technical Analysis, there are multiple techniques such as gap analysis, breakout system, market models, momentum precedes price and neural networks.

Artificial intelligence has gained a significant amount of importance in predicting stock trends. Techniques in Artificial intelligence such as neural network are used in order to capture patterns, relationships and environmental changes based on historical data and determine future trends of a stock. We have developed an environment that will be able to combine technical analysis tools and provide a blackboard based architecture based on the literature survey.

2. RELATED WORK

Andrea.S et.al proposed that a good prediction can be done by using macroeconomic variables, time series combination and temporal data mining [1]. It can also be done by combining fundamental analysis and technical analysis, with a multi agent system.[2][3]. D.Maldovan [4] uses macroeconomic variables because a change in the rule should be considered as a random event and not predictable.

The most popular approach in recent times is predicting stock using Neural Networks Models for good estimation of a non-linear function without knowing the characteristics of the data [4], [5], [6] and Markov Regime Switching Models due to the fact that it can capture discrete shifts which can appear in the behaviour of economic variables [5] for forecasting financial time series.
Numerous approaches have been used in the past to create expert systems which deal with stock forecasting by using fundamental and technical analysis such as MASST (Multi-Agent System for Stock Trading) [7] which was designed to be an agent-based environment able to collect, filter and manage data in order to make suggestions to the user. The architecture of this system lies on three agents which are interconnected.The agents were Location agent, stock sample agent and symbol agent.

G. Preethi has proposed a trading algorithmic model that uses the signal of three technical indicators to produce a trading signal. These technical indicators are MACD (Moving Average Convergence-Divergence), ROC (Price Rate of Change) and STS (Stochastic Oscillator) [8].
G.Marketos et.al have worked on "Intelligent Stock Market Assistant using Temporal data mining". He discuss about portfolio management solutions using business intelligence by the use of temporal data mining patterns.

3. MOTIVATION

The motivation behind the paper is to find the most efficient method of prediction with less computation and utilizing fewer system resources. The goal is to forecast the stock market based on the first 45 minutes of the day's data. This method is quite famously known as Opening Range Breakout. Based on research conducted on ORB trading it gives a better prediction result than those based on historical data. We convert this technique into an algorithm form and make it an Algorithmic Trading Platform so that the entire process of calculating would be done in a matter of seconds.

4. PROBLEM STATEMENT

One of the major problems faced in modelling financial market movements is the fact that information comes in from a very large number of sources. With many models developed in this field, we decided to take an approach away from such large data analysis (historical data). The challenge here is to develop a model that has a good performance and best accuracy. While taking very less amount of data analysis, the end goal is to find the best configuration for the model to give the maximum performance. In our project, we are considering 50 stocks in all the twelve sectors of Nifty, an index composed by National Stock Exchange of India. In our model, we are aiming to achieve an accuracy of approximately 60-70%.

5. PROPOSED METHODOLOGY

Traditional Stock Market analysis mainly depends on data. Different techniques such as artificial neural network, genetic algorithm and so on depends on historical data. The main problem with historical data is that sometimes the data on some particular day won't be available and also the data will be very large. Our project forecasts the stock market based on the first 45 minutes of the opening data. This method is popularly known as Opening Range Trading. Based on the research conducted, Opening Range Breakout trading gives better results than those predictions which are based on the historical data.

We convert this technique into an algorithm form and make it as an algorithmic trading platform. So that the entire process of calculation would be done in a matter of seconds and by adding customized filters to the algorithm increases the efficiency, compared to conventional method, thereby increases the chances of high profitability. The main objective of this project is to determine the right opportunity to invest in a particular stock, to maximize the profit and minimize the loss.

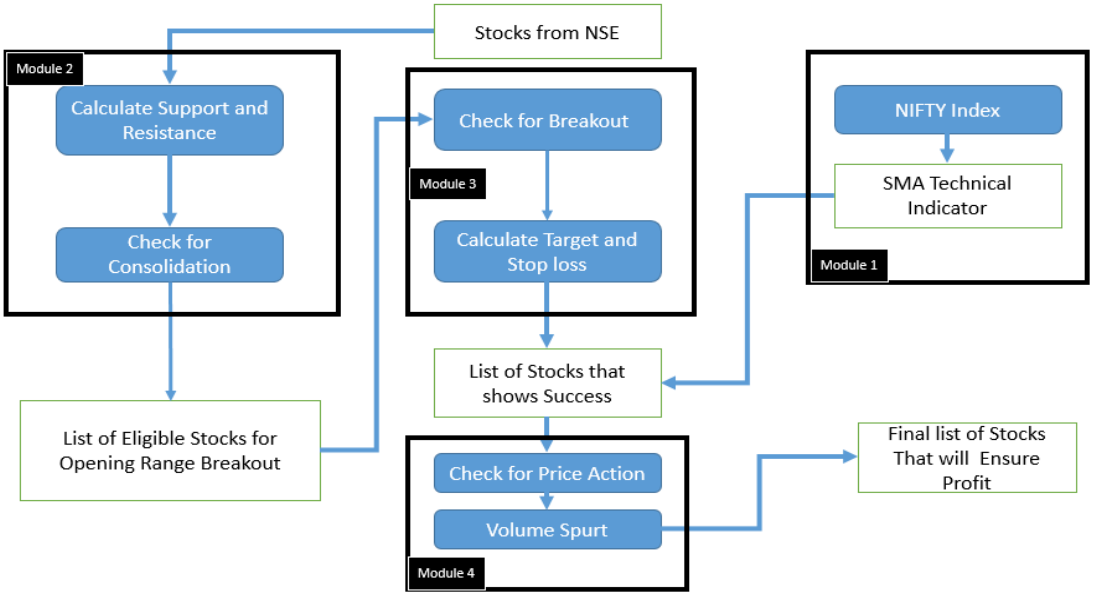

Fig 1 – Methodology

6. IMPLEMENTATION

The solution has been divided into modules in order to implement. Our data source for the project is Google finance that provides real-time data for the application

6.1 Simple Moving Average

Access the Nifty 50 and plot simple moving average on the accessed 50 stocks of nifty. A simple moving average is calculated by adding the closing price of the stock for a number of time periods and then dividing this total by the number of time periods. We consider two moving averages – a short period and a long period. If the shorter period, crosses and goes above the longer period, we know that the market is going up but if the opposite happens, we come to know that the market is going down. The relationship between shorter and longer moving average trend lines is the subject of many studies and traders look to crossovers for opportunities to buy, sell or short.

6.2 Calculation of Support and Resistance

Scans the accessed 50 stocks and finds out support and resistance based on the first thirty minutes and also check if support and resistance are broken or not during the consolidation period. If consolidation period is not broken then stocks are eligible for trading and rest of the stocks are eliminated for the day. The support and resistance lines are set by observing the time between 9:25 a.m. and 9:55 a.m. [9]. The high and low for that period is set as the support and resistance.

6.3 Setting the Buying Price, Target, Stop Loss

Post consolidation period, the program checks if the support and resistance are broken and if it has, then the buying price, target and stop loss is printed. The target is calculated by computing the difference between the support and resistance and the dividing that by 2. The stop loss is calculated by dividing the difference by 3. The objective of setting the target is to ensure that the investor gets a fair share of the market's profit. The purpose of the stop loss is to guarantee a fail-safe method of losing money. The investor does lose money, but at minimum risk.

6.4 Monitoring the Price Action

Once the Breakout occurs, it checks if the breakout occurred is a false breakout or true breakout by comparing the breakout bar with the next bar. We use an active price filter and a volume spurt filter. If the first breakout bar is bullish, the second bar needs to be bullish too. Otherwise, there is a chance of the market going down and the investor losing his money. The same applies for a bearish bar too. If this pattern isn't followed, it means that it is a false breakout and the target will not be reached. Sequence diagram described in fig [2] will show the order of execution of the modules.

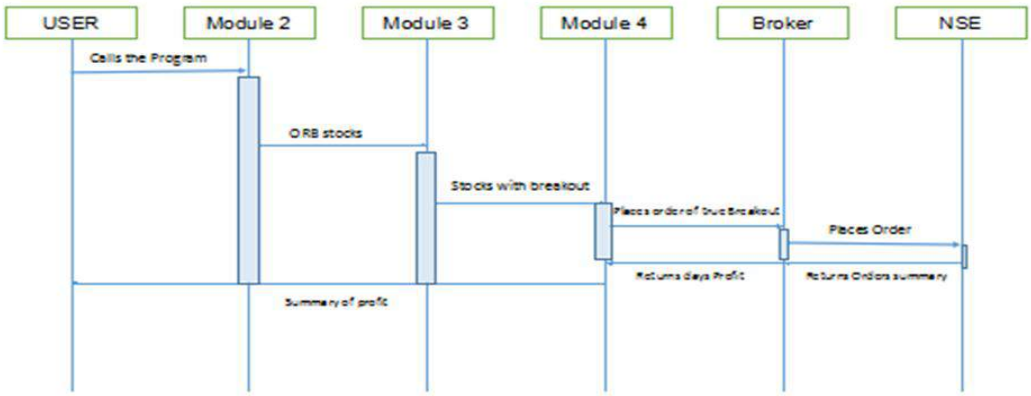

Fig 2. Sequence Diagram

7. TESTING

7.1 Accuracy Testing Results

The algorithm was tested for a period of 7 trading days from 25 Mar 2015 to 02 Apr 2015. This period was chosen randomly. On an average 25 trades were done on each day, of which a

prediction accuracy of 70% was achieved by testing the algorithm in the real-time market. The results are tabulated in the table [1].

7.2 Single Day Real Time Test Results

A single random day test was carried out on 19-05-2015 (Tuesday) to test the performance of the algorithm. The following was observed and recorded in table [2]. It was noted that stocks in the automobile, banks, and steel companies achieved the target. On the other hand, cement and oil companies failed to achieve the target and few were with no trade.

Table1. Prediction Accuracy Percentage

			Testing			
Date	Number of Eligible Stocks	Stocks That Achieved the Target	Stocks That did not reach the target		Predication accuracy %	Loss of the day %
			With Loss (False Breakout)	Without loss (No breakout)		
25-03-2015	25	15	3	7	60	28
26-03-2015	19	17	1	1	89.21	0.05
27-03-2015	18	10	4	4	55	22
30-03-2015	22	16	3	3	72.72	13.63
31-03-2015	26	16	6	4	61.53	15.3
01-04-2015	23	17	1	5	73.91	21.73
02-04-2015	23	17	2	4	73.91	17.39
					∑%=69.7	∑%=16.87

Table 2. Single Day Real Time Test Results

Date	List of Eligible Stocks	Stock Achieved the Target	Stocks That did not reach the target		BUY/SELL	Prediction accuracy %	Loss of the day %
			With Loss (False Breakout)	Without loss (No breakout)			
19-05-2015	ACC	-	✓	-	-	60	28
	AMBUJACEM	✓	-	-	Sell->Buy		
	ASIANPAINT	✓	-	-	Sell->Buy		
	AXISBNAK	✓	-	-	Buy->Sell		
	BAJAJ-AUTO	-	-	✓	-		
	BHARTIARTL	✓	-	-	Buy->Sell		
	CAIRN	✓	-	-	Buy->Sell		
	CIPLA	-	✓	-	-		
	DRREDY	✓	-	-	Buy->Sell		
	GAIL	-	-	✓	-		
	HINDUNILVR	✓	-	-	Sell->Buy		
	IDFC	✓	-	-	Sell->Buy		
	INFY	✓	-	-	Sell->Buy		
	ITC	-	✓	-	-		
	JINDALSTEL	✓	-	-	Sell->Buy		
	LT	✓	-	-	Sell->Buy		
	MARUTI	✓	-	-	Buy->Sell		
	NMDC	-	✓	-	-		
	ONGC	-	✓	-	-		
	POWERGRID	-	✓	-	-		
	RELIANCE	-	-	✓	-		
	SBIN	✓	-	-	Sell->Buy		
	SSLT	✓	-	-	Buy->Sell		
	TATAMOTERS	-	✓	-	-		
	WIPRO	✓	-	-	Buy->Sell		
						60	28

8. CONCLUSION

The Opening Range is a powerful concept and yields significant profits when traded with the right stock. It works best with a consolidation period of 25 minutes, an active price filter, and volume spurt filter. Sometimes the market is very volatile due to external influences like politics, company mergers etc., therefore on those days it is difficult to have a high prediction accuracy. Overall, we are able to achieve an accuracy of almost 70%. In future, we can automate this process by linking it with iBroker, which is an interactive broker system to make it completely automated.

9. SCREENSHOT'S

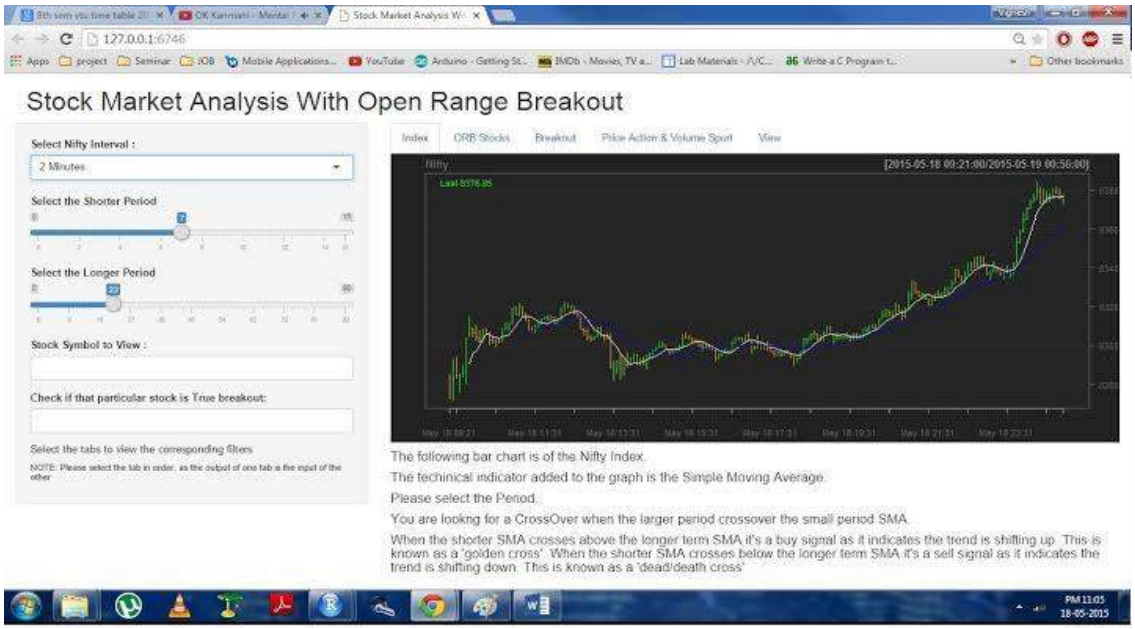

Fig 3. SMA

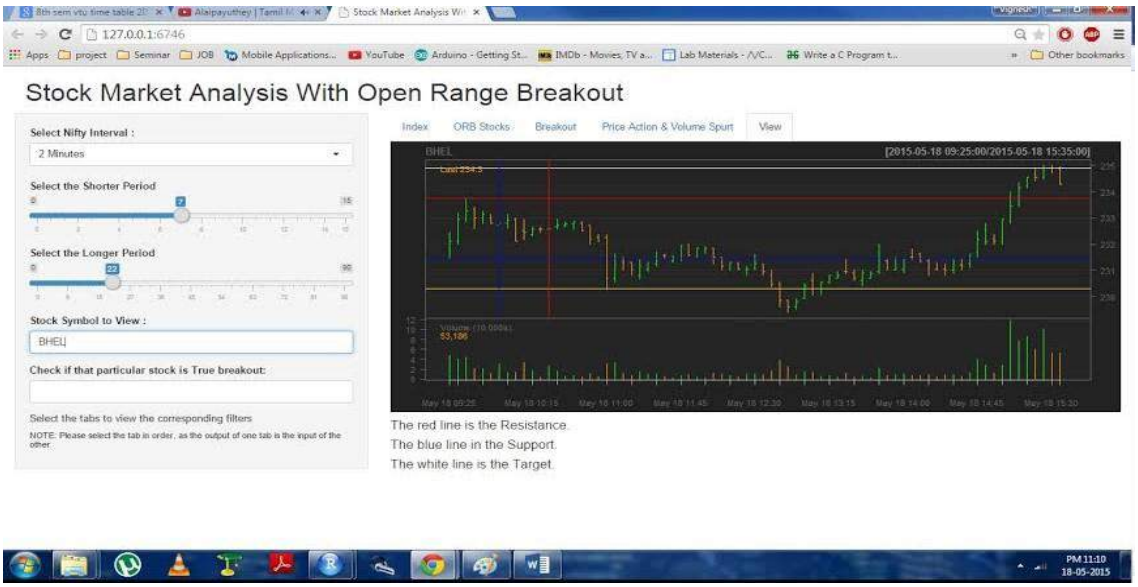

Fig 4. Breakout

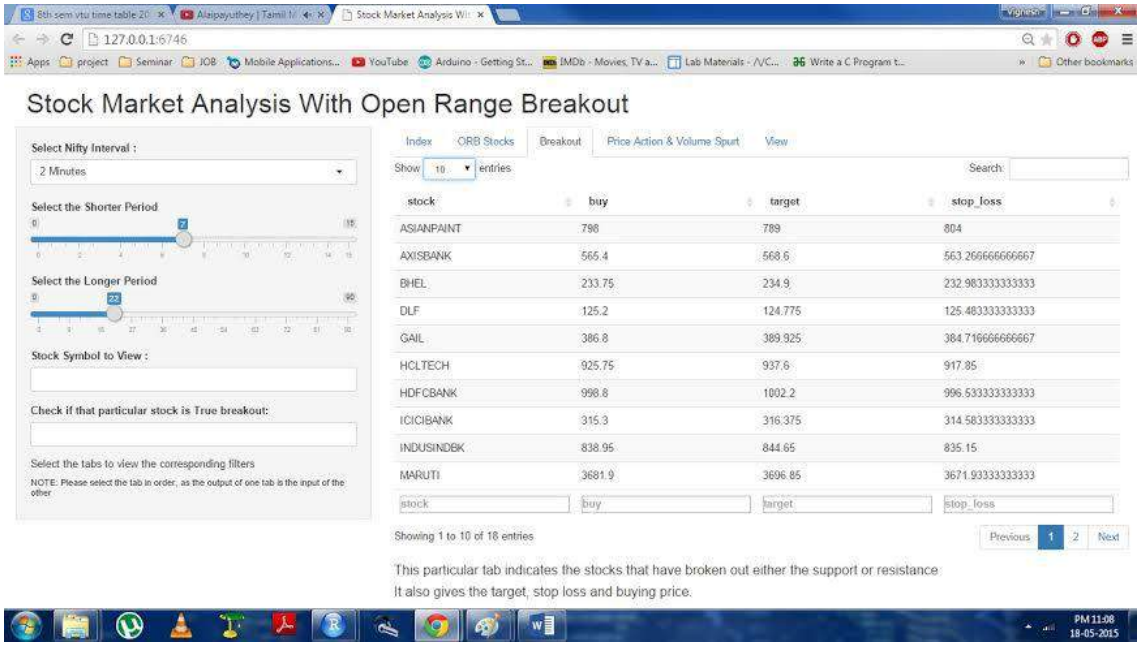

Fig 5. Buying Price, Target, Stop Loss

REFERENCES

[1] Andreas S. Andreou, Constantinos C. Neocleous, Christos N. Schizas, "Testing the predictability of the Cyprus Stock Exchange :The case of an emerging market in Proceedings of the IEEE-INNS-ENNS International Joint Conference on Neural Networks,Vol:6,2000

[2] Andrew Pole, Statistical Arbitrage: Algorithmic Trading Insights and Techniques, John Wiley & Sons, 2007

[3] Monica Tirea, Viorel Negru, "Stock Market Analysis - Strongest Performing Stocks Influence on an Evolutionary Market" in Proceedings of the 35th International Conference on Information Technology Interfaces (ITI),2013

[4] D. Moldovan, M. Moca, t. NitchiI, "A Stock Trading Algorithm Model Proposal, based on Technical Indicators Signals", Informatica Economic, Vol 15, Issue No 1, pp.183-188, 2011

[5] Fluctuations Gabriel Iuhasz, Monica Tirea and Viorel Negru, "Neural Network Predictions of Stock Price", Published in 14th International Symposium on Symbolic and Numeric Algorithms for Scientific Computing (SYNASC), 2012

[6] C. Xiang and W. M. Fu, "Predicting the Stock Market using Multiple Models", in 9th International Conference on Control, Automation, Robotics and Vision, 2006.

[7] D. Liu, L. Zhang, "China Stock Market Regime Prediction with Artificial Neural Network and Markov Regime Switching", in Proceedings of the World Congress on Engineering, Volume 1, 2010, London.

[8] G.Preethi, B. Santhi, "Stock Market Forecasting Technique: a Survey", Journal of Theoretical and Applied Information Technology , Vol. 46 ,pp:No.1 , 2012.

[9] http://www.marketgauge.com/ TradingThe10OclockBulls Winning Strategies for Active Traders by Geoff Bysshe

[10] Wei Yang, "Stock Price Prediction Based On Fuzzy Logic", Published in Proceedings of the Sixth International Conference on Machine and Cybernetics ,Vol: 3,2007

[11] Marketos et.al, "Intelligent Stock Market Assistant Using Temporal data mining", published in Proceedings of 10th Panhellenic Conference in Informatics (PCI'05), Volos, Greece, November 2005.

INTENTIONAL BLANK

BIG DATA ANALYTICS AND E LEARNING IN HIGHER EDUCATION

Tulasi.B[1] and Suchithra.R[2]

[1]Department of Computer Science, Christ University, Bangalore, India
[2]Department of Computer Science , Jain University, Bangalore, India

ABSTRACT

With the advent of internet and communication technology the penetration of e-learning has increased. The digital data being created by the higher educational institutions is also on ascent. The need for using "Big Data" platforms to handle, analyse these large amount of data is prime. Many educational institutions are using analytics to improve their process. Big Data analytics when applied onto teaching learning process might help in improvising as well as developing new paradigms. Usage of Big Data supported databases and parallel programming models like MapReduce may facilitate the analysis of the exploding educational data. This paper focuses on the possible application of Big Data Techniques on educational data.

KEYWORDS

Big Data, e-learning, Higher Education, MapReduce, MongoDB, Association rule mining

1. INTRODUCTION

Operational processes of higher educational institutions are increasing becoming complex. The quality of learning, accountability to the stake holders, the requirements of the digital-era Millennials are few of the issues which are currently associated with higher education. The digital revolution has given rise to newer approaches to learning in form of Massive Open Online Courses and Learning Management Systems where the interaction of the learner with the teacher moves beyond the physical walls of the class room leading to design of flexible class room sessions [1]. With the augmentation of internet and communication technology, demand for online learning has seen greater growth. The amount of data being stored by higher educational institutions has always had been huge. But the digital penetration into the processes of teaching-learning and evaluation has paved way to availability of huge amount of data which can be termed as "Big Data". Big Data is loosely defined as data sets which are of very large scale and complex in nature [2]. With the penetration of digital and mobile communication into the field of education data being stored has exponentially grown.

The digital learning or e-learning is being seen as a futuristic approach of learning by the current generation of learners [3]. The ease of availability and usage of handheld devices like Tablets has provided the required leap for e–learning. Open source LMS like MOODLE provide avenues for the students to interact not only with the teacher but also with their peers which would result in richer learning experience. The huge amount of data being generated by these educational modules is on ascent. This data when analysed can provide greater insights on learning patterns of students, gaps in the teaching learning processes and many more. The storage requirements of this humongous data are quite different from the traditional storage. The analytics to be applied on this data also would require newer technologies and platforms. Parallel computation of these large

data sets would be required to derive actionable knowledge. The horizontal scalability feature of "NoSQL" data stores makes it a potential alternative over the traditional storage. The trait of NoSQL "shared nothing, replicating and partioning of data over many servers" allows it to support large number of read/write operations per second [4].

This paper explores the possible role of big data analytics, e-learning in higher education. Big Data analytics can be applied at various levels in higher education like teaching learning, resource allocation, student retention, course advisor. The paper tries to identify the penetration of e-learning into higher education and the impact big data analytics could provide to the various processes of higher education.

2. BACKGROUND

Digital data being created as a result of direct, indirect usage of technology and communication when analysed would provide profound data on the teaching- learning trends. This would facilitate in providing recommendations to both the students and the teachers regarding the learning curve. Tools like NodeXL, SNAPP, Gelphi are being utilized by researchers and educational institutions to obtain information regarding learning advancement of a student [5]. "Signals" at Purdue University has helped students, teachers, administrators through the intervention model [6]. With digitalization of most of the activities of a higher educational institution the digital trail left by the student plays an important role in analysing his learning [7].

3. "BIG DATA" IN HIGHER EDUCATION

The environment of higher education is transforming to cater the changing learning needs and diversity of students. Global changes like advancement, availability and ease in use of technology has steered the change in higher education. Though there have been developments in the educational field, the role of data has been overlooked [1]. E-learning technologies have provided a new platform to enhance the teaching learning .The data trails left by them provide higher education institutions actionable data to adapt to the required changes. The data being stored by the higher education institutions along with the digital data being created by the use of technology has resulted in huge chunks of data which can be termed as "Big Data". Big Data is associated with fives V's Velocity, Volume, Variety, Value and Veracity. The same is depicted in the figure 1. The exploration of Big Data in association with higher education would be beneficial in understanding the social, cognitive and emotional aspects of students and teachers.

Educational data is not just humungous data but also heterogeneous data [9]. Traditional data mining approaches are applied to obtain patterns and move towards predication. But mining of educational data tends to focus on development of new tools to determine patterns and apply techniques to analyse large data sets [13]. Due to the sheer volume and variety associated with Big Data the traditional approaches might fall short for deliverance. The big storage requirement is also one of the major concerns to be handled. Big Data is usually associated with no-schema, high scalability. NoSQL data stores like Cassandara, MongoDB, CouchDB try to meet the requirements of "Big Data"

3.1. Big Data Supportive databases

NoSQL databases are inherently schema less and highly scalable [9]. These databases support parallel processing of the large amount of data. MapReduce is a data processing paradigm for squeezing the large volumes of data into useful and comprehensive results [10]. MapReduce provides platform to access data in distributed file systems with intermediate data being stored on

local disks. MongoDB, Cassandra, Accumulo, MonetDB, Apache Hadoop, Hive are few platforms which have emerged to store large chunks of data [11]. This section deals with "MongoDB" and how it is suitable for storing educational data.

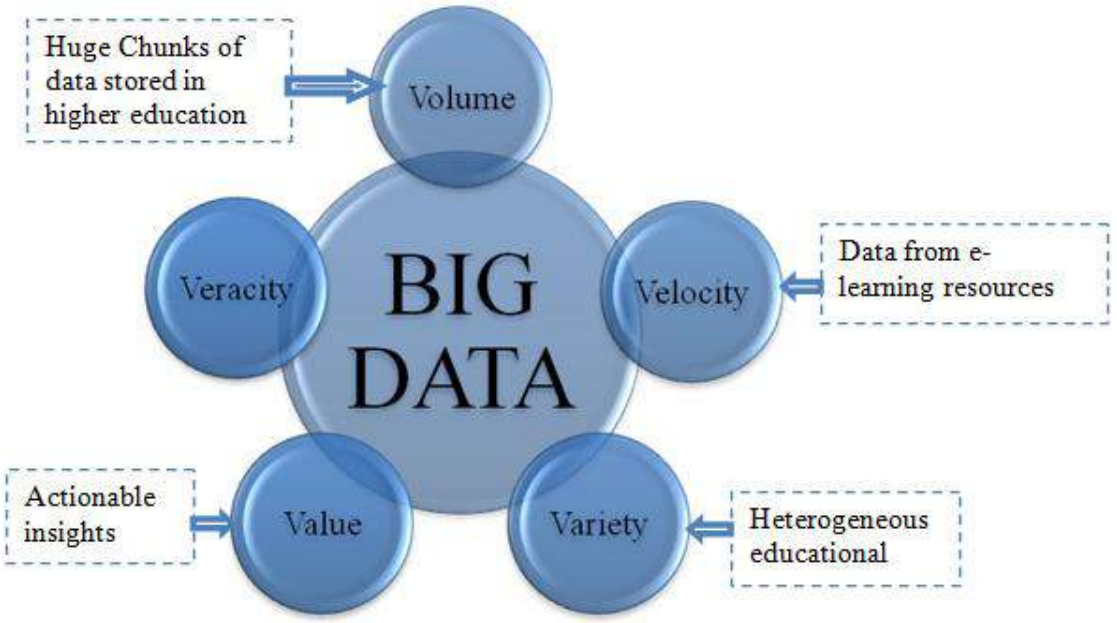

Figure 1: Big Data – Five V's

MongoDB stores data in form of documents which are JSON like field and value pairs [12]. MongoDB documents are BSON, which is binary representation of JSON. All documents are stored in collections. Due to non enforcement of document structure to collections, there is a greater flexibility in mapping a document to an object. To tackle large datasets and the issues of scalability MongoDB uses the concept of "sharding". It achieves sharding through configuration of sharaded clusters [10]. MongoDB provides rich set of aggregation and map-reduce operations to perform aggregation. The two stages of map-reduce: map phase which processes each document and emits one or more objects. Reduce phase that combines the output of map phase. The flexibility and scalability features of MongoDB makes it suitable to store educational data .Few salient features are mentioned in the Table 1.

Table 1: Features of MongoDB

Sno	Feature
1	Schema less document based database
2	MapReduce and Aggregation tools
3	Use of secondary and geospatial indexes
4	Designed for High performance
5	Easy to scale
6	Supports Sharding, Replication and high availability

CRUD operations in MongoDB are simpler and flexible when compared to the traditional SQL statements. The following example depicts the flexibility in storing documents with dynamic schemas which stores student information into the collection "Studentdetails".

Student1= {
"Student_id": "1"
"Deptid":"D1"
"FirstName":"Ravi"
"LastName":"Kumar"
"Age" :20

"Email":ravi.kumar@gmail.com
"CoreCourses": ["Java Programming",
"Computer Networks"],
"InternalAssesmment" :[78,56] }

Student2={
"Student_id": "2"
"Deptid":"D1"
"FirstName":"Geeta"
"LastName":"Rao"
"CoreCourses":[" Java Programming",
"Computer Networks"],
"Certifications":["Oracle","RedHat"] }

3.2. Analytics in higher education

In recent years, there has been increasing focus on the use of data in the processes of educational institutions. Data-driven decisions would help the teaching learning process to evolve and also indulge in creation of new pedagogy. Learning Analytics would pave way to identify the learning patterns and behaviours of students [16]. Few popular methods which being used on educational data are clustering, classification, discovery with models, Association rule mining.

Association Rule Mining (ARM) is one of the most useful methods and has been successfully applied on educational data [18]. Association rule mining is a procedure which is used to find frequent patterns, associations from data sets. Though the main applications of it have been basket data analysis, cross marketing, it would be applicable to the field of education. Association rule consists of two parts: the antecedent which an element available in the data and the consequent which is the element obtained along with the antecedent. These kinds of if/then rules can be applied on educational data to frame a hypothesis which can be investigated further. A sample rule can be "Student spends daily a minimum of a hour in library"$\Longrightarrow$ "Good Learning behaviour". The if/then patterns identified by association rules by analysing the data help in identification of important relationships. In the large data sets of educational data this would provide information regarding the most significant relationship.

4. CONCLUSIONS

Educational institutions are generating huge volumes of data through the admission process, evaluation and teaching learning. The field of education is gaining insight and is obtaining actionable data from large chunks of varied data known as Big Data. With the advent of e-learning provide in many universities, the amount of data available to all the stake holders of the educational system is enormous. The Big Data paradigms are needed in current world to add value to the processes of educational institutions.

REFERENCES

[1] Ben Daniel ,"Big Data and analytics in higher education: opportunities and challenges" , British journal of educational technology 2014.

[2] Ahmed Ashraf,Hazem M, Yehia El-Mashad, Nikos MAstorakis ,"Enhancing Big Data processing in Educational Systems" , Advances in Computer and Technology for Education,2014

[3] Anthony G.Picciano, "Big Data and Learning Anlytics in Blended Learning Environment; Benifits and Concerns", International Journal of Artificial Intelligence and Interactive Multimedia, Vol2, No7,2014

[4] Cattell R (2011) ,"Scalable sql and nosql data stores". ACM SIGMOD Record 39(4):12–27

[5] http://learninganalytics.net/LearningAnalyticsDefinitionsProcessesPotential.pdf <accessed on 2nd October 2015>.

[6] Arnold, K. E. (2010). "Signals: Applying Academic Analytics", EDUCAUSE Quarterly 33(1).

[7] Phil Long and Gorge Siemens ,"Penetrating the fog: Analytics in learning and education", EDUCAUSE Review vol 46,no 5 September/October 2011

[8] A survey of use of weblogs in education, Current developments in technology-assisted education ,1,260-264

[9] Jyotsna Talreja Wassan ,"Discovering big Data Modelling for Educational World" , Procedia- Social and Behavioral Sciences 176(2015) 642-649

[10] https://docs.mongodb.org/manual/core/map-reduce/ <accessed on 5th October 2015>.

[11] http://nosql-database.org/ <accessed on 5th October 2015>

[12] https://docs.mongodb.org/manual/core/crud-introduction/ <accessed on 7th October 2015>

[13] Rmoero.C.R and Ventura.S ,"Educational Data Mining: A Review of the State of the Art" , IEEE Transactions on Systems, Man and Cybernetcs, Part C:Applications and Reviews, 40,6,610-618

[14] Pradeep soni, narendra singh yadav, "Quantitative analysis of document stored databases" International journal of computer applications Volume 118 – No.20, May 2015

[15] Ciprian-Octavian Truică, Alexandru Boicea ,"Operations in MongoDB ", International Conference on Advanced Computer Science and Electronics Information (ICACSEI 2013),

[16] Mr.Suhas G. Kulkarni , Mr.Ganesh C. Rampure , Mr.Bhagwat Yadav ,"Understanding Educational Data Mining (EDM)", International Journal of Electronics and Computer Science Engineering, volume 2, Number 2, 2013.

[17] Rodrigo, M.M.T., Baker, R.S.J.d. (2011) "Comparing Learners' Affect While Using an Intelligent Tutor and an Educational Game", Research and Practice in Technology Enhanced Learning, 6 (1), 43-66

[18] ROMERO, C., ROMERO, J.R., LUNA, J.M., VENTURA, S.," MINING RARE ASSOCIATION RULES FROM E-LEARNING DATA", PROC. OF EDUCATIONAL DATA MINING CONFERENCE, PP. 171–480 (2010)

INTENTIONAL BLANK

FINGERPRINT MATCHING USING HYBRID SHAPE AND ORIENTATION DESCRIPTOR -AN IMPROVEMENT IN EER

Dr. Parvinder Singh[1] and Anisha Rana[2]

[1-2]Department of Computer Science & Engineering
Deenbandhu Chhotu Ram University of Science and Technology, Murthal

ABSTRACT

Fingerprint recognition is a promising factor for the Biometric Identification and authentication process. Fingerprints are broadly used for personal identification due to its feasibility, distinctiveness, permanence, accuracy and acceptability. This paper proposes a way to improve the Equal Error Rate (EER) in fingerprint matching techniques in the domain of hybrid shape and orientation descriptor. This type of fingerprint matching domain is popular due to capability of filtering false and strange minutiae pairings. EER is calculated by using FMR and FNMR to check the performance of proposed technique.

KEYWORDS

Fingerprint, Minutiae, Feature Extraction, Shape Descriptor, Orientation Descriptor, EER

1. INTRODUCTION

In an increasingly digitized world the reliable personal identification has become an important human computer interface activity. Fingerprints are gaining popularity because it is distinct for every person and one need not to remember them like password. Apart of it, Fingerprints are always with a person and one need not to carry like cards.

Fingerprint is a pattern of ridges, furrows and minutiae, which are extracted using inked impression on a paper or sensors. A good quality fingerprint contains 25 to 80 minutiae depending on sensor resolution and finger placement on the sensor [1]. The purpose of ridges is to give the fingers a firmer grasp and to avoid slippage. These ridges allow the fingers to grasp and pick up objects [2]. In a fingerprint image, the ridges appear as dark lines while the valleys are the light areas between the ridges. Minutiae points are the locations where a ridge becomes discontinuous. A ridge can either come to the end, or can split into two ridges, which is called as Bifurcation. The two minutiae types i.e. terminations and bifurcations are of more interest for matching of fingerprints.

II. IMPROVING EER OF FINGERPRINT MATCHING USING HYBRID SHAPE AND ORIENTATION DESCRIPTOR

We propose minutiae based matching technique for fingerprint comparison. This technique improves the EER of fingerprint matching using hybrid shape and orientation descriptor described in [6]. The proposed algorithm is:

Algorithm:

Step 1: We have a database of fingerprints. In this database, 8 impressions of each fingerprint are stored with noticeable differences in region overlap, orientation, image quality.
Step 2: Now we have a fingerprint which has to be matched with the database fingerprints. If this test fingerprint image is in color then it has to be converted it into gray scale image.
Step 3: Convert the gray-scale image to binary image, by using:

$$I(x,y) = \begin{cases} 1 & if\ I(x,y) \geq t \\ 0 & otherwise \end{cases}$$

Where *t* is the threshold

Step 4: Next step is image improvement. For this, following functions are performed:

- ridgesegment() operation performs which returns normalized image.
- ridgeorient() estimates local orientation of ridges (not minutiae).
- ridgefreq() estimates the ridge frequency.
- ridgefilter() finally enhances the fingerprint image via oriented filters.

Watch carefully these operations are performed on ridges (not on minutiae).

Step 5: Then the analysis of this enhanced image is done so that features can be obtained.
Step 6: Now registration is done. It concerns the alignment and overlay of the template and test fingerprints so that corresponding regions of the fingerprints have minimal geometric distance to each other.
Step 7: Now the Orientation descriptor is used which describes the orientation of fingerprint.
Step 8: Now construct shape descriptor. In order to improve accuracy, the shape context includes contextual information, such as minutiae type (i.e., bifurcation and ridge endings) and minutiae angle.
Step 9: Each minutiae is stored in vector form which has 5 values [x, y, cn, Theta, Flag].
Where,

x & y = co-ordinates of a minutiae
Theta = orientation of that minutiae

cn = crossing number
Flag = 0 for permissible minutiae, 1 for non-permissible minutiae.

Step 10: Now transform minutiae (i.e. x, y, theta) according to i-th reference point.

Step 11: Find the best matching using Euclidean distance between both transformed minutiae with the help of

$$r_{affine} = \sqrt{a_{1,x}^2 + a_{1,y}^2} < r_{max}$$

And computes the similarity score by using

$$sim(A,B) = \frac{n_{match}^2}{n_A n_B}$$

Step 12: It compares the test fingerprint to whole database and returns similarity score of all comparisons.
Step 13: Finally returns the matching fingerprint index which has similarity score > threshold value.

III. EXPERIMENTAL RESULTS AFTER IMPLEMENTATION

The experiment is implemented in MATLAB 7.10.0.499 by using FVC2002 DB1 Set B database. Fingerprint images were taken on optical scanner. Image size is 388x374, resolution is 500 dpi and format is .tif. A hybrid shape and orientation descriptor is used for matching the fingerprints. EER value is calculated by using FMR and FNMR.

Following figure shows the similarity between two fingerprints:

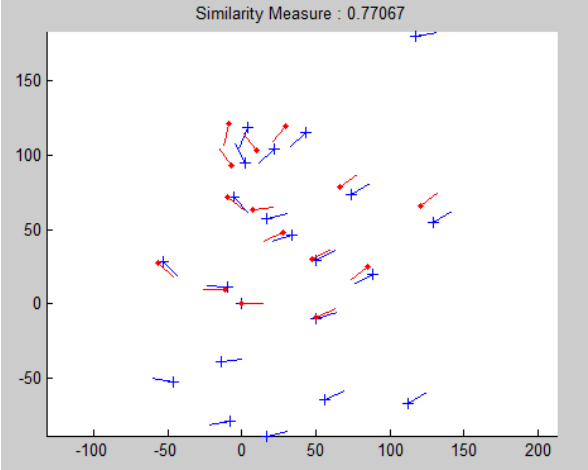

Fig. 2: Similarity measure between two fingerprints

Following graph shows the FMR, FNMR & EER of proposed technique:

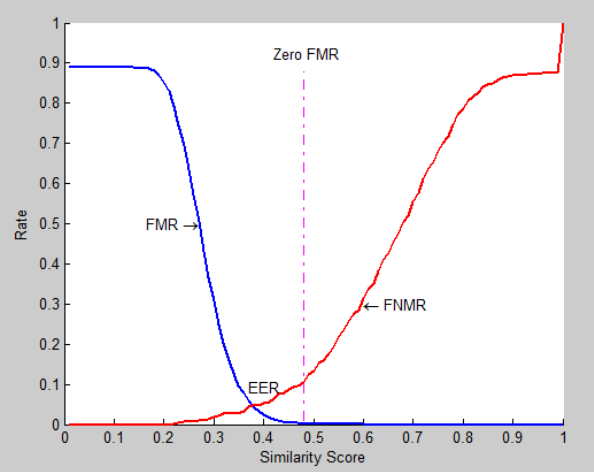

Fig. 3: FMR, FNMR & EER

In the graph, EER value of proposed technique is shown which is 0.37. Because of this value FMR and FNMR curves are intersecting.

Following table summarizes the performance of our proposed algorithm against numerous well-known algorithms on the FVC2002 database:

Table 1: Performance comparison of matching algorithms on FVC2002 Db1 Set B

We see that proposed technique improves the EER by minimizing its value.

Table 1: Performance comparison of matching algorithms on FVC2002 Db1 Set B

Matching Algorithm	EER
CBFS Chikkerur & Govindaraju [8]	1.50
TPS based Kwon et al. [9]	0.92
Meshgrid based Kwon et al. [10]	0.82
Hybrid Spiral based Shi & Govindaraju [11]	1.98
PA08 Maio et al.	0.98
Orientation based Joshua abrahm [6]	0.75
Proposed method	**0.37**

IV. CONCLUSION

We have obtained number of fingerprints from standard databases. In our proposed technique, the fingerprint image is improved using image-processing operations before obtaining features. This paper proposes a way to improve the Equal Error Rate (EER) in fingerprint matching techniques in the domain of hybrid shape and orientation descriptor. Experimental results show that the presented method has the better recognition accuracy compared with the previous recognition methods.

REFERENCES

[1] Ravi. J et al., "Fingerprint recognition using minutiae score matching", International Journal of Engineering Science and Technology Vol.1(2), 2009, 35-42

[2] Muzhir Shaban Al-Ani, "A Novel Thinning Algorithm for Fingerprint Recognition", International Journal of Engineering Sciences, 2(2) February 2013, Pages: 43-48

[3] Pedro Ribeiro Mendes et al., "A Complete System For Fingerprint Authentication Using Delaunay Traingulation", 2010

[4] E. Hastings, "A Survey of Thinning Methodologies", Pattern analysis and Machine Intelligence, IEEE Transactions, vol. 4, Issue 9, pp. 869-885, 1992.

[5] A. K. Jain, F. Patrick, A. Arun, "Handbook of Biometrics", Springer science + Business Media, LLC, 1st edition, pp. 1-42, 2008.

[6] Joshua Abraham, Paul Kwan and Junbin Gao, "Fingerprint Matching using A Hybrid Shape and Orientation Descriptor, State of the art in Biometrics, Dr. Jucheng Yang (Ed.), ISBN: 978-953-307-489-4, InTech, 2011 Available from: http://www.intechopen.com/books/state-of-the-art-in-biometrics/fingerprint-matchingusing-a-hybrid-shape-and-orientation-descriptor

[7] Muzhir Shaban Al-Ani, "A Novel Thinning Algorithm for Fingerprint Recognition", International Journal of Engineering Sciences, 2(2) February 2013, Pages: 43-48.

[8] Chikkerur, S. & Govindaraju, " K-plet and CBFS: A graph based fingerprint representation and matching algorithm", International Conference on Biometrics, 2006.

[9] Kwon, D., Yun, I. D., Kim, D. H. & Lee, S. U, "Fingerprint matching method using minutiae clustering and warping, Pattern Recognition", International Conference on 4: 525–528, 2006.

[10] Kwon, D., Yun, I. D. & Lee, S. U, "A robust warping method for fingerprint matching, Computer Vision and Pattern Recognition", IEEE Computer Society Conference on 0: 1–6, 2007.

[11] Shi, Z. & Govindaraju, " Robust fingerprint matching using spiral partitioning scheme", ICB '09: Proceedings of the Third International Conference on advances in Biometrics, Springer-Verlag, Berlin, Heidelberg, pp. 647–655, 2009.

PREDICTING BANKRUPTCY USING MACHINE LEARNING ALGORITHMS

Abhishek Karan[1] and Preetham Kumar[2]

[1]Department of Information & Communications Technology, Manipal Institute of Technology, Manipal University, Manipal, Karnataka, India
[2] Professor & Head Department of Information & Communications Technology, Manipal Institute of Technology, Manipal University, Manipal, Karnataka, India

ABSTRACT

This paper is written for predicting Bankruptcy using different Machine Learning Algorithms. Whether the company will go bankrupt or not is one of the most challenging and toughest question to answer in the 21st Century. Bankruptcy is defined as the final stage of failure for a firm. A company declares that it has gone bankrupt when at that present moment it does not have enough funds to pay the creditors. It is a global problem. This paper provides a unique methodology to classify companies as bankrupt or healthy by applying predictive analytics. The prediction model stated in this paper yields better accuracy with standard parameters used for bankruptcy prediction than previously applied prediction methodologies.

KEYWORDS

Machine Learning, Classification, Regression, Correlation, Error Matrix, ROC

1. INTRODUCTION

Bankruptcy is a legal status of a firm that cannot repay the debts it owes to creditors. The latest research within the field of Bankruptcy and Predictive Analytics compares various different approaches, modelling techniques, and individual models to ascertain whether any one technique is superior to its counterparts and if so then which all parameters will help better predict the outcome of bankruptcy.

Bankruptcies affect all stakeholders: from employees to regulators, investors or managers. Therefore, it is very interesting to understand the phenomenon that leads to a company going bankrupt in order to take advantage over their competitors. Companies are never protected against going bankrupt. Either in an economic expansion or in a recession, firms are likely to go bankrupt.

Financial ratios are a tool to determine the operational & financial efficiency of business undertakings.

2. LITERATURE REVIEW

2.1 Machine Learning

Machine learning comes under artificial intelligence that provides computers with the ability to learn without being explicitly programmed. It makes the machine learn on its own in overdue

course of time and also with increase in volume of datasets. It focuses on the development of computer programs that can teach themselves to grow and change when exposed to new data in a trained environment.

It is a mature and well-recognized research area of information technology, mainly concerned with the discovery of models, patterns, and other regularities in data. Machine learning is closely related to and often overlaps with computational statistics: a discipline that also specializes in prediction-making. It has strong ties to mathematical optimization, which deliver methods, theory and application domains to the field.

Machine learning is employed in a range of computing tasks where designing and programming explicit algorithms is infeasible. Example applications include spam filtering, search engines and computer vision.

2.2. Predictive Model Approach

There are 5 approaches to follow and create the best model possible with given dataset.

2.2.1. Model Creation

Models are basically algorithms and approaches to deal with certain predictive environment. Many different software models are available which allows to create models to run one or more algorithms on the data set and predict the answers with certain percentage of probability.

2.2.2. Model Testing

Testing models on new and unknown dataset helps us to estimate the accuracy of the constructed model. In most cases, the testing is done on past data to see how best the model predicts.

2.2.3. Model Validation

Validation is also done on previously unknown datasets to tweak and optimize the existing model and hence create an airtight one. Results of these tests are run on visualization tools and business data as well.

2.2.4. Model Evaluation

Evaluate the best fit model from different models used and choose the model right fitted for the dataset. This approach is taken when more than one model have to be compared which is most often than not a general situation. It uses tools like Receiver Operating Curves, Confusion Matrices, Accuracy and Precision.

2.2.5. Deploying of Model

The model created to be deployed in forms of graphs, trees or equations. In real world a simple GUI (Graphical User Interface) is created of the model and presented to the clients.

2.3. Tools Used

1.2.1 R & RStudio
1.2.2 Rattle
1.2.3 Microsoft Excel 2013

R Libraries: Library(rattle), Library(rpart), Library(MASS), Library(e1071), Library(caret) & Library(corrgram)

3. METHODOLOGY

3.1. Dataset

3.1.1. Collection

The Financial Ratios, Bankruptcy Prediction dataset was received from Alto University's Application of Machine learning dataset [5].

3.1.2. Description of Dataset

The dataset consists of 500 samples or instances based on 41 attributes. The Output is a class type variable describing the instance as 'Bankrupt' (250 cases) & 'Healthy' (250 cases). The attributes are financial indicators from several anonymized companies of 2002 for bankruptcy prediction task.

3.1.3. Data Cleaning

3.1.4. The NULL factor

Removing NULLs

If less number of NULL values are present in dataset as compared to actual number of records, then those records can be removed.

Domain Expertise

Domain experts can contribute valuable knowledge with respect of data quality, i.e. selection of attributes /data quality.

Mark as N.A

Certain NULL values can be replaced with 'N.A' values for easier calculations in statistics [13]. This dataset doesn't contain any missing values.

3.1.5. The Outlier Factor

Removing outlier through Box Plot

Box Plot of all attributes are drawn. The values which are irrelevant, outliers and are not making sense to the dataset are removed.

Sorting

Each attribute is sorted in any order (Ascending/Descending). Values which seems to be absurd or out of bounds are removed.

After applying the Outlier methodology, 59 records were removed. Now, the dataset contains 441 samples based on 41 attributes and 1 Target variable (Bankrupt).

3.1.6.The Correlation Factor

Correlation is statistical tool which is used to measure the degree to which the movements of independent variables or attributes are related. Correlations are useful because they can indicate a predictive relationship that can be exploited in practice. The correlation coefficient, often denoted 'ρ' or 'r', measures the degree of correlation. The most common of these correlations is the Pearson correlation coefficient (used in this paper as well), which is sensitive only to a linear relationship between two variables. The correlation is defined as:

$\rho_{x,y} = E\,[(X-\mu_x)\,(Y-\mu_y)] \,/\, (\sigma_x\,\sigma_y)$ Where μ_X and μ_Y are expected values & σ_X and σ_Y are standard deviations. E is the expected value operator. The correlation coefficient 'r' ranges from -1.0 to +1.0. The closer it is to +1 or -1, the more closely the two variables are related.

1. If 'r' is close to 0, it means there is no relationship between the variables.
2. If 'r' is positive, it means that as one variable gets larger the other gets larger.
3. If 'r' is negative it means that as one gets larger, the other gets smaller (an "inverse" correlation).

3.1.7. Correlation Matrix

Correlation Matrix is a matrix giving the correlations between all pairs of data sets. The Correlation between the target variable and other predictors is viewed in this matrix. These 2 predictors have the least correlation with Bankrupt (1 = Healthy, 2 = Bankrupt)

Total Sales/Total Assets: -0.007816907
Labor Expenses/Total Sales: -0.002093413

Correlation Plot

The Correlation Plot helps us to visualize the data in correlation matrices. The correlation values of predictors Total Sales/Total Assets & Labor Expenses/Total Sales is the least with target variable (Bankrupt) from the correlation matrix as well as the correlation plot. After applying the Correlation Factor, 2 columns (Total Sales/Total Assets & Labor Expenses/Total Sales) were removed from dataset. Now, the dataset contains 441 samples based on 39 attributes and 1 Target variable (Bankrupt).

3.1.8. The Mean & Median Factor

The summary of entire dataset is found which contains the Mean, Median, Minimum, Maximum values along with 1st and 3rd quartiles in R. Predictors having very different Mean and Median are removed as that data seems to be faulty. But as a judgement call certain predictors are not removed because they share high affinity with those of real world bankruptcy factor.
Duplication of Column names

There are 2 columns with same names (LI7 Quick Assets/Total Assets & LI9 Quick Assets/Total Assets). We remove the L19 column. Now, the dataset contains 441 samples based on 38 attributes and 1 Target variable (Bankrupt).

3.2. Distribution of Dataset

In building a model 70% subset of all of the available data is used. We call this 70% sample as training dataset. The remainder is split equally into a validation dataset (15%) and a testing dataset (15%).

1. The validation dataset is used to test different parameter settings or different choices of variables. It is important to note that this dataset should not be used to provide any error estimations of the final results from machine learning algorithms since it has been used as part of the process of building the model.
2. The testing dataset is only to be used to predict the unbiased error of the final results. It is also a new and previously unknown dataset.

In our Model the dataset is divided into 70/30. There is no validation dataset. Only Training (70%) & testing (30%) dataset is present. The division of samples into testing and training datasets are done randomly, keeping in mind the seed value for the random function used for distribution.

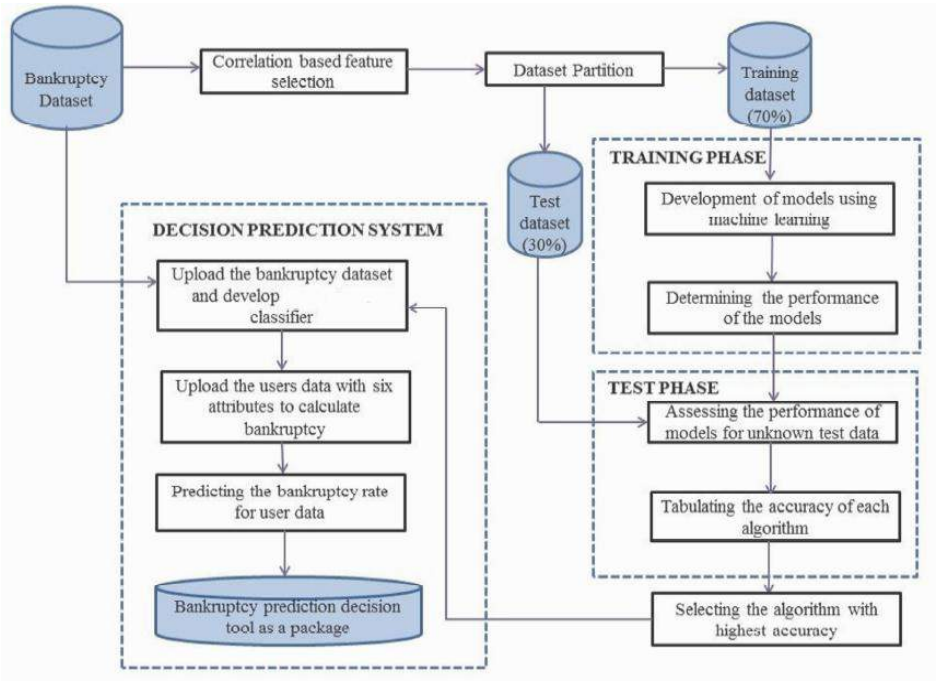

Figure 1: Decision Support System for predictive Bankruptcy [1]

3.3. Building a Model

3.3.1. Classification Algorithm

Following algorithms are used in the paper

1. Decision Tree
2. SVM (Support vector machines)
3. Logistic Regression

Decision Tree

The building of a decision tree starts with a description of problem which should specify the variables, actions and logical sequence for a decision-making [10]. In a decision tree, a process leads to one or more conditions that can be brought to an action or other conditions, until all conditions determine a particular action, once built you can have a graphical view of decision-making[4]. The tree model is created using the "rpart" library of R.

Which variables are best Classifiers?

The answer to this lies in Entropy and Information Gain.

Entropy: Entropy characterizes the purity or impurity of an arbitrary collection of examples. It is defined as:

$$Entropy(S) = (-p_{+}log_2 p_{+}) + (- p_{-} log_2 p_{-}) \quad [16]$$

Where S is a collection. Entropy is very common in Information Theory.

Information Gain: Information Gain measures how well a given attribute separates the training examples according to their target Classification. Entropy is a fundamental attribute in finding this gain. It is defined as:

$$Gain\ (S, A) = Entropy\ (S) - \sum |S_v| / |S| * Entropy\ (S_v)$$ [16] Where S is a collection and A is a chosen attribute.

The best Classifiers for this dataset are:

1. Accounts Receivable/ TotalSales
2. Cash Total Debt
3. Net Income Shareholder's Funds
4. Profit before Tax/Shareholder's Funds
5. Shareholder's Funds/Total Assets

After getting these parameters from R we create a decision tree. This tree may be subjected to overfitting so we chose to prune this tree on basis of certain parameters as discussed below

Table 1: 'rpart' Result of Decision Tree

CP	*NSPLIT*	*REL_ERROR*	*XERROR*	*XSTD*
0.753695	0	1.000000	1.00000	0.051561
0.093596	1	0.246305	0.28571	0.034962
0.019704	2	0.152709	0.21182	0.030687
0.014778	4	0.113300	0.23645	0.032218
0.010000	5	0.098522	0.23153	0.031921

Table 2: Confusion Matrix and Statistics before pruning

Predicted	**Actual**		
		1	2
	1	57	5
	2	3	67

Pruning is a technique in decision tree model of machine learning that reduces the size of decision trees by removing sections of the tree that provide little power to classify instances. Pruning reduces the complexity of the final classifier, and hence improves predictive accuracy by the reduction of overfitting [8].

The 'rpart' function in R gives 3 important columns:

- rel_error,
- xerror
- xstd

Cross-validation error will actually grow as the tree gets more levels (at least, after the 'optimal' level). The optimum value is usually the lowest level where the (rel error + xstd) < xerror [15]. As per table 1, lowest level is level 3 thus advisable to prune at level 3.

Also, after plotting the graph of xerror (cross validation error) as shown in figure 2, it was very clear that the least error was found at 3rd level where CP value is: 0.019704. Hence, the optimal level of tree is till 3rd.

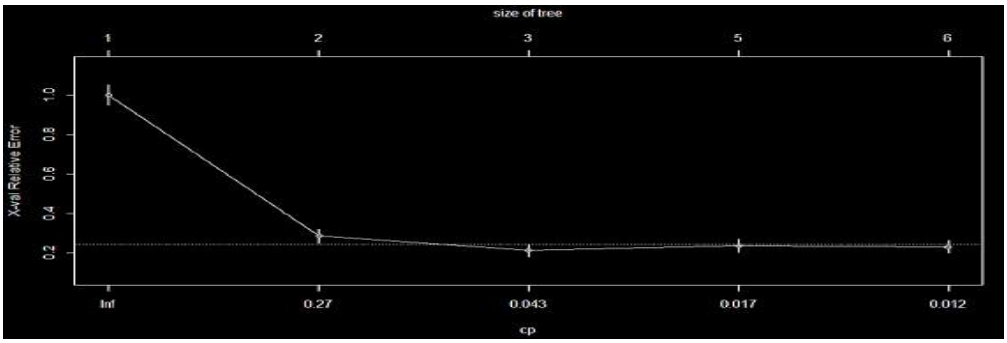

Figure 2: 'xerror' Plot of Decision Tree

Based on the above 2 factors, optimal level of pruning is at level 3.

Table 3: Decision Tree confusion matrix after Pruning

Predicted	**Actual**	
	1	2
1	58	6
2	2	66

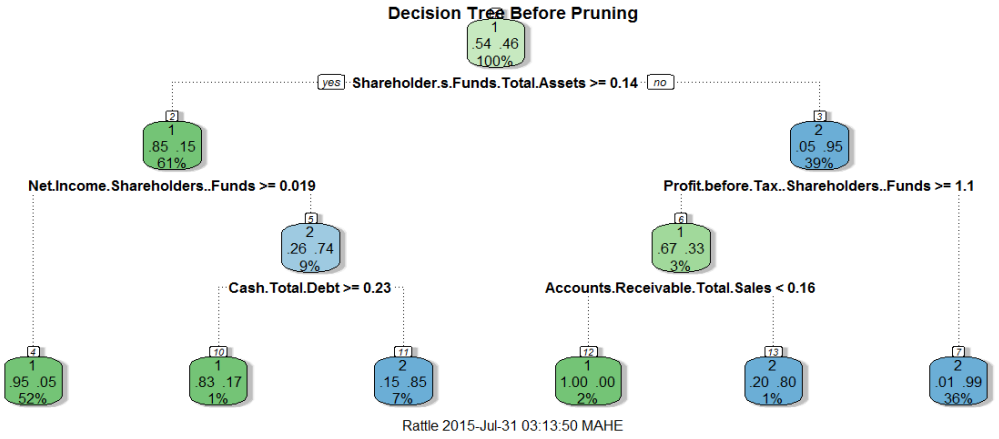

Figure 3: Decision Tree before Pruning

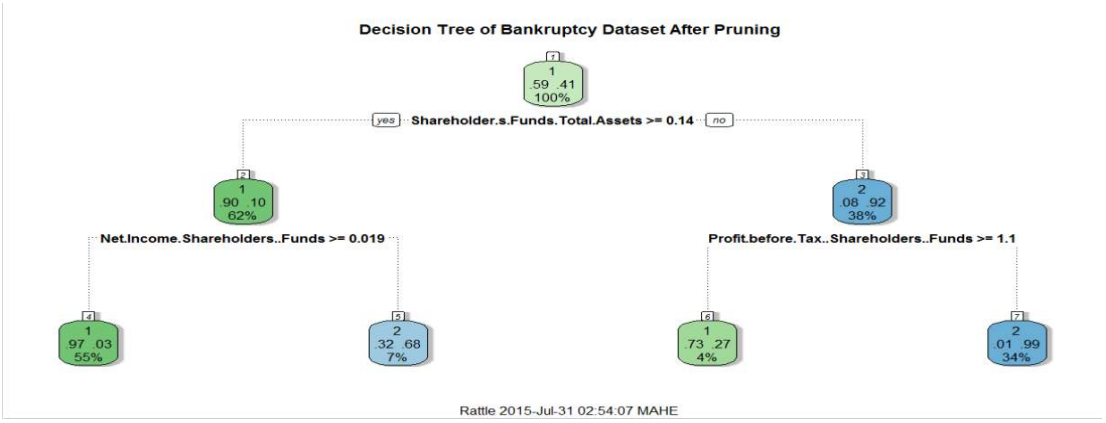

Figure 4: Decision Tree after Pruning

Decision Tree Traversal Rules from Rattle:

Rule #7:
Bankrupt=2 cover=132 (34%) prob = 0.99
Shareholder's Funds / Total Assets < 0.14
Profit before Tax/Shareholder's Funds < 1.1

Rule #5:
Bankrupt=2 cover=16 (7%) prob = 0.68
Shareholder's Funds / Total Assets >= 0.14
Net Income Shareholder's Funds < 0.01906

Rule #6:
Bankrupt=1 cover=12 (4%) prob = 0.27
Shareholder's Funds / Total Assets < 0.14
Profit before Tax/Shareholder'sFunds >=1.1

Rule #4:
Bankrupt=1 cover=148 (55%) prob = 0.03
Shareholder's Funds / Total Assets >= 0.14
Net Income Shareholder's Funds >= 0.01906

Support Vector Machine (SVM)

Basic idea of support vector machines:

An optimal hyperplane for linearly separable patterns is used. Extend the patterns that are not linearly separable by transformations of original data to map into new space – Kernel function.

- SVMs Support vectors Maximize margin.
- SVMs maximize the margin around the separating hyperplane.
- The decision function is fully specified by a subset of training samples, the support vectors.

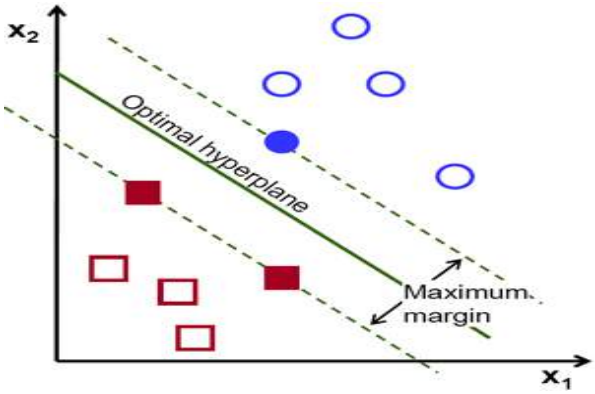

Figure 5: SVM Hyperplane [7]

Factors that influence SVM Model [9]

1. Cost (c): Measure of misclassification.

'c' is the parameter for the soft margin cost function, which controls the influence of each individual support vector. This process involves trading error penalty for stability. A large 'c' gives low bias and high variance. Low bias because it penalizes the cost of misclassifications a lot.

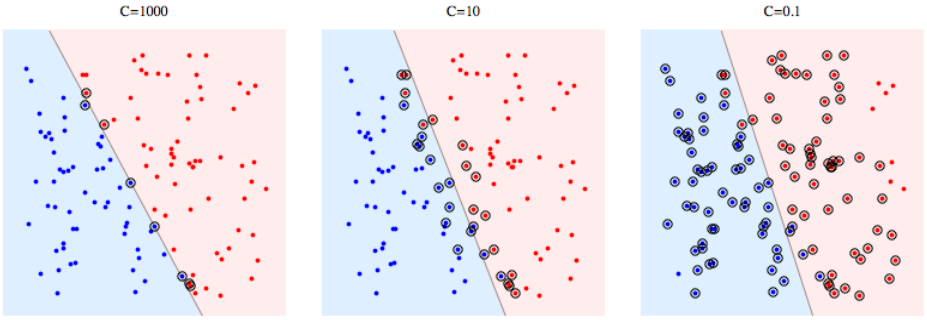

Figure 6: Cost Representation

2. Gamma:

Raise a hyperplane between blue circles and red squares from figure 8. Peak measures Gamma. It is the parameter of a Gaussian Kernel (to handle non-linear classification). They are not linearly separable in 2D so it should be transformed to a higher dimension where it'll will be linearly separable. Imagine "raising" the blue points, then it can be separated from the red points with a plane (hyperplane). To "raise" the points use the RBF kernel function. Gamma controls the shape of the "peaks" where the points are raised. A small gamma gives a pointed bump in the higher dimensions, a large gamma gives a softer, broader bump. So a small gamma will give low bias and high variance while a large gamma will give higher bias and low variance.

- The optimal gamma and cost factors are chosen.
- The SVM Model is created using the "e1071" library in R.
- Error Matrix is created to check the accuracy of the model.

Table 4: Snapshot of SVM Performance Results

S.NO.	*GAMMA*	*COST*	*ERROR*	*DISPERSION*
1	0.001000	1	0.11241808	0.02928308
2	0.010000	1	0.07524877	0.02914474
3	0.100000	1	0.11797534	0.0274428

Summary Result of SVM Function Model from R:

1. Best parameters: Gamma=0.01, Cost=1
2. Best performance: 0.07524877

3.3.2. Regression Model

Logistic Regression
Logistic Regression seeks to:

1. Model the probability of an event occurring depending on the values of the independent variables, which can be categorical or numerical.
2. Estimate the probability that an event occurs for a randomly selected observation versus the probability that the event does not occur.
3. Predict the effect of a series of variables on a binary response variable(1 & 0)
4. Classify observations by estimating the probability that an observation is in a particular category (such as approved or not approved).

To understand Logistic Regression first understand Odds.

- Odds = P(Occurring of an event) / P(Not Occurring of the event)

Odds Ratio:

- Odds Ratio = odds1 / odds2

The dependent variable in Linear Regression follows Bernoulli distribution having an unknown probability 'p'. In Logistic Regression we are estimating an unknown 'p' for any given linear combination of independent variables. Thus we need to link together our independent variable to Bernoulli distribution, this link is called LOGIT. Bernoulli is a special case of Binomial distribution where n=1.

Now, when the points on graph follows an approximately straight line. $\boldsymbol{Logit\ (p) = \beta_0 + \beta_{1x}}$ Although this model looks similar to a simple linear regression model, the underlying distribution is binomial and the parameters β_0 and β_1 cannot be estimated in exactly the same way as for simple linear regression. Instead, the parameters are usually estimated using the method of Maximum Likelihood Estimation (MLE).

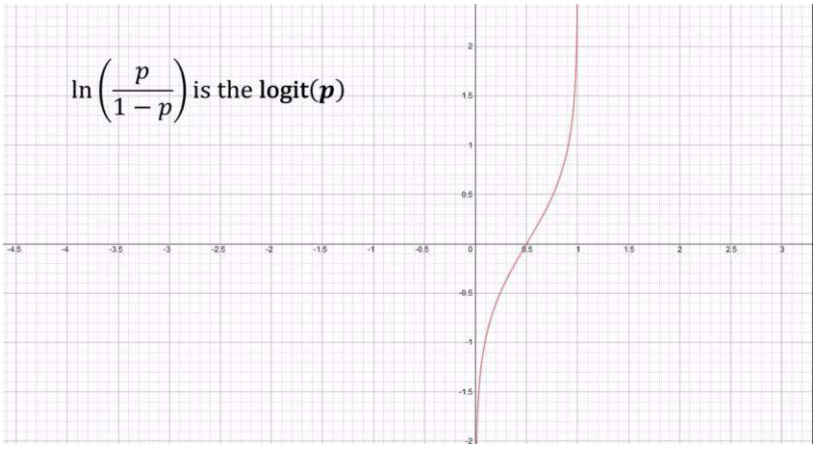

Figure 7: Log Curve

To get Probabilities on Y-Axis we take its inverse.

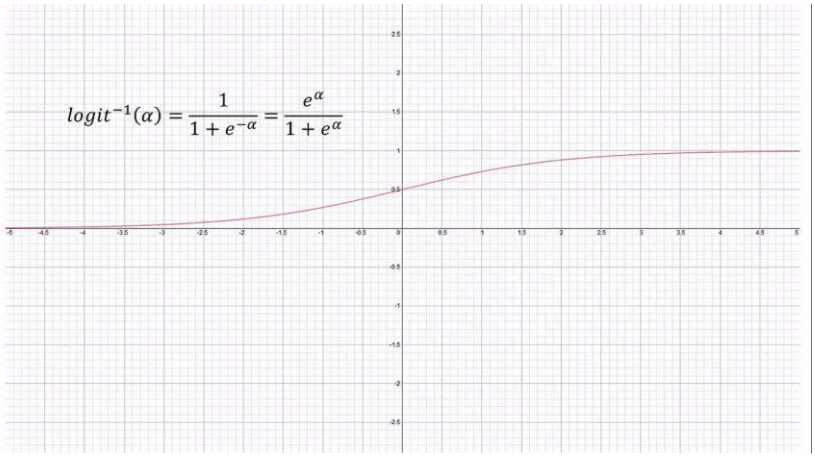

Figure 8: Inverse Logit Curve

Where $\boldsymbol{a = \beta_0 + \beta_{1x}}$ Thus, the Logistic function can now be written as: $\boldsymbol{F(x) = 1/(1 + e^{-(\beta 0 + \beta 1x)})}$
Where β_0 and β_1 are coefficients for input variable x. F(x) is the probability of the event to occur.

The value of F(x) ranges from zero to one.

Approach Taken for Logit Regression

Using all 38 variables:

Firstly, the Logit Model was made using all available 38 variables:

1. This gave very low AUC (Area Under Curve) value of 0.9097 compared to other models.
2. Also, this gave high p-value test results for a lot of variables.
3. Using 16 Variables

Finally only 15 variables were chosen which has acceptable p-values of less than or equal to 0.05 Same, Logit Model test was done in this new dataset of 15 variables.

Following are results.

- High AUC of 0.9697
- High Accuracy of 94.73%

3.4. Evaluating Model

After all the machine learning models are created they are then evaluated on the basis of test dataset.

3.4.1. Error Matrix

3.4.2.

An Error matrix is a table that is used to describe the performance of a classification model (or "classifier") or regression model on a set of test data for which the true values are known. It is also known as a contingency table or a confusion matrix.

Table 5: Decision Tree Error Matrix

Predicted	**Actual**		
	1	2
1	58	6
2	2	66

Table 6: SVM Error Matrix

Predicted	**Actual**		
	1	2
1	57	10
2	3	62

Table 7: Logistic Regression Error Matrix

Predicted	**Actual**		
	1	2
1	78	2
2	5	48

3.4.3. Receiver Operating Characteristic (ROC) [3]

3.4.4.

ROC curve, is a graphical plot that assesses predictive behaviour independent of error costs or class distributions. The curve is created by plotting the true positive rate (TPR) against the false positive rate (FPR) at various threshold settings.

- True positive (TP): The actual negative class outcome is predicted as negative class from the model.
- False positive (FP): The actual negative class outcome is predicted as a positive class outcome.
- False negative (FN): The actual positive class outcome is predicted as negative class from the model.
- True negative (TN): The actual class outcome excluded is also predicted to be excluded from the model.

Positive is taken as the company going bankrupt (Bankrupt=2) and Negative is taken as company being healthy (Bankrupt=1).Based on these four parameters the performance of algorithms can be adjudged by calculating the following ratios.

- Accuracy (%) = (TP + TN) / (TP +FP +TN + FN)
- TPR (%) = TP / (TP + FN)
- FPR (%) = FP / (FP + TN)
- Precision (%) = TP / (TP +FP)

ROC curve represents the accuracy of a classifier or Model. Accuracy, Area under Curve & Precision were calculate for all models and represented in Table 10.

Table 8: Result of Bankruptcy prediction using machine learning algorithm

S.NO.	***RESULT***	***ACCURACY***	***AUC***	***PRECISION***
1	Decision Tree	93.94 %	0.9423	97.05 %
2	SVM	90.15 %	0.9495	95.38 %
3	Logistic Regression	94.73 %	0.9697	93.97 %

Summary from Rattle:

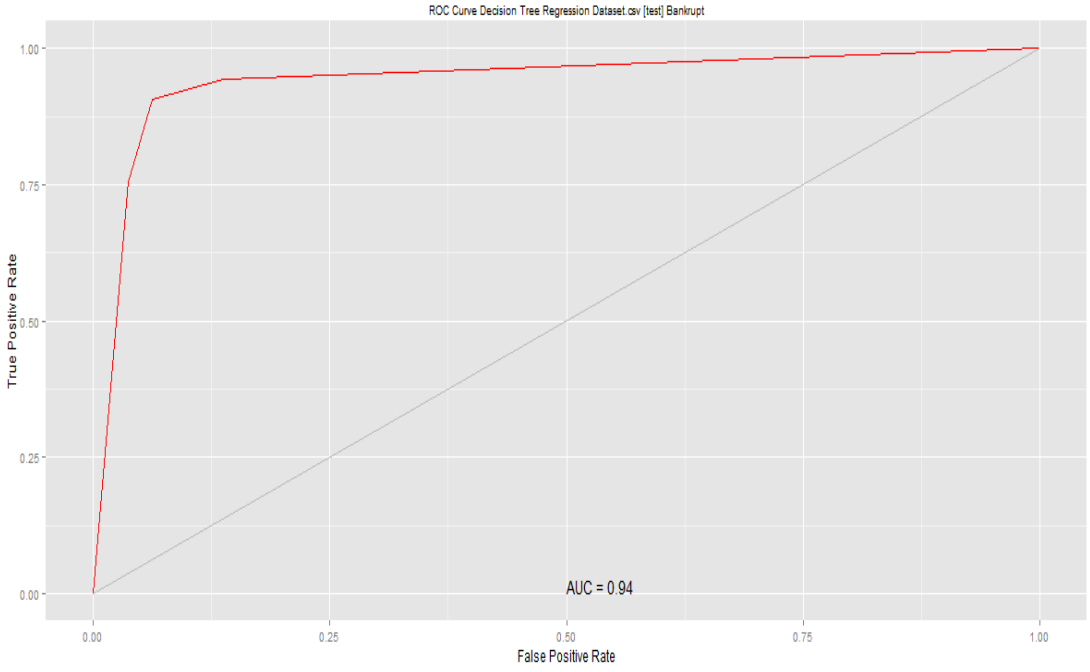

Figure 9: ROC of Decision Tree

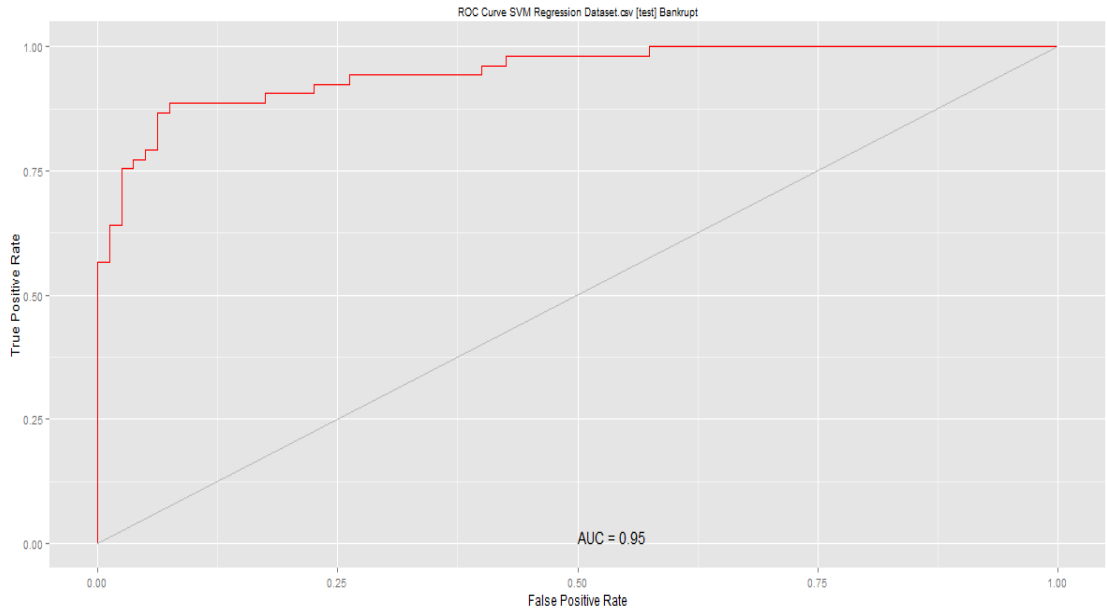

Figure 10: ROC of SVM

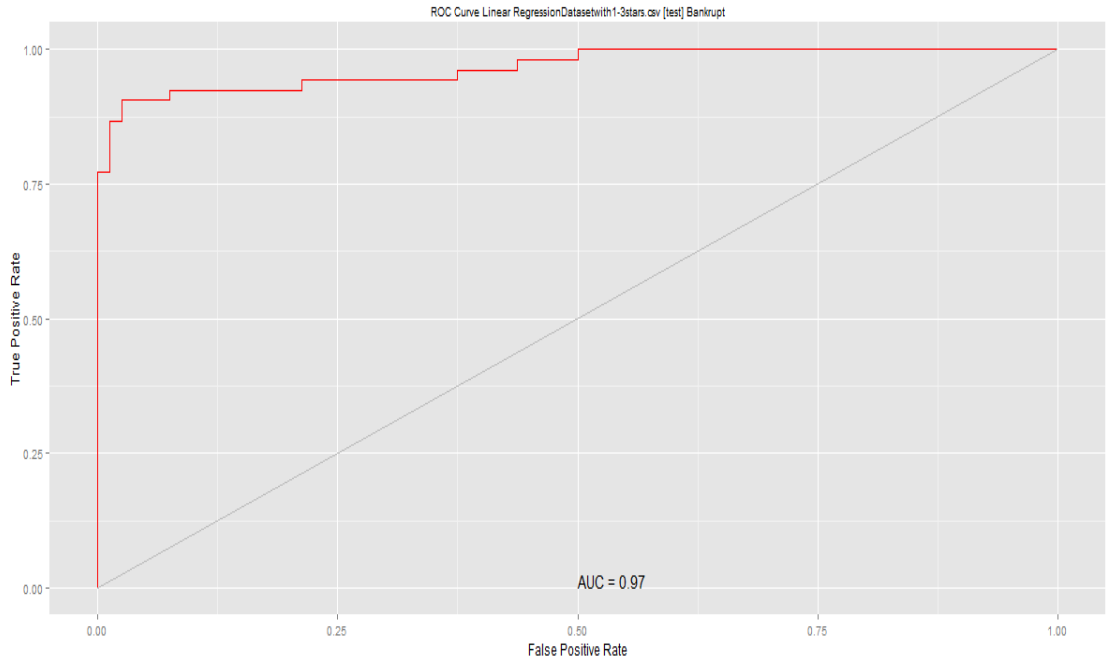

Figure 11: ROC of Logistic Regression

4. RESULT

Accuracy, Area under Curve (AUC) & Precision were calculated for all models and represented in the table 8. Logistic Regression has highest Accuracy and Precision and very high value of Area under Curve from ROC. Hence, Logistic Regression is chosen as it has outperformed other machine learning algorithms.

5. CONCLUSION

In this paper we presented an efficient classification model using Logistic regression for predicting Bankruptcy for an organization. The experimental result shows that after iteration of model with different number of variables improved the effectiveness and efficiency of the model. The experimental result suggests that Logistic regression seems to be more accurate machine learning algorithm for prediction of bankruptcy.

5.1. Limitation of study

- Data is not adjusted for Inflation and seasonal changes. Thus, Results may differ.
- This dataset includes many companies but for different business domains like manufacturing, finance, ecommerce and medical which usually have their own peculiarity and similarities, this model should be used with caution.

5.2. Suggestions

- Researchers should work on Industry based modeling.
- Three algorithms have been used in this paper, however more algorithms like Naïve Bayes, Genetic, and KNN exists.
- Each country has their own laws, culture, socio demographic patterns and economical status. To get reliability in predictions, country wise parameters must be included.
- The study should be done for longer periods.

REFERENCES

[1] Kalyan Nagaraj,Amulyashree Sridhar,(January 2015) "A Predictive System for Detection of Bankrupty using Machine Learning Tecniques", IJDKP-Vol.5, No.1.
[2] Graham Williams,(January 1, 2011) "Data Mining With Rattle and R_ The Art of Excavating Data for Knowledge Discovery".
[3] Sadiq Hussain, G.C. Hazarika, (2014) "Educational Data Mining Model Using Rattle" Vol. 5, No. 6
[4] Prajwala T R,(January 2015) "A Comparative Study on Decision Tree and Random Forest Using R Tool", IJARCCE,-Vol. 4, Issue 1
[5] Financial Ratios, Bankruptcy Prediction –"http://research.ics.aalto.fi/eiml/datasets.shtml"
[6] Eibe Frank ,(January 2000) "Pruning Decision Trees and Lists"
[7] R. Berwick, "An Idiot's guide to Support vector machines (SVMs)"
[8] Tree Based Model, 'http://www.statmethods.net/advstats/cart.html'
[9] SVM hard or soft Margins, 'http://stackoverflow.com/questions/4629505/svm-hard-or-softmargins'
[10] M.A. Sprengers (21st August 2005) "Bankruptcy Prediction Using Classification and Regression Trees".
[11] Charles X. Ling , Jin Huang, 'AUC: a Better Measure than Accuracy in Comparing Learning Algorithms'.
[12] Qi Yu, Amaury Lendasse and Eric S´everin,'Ensemble KNNs for Bankruptcy Prediction.
[13] Q. Yu, Y. Miche, A. Lendasse and E. Séverin,'Bankruptcy Prediction with Missing Data'.
[14] Correlation and dependence 'https://en.wikipedia.org/wiki/Correlation_and_dependence'
[15] 'http://stackoverflow.com/questions/29197213/what-is-the-difference-between-rel-error-and-x-error-in-a-rpart-decision-tree'-Stack OverFlow
[16] Tom Mitchell (1997), Machine Learning, McGraw Hill.

INTENTIONAL BLANK

MANET ROUTING PROTOCOLS ON NETWORK LAYER IN REALTIME SCENARIO

Mamata Rath*, Binod Kumar Pattanayak** and Bibudhendu Pati***

*C.V.Raman Computer Academy,Bhubaneswar,India
**Department of Computer Science and Engineering, Siksha 'O' Anusandhan University, Bhubaneswar,India
***Department of Computer Science and Engineering, C. V. Raman College of Engineering, Bhubaneswar,India

ABSTRACT

A Mobile Ad hoc Network comprises of a group of mobile nodes that are connected in wireless medium and they dynamically form a self-organizing mobile network for temporary period of time. Due to ease of deployment, MANET is very effective in situations where it is difficult to create infrastructure based network. Nodes in a MANET are self configured and self governed without being controlled by any central administrator. Mobile Adhoc Network (MANET) has always been a rising technology which supports real time multimedia transmission service, a common trend in current communication technology that uses maximum real time applications with dynamic mobility of the mobile devices. Offering Quality of Service is also an important parameter during communication in real time scenario.Many routing protocols for Mobile Adhoc Network Supporting Real Time Applications have been developed, basic intention being maximum utilization of resource in resource constraint environment, minimum power consumption using limited residual battery power of the highly movable mobile nodes. This paper presents an intensive study and analysis of MANET based effective routing protocols and secondly, it provides report on comparative analysis of efficient real time supported protocols based on power consumption, delay analysis and packet delivery ratio.

KEYWORDS

MANET,AODV,PDR,Throughput,Delay,Real Time Appliction

1. INTRODUCTION

Real time data transmission in Mobile Adhoc Network is a challenging issue due to the self-directed nature of mobile devices which are connected with each other by wireless links. Nodes frequently changes their position and location by forming a network without any base or any infrastructure. Careful considerations have to be made during designing the protocols for real time data transmission which are highly sensitive. Common challenges faced by real time data during transmission are energy utilization, scalability of the network, optimized use of bandwidth, resource reservation, reducing chance of link failure, security, take care of Qos, dynamically changing topology etc.

2. LITERATURE REVIEW

Many researchers have done analysis e regarding successful transmission of real time data over MANETs, some of which are discussed in this section. Scheduling algorithms basically classifies

and categorizes high priority-based real time applications to enhance the efficient delivery of realtime packets in the channel. In paper[11] five types of such scheduling algorithms are examined under real time traffic condition. They are First-In-First-Out (FIFO) Scheduling Algorithm, Priority Queuing Algorithm, Weighted Fair Queuing (WFQ) Algorithm, Class Based Weighted Fair Queuing (CBWFQ) Algorithm and Low Latency Queuing (LLQ) Algorithm.After simulation was done in OPNET, the results were compared and evaluated for the following parameters for the above five algorithms.a.Voice traffic receivedb. video traffic receivedc. voice packet end-to-end delay d. voice packet delay variation.In every case the performance of LLQ algorithm was found to be better with lower delay and higher throughput.

In a dense MANET scenario, where the source is situated far away from the destination, proper data delivery for real-time video streaming is a difficult task. In video traffic flows which is too heavy and need to be continuously flowed without interruption, so sending packets continuously without pause causes congestion of its own flow.In [3] the authors propose a method of periodically delaying the realtimedata transmission specifically video stream at source itself just to avoid more congestion at the next-hop relaying node level.

3. REAL TIME TRAFFIC AND ROUTING PROTOCOLS

Detail study and analysis of Real Time Protocols have been done in this section. Table 1. Provides description of studied protocols and analysis based on Real Time Support.

Table.1 Details of studied and analyzed Protocols

Sl.No	Literature	Year	Protocol/Proposal	Feature	Advantage	Simulation Tool
1	D.Tardioli, *et al* [1]	2015	RT-WMP Real Time Wireless Manet Protocol	Proposes a cross-layer strategy with a novel MAC mechanism	Priority ad mobility support for real-time communications	Real-world application Linux Kernel
2	H.Xie, *et al* [2]	2015	An error-recovery mechanism is proposed for real-time video streaming called MERVS	Transmission of video through multiple channels and priority queue is used	High quality video streaming with FEC (Forward Error Correction)	NS2
3	P.Sondi, *et a*l [3]	2014	A new MANET based strategy to handle real time application is presented	At source periodical delay is maintained to avoid congestion and hence avoids interruption	30% improvement in delivery of video packets between source and destination	OPNET
4	G.Yasin, *et al* [4]	2013	Performance comparison of protocols	Study of different routing protocols, specifically OLSR,AODV,DSR, TORA	Gives idea about the routing nature for real time traffic	OPNET
5	I.Ahmad, *et al* [5]	2013	TSBR-Time Slot Bandwidth Reservation	Presents a technique that provides better QoS using time-slot bandwidth	Reduces queuing delay	NS2

				reservation method		
6	P.Vijaya Kumar, *et al* [6]	2013	A Multicast tree structure protocol	Challenge of transmission of multimedia stream is investigated	A new technique for multimedia stream is presented here	NS2
7	Z.Yuan, *et al* [7]	2013	iPAS-intelligent Prioritized Adaptive Scheme	Mainly discusses suitable routing method for multimedia data	Proposes an efficient scheme called iPAS(Intelligent Prioritised Adaptive Scheme)	Real-life test bed set up with multimedia server
8	R.Viegas, *et al* [8]	2013	A new Real time communication scheme	Proposes a new idea to prioritize real time flow in a network	Proves better throughput for real time data flow	NS2
9	D.Sicignano, *et al* [9]	2013	Real time multi-hop protocol with Qos extension	Proposes the use of multi-hop adhoc network to provide multimedia communication between mobile nodes	Use of low cost s/w and h/w platform to run the protocol, easy to set up solution.	Real application in Somport tunnel, France
10	J.Boksiner, *et al* [10]	2013	MRFM-MANET Real time Frequency Management approach is proposed	Frequency re-use automation, and spectrum sharing with centralized control	Dynamic Spectrum Access capability among MANET radio layer	Real implementation in android device
11	P.Rukmani, *et al* [11]	2013	Analysis of five scheduling algorithm for real time transmission	Voice and video traffic simulated using WFQ & LLQ algorithm.	LLQ(Low Latency Queuing) algorithm improves the overall performance of real time applications	OPNET
12	H.Mewara, *et al* [12]	2013	Evaluation of protocols based on Pattern of traffic and Node density	AODV,DSR,OLSR,TORA are evaluated for delay, n/w load, throughput	Gives a better knowledge of protocol selection for Qos-aware traffic.	OPNET Ver 14.5
13	G.Aujla, *et al* [13]	2013	Evaluation of Behavior of GRP,TORA,OLSR protocols for video conferencing application	Simulation shows that TORA has highest throughput in most scenarios.	Better analysis of protocols to select a suitable one for real time transmission.	OPNET Modeler 14.5
14	C.Lal, *et al* [14]	2013	QARP-Qos Aware Routing Protocol using cross-layer design proposed	Session Admission Control method is used in the protocol	Normal periodic message format can be extended to minimize the effect of mobility	NA

In paper [9] a survey of multi-path video transmission in MANETs has been done. Parameters which were considered during the analysis were Coding methods, Optimal number of streams, video data rate, multi-path routing etc. A coding intrusive algorithm was presented for choosing optimal parameters for successful "network friendly" video transmission over MANET.

4. COMPARATIVE ANALYSIS OF REALTIME PROTOCOLS

Three important real time supported protocols were selected for their performance comparison and analysis to highlight on the functionality used by them in order to improve the network performance in real time scenario. They are RT-WMP[1], MCT[6] and MRFM [10] approach with Real Time Support.

Table 2. Describes studied performance of the three selected protocols.

Table 2. Comparison of Network Performance Parameters in three leading protocols

Protocol	Power Consumed	End to end delay	Network Life time	PDR	QoS Support
RT WMP	Low	Low	More	High	Medium
MCT	Medium	Medium	Medium	Medium	Low
MRFM	High	High	Low	low	High

5. SIMULATION AND RESULT

We have done simulation of above considered protocols for their performance evaluation based on Packet Delivery Ratio, Power Consumption, Delay and Network Lifetim .Ns 2.35 simulation tool was used for simulation purpose.120 number of nodes were scattered randomly in an area of 2000 x 2000m during beginning of the simulation. In mobility scenario, mobiles nodes were moving in six different speeds within a range of 0 to 10 m/s. Table 3 shows the simulation parameters used in the simulation.

Table 3. Simulation Parameters

Simulation parameters	Data/Value
Channel Type	Wireless Channel
MAC Protocol	802.11
Traffic Type	CBR
Packet Size	512 Bytes
No. of Mobile Nodes	120
Simulation Time	600 seconds (10 mins)
Simulation area	2000 x 2000 m
Protocols Name	RTWMP,MCT,MRFM
Model for Node Movement	Random way point
Data rate	11 mbps
Application Type	Video Transmission (Real Time)
Bandwidth	2Mb/s for both
Simulator	Ns2.35

Comparative analysis of the three discussed protocols has been done in the following section based on network parameters such as power consumption, delay rate, packet delivery ratio and network lifetime.

Fig.1 shows the comparison between three Protocols for packet delivery ratio nd it was observed that RTWMP performs better than MCT and MRFM.

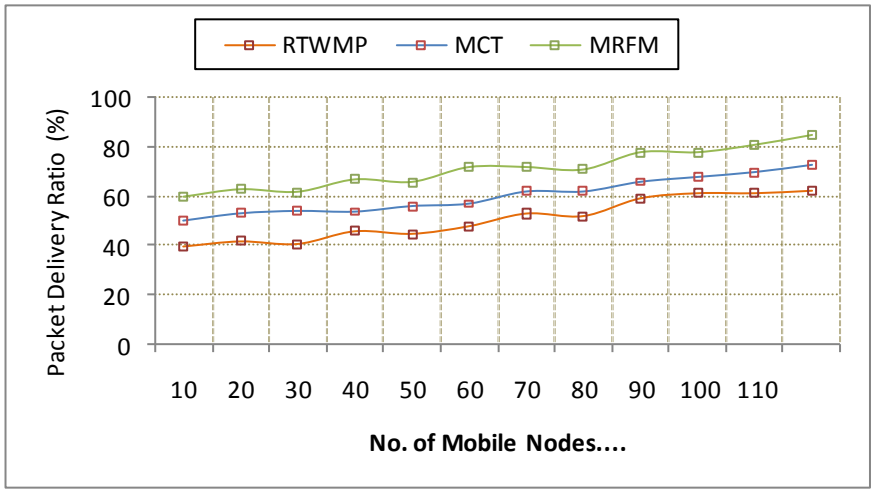

Fig.1 PDR Analysis in Video Conference Application

6. CONCLUSION

The above discussed theme first presents detailed study on challenging protocols, highlights on the mechanisms usded by important real time based routing protocols in MANET and some analysis which has been done to evaluate their performance. Secondly, three leading protocols are selecetd based on specturm distribution in the wireless channel and on the basis of their technical mechanism and approches for comparative analysis, the result of simulation are presented which we believe will be useful for further analysis and development of a robust and versatile realtime based protocol for the magnificent area of MANET.

REFERENCE

[1] DaniloTardioli ,DomenicoSicignano , José Luis Villarroel,(2015)" A wireless multi-hop protocol for real-time applications",*Computer Communications* ,Vol 55, Pages-4-21.

[2] Xie, H., Boukerche, A., Loureiro, A.,(2015) "MERVS: A Novel Multi-channel Error Recovery Video Streaming Scheme for Vehicle Ad-hoc Networks," *Vehicular Technology, IEEE Transactions on* ,Vol 99.

[3] Sondi, P., Gantsou, D.,(2014) "Improving real-time video streaming delivery over dense multi-hop wireless ad hoc networks," *Wireless Days (WD), 2014 IFIP*, Pages 1-4.

[4] GhulamYasin, Syed Fakhar Abbas, S. R. Chaudhry, (2013)" MANET Routing Protocols for Real-Time Multimedia Applications," *WSEAS Transactions on Communications* , Vol 12, Issue 8, Pages 386-395.

[5] Ahmad, Iftikhar, SamreenAyaz, Syed Yasser Arafat, Faisal Riaz, and HumairaJabeen,(2013) "QoS routing for real time traffic in mobile ad hoc network", *Proceedings of the 7th International Conference on Ubiquitous Information Management and Communication.*

[6] P.D.R. Vijaya Kumar and T. Ravichandran,(2013) " A Real Time Multimedia Streaming in Mobile Ad Hoc Networks using Multicast Tree Structure" Research Journal of Information Technology, Vol 5,Issue 1,Pages 24-34.

[7] Zhenhui Yuan, and Gabriel-MiroMuntean,(2013)" A Prioritized Adaptive Scheme for Multimedia Services over IEEE 802.11 WLANs," IEEE Transactions on Network and Service Management , Vol. 10, No. 4.

[8] RaimundoViegas, Jr., LuizAffonsoGuedes , (2013) Francisco Vasques , Paulo Portugal , Ricardo Moraes "A new MAC scheme specifically suited for real-time industrial communication based on IEEE 802.11e" ELSEVIER, Computers and Electrical Engineering, Pages-1684–1704.

[9] D. Sicignano, D. Tardioli, S. Cabrero, J.L. Villarroel,(2013) " Real-time wireless multi hop protocol in underground voice communication," Ad Hoc Networks Vol.11,Issue 4, Pages- 1484–1496.

[10] Boksiner, J., Posherstnik, Y., May, B., Saltzman, M., Kamal, S.,(2013) "Centrally Controlled Dynamic Spectrum Access forMANETs,", Military Communications Conference, MILCOM 2013 - 2013 IEEE ,Pages 641-646, 18-20.

[11] P.Rukmani,R.Ganesan, (2013) "Scheduling algorithm for real time applications in mobile ad hoc network with opnet modeler," International Conference On Design And Manufacturingg, IConDM 2013,Procedia Engineering, Vol 64, Pages. 94 – 103.

[12] Mewara, H.S., Porwal, S.,(213) "Node density and traffic based modelling and analysis of routing protocols for MANETs," Advances in Technology and Engineering (ICATE), 2013 International Conference on ,Pages 1-6.

[13] G. S. Aujla, S. S. Kang,(2013) "Simulation based comparative analysis of TORA, OLSR and GRP routing protocols for email and video conferencing applications over MANETs", International Journal of Computer Networking Wireless and Mobile Communications Vol. 3, Pages- 353-362.

[14] Lal, C., Laxmi, V., Gaur, M.S.,(2013) "QoS-aware routing for transmission of H.264/SVC encoded video traffic over MANETs," Communications (APCC), 2013 19th Asia-Pacific Conference on , Pages 104-109.

SOFTWARE COST ESTIMATION USING FUZZY NUMBER AND PARTICLE SWARM OPTIMIZATION

Divya Kashyap[1] and D. L. Gupta[2]

[1]Computer Science and Engineering Department, IADC, Bangalore
[2]Computer Science and Engineering Department, KNIT, Sultanpur

ABSTRACT

Software cost estimation is a process to calculate effort, time and cost of a project, and assist in better decision making about the feasibility or viability of project. Accurate cost prediction is required to effectively organize the project development tasks and to make economical and strategic planning, project management. There are several known and unknown factors affect this process, so cost estimation is a very difficult process. Software size is a very important factor that impacts the process of cost estimation. Accuracy of cost estimation is directly proportional to the accuracy of the size estimation.

Failure of Software projects has always been an important area of focus for the Software Industry. Implementation phase is not the only phase for Software projects to fail, instead planning and estimation steps are the most crucial ones, which lead to their failure. More than 50% of the total projects fail which go beyond the estimated time and cost. The Standish group's CHAOS reports failure rate of 70% for the software projects. This paper presents the existing algorithms for software estimation and the relevant concepts of Fuzzy Theory and PSO. Also explains the proposed algorithm with experimental results.

KEYWORDS

Software Cost estimation, Particle swarm optimization, Fuzzy logic etc

1. INTRODUCTION

Software cost prediction is a crucial, essential and an important issue for software engineering research communities. As the software size varies from small to medium or large, the need for accuracy or correctness in software cost estimation with understanding has also grown. Software cost estimation is a method to determine effort, time and cost of a project, which in turn helps in better decision making about the feasibility and/or viability of the project. To effectively organize the project development tasks and make considerable economical and strategic planning, project management requires accurate software cost estimation. Cost estimation is a very difficult process because several known and unknown factors affect the estimation process. Software size is a very important (desirable) factor that impacts the process of cost estimation. Accuracy of cost estimation is directly proportional to the accuracy of the size estimation.

Software estimators sometimes confuse size and effort. Size, in a software development context, is the complete set of business functionalities that the end user gets when the product is deployed and is in use, and the Person months required to produce the software application of a given size is the effort.

Failure of Software projects has always been an important area of concern for the Software Industry. Implementation phase is not the only phase for Software projects to fail, instead planning and estimation steps are the most crucial ones, which leads to their failure. More than 50% of the total projects which go beyond the estimated time and cost fail.

DOI: 10.5121/ijci.2016.5112

2. MOTIVATION

Based on literature review and current trends in the software industry, some of the important motivators for this research work are discussed below:

1.) Insignificant Contribution by the various Algorithmic Techniques

There are multiple studies available which accounts for the incorrect and inaccurate contribution by the various algorithmic techniques for software cost estimation for various projects. The errors are far beyond the acceptable limits and hence impacting the overall project. Since these types of traditional techniques and modeling equations based on algorithmic approach has failed, it has become imperative for us to look out for better options either in terms of new methods or optimization of the existing ones. This is quite motivating for a researcher to explore new options.

2.) Emergence of Soft Computing & Meta-heuristic Techniques

Soft Computing techniques like Fuzzy systems and meta-heuristic algorithms like particle swarm optimization, firefly algorithm, harmony search, and the likes have enhanced their presence and utility in the software industry. With so many applications existing for such techniques, software cost estimation is an area which can be explored through their applications. Their advantageous characteristics can be imparted on the estimation techniques which can become more efficient. So it is also an important motivation to study the application of such techniques in the software cost estimation scenario.

3.) Increasing criticality of Software Cost Estimation techniques & rising impact on Business Activities

These days, the importance of Software Cost Estimation has gone beyond limits. The criticality of the software is increasing exponentially and thus cost is becoming a very important parameter. A small error in the process of cost estimation can destroy the organization's reputation and recognition in the market. With digital world becoming so powerful, this negative publicity can spread virally. Thus cut-throat competitions are making it very difficult for everyone to survive and better techniques must be researched for cost estimation. Once the estimation process is completed successfully, one can easily execute the project without much pressure from the costing point of view.

3. INTRODUCTION TO SOFTWARE EFFORT ESTIMATION

Estimation of effort and time involved in the development of the software product under consideration are the most critical activities of the software life cycle. This process may be performed at any stage during the software development and is termed as software cost estimation. It is necessary to perform the estimate during early phases of the Software Development Life Cycle (SDCL), which helps us in taking an early decision regarding feasibility of the software development project. The results of estimation are also used for early analysis of the project efforts [1].

The primary components [2] of project development costs are: Hardware costs, Operational costs and Effort costs (in terms of Man-hours deployed on a particular project with their salaries as per their time utilized on it). The most important (dominant) cost out of all the three is the effort cost. It has been found to be very difficult to estimate the effort cost and control it, which can have a significant effect on overall costs. Software cost estimation is an ongoing process which starts at

the beginning of the SDLC at the requirement gathering and proposal stage and continues throughout the conduction of a project. Projects are bound to have a specific monetary plan in terms of revenue and expenditure, and consistent cost estimation technique is necessary to ensure that spending is in line with the budget plan. Man-hours or man-months are the units used to measure the effort. An ill estimated project or poor feasibility study for a project hampers the image of the software development organization. If a project cannot be completed within the estimated time or efforts, the budget may get disturbed. This in turn can bring lots of losses for both the client and the organization. Thus we need to have a strong estimation model available with us, which can facilitate us in preparing a correct and feasible plan.

Though there has been various models proposed in the past [1] [6], but still the accuracy levels are not that satisfactory and leaves a scope of improvement over the previous work. In this paper, a new algorithm which is combination of Particle swarm optimization and fuzzy theory has been proposed and discussed for the Software cost, effort and time estimation.

4. BACKGROUND

Software cost estimation methods can be majorly categorized into three types: Algorithmic method, Expert judgment and Analogy based method [7].Machine learning is also an estimation method but is not a prominently different one in regular practices and is more categorized under the Analogy based methodology only. Each technique has its own advantages, disadvantages and limitations. With projects of large cost magnitude, many cost estimation methods should be used in parallel. This way one can compare the results produced from these methods and reliability over one particular methodology gets reduced and hence risk is also minimized [8]. But for smaller or medium sized projects, applying all the cost models might become costly affair thus making it an expensive start of the project [8].

5. FUZZY LOGIC

Fuzzy logic is a kind of multi-valued logic, which deals with approximate reasoning rather than exact and absolute reasoning. It is an approach for computing based on degree of truth rather than just true or false (1 or 0). There are few terms associated with fuzzy logic which are mentioned as below:

5.1 Fuzzy Number

A fuzzy number is a quantity whose value is uncertain rather than exact as in case of single valued numbers. Fuzzy number refers to a connected set of possible values with each value having its own weight in range 0 to 1. The weight assigned to each value is called the membership function.

5.2. Membership Function

As per the definition, for a fuzzy set A on the universe of discourse X, membership function is defined as

$$\mu A: X \rightarrow [0,1] \qquad (1)$$

where, each element of X is mapped to a value between 0 and 1[3].It represents degree of truth as an extension of valuation. Membership functions are of different shapes [9] such as triangular, trapezoidal, piecewise linear, Gaussian, bell-shaped, etc.

Trapezoidal Function: It is defined by a - lower limit, d- an upper limit, b- lower support limit, and an upper support limit c, where a < b < c < d. [3]. The Membership function depicting the Trapezoidal Function is shown below in equation 2.

$$\mu_A(x) = \begin{cases} 0, & (x < a) \text{ or } (x > d) \\ \dfrac{x-a}{b-a}, & a \le x \le b \\ 1, & b \le x \le c \\ \dfrac{d-x}{d-c}, & c \le x \le d \end{cases} \quad (2)$$

Let A be a fuzzy number, A = [a, b, c, d; w] , w is the weight, 0 < w ≤1 .The Trapezoidal membership of this Fuzzy number A should satisfy the following conditions:

(a) A is a continuous mapping from R to the closed interval in [0, 1].
(b) A(x) = 0, where infinite ≤ x ≤ a and d ≤ x ≤ infinite.
(c) A(x) is monotonically increasing in [a, b].
(d) A(x) = w where b≤ x≤ c.
(e) A(x) is monotonically decreasing in [c, d].

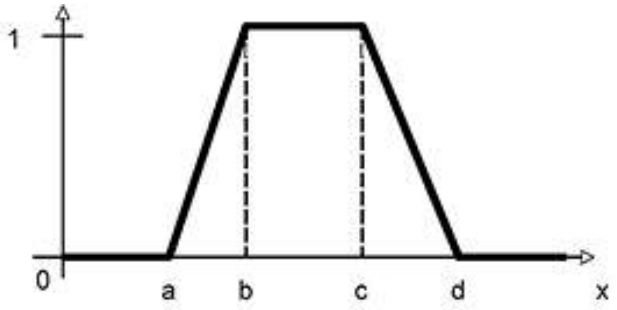

Figure 1 Trapezoidal Membership Function within the range of 0 and 1 [4]

In the Figure 1, the x axis represents the universe of discourse, whereas the degrees of membership in the [0, 1] interval is represented by y-axis [3].

6. PARTICLE SWARM OPTIMIZATION (PSO)

Particle swarm optimization (PSO) is a stochastic optimization technique invented by Dr. Eberhart and Dr. Kennedy in 1995[5], used the concept of population and social behaviour of bird flocking or schooling. PSO is an evolutionary computation technique such as Genetic algorithm. PSO optimizes problem by iteratively trying to improve a candidate (initial) solution with regard to a given measure of quality or fitness function. Initially PSO starts with candidate solutions, known as particles and move these particles around in the search-space according to the mathematical formulae describing the particle's position and velocity. Each particle's movement depends on its local best known position but, is also diverted toward the best known positions in

the search space [10], [11]. These local best positions are updated as better positions are found by other particles.

6.1. PSO Algorithm

The steps of PSO Algorithm [5] are summarized as follows

1. For each particle i = 1, ..., S do:
   1.1 Initialize the particle's position with a uniformly distributed random vector: xi ~ U(blo, bup), where blo and bup are the lower and upper boundaries of the search-space.
   1.2 Initialize the particle's best known position to its initial position: pi ← xi
   1.3 If (f(pi) < f(g)) update the swarm's best known position: g ← pi
   1.4 Initialize the particle's velocity: vi ~ U(-|bup-blo|, |bup-blo|)
2. Until a termination criterion is met (e.g. number of iterations performed, or a solution with adequate objective function value is found), repeat:
   2.1 For each particle i = 1, ..., S do:
      2.1.1 Pick random numbers: rp, rg ~ U(0,1)
      2.1.2 For each dimension d = 1, ..., n do:
         2.1.2.1 Update the particle's velocity: vi,d ← ω vi,d + φp rp (pi,d-xi,d) + φg rg (gd-xi,d)
      2.1.3 Update the particle's position: xi ← xi + vi
      2.1.4 If (f(xi) < f(pi)) do:
         2.1.4.1 Update the particle's best known position: pi ← xi
         2.1.4.2 If (f(pi) < f(g)) update the swarm's best known position: g ← pi
3. Now g holds the best found solution.

The parameters ω, φ_p, and φ_g are selected by the practitioner and control the behaviour and efficacy of the PSO method.

7. COCOMO MODEL

Developed by Barry Boehm in 1981 [12], Cost Constructive Model or COCOMO is a cost estimation model based on algorithmic properties. There were more than 60 projects which were tested and analyzed under this model before it was formally announced. Since the beginning, there were three levels of this model which were defined by Boehm. They were Basic, Intermediate and Detailed. For the purpose of this research, Intermediate COCOMO model has been used.

7.1. Intermediate COCOMO

The basic COCOMO model is based on the relationship:

$$DE = a*(SIZE)b \quad (3)$$

where SIZE is measured in thousand delivered source instructions. The constants a, b are dependent upon the 'mode' of development of projects, DE is Development Effort and is measured in man-months.

There were three modes proposed by Boehm- Organic, Semi-detached and Embedded Mode. Organic was associated with small teams with known development environment, Semi-detached followed a mixture of experience and fresher with mode lying between organic and embedded and finally, Embedded was used for real time projects with strict guidelines and very tight schedule. The development efforts for various modes of software in Intermediate COCOMO are

calculated by equations given in table 3.1. Since the basic COCOMO was not that much accurate, intermediate COCOMO was developed with introduction of Cost Drivers.

The EAF term is the product of 15 Cost Drivers [12] that are presented below. The various multipliers of the cost drivers can be categorized from Very Low to Extra High as given.
The 15 cost drivers are broadly classified into 4 categories of product, platform, personnel and project. The meaning and classification of the cost drivers are as follows:

Table 1 Development Efforts for various modes in Intermediate COCOMO

Development Mode	Intermediate Effort Equation
Organic	$DE=EAF*3.2*(SIZE)^{1.05}$
Semi-detached	$DE=EAF*3.0*(SIZE)^{1.12}$
Embedded	$DE=EAF*2.8*(SIZE)^{1.2}$

a) Product: RELY - Required software reliability
DATA - Data base size
CPLX - Product complexity
b) Platform: TIME - Execution time
STOR- Main storage constraint
VIRT - Virtual machine volatility
TURN - Computer turnaround time
c) Personnel: ACAP - Analyst capability
AEXP - Applications experience
PCAP - Programmer capability
VEXP - Virtual machine experience
LEXP - Language experience
d) Project: MODP - Modern programming
TOOL - Use of software tools
SCED - Required development schedule

With a dependency on the projects, various multipliers of the cost drivers will differ and thereby the EAF may be greater than or less than 1, thus affecting the Effort.

8. PROPOSED EFFORT ESTIMATION APPROACH

Analogy based approach [13] operates with one or two past projects selected on the basis of their similarity to the target project. Based on this approach following algorithm has been developed to estimate the effort.

ALGORITHM 1:

1. Establish attributes of planned project i.e. select all the attributes that are required for the estimation.
2. Estimate the values of attributes established in step 1.Since estimates are uncertain so fuzzy numbers are used to depict the generated values for attributes.
3. Now from the repository of historical projects find the project that closely matches the attributes of planned project.
4. Similarity distance is calculated by comparing attribute values of planned project to that of historical project. The most similar project, though closest, is still not ‘identical’ to the considered project. Hence, its ‘weight’ (as described in step 6) will be 1.

5. At this step, the values of linear coefficients may be computed using the inputs of 'similarity distances' from the existing project using PSO algorithm.
6.

The equation will be similar to linear equation, except that the weights will be adjusted in powers of distance ratios (powered to s/si, where s is the minimum distance for the best project and si for the target project).

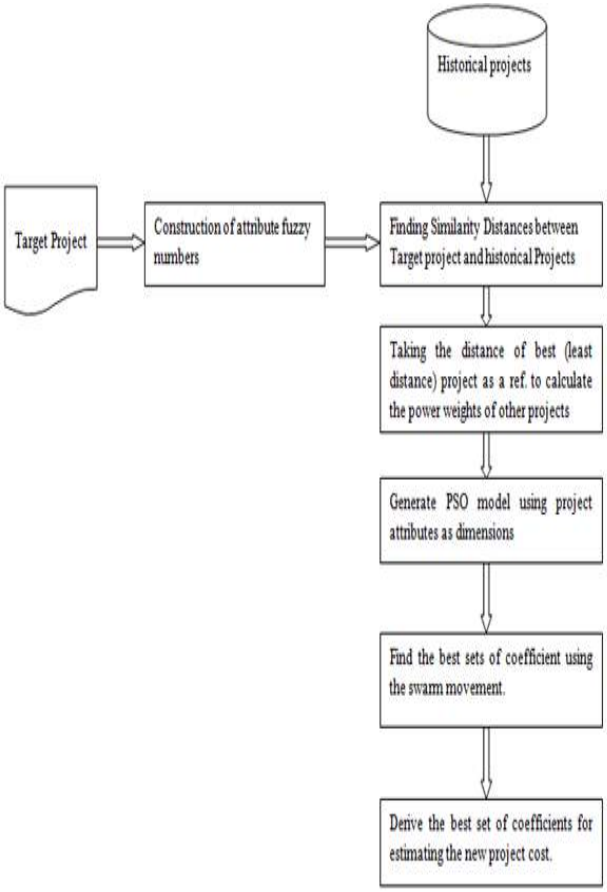

Figure 2 Generalized framework for estimation using Fuzzy numbers and PSO

The proposed model as shown in Figure 2 is considered as a form of EA (Estimation by Analogy) and comprises of following main stages:

i. Construction of fuzzy number of attributes.
ii. Finding Similarity distance between planed project and historical project.
iii. Deriving project weights according to the distance.
iv. Applying PSO algorithm to find B, as per the equation Y = B*X, where B is the coefficient vector, Y is the matrix for current project and X is the matrix for historic projects.

Construction of fuzzy number of attributes

The proposed method chooses COCOMO81 Dataset that describes the project using 15 attributes. Firstly, value of each attribute is replaced by its corresponding Fuzzy number in order to depict uncertainty. Fuzzy numbers can be constructed by any of the following two methods: [15].

a. Expert opinion
b. From data

Expert opinion is a totally subjective technique. It depends on identifying pessimistic, optimistic and most likely values for each Fuzzy number [16], whereas construction using data is based on the structure of data only. Therefore based on DATA, and using Fuzzy modelling [14], the approach develops the membership functions for each attributes. Let the numeric value of attributes in Fuzzy Number is represented in the following sequence, where trapezoidal membership has been considered as given in the section 4.

- Planned Project (P): [a1, a2, a3, a4; wa]
  and [a1, a2, a3, a4; wa] represents a fuzzy number for one attribute, where $0 \leq a1 \leq a2 \leq a3 \leq a4 \leq 1$ and all are real numbers. Therefore, planned project will also have 15 sets of this type representing 15 attributes.

- Historical Project (H): [b1, b2, b3, b4; wb]
  and [b1, b2, b3, b4; wb] represents a fuzzy number for one attribute , where $0 \leq b1 \leq b2 \leq b3 \leq b4 \leq 1$ and all are real numbers. Therefore, historical project will have 15 sets of this type representing 15 attributes.

Finding Similarity between planned project and historical project

To calculate the similarity distance between two fuzzy numbers, the method proposed by Azzehet. Al has been used [14] which combines the concept of geometric distance, Center of Gravity (COG) and height of generalized fuzzy numbers. The degree of similarity S(P,H) between two generalized Fuzzy numbers comprises of three elements:

a) Height of Adjustment Ratio (HAR)
b) Geometric Distance (GD)
c) Shape of Adjustment Ratio (SAF)

Equation for S(P,H) is given by the following equation[14]:

- HAR is used to assess the degree of difference in height between two generalized Fuzzy numbers. Equation for HAR is given by[4]:

  $$HAR = \sqrt{(\min(wa/wb, wb/wa))} \quad (4)$$

  where, wa is weight for attribute of P and wb is weight for attribute of H.

- GD is used to measure the geometric distance between two generalized Fuzzy numbers including the distance between their x-axis centroid. Equation for GD is given by:

  $$GD = 1 *((a1-b1) + (a2-b2) + (a3-b3) + (a4-b4) + (xa- xb))/5 \quad (5)$$

- SAF is used to adjust the geometric distance, like, when the 2 Fuzzy numbers are having different shapes. Equation for SAF is given by:

  $$SAF = 1 + abs (ya-yb) \quad (6)$$

  Equation for S(P,H) is given by the following equation

  $$S(P,H) = HAR*(1-GD)/SAF \quad (7)$$

  (xa, ya) and (xb, yb) presents the centre of gravity of generalized fuzzy numbers P and H respectively and calculated using equations 8 and 9:

$$ya = \begin{cases} \frac{wa \times (\frac{a3-a2}{a4-a1}+2)}{6} & , if\ a1 \neq a4 \\ \frac{wa}{2} & , \quad if\ a1 = a4 \end{cases} \quad (8)$$

$$xa = \frac{ya(a3+a2)+(a4+a1)(wa-ya)}{2wa} \quad (9)$$

Substituting the values of HAR, GD, SAF from equations 4, 5 and 6 respectively in equation 7, will give the similarity distance between one pair of attribute. Similarly, similarity distances for rest of the 14 attributes are calculated.

Now, Let Si where i varies from 1 to 15, denote similarity distance between ith attribute of the two projects we are comparing, then collectively it will give the similarity distance between two projects denoted by S, given by equation 10:

$$S = \sum_{i=1}^{15} S_i \quad (10)$$

In a similar way, similarity distance between planned project and each of historical projects are calculated to get the most similar project.

Ranking the Closest Project

After calculating the aggregated similarity measure S between the planned project and each individual analogue project, we will sort the similarity results according to their value. The project with highest similarity to target project is chosen. We choose project with least similarity distance because it has highest potential to contribute to the final estimate. We assume that the effort of the closest project is E which will be utilized for Effort adjustment.

Application of PSO algorithm for determination of Coefficients

For deriving the new estimate only using the closest project is not sufficient in many cases as [6] it may lead to bad estimation accuracy. Therefore Particle Swarm Algorithm is used to ensure that all projects are considered according to the extent to which they are similar to the test project. The framework of implementation of PSO model is shown in Figure 3. Here, the potential benefits of applying PSO to analogy-based software effort estimation models based on Fuzzy Numbers are evaluated. A suitable linear model is derived from the similarity distances between pairs of projects for obtaining the weights to be used for PSO. PSO may be considered as a process of random allocation of coefficient values, and then randomly changing them till they are closest in linking the projects (minimum error).

Figure 3, presents the iterative process to optimize the coefficients of linear equation and software cost estimation process that combines the best linear equation with estimation by analogy using Fuzzy number [15].

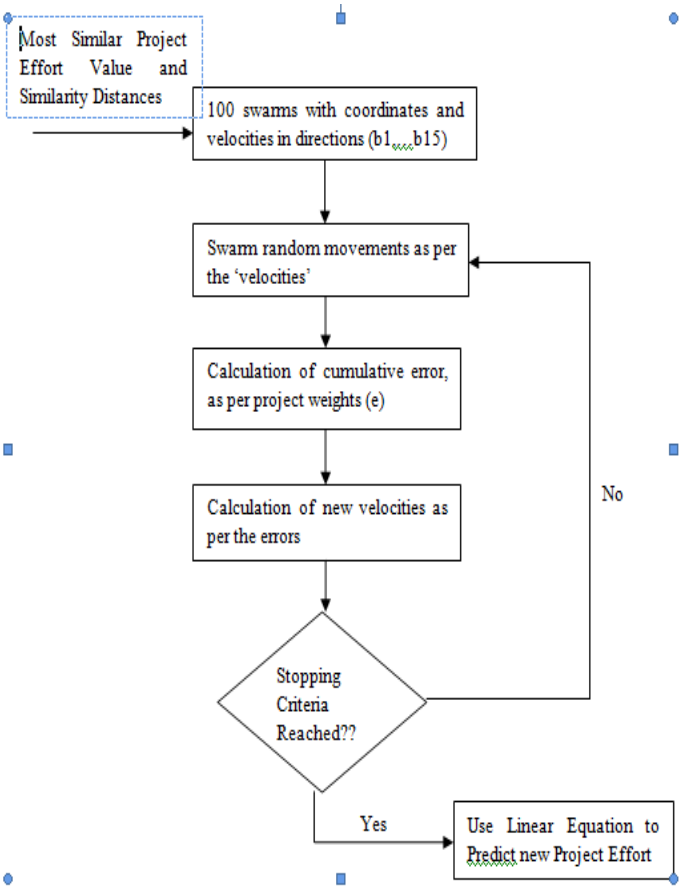

Figure 3 Framework of Adjusted Fuzzy Analogy based Estimation

The algorithm for PSO implementation goes as follows:

1. Pick 100 swarms corresponding to the coordinates of 15 attributes for the equation e = Sum (abs((A(i,j)*B(j)) – E(i))^(s/si))/(no. of past projects), where A represents the values corresponding to the original scaled ratings (1-6), B is the quantity to be measured, and s is similarity ratings. Thus, dissimilar projects get lower share of contribution.
2. Pick random positions and velocities for 15 attributes for each of the swarms. Random velocity would be in the range (-x,+x), where x could take a value like 1, and position can be taken in range (0,y). Later, when equation was modified as e = Sum (abs((B(j)/A(i,j)) – E(i))^(s/si))/(no. of past projects), most of the coefficients were found in the range (0,10). The first attempt would take y = 10.
3. Compute total Error = Sum (| Estimated – Actual effort|/(Actual effort + Estimated effort)), for each project.
4. New velocity = unit random velocity * error for the swarm
5. No. of iterations may be varied as per the accuracy requirements.
6. The 'particle best' and 'global best' coordinates may be computed as per the standard PSO method.

A representation of the PSO algorithm for the project is shown in Fig. 4.

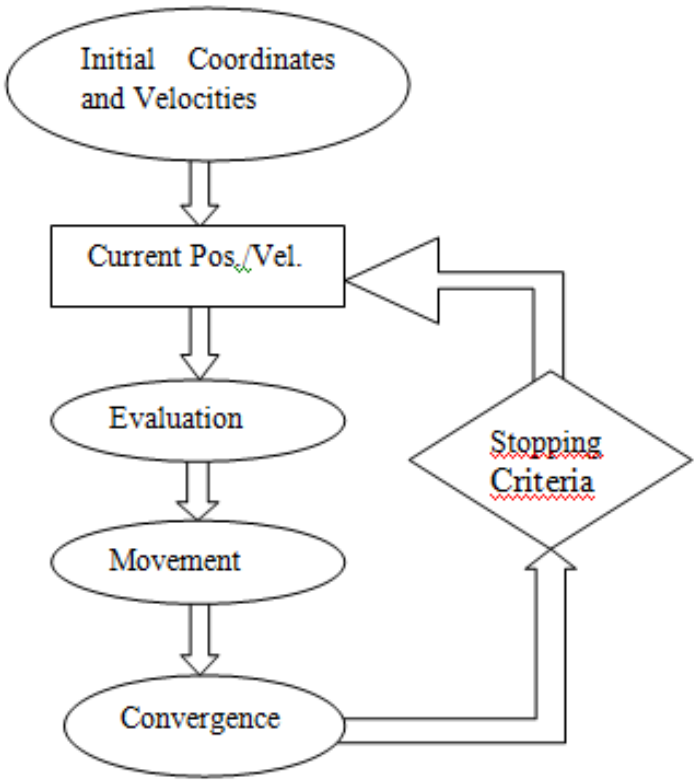

Figure 4 Adjusting Reused Effort process diagram

The failure of implementation of an iterator may come in several forms, such as

(i) Poor/Slow convergence, or slowdown before convergence near the required point,
(ii) Divergence
(iii) Undesirable oscillations
These problems may be prevented if the iteration function is mathematically consistent. This may be ensured as follows:

- The swarm movement starts slowing down when the error value start decreases, leading to a tendency to converge around the best value, as the number of iterations are increased.
- To ensure that the 15 coefficients do not go too high, the normalized data is inverted to form the equation E = Sum (B/S) + e implies e = E – sum (B/S);
  e (total) = sum [abs({ E – sum(B/S) }) ^ s/si]
  If the absolute value of S increases, the error grows to bring it down again. This keep the values of coefficients represented by 'S' in a narrow range.
- An important mathematical step in the algorithm was that of 'initialization'. If initial coefficients are taken in the range (0, 10), then there are good chances that the errors would be in the range (0, 1). If velocities are allocated in (0, 1) range, a fast convergence may be expected.

9. EXPERIMENTAL RESULTS

Using the effort of most similar project and calculated similarity distances between each attribute, the coefficients of all effort drivers in OPTIMTOOL (MATLAB (R2011a)) [104] are found that results in significantly lesser errors. There is no proof on software cost estimation models to perform consistently accurate within PRED 25% (number of observation for which MRE is less than 0.25). Applying PSO algorithm, the value of coefficients of effort drivers (shown in Table 3) is obtained that aim to minimize the MRE [204] of projects. For some of the effort drivers the coefficient value is very very less. So we can deduce that these drivers does not play important role in the adjustment of effort. For the proposed PSO algorithm, Figure 5 shows how algorithm converges with the number of iterations. Two sets of iterations per simulation set were performed in order to note the variation of precision as well. It was found that the precision also improves with the number of iterations, since the absolute difference of error of each pair of simulation decreases with the number of runs.

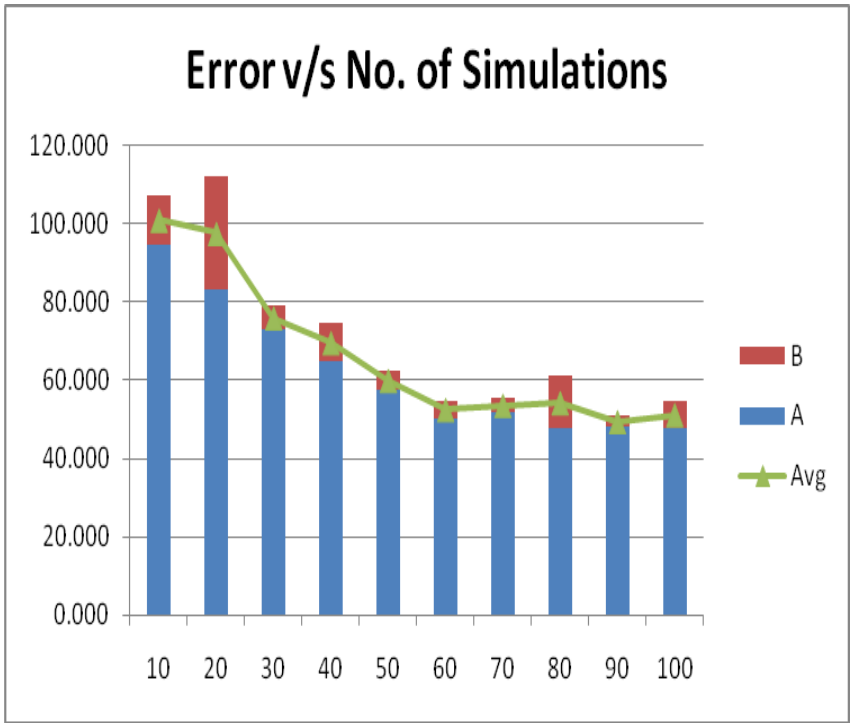

Figure 5 PSO algorithm stabilizes as the number of iterations is increased

Table 2 Corresponding to Figure 3.6

	A	B	Avg
10	94.514	12.909	100.968
20	83.157	28.896	97.605
30	73.032	5.996	76.030
40	64.894	9.600	69.694
50	57.730	4.567	60.014
60	50.379	4.414	52.586
70	51.989	3.388	53.683
80	47.565	13.645	54.387
90	48.159	2.691	49.505
100	47.819	6.980	51.309

Table 3 Best Coefficient Values Obtained through PSO

Cost Driver	Coefficents of drivers (Bi)
ACAP	-1.74
AEXP	4.51
CPLX	8.84
DATA	0.39
LEXP	5.43
MODP	6.33
PCAP	3.89
RELY	9.60
SCEP	1.86
STOR	0.97
TIME	-2.37
TOOL	-1.78
TURN	7.75
VEXP	0.51
VIRT	5.87

10. CONCLUSION AND FUTURE WORK

To solve the problem of uncertain, lost values and ambiguous and vague values of attributes related to project, the concept of fuzzy numbers is used in the present proposed approach. The fuzzy model is employed in Estimation by Analogy to reduce uncertainty and improving the way to handle both numerical and categorical data in similarity measurement. Converting each attribute (real number) in to fuzzy number solve the problem of ambiguous data. Once it gets over, calculating the similarity distance of the target project with all historical projects results the most similar project. But the most similar project still has similarity distance with the project being estimated. Hence, all projects were considered in varying weights, as per their similarity distance with the proposed project – the lower the distance, the higher the weight.

Combining the concept of Fuzzy logic and PSO algorithm in a model to estimate the software effort improves the accuracy of estimation techniques. The experiments, which were conducted applying this model to NASA63 dataset, establish significant improvement under various accuracy measures. Case Based Reasoning (CBR), traditional COCOMO and estimation analogy based Fuzzy Model (EA) have been used for the comparison purpose with the proposed technique. The evaluation parameter used for the comparison is Mean Magnitude of Relative Error (MMRE).

REFERENCES

[1] Martin Shepperd, and Schofield Chris, "Estimating software project effort using analogies." Software Engineering, IEEE Transactions on 23.11, pp: 736-743, 1997.

[2] Practical Software Engineering, Accessed from http://ksi.cpsc.ucalgary.ca/courses/451-96/mildred/451/CostEffort.html on September 5, 2013.

[3] Mohammad Azzeh, Daniel Neagu, Peter I. Cowling, "Fuzzy Grey Relational Analysis for Software Effort Estimation", Empirical Software Engineering, Vol. 15, No. 1, pp. 60-90, 2010.

[4] The fuzzy descriptive Logic System, http://gaia.isti.cnr.it/straccia/software/fuzzyDL/fuzzyDL.html

[5] R. C. Eberhart and Y. Shi, "Particle swarm optimization: Developments, applications and resources," in Proc. IEEE International Conference on Evolutionary Computation, vol. 1, pp. 81–86, 2001.

[6] MATDOCS : http://www.mathworks.in/matlabcentral/fileexchange

[7] Fiona Walkerden, Ross Jeffery, "An empirical Study of Analogy-based Software Effort Estimation", Empirical Software Engineering, Kluwer Academic Publishers, Boston, Volume 4, pp. 135-158, 1999.

[8] Giancarlo Attolini , "Guide to Practice Management for Small- and Medium-Sized Practices", International Federation of Accountants ,Third Edition, 2012.

[9] Fuzzy logic membership function, http://www.bindichen.co.uk/post/AI/fuzzy-inference-membership function.html

[10] K. Vinay Kumar, V. Ravi and Mahil Carr, "Software Cost Estimation using Soft Computing Approaches", Handbook of Research on Machine Learning Applications and Trends: Algorithms, Methods, and Techniques, pp. 499-518, IGI Global, 2010.

[11] Y. Shi, R. C. Eberhart , "A modified particle swarm optimizer", Proceedings of IEEE International Conference on Evolutionary Computation, pp. 69–73, 1998.

[12] B. Boehm, "Software Engineering Economics", Prentice Hall, 1981.

[13] Nikolaos Mittas, Marinos Athanasiades, Lefteris Angelis, "Improving Analogy-based Software Cost Estimation by a Resampling Method", Information and Software Technology, 2007.

[14] Mohammad Azzeh, Daniel Neagu, Peter I. Cowling, "Analogy-based Software Effort Estimation Using Fuzzy Numbers", The journal of Systems and Software 84, 2010.

[15] M. Jorgensen, "Realim in Assessment of Effort Estimation Uncertainty: It Matter How You Ask." IEEE Transaction on software Engineering 30, 2004.

[16] Barry Boehm, Chris Abts, "Software Development Cost Estimation Approaches – A Survey", 650 Harry Road, San Jose, CA 95120: IBM Research, pp.1-45, 1998.

A SURVEY ON CROSS LANGUAGE INFORMATION RETRIEVAL

Prof. Sanjay K.Dwivedi[1] and Ganesh Chandra[2]
[1-2]Department of Computer Science, BBAU (A Central University), Lucknow

ABSTRACT

Now a days, number of Web Users accessing information over Internet is increasing day by day. A huge amount of information on Internet is available in different language that can be access by anybody at any time. Information Retrieval (IR) deals with finding useful information from a large collection of unstructured, structured and semi-structured data. Information Retrieval can be classified into different classes such as monolingual information retrieval, cross language information retrieval and multilingual information retrieval (MLIR) etc. In the current scenario, the diversity of information and language barriers are the serious issues for communication and cultural exchange across the world. To solve such barriers, cross language information retrieval (CLIR) system, are nowadays in strong demand. CLIR refers to the information retrieval activities in which the query or documents may appear in different languages. This paper takes an overview of the new application areas of CLIR and reviews the approaches used in the process of CLIR research for query and document translation. Further, based on available literature, a number of challenges and issues in CLIR have been identified and discussed.

KEYWORDS

Cross language information retrieval, query translation, document translation, corpora based translation, dictionary based translation, machine translation

1. INTRODUCTION

Information retrieval (IR) generally refers to the process where the users search for required information from a large number of documents. Traditional IR systems are implemented mainly for monolingual documents. However, with rapid development of the Internet, the demand for searching information from multi-lingual documents is increasing, which results in the great challenge of how to match the users query written in one language with the documents written in other languages. Therefore, suitable techniques are required to enhance the performance of IR, CLIR & MLIR. The Cross Language Information Retrieval (CLIR) [1] provides a convenient way that can solve the problems of language boundaries, where users can submit queries written in their own language and retrieve documents in another language [2]. For example, a query in Hindi will return the related information description in Chinese language, as given in figure1.

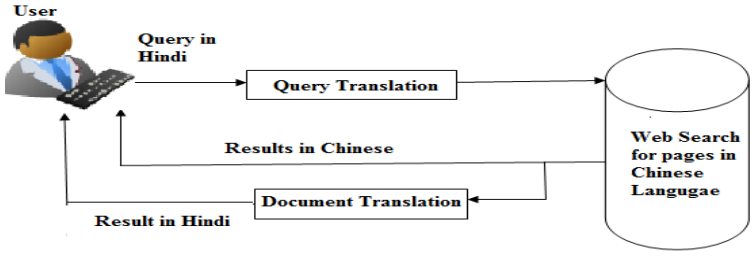

Figure.1 Cross Language Information Retrieval System

DOI: 10.5121/ijci.2016.5113

With the rapid development of Internet technology, globalization of information structure caused the urgent demand to CLIR, because CLIR allows the usage of information exchanges between different languages, remove linguistic disparity between the queries that are submitted and documents that are retrieved using resource over the network, and also decreases the communication cost [3]. The research on information retrieval, came into existence since early 1970s where as experiments for retrieving information across languages were first initiated by Salton in 1973[67]. However, most of the modern research on CLIR started in 90's, and now a day's it has become one of the most important research topic in the area of information retrieval.
An ever active research field, a vast number of researches and studies have been published on CLIR and various issues are addressed in several evaluation forums such as TREC [64], NTCIR [65], and CLEF [66] while each of them cover different languages: TREC includes Spanish, Chinese, German, French, Arabic and Italian; NTCIR includes Japanese, Chinese and Korean and CLEF includes French, German, Italian, Spanish, Dutch, Finnish, Swedish and Russian [4]. The most effective way to solve the problem of language barriers may be achieved through CLIR by using query translation approach, document translation approach, or by using both query and document translation approach.

This paper is organised as follows: section 2, 3, 4 consists of query translation, document translation and dual translation respectively. Section 5, 6, 7 describes the comparative study of the three approaches, challenges of CLIR and CLIR tools respectively. Section 8 describes the application areas of CLIR, section 9 describes CLIR researches in Foreign & Indian languages and section 10 describes the conclusion and future of CLIR.

2. QUERY TRANSLATION APPROACH

A major challenge in CLIR is to bridge the language gap between query and documents. Query translation is now serving as a major cross-lingual mechanism in current CLIR systems [5], [40], [70] as shown in figure2. CLIR search engines enable users to retrieve content in a language different from language used to formulate the query. Translation of query has the advantage that the computational effort i.e. time and space, is less as compared with other methods. Query translation has following disadvantages:

(i) Usually a query does not provide enough contexts to automatically find the intended meaning of each term in the query.
(ii) Translation errors affect retrieval performance sensibly.
(iii) In case of searching a multilingual database, query has to be translated into each one of the languages of database.
In CLIR query translation play an important role that can be achieved by following approaches: dictionary based translation approach, corpora based translation approach and machine translation based approach.

2.1. Dictionary Based Translation Approach

In dictionary-based query translation, the query will be processed linguistically and only keywords are translating using Machine Readable Dictionaries (MRD), given in figure3. MRDs are electronic versions of printed dictionaries, either in general domain or specific domain. The use of existing linguistics resources, especially the MRDs, is a natural approach to cross-lingual IR. Translating the query using the dictionaries is much faster and simpler than translating the documents [6], [7], [41]. Some common problems associated with dictionary-based translation [8] are:

(i) Untranslatable words (like new compound words, proper names, spelling variants, and special terms): Not every form of words used in query is always found in dictionary. Some time problem occurs in translating different compound words (formed by combination of new words) due to the unavailability of their proper translation in dictionary [42].

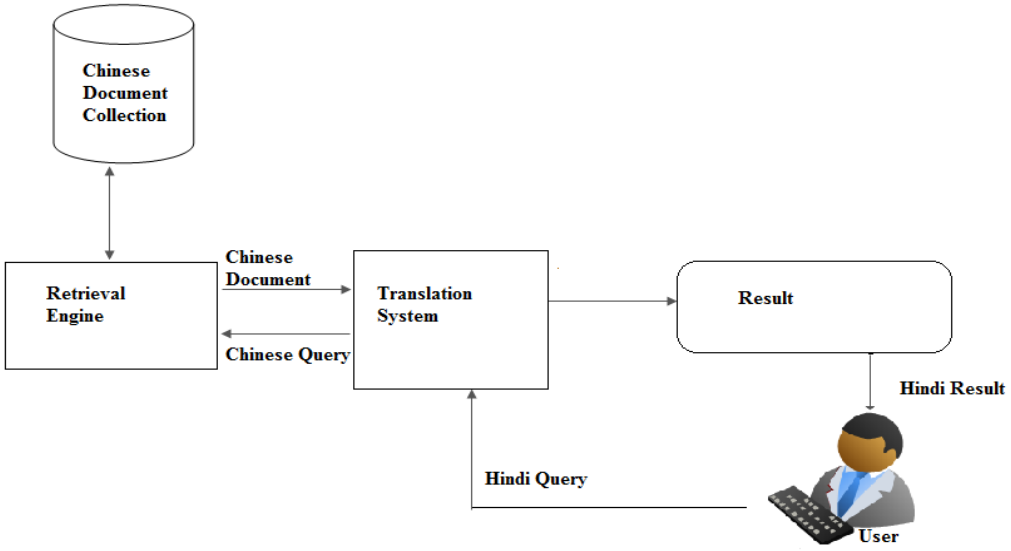

Figure 2: Query Translation

(ii) Processing of inflected words: Inflected word forms are usually not found in dictionaries [43].
(iii) Lexical ambiguity in source and target languages: Relevant forms of lexical meaning for information retrieval are: 1) homonymous and 2) polysemous words. Two words are homonymous; if they have at least two different meanings and senses of words are unrelated e.g. bank (river bank) and bank (financial institution). Polysemous words should have related senses e.g. star in the sky and star. Due to ambiguity in the search keys, matching for retrieving relevant documents may not be successful [46].

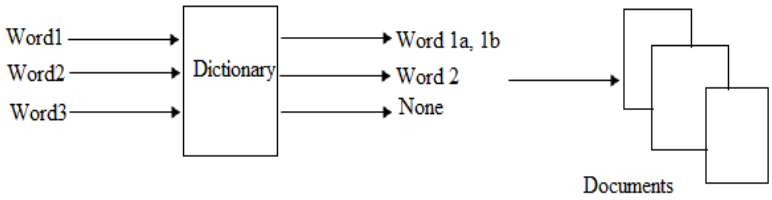

Figure3.Dictionary Based Translation

2.2. Corpora Based Translation Approach

Query translation using corpora requires single corpus or many corpuses. Corpora, (plural of corpus) are the systematic collection of naturally occurring language material, such as texts, paragraphs and sentences from one or many languages. In corpus-based methods [9], [12] queries are translated on the basis of multilingual terms extracted from parallel or comparable document collections. A parallel corpus has been used since the early 1990's for translation of given word. A parallel corpus is a collection of texts, each of which is translated into one or more languages other than the original language. Parallel corpora are also used to decide the relationships, such as co-occurrences, between terms of different languages. A parallel corpus is an important kind of

source of linguistic meta-knowledge, which forms the basis of techniques such as tokenization, morphological and syntactic analysis [15], [10].

A comparable corpus is one of the important concepts in corpus-based translation study, introduced by Baker [38]. Comparable corpora contain text in more than one language. The texts in each language are not translations of each other, but cover the same topic area, and hence contain an equivalent vocabulary. A good example of corpora is the multilingual news feeds produced by news agencies such as Reuters, CNN, BBC, Xinhua News and BERNAMA. Such texts are widely available on the Web for many language pairs and domains. They often contain many sentence pair that are fairly good translations of each other [11], [12] [13].

2.3. Machine Translation Based Approach

Cross-lingual IR with query translation using machine translation [6] seems to be an obvious choice compared to the other two above, as shown in figure4. The advantages of using the machine translation is that it saves time while translating large texts. Manning and Schutze [16] distinguished four different approaches to deal with machine translation: (a) Word-for-word approach, (b) Syntactic transfer approach, (c) Semantic transfer approach, and (d) Interlingual approach. The ultimate goal of CLIR machine translation (MT) systems is to translate queries from one language to another by using a context. Many factors contribute the difficulties of machine translation, including words with multiple meanings, sentences with multiple grammatical structures, uncertainty about what a pronoun refers to, and other problems of grammar.

Many researchers criticize MT-based CLIR approach. The reasons behind their criticisms mostly stem from the fact that the current translation quality of MT is poor. Another reason is that MT systems are expensive to develop and their application degrades the retrieval efficiency (run time performance) due to the lengthy processing times associated with linguistic analysis.

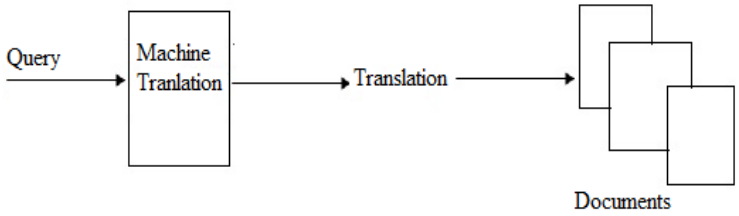

Figure4. Machine Translation

MT based approaches seems to be the ideal solution for CLIR. It is mainly because MT systems translate the sentence as a whole, and the translation ambiguity problem is solved during the analysis of the source sentence. Table 1, describes the differences between various techniques of query translation.

Table1: Comparison between Techniques of Query Translation

Parameters	**Dictionary Based Translation Approach**	**Corpora Based Translation Approach**	**Machine Translation Based Approach**
Ambiguity	High	Low	Low
Offline Translation	Possible	Possible	Not possible
Working Architecture	Visible as like white box testing.	Visible as like white box testing.	Works similar to black box testing
Development	Less expansive	More expensive than	More Expensive

expenses		DBT	
Translation Availability	Highly available in many languages	Available only in few languages	Available only in few languages

3. DOCUMENT TRANSLATION APPROACH

Document Translation [44], [45] can be the most desirable scenario in CLIR, if the purpose is to allow the users to search the documents different from their own language and receive results back in user's language, as given in figure5. In this sense, it is truly a better option which does not require a passive knowledge of the foreign language from the user. In document translation approach, all target languages are translated to the source language [63]. The function of this translation is twofold. First, post translation or 'as-and-when-needed' or 'on-the–fly translation', where documents of any other language being searched by user are translated into user language at query time. IR process mostly uses indexing technique to speed up the searching process of documents. But indexing is not possible in post translation, so this approach is infeasible because it requires more time for translation.

Second, pre translation or 'all together before any query is processed' used to browse through a translated version of an original translation in user language or in a language which user can understand (figure 5). This translation can be called as offline translation. In this approach, documents that are written in different languages are translated to all desired source languages and these documents are indexed before query time. This translation is impossible as a solution for large collection of distributed documents, which are managed by different groups of people, for example internet. Document translation has its own advantages and disadvantages compared to query translation. Some researchers have used it to translate large sets of documents (e.g., Braschler & Schauble, 2001 [17]; Franz, Scott McCarley, & Todd Ward, 2000 [18]; Oard & Hackett, 1998 [19]) since more varied context within each document is available for translation, which can improve translation quality. The document translation approach has certain benefit over query translation. These include the following:

(i) A long document provides more contexts to perform translation, so that terms in the target language can be chosen more accurately.
(ii) Translations errors should not harm retrieval too much, as they are weighted against a whole document.
(iii) The translation effort is done at indexing time, thus getting faster retrieval at run time.
However, there are certain issues with document translation as well, such as:
(i) Much more computational effort is needed to index collections.
(ii) Bad scaling performed in case of more than two languages.

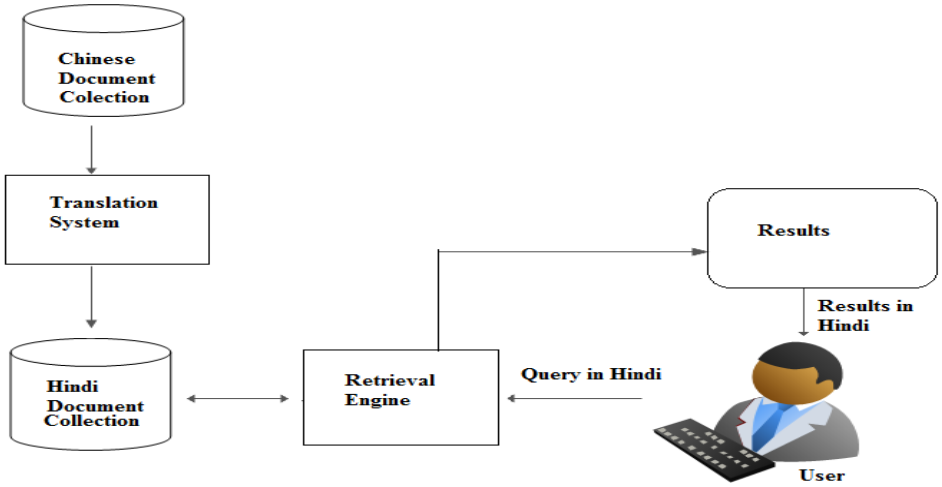

Figure5. Document translation

4. DUAL TRANSLATION (BOTH QUERY AND DOCUMENT TRANSLATION APPROACH)

In this approach – both queries and documents are translated into a common representation (figure 6). This approach requires additional storage space for translated documents but provides scalability when same collection of documents is required in multiple languages. One of the examples of such approach is controlled vocabulary systems [20]. These systems represent all documents using a pre-defined list of language-independent concepts, and enforce queries in the same concept space. This concept space defines the granularity or precision of possible searching. The major issue of controlled vocabulary systems is that, non-expert users usually require some training and also require interfaces to the vocabularies in orderable to generate effective queries.
Dual translation approach also called as hybrid translation approach can be performed by pivot language. Direct translation between two languages may not always be possible due to the limitation of translation resources. To perform such type of translation, a resources or a third language is required between these languages, called pivot language. In this process, two types of approaches are possible: either the query or the document is translated first to pivot language, then to the target language; translate both document and query into pivot language as shown in figure 6.

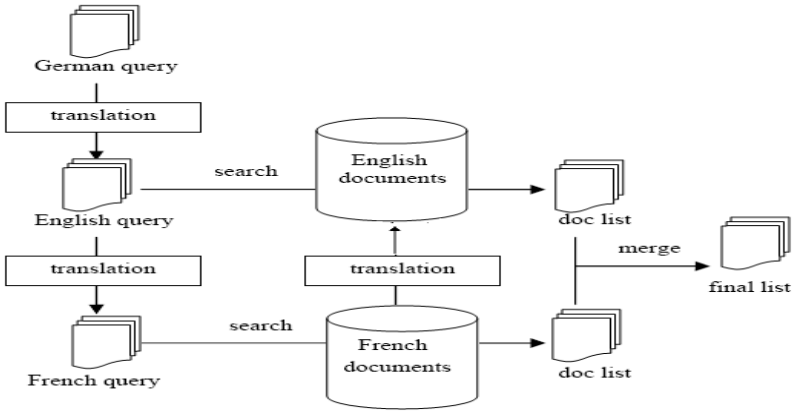

Figure 6. Dual Translation (Pivot Language)

5. COMPARATIVE STUDY OF THE THREE APPROACHES

The need for translation has itself been questioned because non-translation based methods of CLIR, such as cognate-matching [21] and cross-language Latent Semantic Indexing [22] have been developed. Document translation into query language or query translation into documents language are the two approaches that couples machines translation and information retrieval. Query translation and document translation approaches are neither equivalent nor mutually exclusive. They are not equivalent because machine translation is not an invertible operation. Query translation and document translation become equivalent only if each word in one language is translated into a unique word in other languages.

Various researches suggest that document translation should be competitive or superior to query translation. Typical queries are short and may contain key words or phrases only. When these are translated inappropriately, the IR engine has no chance to recover. Translating a long document, MT engine offers the many more opportunities to translate key words and phrases. If some of these are translated inappropriately, the IR engine has at least a chance of matching these to query terms. Query translation approach is flexible and allows for more interactions with the user. However, query translation often suffers from the problem of translation ambiguity, and this problem is amplified due to the limited amount of context in short queries. From this perspective, document translation seems to be more capable of producing more precise translation due to richer contexts.

One of the critical aspects of document translation approach is that one has to determine in advance to which language each document should be translated and that all the translated versions of the document should be stored. In a multilingual IR environment, one would desire to translate each document to all other languages. This is impracticable because of the multiplication of document versions and the increase in storage requirement. Once a document is pre-translated into the same language as the query, user can directly read and understand the translated version. Otherwise, a post-retrieval translation is often needed to make the retrieved documents readable by the user (if he/she does not understand the document language).

Query translation and document translation become equivalent only if each word in one language is translated into a unique word in the other languages. Document translation can be performed off-line and on-line but query translation is performed only on-line. Hybrid system that uses both query and document translation are possible because of a trade off between computer resources and quality of translation. Hybrid or dual translation approach provides the relationship between multilingual and the key advantages of these systems are that queries can be expressed and matched unambiguously. In this approach the additional storage space requirement is independent to the number of languages supported. The major problems occurs in this approach are to define the concept space, intermediate representation and conversion of documents into intermediate representation. Differences between two approaches (query translation and documents translation) of CLIR are described in table2. Table3 describes the comparative study of three approaches of CLIR.

Table2: Difference between Query and Document Translation

Parameter	Query Translation	Document Translation
Size	Small	Large
Language	Prior knowledge of translation language is not required	Prior knowledge of translation language is required
Overhead	Low	High
Recovery	When these are translated inappropriately, the IR engine has no chance to recover	Chance to recover
Ambiguity	Maximum chances of occurring ambiguity	Minimum chances of occurring

		ambiguity
Cost	Low cost	High cost

Table 3: Comparison of three Translation Approaches

Parameter	Query Translation	Document Translation	Both Query & Document Translation
Ambiguity	Maximum	Minimum	More than both
Additional Storage Space	Not required	Required	Not required
Translation time	Less	More than query	More than both
Information retrieval	Bilingual	Bilingual	Bilingual and Multilingual
Flexibility	Highly	Less	Less
Working nature	Can provide interface between two language at a time	Can provide interface between two language at a time	Can provide interface between more than two language at a time

6. CHALLENGES IN CLIR

Queries from users are often too short, which produce more ambiguity in query translation, and reduce the accuracy of the cross language retrieval results. Since the problem of language mismatch in CLIR are more serious than in monolingual IR, it is necessary to exploit techniques for improving the multilingual retrieval performance. In CLIR systems, users often present their query in their native language, and then the system automatically searches documents written in other languages. Therefore, it is a challenge for CLIR to conquer the barrier between the source language (SL) in query sentences and the target language (TL) in documents to be searched. As discussed in the previous section, most CLIR systems utilize MT technology to resolve this problem. As MT research itself has a number of issues (such as accuracy), the research in CLIR also faces critical issues and challenges that must be addressed.

6.1. Ambiguity

Ambiguity [15] occurs when words have multiple meaning which also referred to as homonymy or polysemy. Ambiguity in IR are semantic and syntactic in nature, where as ambiguity in CLIR are semantic and lexical. So the probability of occurrence of ambiguity in CLIR is higher than normal IR, due to the availability of different languages [39].

6.2. Effective User Feedback

Effective user functionality can be incorporated by the user feedback, about their requirements and information needs. It should also provide readable translations of the retrieved documents to support document selection. System should also provide better support for query formulation and reformulation based on some set of intermediate results.

6.3. Complexity in New Applications

Question/Answering is relatively a new stream of Information Retrieval. In Question/Answering end-users throw a question in a form of query and retrieve answers for that. However, challenge is to retrieve answers of English questions in different language.

6.4. Specialized Terminology and Proper Nouns

Specialized terminology, such as scientific names, is often difficult to translate and is often found in specialized dictionaries or term banks. Specialized terminology tends to be less ambiguous than regular vocabulary although regular vocabulary can have a specialized meaning when used in a certain subject area.

7. CLIR RESEARCHES IN FOREIGN & INDIAN LANGUAGES

India is a multilingual country, with 22 constitutionally recognized languages and 12 scripts. A huge amount of information on Web is available in English. In view of the fact that a small number of people know English in India, others are familiar with Hindi and other local languages. In order to solve the language gap between people of India, many government [14] and private organisations are working on CLIR research field. Some of the prominent organisations working in CLIR [47] field are:

(i) Indian Institute of Technology, Bombay, Maharashtra, India.
(ii) Indian Institute of Technology, Kharagpur, West Bengal, India.
(iii) Indian Institute of Technology, Hyderabad, Telangana, India.
(iv) Anna University- K B Chandrasekhar (AUC-KBC), research centre, Chennai, India.
(v) Indian Statistical Institute, Kolkata, West Bengal, India.
(vi) Jadavpur University, Kolkata, West Bengal, India.
(vii) Centre for Development of Advanced Computing (C-DAC), Pune, India.
(viii) Centre for Development of Advanced Computing (C-DAC), Noida, UP, India.
(ix) Utkal University Bhubaneswar and STDC, Orissa, India.
(x) Department of Information Technology (DIT), New Delhi.
(xi) Microsoft research centre, Bangalore, Karnataka, India.
(xii) Technology Development for Indian Langauge (TDIL), government of India.

The objective of these organisations is to help any user to give a query in one Indian language, can access documents in any other language. Some Foreign organisation that working on CLIR are as follows:

(i) Centre for Intelligent Information Retrieval (CIIR), School of Computer Science, University of Massachusetts Amherst.
(ii) National Institute of Standard and Technology (NIST), U.S. department of research.
(iii) Johns Hopkins University, Baltimore, Maryland.

Some of the prominent researches in Foreign & Indian languages are described in table 4 and table5 respectively as follows:

Table 4: Prominent CLIR research in foreign languages

Languages	Authors	Year
English and French	David A. Hull, Gregory Grefenstette [48]	1996
Japanese and English	Fujii, A., Ishikawa, T.,[49]	2001
English and Chinese	Su Liu [50]	2001
Japanese, English and Chinese	Wen- Cheng Lin Hsin- Hsi Chen [51]	2003
Greek, Latin and Old Norse	Jeffrey A, Rydberg-Cox, Lara Vetter, Stefan M, Ruger Daniel Heesch [52]	2004
Chinese, Japanese and Korea	Chen-Yu Su, Tien-Chien Lin , Shih- Hung Wu [53]	2007
English and Chinese	Hsin-Chang Yang, Chung-Hong Lee [54]	2008

Table 5: A brief description of some CLIR research in Indian languages

Languages	Name of Researcher's	Year
Hindi, Telugu, English	Prasad Pingali,Vasudeva Verma [56]	2006
Hindi,Tamil, Telugu, Bengali, Malyalam and English	Jagdeesh, J. , Kumaran, K. [57]	2007
Telugu, English	Ranbeer Makin, Nikita Pandey, Prasad Pingali, Vasudeva Verma [58]	2007
English, Hindi	Anurag Seetha, Sujoy Das, M. Kumar [59]	2007
Hindi, English	Sethuramalingam S, Vasudeva Verma [60]	2008
English, Hindi, Telugu, Tamil	Manoj Kumar Chinnakotla, Om P. Damani [61]	2009
English, Telugu, Tamil	P. Sujatha, P. Dhavachelvan, V. Narasimhulu [62]	2010
Tamil to English	S.Saraswathi & A. Siddhiqaa [55]	2010

8. CLIR TOOLS

Over the past few years, research in CLIR has progressed and a many systems have been developed. Some of the prominent systems of CLIR are as follows:

8.1 SAPHIRE

The architecture of SAPHIRE system is based on multilingual aspects of UMLS (Unified Medical Language System). In this system a dictionary based approach of CLIR is used [27]. It provides an intelligent healthcare monitoring architecture for high quality health care services with reasonable cost.

8.2. KEIZAI

KEIZAI [24] was developed at New Mexico State University and its aim is to provide the Web-based cross language text retrieval system, which searches the documents of Korean or Japanese language on the web for English query. Keizai examines the effectiveness of representing the retrieved documents together with small images, which are called Document Thumbnail Visualizations. The advantage of visualization is to improve the recall and efficiency.

8.3. MULINEX

MULINEX system [26] was developed at German Research Center for Artificial Intelligence (DFKI), whose aim is to allow the user to search the collection of multilingual document, supported by an effective combination of linguistic and IR technologies. There are three document categorisation algorithms are used in Mulinex for different tasks: n-gram categoriser for noisy input, k-nearest-neighbour (KNN) algorithm for normal documents, and pattern-based categoriser for every short documents.

8.4. MIRACLE

MIRACLE (Maryland Interactive Retrieval Advanced Cross-Language Engine), deals with a combination of statistical and linguistic resources, for monolingual, cross-lingual and multilingual search. In MIRACLE two types of query translation are performed: fully automatic query translation and user assistant query translation [25].

8.5. UCLIR

The core process of UCLIR (Unicode Cross-language Information Retrieval system) includes machine translation and standard monolingual information retrieval, which accepts the query in one language and retrieves relevant documents in other language. The UCLIR retrieval system is based on URSA (Unicode Retrieval System Architecture), which is a high-performance text retrieval system that can index and retrieve Unicode texts [28].

8.6. KANSHIN

KANSHIN collects and analyzes the multilingual articles of Japanese, Chinese, Korean and English languages [23]. The system provides a various view points for user such as temporal, focal, geographical, and network. It also provides a cross-lingual keyword navigation tool between splog survey tools (called SplogExplorer) and inters language links of Wikipedia.

9. APPLICATION AREAS OF CLIR

The core field of information retrieval where research on CLIR is needed for effective results are:

9.1. Medical

A number of resources available on Web provide the public and healthcare professionals with the most up-to-date findings in medical research, such as PubMed [68] and MedlinePlus [69].

Table6: List of some prominent CLIR tools from 1990's

Name	Language	Developed At	Year
SAPHIRE [27]	English, German, French, Russian, Spanish, and Portuguese.	School of Medicine Oregon Health Sciences University Portland, OR, USA by William R. Hersh, M.D., Laurence C. Donohoe, M.L.I.S	1998
KEIZAI [24]	English , Japanese & Korean	Computer Research Lab New Mexico State University, Las Cruces USA by William Ogden & James Cowie et.al	1999
MULINEX[26]	French, German and English	German research Centre for artificial Intelligence by Capstick et.al	2000
MIRACLE [25]	English , French, German, Spanish, Cebuano and Hindi	Spanish University (Universal Politecnica de Madrid, Universidad Autonoma de Madrid & Universidad CarlosIII de Madrid) by Julio, Sara et.al	2003
UCLIR [28]	English , Japanese Korean, Arabic	Computing Research Laboratory at New Mexico State University by Ahmed Abdelali et.al	2004
KANSHIN [23]	Japanese, Chinese , Korean & English	University of Tokyo Japan by Tomohiro Fukuhara et.al.	2005

Medline Plus is a Web-based consumer health information resource, made available by the National Library of Medicine. PubMed first released in 1996, is a free search engine for accessing the Medline database of life sciences and biomedical topics.

Most of the high level quality resources that are freely available and unlimited for users all around the world are available only in English language. Therefore Non-English users encounter

a great language barrier when trying to access medical information from these websites such are also not familiar with medical terminology even in their first language (native language). So there is a big platform for researcher to work on medical information retrieval system, in order solve the problem of language barrier [29].

9.2. Multimedia

Multimedia Information Retrieval (MMIR or MIR) is a hot research discipline whose objective is to extract the semantic information from multimedia data sources such as audio, video, and image [1]. MMIR implies that multiple channels are employed for the understanding of media content, each of these channels are described by media-specific features transformations [30].

The first version of the Multilingual Multimedia Information Retrieval (MMIR) prototype involves short videos in the domain of news, that are selected from online web TV channels, from UGC portals, or from online news agencies [31]. There has so far been very little work in the area of Cross-Language Multimedia Information Retrieval (CLMIR). This is an important future research topic as the growth of multilingual and multimedia document collections is likely to lead inevitably to the growth of multilingual multimedia collections [32], [33].

9.3. Mobile Network

This research proposes a Cross-Lingual Information Retrieval approach that is used to search Internet resources for appropriate content and summarize it into another form using the content specification meta-language. This content is then mapped to the target language [34].

9.4. Video Question/Answering system

Question/Answering on multi-media is a new research issue in recent years. The cross-language QA system have some fundamental problems like video processing, i.e. video Optical Character Recognition (OCR) [32], [35], [36] and video segmentation.

9.5. Enterprise Competition

Along with the economic globalization, the information resource in a modern society becomes an important element for modern enterprises competition. CLIR is introduced to the enterprise competitive intelligence collections can effectively resolve the low recall and veracity rate of intelligence collections to some extent and promote the development of CLIR in the enterprise competition intelligence [37].

10. CONCLUSION AND FUTURE OF CLIR

Cross-lingual IR provides new mirror in searching documents through multitude varieties of languages across the world and it can be the baseline for searching not only between two languages but also in multiple languages. Today, most of the cross-lingual researches involved only few famous languages like English, Hindi, Spanish, China and French. Research on languages has increases the development of country. As the world becomes more connected by technology, cross language IR in every language is needed. CLIR is a multidisciplinary area that has been increasingly gaining more attention from the research community. Despite recent advances and new developments, there are still many aspects to be explored.

In Indian context, which is one of the hotspots of linguistic diversity (350 languages) in the globe, and the fact that a dominant language of one region may be a language of a linguistic minority in other region, cross languages information retrieval systems would play a very important role in allowing the people to go through the documents and literatures of other languages thus breaking the language barrier. We work out here to give a broad overview of the speedy demanding work in the field of CLIR by exploring its aspiration, difficulties, basic tools, major works and future research goals. In reviewing this information, it becomes possible to gain a larger picture of the CLIR field.

REFERENCES

[1] Gaillard, B., Bouraoui, J. L., De Neef, E. G., & Boualem, M., (2010, May), "Query expansion for cross language information retrieval improvement", In Research Challenges in Information Science (RCIS), 2010 Fourth International Conference on (pp. 337-342). IEEE.

[2] Pigur, V. A., (1979, "Multilanguage information-retrieval systems: Integration levels and language support", Automatic Documentation and Mathematical Linguistics, 13(1), 36-46.

[3] Peng, Qu, Lu, Li & Zhang lili, (2008) "A Review of Advanced Topics in Information Retrieval", Library and Information Service, Vol.52.No 3. pp. 19-23.

[4] Ahmed, F., & Nurnberger, A., (2012), "Literature review of interactive cross language information retrieval tools", Int. Arab J. Inf. Technol., 9(5), 479-486.

[5] Narasimha Raju, B. N. V., Bhadri Raju, M. S. V. S., & Satyanarayana, K. V. V. (2014, December). Translation approaches in Cross Language Information Retrieval. In Computer and Communications Technologies (ICCCT), 2014 International Conference on IEEE, pp. 1-4.

[6] Carley Mc & S.J. (1999, June), "Should we translate the documents or the queries in cross-language information retrieval?" In Proceedings of the 37th annual meeting of the Association for Computational Linguistics on Computational Linguistics. Association for Computational Linguistics, pp. 208-214.

[7] Aljlayl, M., & Frieder, O., (2001, October), "Effective arabic-english cross-language information retrieval via machine-readable dictionaries and machine translation", In Proceedings of the tenth international conference on Information and knowledge management ACM, pp. 295-302.

[8] Pirkola, A., Hedlund, T., Keskustalo, H., & Jarvelin, K., (2001), "Dictionary-Based Cross-Language Information Retrieval: Problems, Methods, and Research Findings," Information Retrieval, 4(3/4), pp. 209-230.

[9] Picchi, E. & Peters, C, (2000) "Cross-language information retrieval: a system for comparable corpus querying, in Cross-Language Information Retrieval," G. Grefenstette, Editor. 2000, Kluwer Academic Publishing: Massachusetts. pp. 81-90.

[10] Manning, C. D., Raghavan, P., & Schütze, H. (2008). Introduction to information retrieval (Vol. 1, p. 496). Cambridge: Cambridge University Press.

[11] Munteanu, D.S. and D. Marcu. (2005) "Extracting parallel subsentential fragments from non-parallel corpora", In Proceedings of the 21st international Conference on Computational Linguistics. Sydney, Australia: Association of Computational Linguistics.

[12] Landauer, T.K. & Littman, M.L.,(1990) "Full Automatic Cross Language Document Retrieval using Latent Semantic Indexing" , In Proc. of the 6th Conference of UW Center for New OED and Text Research, pp. 31–38.

[13] Sheridan, P., & Ballerini, J.P., (1996) "Experiments in Multilingual Information Retrieval using the SPIDER System", In Proc. of the 19th Annual International ACM SIGIR, pp. 58–65.

[14]Sourabh, K., (2013) "An Extensive Literature Review on CLIR and MT activities in India", International Journal of Scientific & Engineering Research.

[15] Chandra, G.; Dwivedi, S.K., "A Literature Survey on Various Approaches of Word Sense Disambiguation," in Computational and Business Intelligence (ISCBI), 2014 2nd International Symposium on , vol., no., pp.106-109, 7-8 Dec. 2014.

[16] Manning, C.D., & Schutze, H., (1999) Foundations of statistical natural language processing. MIT Press.

[17] Braschler, M., & Schauble, P., (2000), "Using corpus-based approaches in a system for multilingual information retrieval." Information Retrieval, 3, pp. 273–284.

[18] Franz, M., Scott McCarley, J., & Todd Ward, R. (2000), Ad hoc, cross-language and spoken document information retrieval at IBM. In Proceedings of TREC-8. Gaithersburg, MD: National Institute of Standards and Technology. Available: http://trec.nist.gov/pubs/.

[19] Oard, D. W., & Diekema, A. R., (1998) "Cross-language information retrieval", Annual Review of Information Science and Technology, 33, pp. 223–256.

[20] Oard D and Dorr B. (1996), "A Survey of Multilingual Text Retrieval", Technical Report UMIACS-TR-96-19, University of Maryland, Institute for Advanced Computer Studies.

[21] Buckley, M. Mitra, Wals, J. & Cardie, C., (1998), "Using clustering and superconcepts within SMART: TREC-6", In E.M. Voorhees and D.K. Harman, editors, The 6th Text REtrieval Conference (TREC-6).

[22] Dumais, S. T., Letsche, T. A., Littman, M. L., & Landauer, T. K., (1997, March) "Automatic cross-language retrieval using latent semantic indexing", In AAAI spring symposium on cross-language text and speech retrieval, Vol. 15,pp. 21.

[23] Fukuhara, T., Kimura, A., Arai, Y., Yoshinaka, T., Masuda, H., Utsuro, T., & Nakagawa, H., (2008, April) "KANSHIN: A cross-lingual concern analysis system using multilingual blog articles", In Information-Explosion and Next Generation Search, 2008. INGS'08. International Workshop on IEEE, pp. 83-90.

[24] Ogden, W., Cowie, J., Davis, M., Ludovik, E., Nirenburg, S., Molina-Salgado, H., & Sharples, N. (1999, September). Keizai: An interactive cross-language text retrieval system. In Proceeding of the MT SUMMIT VII workshop on machine translation for cross language information retrieval, Vol. 416.

[25] He, D., Oard, D. W., Wang, J., Luo, J., Demner-Fushman, D., Darwish, K., & Leuski, A., (2003), "Making miracles: Interactive translingual search for cebuano and hindi", ACM Transactions on Asian Language Information Processing (TALIP), 2(3), 219-244.

[26] De Luca, Ernesto William, Ernesto William, Stefan Hauke De Luca, Andreas Nürnberger, and Stefan Schlechtweg., (2006) "MultiLexExplorer-Combining Multilingual web Search with Multilingual Lexical Resources", In Proceedings of the combined workshop on Language-Enabled educational technology and Development and evaluation of Robust Spoken Dialogue Systems, Germany, pp. 17-21.

[27] Hersh, William R., and Larry C. Donohoe, (1998) "SAPHIRE International: a tool for cross-language information retrieval.", Proceedings of the AMIA Symposium. American Medical Informatics Association, pp673.

[28] Abdelali, A., Cowie, J. R., Farwell, D., & Ogden, W. C., (2004) "UCLIR: a Multilingual Information Retrieval Tool", Inteligencia Artificial, Revista Iberoamericana de Inteligencia Artificial, 8(22), pp103-110.

[29] Lu, Wen-Hsiang, et al. (2008), "Using Web resources to construct multilingual medical thesaurus for cross-language medical information retrieval." Decision Support Systems 45.3: 585-595.

[30] Arrieta, K., Leturia, I., Iturraspe, U., de Ilarraza, A. D., Sarasola, K., Hernáez, I., & Navas, E. (2008, December). AnHitz, development and integration of language, speech and visual technologies for Basque. In Universal Communication, 2008. ISUC'08. Second International Symposium on IEEE, pp. 338-343.

[31] Wu, Y. C., Chang, C. H., & Lee, Y. S., (2004, December) "CLVQ: Cross-language video question/answering system", In Multimedia Software Engineering, 2004. Proceedings. IEEE Sixth International Symposium on IEEE, pp. 294-301.

[32] Lin, C. J., Liu, C. C., & Chen, H. H., (2001) "A simple method for Chinese video OCR and its application to question answering", Computational linguistics and Chinese language processing, 6(2), pp11-30.

[33]Wu, V., Manmatha, R., & Riseman, E. M., (1999) "Textfinder: An automatic system to detect and recognize text in images", IEEE Transactions on Pattern Analysis & Machine Intelligence, (11), pp1224-1229.

[34] Kumar, B. A. (2012, January). Profound survey on cross language information retrieval methods (CLIR). In Advanced Computing & Communication Technologies (ACCT), 2012 Second International Conference on IEEE, pp 64-68.

[35] Shim, J. C., Dorai, C., & Bolle, R., (1998, August) "Automatic text extraction from video for content-based annotation and retrieval", In Pattern Recognition, 1998. Proceedings. Fourteenth International Conference on IEEE, Vol. 1, pp. 618-620.

[36] Yang, H., Chaisorn, L., Zhao, Y., Neo, S. Y., & Chua, T. S. (2003, November). VideoQA: question answering on news video. In Proceedings of the eleventh ACM international conference on Multimedia ACM, pp. 632-641.

[37] Xiang-jun, L., Hong-Na, S., Li-Wen, Y., & Xiao-Kun, Y. (2009, May), "Research of Enterprise Competitive Intelligence Collection System Based on Cross-Language Information Retrieval", In Electronic Commerce and Security, 2009. ISECS'09. Second International Symposium on IEEE, Vol. 1, pp. 601-604.

[38] Fernandes, Lincoln Paulo. (2006), "Corpora in Translation Studies: revisiting Baker's tipology." Fragmentos: Revista de Língua e Literatura Estrangeiras, 30.

[39] Diekema, Anne R., (2003) "Translation events in cross-language information retrieval: lexical ambiguity, lexical holes, vocabulary mismatch, and correct translations".

[40] Wu, D., & He, D., (2010, December) "A study of query translation using google machine translation system", In Computational Intelligence and Software Engineering (CISE), 2010 International Conference on IEEE, pp. 1-4.

[41] Seetha, A., Das, S., & Kumar, M., (2007, December) "Evaluation of the English-Hindi Cross Language Information Retrieval System Based on Dictionary Based Query Translation Method", In Information Technology,(ICIT 2007). 10th International Conference on IEEE, pp. 56-61.

[42] Pfeifer, U., Poersch, T., & Fuhr, N. (1996) "Retrieval effectiveness of proper name search methods", Information Processing & Management, 32(6), pp 667-679.

[43] Fluhr, C., Schmit, D., Ortet, P., Elkateb, F., Gurtner, K., & Radwan, K. (1998). Distributed cross-lingual information retrieval. In Cross-Language Information Retrieval, Springer US, pp. 41-50).

[44] Croft, W. B., Turtle, H. R., & Lewis, D. D. (1991, September), "The use of phrases and structured queries in information retrieval", In Proceedings of the 14th annual international ACM SIGIR conference on Research and development in information retrieval, ACM, pp. 32-45.

[45] Buckley, C., Singhal, A., Mitra, M., & Salton, G., (1995, November), "New retrieval approaches using SMART: TREC 4", In Proceedings of the Fourth Text Retrieval Conference (TREC-4), pp. 25-48.

[46] Lyons, J, (1981), "Language and Linguistics: An introduction", Cambridge University Press.

[47] Nagarathinam, A., & Saraswathi, S. (2011), "State of Art: Cross Lingual Information Retrieval System for Indian Languages", International Journal of Computer Applications, 35 (13).

[48] Hull, D. A., & Grefenstette, G., (1996, August), "Querying Across Languages: A Dictionary-Based Approach to Multilingual Information Retrieval", In Proceedings of the 19th annual international ACM SIGIR conference on Research and development in information retrieval ACM, pp. 49-57.

[49] Fujii, A., & Ishikawa, T., (2001, March) "Evaluating multi-lingual information retrieval and clustering at ULIS", In Proceedings of the Second NTCIR Workshop Meeting on Evaluation of Chinese & Japanese Text Retrieval and Text Summarization. Tokyo. Japan, pp. 5-144.

[50] Su Liu.: ECIRS, (2001), "An English-Chinese Cross-language Information-retrieval System", In: IEEE International Conference on Systems, Man, and Cybernetics, Volume 2.

[51] Lin, W. C., & Chen, H. H., (2003) "Description of NTU approach to NTCIR3 multilingual information retrieval", In Proceedings of the third NTCIR workshop.

[52] Jeffrey A. Rydberg-Cox, Lara Vetter, Stefan M. Ruger, Daniel Heesch, (2004) "Cross-lingual searching and visualization for greek and latin and old norse texts", In: JCDL Vol. 383.

[53] Su, C. Y., Lin, T. C., & Wu, S. H. (2007, May). Using Wikipedia to translate OOV terms on MLIR. In Proceedings of NTCIR-6 Workshop Meeting (pp. 109-115).

[54] Yang, H. C., & Lee, C. H., (2008, November) "Multilingual Information Retrieval Using GHSOM", In Intelligent Systems Design and Applications, 2008. ISDA'08. Eighth International Conference on IEEE, Vol. 1, pp. 225-228.

[55] Dr. Saraswathi, S., Siddhiqaa, Asma, Kalaimagal, M, K., and Kalaiyarasi M (2010, April) BiLingual Information Retrieval System for English and Tamil, Journal Of Computing, 2, 4, 85-89.

[56] Pingali, P., & Varma, V. (2006, September) "Hindi and Telugu to English Cross Language Information Retrieval at CLEF 2006", In Working Notes of Cross Language Evaluation Forum.

[57] Jagadeesh, J. & Kumaran, K, (2007), "Cross-Lingual Information Retrieval System for Indian Languages.In: Advances in Multilingual and Multimodal Information Retrieval: 8th Workshop of the Cross-Language Evaluation Forum, CLEF, pages: 80-87.

[58] Makin, R., Pandey, N., Pingali, P., & Varma, V., (2007) "Approximate string matching techniques for effective CLIR among Indian languages", In Applications of Fuzzy Sets Theory, Springer Berlin Heidelberg, pp. 430-437.

[59] Seetha, A., Das, S., & Kumar, M. (2007, December). Evaluation of the English-Hindi Cross Language Information Retrieval System Based on Dictionary Based Query Translation Method. In Information Technology,(ICIT 2007). 10th International Conference on IEEE, pp. 56-61.
[60] Sethuramalingam, S., & Varma, V. (2008). IIIT Hyderabad's CLIR experiments for FIRE-2008. In The working notes of First Workshop of Forum for Information Retrieval Evaluation (FIRE), Kolkata.
[61] Chinnakotla, M. K., & Damani, O. P., (2009, August) "Experiences with english-hindi, english-tamil and english-kannada transliteration tasks at news 2009", In Proceedings of the 2009 Named Entities Workshop: Shared Task on Transliteration ,Association for Computational Linguistics, pp. 44-47.
[62] Sujatha, P., Dhavachelvan, P., & Narasimhulu, V., (2010) "Evaluation of English-Telugu and English-Tamil Cross Language Information Retrieval System using Dictionary Based Query Translation Method", International Journal of Computer Science and Information Security, 8(2), 314-319.
[63] Ramanathan, A. (2003). State of the Art in Cross-Lingual Information Retrieval.VIVEK-BOMBAY-, 15(2), 16-22.
[64] Voorhees, Ellen M., & Donna K. Harman, eds, (2005), "TREC: Experiment and evaluation in information retrieval. Vol. 63. Cambridge: MIT press, Vol. 63.
[65] Peters, Carol, (2001), "Cross-language information retrieval and evaluation", Berlin Heidelberg: Springer.
[66] Gey, F., Larson, R., Sanderson, M., Joho, H., Clough, P., & Petras, V. (2006) "Geo CLEF: the CLEF 2005 cross-language geographic information retrieval track overview ,Springer Berlin Heidelberg, pp. 908-919.
[67] Salton, G., (1973), "Experiments in multi-lingual information retrieval", Information Processing Letters, 2(1), 6–11.
[68] Chang, D. T. H., Weng, Y. Z., Lin, J. H., Hwang, M. J., & Oyang, Y. J., (2006) "Protemot: prediction of protein binding sites with automatically extracted geometrical templates", Nucleic acids research, 34(suppl 2), W303-W309.
[69] Shatkay, Hagit, (2005) "Hairpins in bookstacks: information retrieval from biomedical text", Briefings in Bioinformatics 6.3 (2005): 222-238.
[70] Oard, D. W., He, D., & Wang, J. (2008). User-assisted query translation for interactive cross-language information retrieval. Information Processing & Management, 44(1), 181-211.

AUTHORS

Prof. Sanjay K. Dwivedi is working as Professor & Head, Department of Computer Science at Babasaheb Bhimrao Ambedkar Central University, Lucknow, India. His research interest is in Artificial Intelligence, Information Retrieval, Web Mining, NLP and WSD. He has published number of research papers in reputed journals and conferences. He is approachable at skd200@yahoo.com.

Ganesh Chandra received his M. Tech. degree from KNIT Sultanpur, U.P. India and is pursuing his Ph.D. degree in Department of Computer Science at Babasaheb Bhimrao Ambedkar Central University, Lucknow, India. His major research interests include Information Retrieval, WSD and Machine Translation. He has published papers in various international journals and conferences. He is approachable at ganesh.iiscgate@gmail.com.

PDE BASED FEATURES FOR TEXTURE ANALYSIS USING WAVELET TRANSFORM

P. S. Hiremath[1] and Rohini A. Bhusnurmath[2]

[1]Department of Computer Science (MCA), KLE Technological University,
BVBCET Campus, Hubli-580031, Karnataka, India.
[2]Department of P.G. Studies and Research in Computer Science,
Gulbarga University, Gulbarga-585106, Karnataka, India.

ABSTRACT

In the present paper, a novel method of partial differential equation (PDE) based features for texture analysis using wavelet transform is proposed. The aim of the proposed method is to investigate texture descriptors that perform better with low computational cost. Wavelet transform is applied to obtain directional information from the image. Anisotropic diffusion is used to find texture approximation from directional information. Further, texture approximation is used to compute various statistical features. LDA is employed to enhance the class separability. The k-NN classifier with tenfold experimentation is used for classification. The proposed method is evaluated on Brodatz dataset. The experimental results demonstrate the effectiveness of the method as compared to the other methods in the literature.

KEYWORDS

Anisotropic Diffusion, Wavelet Transform, Texture Approximation, Partial Differential Equation (PDE).

1. INTRODUCTION

Texture is a recurring pattern in image intensity. Texture can be defined as a similarity grouping in an image [1]. Texture analysis represents mathematical approach that captures gray level variations in an image. Texture perception is a function of radiometric and spatial scales. It is used in computer vision and image analysis. An image is the matrix of pixels and a texture in an image can be considered as descriptors of interrelated pixels. Tuceryan and Jain [2] categorized texture analysis approaches into statistical, signal processing, geometrical, and model based methods. The study of human vision system reveals that spatial or frequency representation preserving local and global information is suitable for quasi periodic signal. Haralick et al. [3] proposed gray level co-occurrence matrix (GLCM) for texture feature extraction. This approach explored spatial gray level dependence of texture. Tamura et al. [4] proposed a computation of six visual properties like contrast, coarseness, likeliness, regularity, directionality and roughness. In [5] wavelet transform is used to obtain features for texture classification. Smith and Chang [6, 7] used the statistical features such as mean and variance from wavelet sub-bands as texture measures. The local directional binary patterns (LDBP) and non-subsampled contourlet transform (NSCT) based texture classification using k-NN classifier is introduced in [8]. The effective LDBP's are investigated which characterize local image texture [9]. In [10], support vector machine is used for rotation and shift invariant texture classification. Thyagarajan et al. [11] proposed wavelet transform with co-occurrence matrix for texture analysis. The commonly used texture descriptors that have been used successfully to real-world textures are the Laws' texture energy measures [12] and Fourier power spectrum [13]. The fractal concept developed by Mandelbrot [14] provides an excellent representation of the roughness of natural textural surfaces. The partial differential equation (PDE) based anisotropic diffusion filter is used for image processing. The PDE techniques are widely used in image and signal processing [15]. Most

DOI: 10.5121/ijci.2016.5114

methods based on PDE are used to smooth the image while preserving the edges [16]. An effective method for texture classification using local directional binary pattern co-occurrence matrix and anisotropic diffusion is presented in [17]. Anisotropic diffusion for color texture image classification is explored on RGB color space [18]. Extraction of LDBP features using diffusion approach on different datasets is presented in [19]. Randen and Husoy [20] concluded in a survey of filtering methods that future direction of research is extraction and classification of powerful texture features with low computational cost. This observation has inspired to develop proposed method.

The combination of transform based method and statistical method for feature extraction is proposed in the paper. The objective of this paper is to obtain better classification accuracy with reduced computational cost. Wavelet transform is used to obtain directional information. Anisotropic diffusion is applied on directional information to find texture approximation. Further, various statistical features are computed from texture approximation. Linear discriminant analysis (LDA) enhances the class separability. The k-NN classifier is used for classification. The method is evaluated on sixteen texture classes from Brodatz image dataset. The average classification accuracies obtained by using various statistical feature sets are compared with other methods in the literature.

2. PROPOSED METHOD

The proposed method comprises the following steps:

i. Apply Haar wavelet transform on input image to yield H, V and D subbands.
ii. Apply anisotropic diffusion on H, V and D components up to n diffusion steps and obtain texture approximation.
iii. Extract statistical features from texture approximation image and use LDA on feature sets for optimization
iv. Use k-NN classifier to classify the feature set of textural image.

These methods are described briefly as given below.

2.1. Wavelet Transform

During the past decades wavelet analysis has become a powerful tool for multi-resolution analysis. Intuitively, multiscale wavelet analysis is an ideal approach to analyze texture because it is well recognized that scale is one of the most important aspects of texture information. The wavelet based methods are computationally effective over other methods for the texture classification. The different wavelet transform functions filter out different range of frequencies (i.e., subbands). Thus, wavelet is a powerful tool, which decomposes the image into low frequency and high frequency subband images. The implementation and theoretical aspects of wavelet based algorithms are discussed in [21, 22, 23]. Time dependent signal analysis at different resolution is achieved by wavelet transform. The wavelet transform has several advantages making it attractive for texture analysis. That include –textures are represented at the suitable scale in varying the spatial resolution. Wavelet functions are available in wide range of choices, so that wavelet best suited for texture analysis can be chosen in a specific application. In an image, the wavelet decomposition is obtained with separable filtering along the columns and the rows and of an image [23]. The decomposition of a signal into a set of detail coefficients (H, V, D) and an approximation coefficient (A) is obtained in discrete wavelet transform. The D subband represents diagonal details (high frequencies in both directions – the corners), H gives horizontal high frequencies, V gives vertical high frequencies, and the image A corresponds to the lowest frequencies. The Figure 1 represents the level 1 (1-scale) image decomposition. The

original Brodatz texture image D51 is shown in the Figure 1(b) and its 1-level Haar wavelet transform is shown in the Figure 1(c).

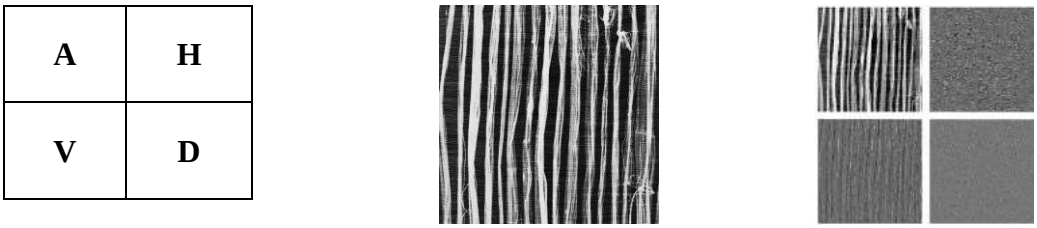

(a) (b) (c)

Figure 1. Wavelet transform (a) Subbands of level 1 decomposition (b) Brodatz texture image D51 (c) 1-level Haar wavelet transform of the image in (b).

2.2. Anisotropic Diffusion

Anisotropic diffusion filter proposed by Perona - Malik [15] is used to smooth an image without altering important parts of the image such as edges. The edge detection is done using scale space approach. The family of parameterized images is produced in combination of original image and image dependent filter. This makes anisotropic diffusion a space variant and nonlinear transformation of the image. The relation between filtered image F(x,y,t) and the original image $F_0(x,y)$ is represented by $F(x,y,t) = F_0(x,y) * GK(x,y,t)$, where GK(x,y,t) is a Gaussian kernel having variable scale parameter t. The filtering is the result of iterative heat diffusion. The initial condition is given by the equation F(x,y,0) = F(x,y) , where t represents time. The diffusion process smoothes the image and is stopped at the edges and boundaries. The method is described in brief in Appendix.

2.3. Statistical Features

Statistical methods are used to compute local features by considering gray values in an image [24]. Statistical methods are classified into first order (one pixel), second order (two pixels) and higher order (more than two pixels) statistics [24]. The first-order statistics captures properties (e.g. average and variance) considering individual pixel values, whereas second and higher order statistics represent the spatial dependency between two or more pixel values relative to each other. Various feature vectors considered for experimentation are described below.

2.3.1. First order statistics for texture analysis (F1)

First order texture features are calculated from the gray values of original image. These statistics do not consider relationships between neighboring pixels. Five features, namely, mean, median, standard deviation, skewness and kurtosis are considered for experimentation. Texture analysis based on these statistical features lacks the information about the relationship between neighboring pixels.

2.3.2. Haralick features (F2)

Haralick et al. [3] suggested second order statistics of textures that considers relationship between pairs of pixels. They used gray level co-occurrence matrices (GLCM) which have become well known and widely used textural features. GLCM shows a function of joint probability distributions of pairs of gray level pixels. The most commonly used seven textural features,

namely, contrast, energy, entropy, homogeneity, maximum probability, cluster shade and cluster prominence over angles 0, 45, 90 and 135 degrees (7 features x 4 angles = 28 number) are considered for the experimentation.

2.3.3. Gray level difference statistics (F3)

This method is described in [25]. Five features, namely, homogeneity, contrast, energy, entropy and mean are calculated from a single grey level difference probability distribution vector. These features are obtained from sum of four vectors for 0, 45, 90 and 135 degrees. Methods based on second-order statistics have higher discrimination capability than the structural and power spectrum (transform based) methods [25].

2.3.4. Neighborhood gray tone difference matrix (F4)

Image texture can be represented as a function of the structural and tonal relationships between the pixels. Tone is based mainly on pixel intensity (gray values), while the structure is the spatial (location) relationship between pixels [26]. A Grey-Tone Difference Matrix (GTDM) was proposed in [27] to correlate texture measures with human perception of textures. A GTD matrix is a vector containing G elements. Its elements are computed as the difference between gray value of pixel and average of gray values over a square by sliding the window centered at the pixel. Features, namely, coarseness, contrast, busyness, complexity, and texture strength are considered.

2.3.5. Statistical feature matrix (F5)

This method of feature extraction was introduced in [28]. Four features, namely, coarseness, contrast, period and roughness are considered.

2.3.6. Law's texture energy measures (F6)

This method is described in [29, 30]. Six texture energy measures are given by standard deviation of convolved image over entire region of interest. The measures are derived from three simple vectors. L3 = (1, 2, 3) which represents averaging; E3 = (-1, 0, 1) calculating first difference (edges); and S3 = (-1, 2, -1) corresponding to the second difference (spots). Mutually multiplying these vectors by considering the first term as a column vector and the second term as row vector, results in 3 X 3 matrix known as Law's masks. The Law's mask is convolved over texture image and six energy statistics are calculated, which are used for texture description.

2.3.7. Fractal dimension texture analysis (F7)

Texture analysis based on fractal was introduced in [14]. The geometric complexity of spatial pattern of textures is represented using fractals [14]. The word `fractal' refers to complex patterns that re-occur at various scales and are independent of scales. Fractal metrics provide features patterns of self similarity at different scales. The fractal dimension gives a global descriptor of complexity or irregularity of a geometric object. It has been found that fractal dimension encode textures in nature, which represents the irregularity of textures. The fractal dimension is used to calculate roughness of a surface. The larger the fractal dimension, the rougher is the texture.

2.3.8. Fourier power spectrum (F8)

Texture descriptors are scale dependant. A texture is described in multiple resolutions to decrease the scale sensitivity. An appropriate scale to achieve the maximum texture discrimination may be

chosen. For calculating multiscale feature, time-frequency method known as Fourier spectral method [31] is adopted. It is an image in a space whose co-ordinate system has an interpretation that is closely related to the characteristics of a texture (such as size or frequency). Two features, namely, radial sum and angular sum features are computed.

2.3.9. Shape (F9)

Five shape features: size (x, y), area, perimeter and perimeter^2 /area are considered for experimentation. Texture size measure may be based on co-occurrences of edge pairs with opposite edge directions at constant distance in a direction perpendicular to the edge directions. These statistics are derived from the second order statistics.

3. FEATURE EXTRACTION AND TEXTURE CLASSIFICATION

Feature extraction is the important stage of texture analysis. Features obtained from this stage are used for texture classification.

3.1. Feature extraction

The steps of the proposed method are given in the Algorithm 1.

Algorithm 1: Training Algorithm	
Step 1 :	Read the training image block I.
Step 2 :	Decompose the image, using Haar wavelet transform, into horizontal (H), vertical (V) and diagonal (D) components.
Step 3 :	Subject the H, V and D components to anisotropic diffusion.
Step 4 :	Obtain texture approximation $I_{Htxr,}$ $I_{Vtxr,}$ I_{Dtxr} for H, V and D components, respectively.
Step 5 :	Compute statistical features (as in section 2.3) for images $I_{Htxr,}$ $I_{Vtxr,}$ I_{Dtxr} obtained in Step 4, which form feature vector F. The F is stored in the feature database, with class label.
Step 6 :	The Steps 1 – 5 are repeated for all the training blocks of all the texture class images and the training feature set (TF) is obtained.
Step 7 :	LDA is applied on training feature set (TF) of Step 6. The discriminant feature set (TFLDA) is obtained, which is then used for texture classification.
Step 8 :	Stop.

The Algorithm 1 is executed up to different numbers of diffusion steps (*t*) and extracted various features as discussed in section 2.3.

3.2. Texture classification

The texture classification is performed using k-NN classifier with ten-fold experimentation, based on Euclidean distance [32]. The steps of testing algorithm are given in the Algorithm 2.

Algorithm 2 : Testing Algorithm (Classification of test images)	
Step 1 :	Read the test image block $I_{test.}$
Step 2 :	Decompose the image I_{test}, using Haar wavelet transform, into horizontal (H), vertical (V) and diagonal (D) components.

Step 3 :	Subject the H, V and D components to anisotropic diffusion.
Step 4 :	Obtain texture approximation $I_{testHtxr,}$ $I_{testVtxr,}$ $I_{testDtxr}$ for H, V and D components, respectively.
Step 5 :	Compute statistical features (as in section 2.3) for images $I_{testHtxr,}$ $I_{testVtxr,}$ $I_{testDtxr}$ obtained in the Step 4, to form feature vector F_{test}.
Step 6 :	Project F_{test} on LDA components stored in TFLDA and obtain the weights which constitute test image feature vector $F_{testLDA.}$
Step 7 :	(Classification) The k-NN classifier (k = 3) based on Euclidean distance is employed to classify the test image I_{test} using $F_{testLDA}$ vectors.
Step 8 :	Stop.

4. EXPERIMENTAL RESULTS AND DISCUSSION

4.1. Dataset

The sixteen texture images from Brodatz album [33] are considered for experimentation and these are shown in the Figure 2. Each Brodatz texture sample represents one class. Each texture image is of 256x256 pixels with 256 gray levels. The experimental dataset includes regular textures, namely, D4, D3, D36, D75, D16, D21, D68, D24, nonregular textures D82, D11, D29, D104, D71 and highly regular textures D6, D52, D51. Each texture image is subdivided into 16 non overlapping blocks of 64x64 pixels. Thus, totally 256 blocks are considered. The texture images in the dataset have different gray scale properties. The performance of unbiased texture classification is estimated by performing ten-fold experiments. The average of ten experimental results is reported in the paper. The images are randomly separated into distinct training and testing sets. The 50% of the sub images are taken as training set and remaining 50% sub images are used for testing.

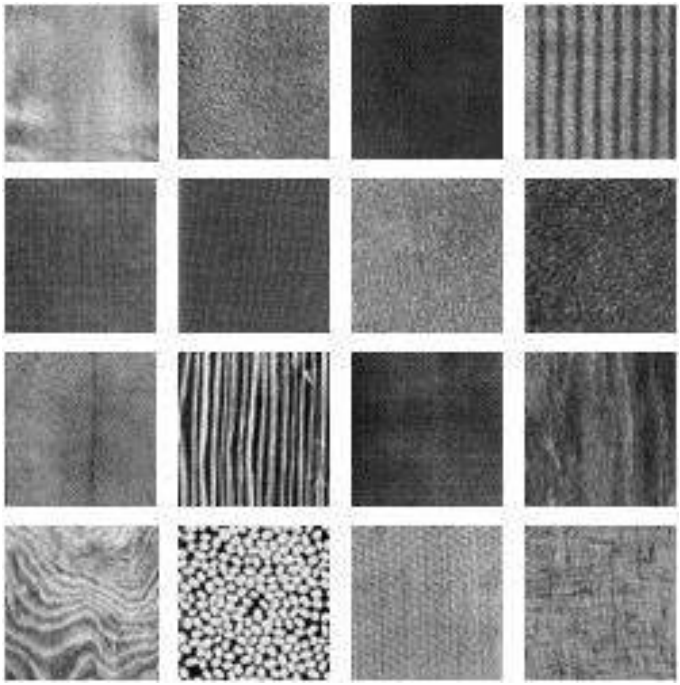

Figure 2. Texture images from Brodatz album from left to right and top to bottom: D3, D4, D6, D11, D16, D21, D24, D29, D36, D51, D52, D68, D71, D75, D82, D104.

4.2. Experimental results

The experimentation of the proposed method is carried out on Intel® Core™ i3-2330M @ 2.20GHz with 4 GB RAM using MATLAB 7.9 software. The Haar wavelet transform is employed to decompose the image, resulting in average (A), horizontal (H), vertical (V) and diagonal (D) components. The H, V and D components of the image are then subjected to anisotropic diffusion to find texture approximation. Further, different statistical features (discussed in section 2.3) are computed from the texture approximations. The LDA is used to enhance the class separability. The k-NN classifier is used for classification. The values for optimization of parameters of anisotropic diffusion are: lambda = 0.25 and conduction coefficient = 60. The experimentation for each feature set is executed up to 10 diffusion steps. The average classification accuracy is computed for the sixteen class problem, where 16 texture classes are considered for the experimentation from Brodatz texture dataset [33].

The Table 1 shows the comparison of average classification accuracy, average training time and average testing time for various feature sets using the optimal number of diffusion steps. Totally, thirty feature sets (including combinations of feature sets in section 2.3) are taken for experimentation. The optimal number of diffusion step is the diffusion step at which the best classification results are obtained for a given feature set. The corresponding training and testing time are recorded.

Table 1. Comparison of average classification accuracy (ACA), average training time (ATrTm) and average testing time (ATsTm) for the various feature sets based on wavelet transform and anisotropic diffusion using the optimal number of diffusion step (DS) for Brodatz dataset.

Sl. No.	**Feature set**	**DS**	**ACA (%)**	**ATrTm (sec.)**	**ATsTm (sec.)**	**No. of features**
1	F1	9	79.30	3.71	0.24	15
2	F2	8	92.89	35.92	2.25	84
3	F3	7	84.69	3.06	0.19	15
4	F4	1	86.17	4.28	0.27	15
5	F5	1	73.44	3.39	0.22	12
6	F6	10	92.11	4.20	0.27	18
7	F7	9	42.19	4.01	0.25	12
8	F8	1	39.84	1.54	0.10	6
9	F9	1	19.84	1.37	0.09	15
10	F1+F3	9	93.20	4.61	0.29	30
11	F1+F3+F4	7	95.78	6.32	0.40	45
12	**F1+F3+F4+F5**	**10**	**98.75**	**8.19**	**0.51**	**54**
13	F1+F3+F4+F5+F6	9	97.58	8.20	0.52	72
14	F1+F3+F4+F5+F6+F7	9	96.41	8.61	0.54	84
15	F1+F3+F4+F5+F6+F7+F8	9	94.84	8.83	0.55	90
16	F1+F3+F4+F5+F6+F7+F8+F9	4	36.09	7.48	0.47	105
17	F1+F3+F5+F6	9	98.36	5.45	0.34	57
18	F3+F4+F5+F6	1	97.73	6.80	0.43	57
19	F1+F4+F5+F6	10	98.28	8.64	0.54	57
20	F6+F7+F8+f9	4	35.78	3.90	0.25	51
21	F1+F3+F5	10	98.36	6.33	0.40	39
22	F1+F3+F6	9	97.42	5.10	0.32	48
23	F1+F4+F5	6	97.81	6.91	0.44	39

24	F3+F4+F5	10	98.05	8.79	0.55	39
25	F6+F7	10	94.06	5.19	0.33	30
26	F4+F5	6	97.66	7.47	0.47	24
27	F3+F4	1	93.20	4.14	0.26	30
28	F5+F6	10	97.34	6.27	0.40	27
29	F8+F9	1	22.58	1.42	0.09	21
30	F2+F4	9	86.88	41.73	2.61	99

It is observed from the Table 1 that the single feature set (F1 to F9) gives poor classification accuracy except F2 and F6. Even though the feature set F2 based on Haralick features gives 92.89% of classification accuracy, it is computationally expensive. The same observation is verified for the combination of feature sets F2+F4. Hence, F2 is not considered with other combinations of feature set. The combination of feature set gives improved classification accuracy compared to the feature set considered alone. Hence, the accuracy of classification depends on the type of features used.

It is also observed from the Table 1 that the feature sets F1, F3, F4, F5 and F6 are dominant feature sets. These feature sets give better classification accuracy in combinations. The optimal average classification accuracy of 98.75% is observed for F1+F3+F4+F5 feature set (Sl. No. 12) at the tenth diffusion step with average training time of 8.19 sec. and average testing time of 0.51 sec.

The proposed method is experimented on same dataset [33] as used in [8] and [19] so that, results can be compared. The methods NSCT and LDBP used in [8] and [19] are briefly described in Appendix. The Table 2 shows comparison of average classification accuracy attained by the proposed method and other methods in the literature on Brodatz dataset.

Table 2. Comparison of average classification accuracy (%) obtained by the proposed method and other methods in the literature [8, 19] on Brodatz dataset.

Image no.	**Average classification accuracy (%)**		
	Method in [8] (NSCT & LDBP)	**Method in [19] (PDE & LDBP)**	**Proposed method (WT & PDE)**
D104	100	100	100
D11	100	96.25	96.25
D16	100	100	100
D21	100	100	100
D24	100	98.75	98.75
D29	100	100	100
D3	100	95	100
D36	87.5	98.75	95
D4	100	100	97.5
D51	100	97.5	95
D52	100	100	97.5
D6	100	100	100
D68	100	100	100
D71	100	97.5	100
D75	100	100	100
D82	87.5	100	100
Average classification	98.43	98.98	98.75

accuracy (%)			
Average training time (sec.)	278.50	14.92	8.18
Average testing time (sec.)	12.42	0.93	0.51

It is observed from the Table 2 that the average classification accuracy of the proposed method is improved as compared to the method based on NSCT and LDBP [8]. It is marginally less compared to the method based on PDE and LDBP [19]. The training time and testing time of the proposed method is considerably reduced. Thus, the proposed method is effective and computationally less expensive.

5. CONCLUSIONS

In this paper, a novel method of PDE based statistical features for texture analysis using wavelet transform is proposed and is implemented on Brodatz dataset. The proposed method is compared with the other methods in the literature [8, 19]. Following conclusions can be made from the experimentation:

- Better classification accuracy using simple statistical descriptors is achieved.
- Combination of feature sets improves the average classification accuracy.
- Feature set F2 (that computes the Haralick features) and other combination of feature sets containing F2 (F2+F4) is observed to be computationally expensive.
- Most feature sets are computationally inexpensive making it suitable for real time applications.
- The classification accuracy can be increased with more sophisticated classifier.
- The computational cost is reduced significantly as compared to other methods in the literature, while better classification accuracy is attained.
-

ACKNOWLEDGEMENTS

The authors are grateful to the reviewers for their valuable comments and suggestion, which substantially improved the quality of the paper.

REFERENCES

[1] Rosenfeld, A. (1976) Digital Picture Analysis, Springer Verlag, Berlin.
[2] Tuceryan, M. & Jain, A.K. (1994) Texture Analysis handbook of Pattern Recognition and Computer Vision.
[3] Haralick, R.M., Shanmuga, K. & Dinstein I., (1973) "Textural features for image classification", IEEE Transactions on Systems, Man and Cybernetics, Vol. 3, pp 610-621.
[4] Tamura H., Mori, S., & Yamawaki, T., (1978) "Textures Corresponding to Visual Perception", IEEE Trans. syst. Man Cybern, Vol. 8, No. 6, pp 460-473.
[5] Hiremath, P.S., & Shivashankar, S., (2008) "Wavelet based co-occurrence histogram features for texture classification with an application to script identification in a document image", Pattern Recognition Letters No. 29, pp 1182–1189.
[6] Smith, J. R., & Chang, S. F., (1997) "Visually searching the web for content", IEEE Multimedia Magazine Vol. 4, No. 3, pp 12–20. [Columbia U. CU/CTR Technical Report 459-96-25].

[7] Smith, J. R., & Chang, S. F., (1994) “Transform features for texture classification and discrimination in large image databases”, in Proc. IEEE Int. Conf. on Image Proc.
[8] Hiremath, P. S., & Bhusnurmath, Rohini A., (2013) “Texture Image Classification Using Nonsubsampled Contourlet Transform and Local Directional Binary Patterns”. Int. Journal of Advanced Research in Computer Science and Software Engineering, Vol. 3, No. 7, pp 819-827.
[9] Hiremath, P. S., & Bhusnurmath, Rohini A., (2014) “A Novel Approach to Texture Classification using NSCT and LDBP”. IJCA Special Issue on Recent Advances in Information Technology, No. 3, pp 36-42 (ISBN-973-93-80880-08-3).
[10] Hiremath, P. S., & Bhusnurmath, Rohini A., (2013) “Nonsubsampled Contourlet Transform and Local Directional Binary Patterns for Texture Image Classification Using Support Vector Machine”. Int. Journal of Engineering Research and Technology, Vol. 2, No. 10, pp 3881-3890.
[11] Thyagarajan, K. S., Nguyen, T., & Persons, C., (1994) “A maximum likelihood approach to texture classification using wavelet transform”, in Proc. IEEE Int. Conf. on Image Proc.
[12] Laws, K. I., (1979) “Texture energy measures,” in Proc. Image Understanding Workshop, pp 47-51.
[13] Lendaris, G. O. & Stanley, G. L., (1970) “Diffraction pattern sampling for automatic pattern recognition,” in Proc. IEEE, Vol. 58, pp 198-216.
[14] Mandelbrot, B. B., (1982) The Fractal Geometry of Nature, San Francisco, CA, Freeman.
[15] Perona, P., & Malik, J., (1990) “Scale-Space and Edge Detection Using Anisotropic Diffusion”, IEEE transaction on pattern analysis and machine intelligence. Vol.12, No.7, pp 629-639.
[16] Witkin, A. P., (1983) “Scale space filtering”, Proc. Int. Joint Conf. Artificial Intelligence pp 1019-1023.
[17] Hiremath, P. S., & Bhusnurmath, Rohini A., (2014) “Texture Classification Using Anisotropic Diffusion and Local Directional Binary Pattern Co-Occurrence Matrix”. Proceedings of the Second International conference on Emerging Research in Computing, Information, Communication and Applications (ERCICA 2014), No. 2, pp 763-769, Aug. 2014. ISBN: 9789351072621, Elsevier Publications 2014.
[18] Hiremath, P. S., & Bhusnurmath, Rohini A., (2014) “RGB – Based Color Texture Image Classification Using Anisotropic Diffusion and LDBP”. Multi-disciplinary Trends in Artificial Intelligence, 8th International Workshop, MIWAI 2014, M.N. Murty et al. (Eds.)LNAI 8875, pp 101–111, DOI 10.1007/978-3-319-13365-2_10, Springer International Publishing Switzerland 2014.
[19] Hiremath, P. S., & Bhusnurmath, Rohini A., (2015) “Diffusion Approach For Texture Analysis Based On LDBP,” Int. Journal of Computer Engineering and Applications, Vol. 9, No. 7, Part I, pp 108-121.
[20] Randen, T., & Husøy, J., (1999) “Filtering for Texture Classification: A Comparative Study”, IEEE Trans. Pattern Analysis and Machine Intelligence, Vol. 21, No. 4, pp 291-310.
[21] Teuner, A., Pichler, O., & Hosticks, B., (1995) “Unsupervised Texture Segmentation of Images Using Tuned Matched Gabor Filters”, IEEE Trans. Image Processing, Vol. 4, No. 6, pp 863-870.
[22] Daubechies, I., (1992) Ten Lectures on Wavelets, SIAM, Philadelphia, PA.
[23] Mallat, S. G., (1989) “A theory of multiresolution signal decomposition: The wavelet representation”, IEEE transactions on pattern analysis and Machine intelligence, No. 11, pp 674-693.
[24] Ojala, T., & Pietikäinen, M, (2004) Texture Classification, Machine Vision and Media Processing Unit, University of Oulu, Finland.
[25] Weszka, J. S., Dyer, C. R., Rosenfield, A., (1976) "A Comparative Study of Texture Measures for Terrain Classification", IEEE Transactions on Systems, Man. & Cybernetics, Vol. 6. Pp 269-285,
[26] Srinivasan, G. N., & Shobha, G., (2008) “Statistical Texture Analysis”, Proc. Of World Academy Of Science, Engineering And Technology, Vol. 36, pp 1264-1269.
[27] Amadasun, M. & King, R., (1989) "Texural Features Corresponding to Texural Properties", IEEE Transactions on Systems, Man, and Cybernetics, Vol. 19, No. 5, pp 1264-1274
[28] Chung-Ming, Wu., & Yung-Chang, Chen, (1992) "Statistical Feature Matrix for Texture Analysis", CVGIP: Graphical Models and Image Processing, Vol. 54, No. 5, pp 407-419.
[29] Laws, K. I., (1980) "Rapid Texture Identification", SPIE, Vol. 238, pp 376-380.
[30] Haralick, R. M., & Shapiro, L. G., (1992) Computer and Robot Vision Vol. 1, Addison-Wesley.
[31] Rosenfeld, A., & Weszka, J., (1980) “Picture Recognition”, in Digital Pattern Recognition, K. Fu (Ed.), Springer-Verlag, pp 135-166.
[32] Duda, R. O., Hart, P. E., & Stork, (2001) Pattern Classification, Wiley publication, New York.
[33] Brodatz, P., (1966) Textures: A Photographic Album of Artists and Designers. Dover publication, New York.

[34] Weickert, J., (1998) Anisotropic Diffusion in Image Processing. ECMI Series, Teubner –Verlag.
[35] Coifman, R. R., & Donoho, D. L., (1995) "Translation Invariant Denoising in Wavelets and Statistics", Lecture Notes in Statistics, pp 125-150.
[36] Cunha, A. L., Zhou, J., & Do, M. N., (2006) "The Nonsubsampled Contourlet Transform: Theory, Design and Applications", IEEE Trans. Image Processing, Vol. 15, No.10, pp 3089-3101.

APPENDIX

1. Anisotropic diffusion

The Partial differential equation (PDE) [19] techniques have been widely used for enhancing images. The diffusion process is equivalent to a smoothing process with a Gaussian kernel (linear diffusion). A major drawback of the linear diffusion is its uniform filtering of local signal features and noise. This problem was addressed by Perona and Malik [15], who proposed a nonlinear diffusion process, where diffusion can take place with a variable diffusion in order to control the smoothing effects [34] is represented by Eq. (1):

$$p(\|\nabla I\|) = e^{(\|\nabla I\|/K)^2} \quad (1)$$

where $p(\nabla I)$ is the conduction function, ∇I is the gradient magnitude and the parameter K controls the conduction.

It was demonstrated [15] that anisotropic diffusion clearly outperforms the canny edge detector, making image boundaries sharp. The Figure A1 represents the anisotropic diffusion on Brodatz texture image D104 of size 64 x 64. The row 1 represents the effect of anisotropic diffusion resulting in smoothing of image (cartoon approximation). The row 3 is the texture component of the corresponding images in the row 1, obtained by the difference between original image and it's cartoon approximation. Row 2 and 4 depict the contour representations of images in row 1 and row 3, respectively.

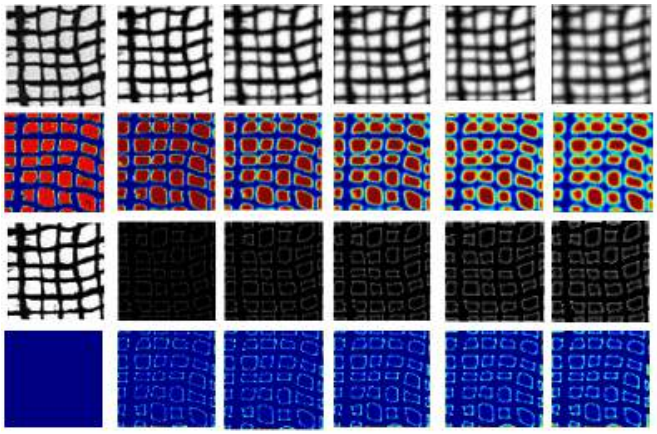

(a) I (b) t_1 (c) t_2 (d) t_3 (e) t_4 (f) t_5

Figure A1. Effect of anisotropic diffusion on Brodatz texture image D104 of size 64 x 64. Row 1 represents the smoothed images [(b) to (f)] of the original image I in (a) at successive diffusion steps t_1 through t_5. Row 3 represents the texture component of the image in row 1. Row 2 and 4 represent the contour plot of the corresponding images in row 1 and row 3, respectively [19].

2. Local directional binary patterns

The most important property of local directional binary patterns (LDBP) [8] is computational simplicity. The basic idea of LDBP is that, 3x3 kernel of image can be treated as basic texture

region. The gray value of central pixel is compared with the gray values of eight pixels around it. The central gray pixel value is the threshold value. If the gray value of surrounding pixel is larger than gray value of central pixel, the surrounding pixel is marked as one otherwise zero. The binary values of all surrounding pixels can be obtained. All surrounding pixels are given different metrics. The metrics is multiplied with a binary value of surrounding pixels as shown in the Figure A2**.** Further, the sum of product of binary value and metrics of all surrounding pixels is set as the value of local directional binary pattern of central pixel. The value of local directional binary patterns of all pixels in an image can be obtained through such calculation neglecting the pixels of edges. The LDBP weight f_b of the central pixel (x_c, y_c) can be calculated using the Eq. (2) and Eq. (3).

$$f_b(x_c, y_c) = \sum_{j=0}^{7} v(f_j - f_c)\cos(j * 45) \tag{2}$$

where

$$v(x) = \begin{cases} 1 & x \geq 0, \\ 0 & x < 0. \end{cases} \tag{3}$$

f_c and f_j are the pixel values at the center and j[th] neighbor in 3x3 kernel of image. Finally, a matrix of LDBP weights is obtained.

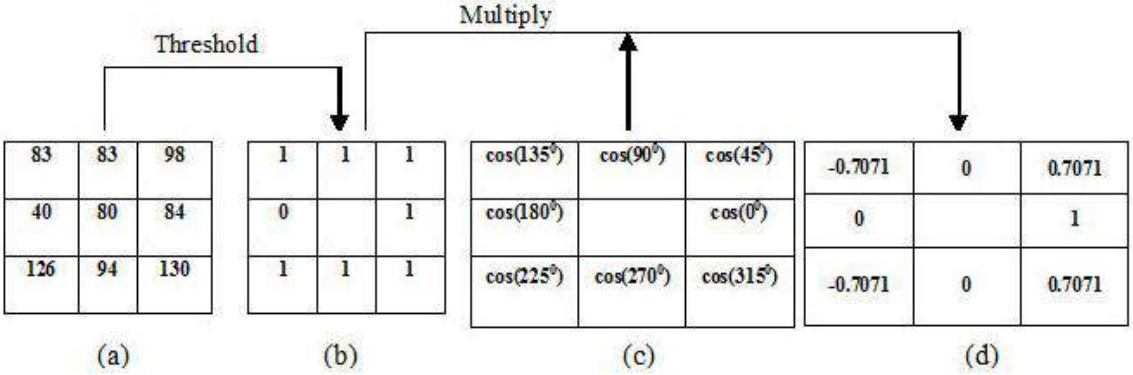

Figure A2. Transformation of neighborhood pixels to calculate central pixel weight in LDBP. (a) A sample neighborhood, (b) Resulting binary thresholded result, (c) LDBP mask, (d) Resultant weights after multiplying corresponding elements of (b) and (c) [18].

3. Nonsubsampled contourlet transform

An important feature of nonsubsampled contourlet transform (NSCT) is its stability with respect to shifts of the input signals [35]. The lack of shift invariance during image processing will cause pseudo Gibbs phenomena around singularities. In order to enhance directional selectivity and shift invariance and to get rid of the frequency aliasing of contourlet, Cunha et al. [36] presented a shift invariant version of the contourlet transform namely, NSCT. To obtain a shift invariant, directional multiresolution image representation, the NSCT is built upon iterated nonsubsampled filter banks. The NSCT combines nonsubsampled pyramids to provide multi scale decomposition and nonsubsampled directional filter bank (DFB) to provide directional decomposition. The two level NSCT decomposition is shown in the Figure A3.

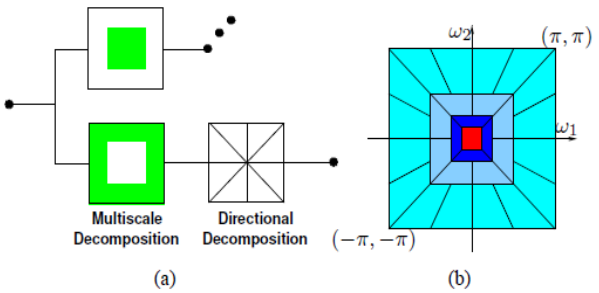

Figure A3. Nonsubsampled contourlet transform (a) Nonsubsampled filter bank (b) Idealized frequency partitioning [36].

The building block of the nonsubsampled pyramid is shown in the Figure A3(a). It is a two channel nonsubsampled filter bank which has no downsampling or upsampling and therefore is shift invariant. The ideal frequency response of a nonsubsampled DFB is shown in the Figure A3(b). The building block of a nonsubsampled DFB is a two channel nonsubsampled filter bank

AUTHORS

Dr. P.S. Hiremath Professor, Department of Computer Science (MCA), KLE Technological University, BVBCET Campus, Hubli- 580031, Karnataka, India. His research areas of interest are Image Processing, Pattern Recognition, Computational Fluid Dynamics, Optimization Techniques, Data Mining, Web Mining and Knowledge Discovery Techniques. He has published 190 research papers in peer reviewed International Journals.

Rohini A. Bhusnurmath is currently pursuing her Ph.D. in Computer Science in the Department of P.G. Studies and Research in Computer Science at Gulbarga University, Gulbarga- 585106, Karnataka, India. Presently she is working as a Lecturer in the department of Computer Science, at Govt. P.U. College for Girls, Bijapur, Karnataka, India. Her research areas of interest are Image Processing and Pattern Recognition.

INTENTIONAL BLANK

CONVEX OPTIMIZATION BASED CONGESTION CONTROL IN LAYERED SATELLITE NETWORKS

R. R. P. Kumar[1], S. Muknahallipatna[2] and J. E. McInroy[3]

[1]National Center for Atmospheric Research, Colorado & Univ. of Wyoming, Wyoming
[2]Dept. of Electrical & Computer Engineering, University of Wyoming, Wyoming, USA
[3]Dept. of Electrical & Computer Engineering, University of Wyoming, Wyoming, USA

ABSTRACT

A multi-layered satellite network consisting of geosynchronous and nano-satellites is suited to perform space situational awareness. The nano-satellites collect information of space objects and transfer data to ground stations through the geosynchronous satellites. The dynamic topology of the network, large propagation delays and bulk data transfers results in a congested network. In this paper, we present a convex optimization based congestion control algorithm. Using snapshots of the network, operating parameters such as incoming, outgoing rates and buffer utilization are monitored. The operating parameters of a satellite are formulated as a convex function and using convex optimization techniques, the incoming data rates are evaluated to minimize congestion. Performance comparison of our algorithm with Transmission Control Protocol congestion control mechanism is presented. The simulation results show that our algorithm reduces congestion while facilitating higher transmission rates.

KEYWORDS

Congestion control, Convex Optimization, Multi-layered satellites.

1. INTRODUCTION

A Single layer satellite networks (SLSN) have the potential to provide global coverage with high bandwidth availability. SLSN can be used to provide communication infrastructure in remote areas and allow also interconnection of local area networks and individual hosts. SLSN is highly reliable due to reduced link failure instances. However, SLSN is shown to be inefficient with respect to data transmissions [1]. To address this issue, in the past two decades, multi-layered satellite network (MLSN) has been proposed by a number of researchers [2, 3].

A MLSN consisting of geosynchronous satellites and a large number of nano-satellites with different capabilities distributed across multiple layers is ideally suited to perform space situational awareness (SSA). SSA involves collecting visual information of space objects like stars, planets, satellites etc. SSA using a MLSN involves the use of nano-satellites to collect visual information and transfer the data to ground stations via multiple geosynchronous satellites through the layered network in real time. The visual information has dense data transmissions between satellites. Furthermore, the large physical distances between satellites will result in large transmission (propagation) delays, causing congestion. Packet drops due to congestion and the associated re-transmission of dropped packets makes the MLSN unsuitable for real-time SSA. Hence the need for an algorithm that can reduce the congestion by maintaining maximum possible data rates is required.

DOI: 10.5121/ijci.2016.5115

A number of satellite networks using different flavors of TCP implementations [4] have been proposed. A number of researchers [5, 6, 7, and 8] have analyzed the reduced throughput of the TCP based satellite network due to large propagation delay, slow start, packet loss assumption due to congestion. The packet loss assumption due to congestion will unduly trigger, congestion control mechanisms resulting in further throughput degradation [9]. A number of modifications to TCP congestion control mechanism (TCP-CCM) have been proposed in the past two decades [10, 11, 12, 13, 14, and 15]. The first set of modifications proposed, address either preventing congestion or reduce the congestion rapidly, while a second set of modifications (Fast Retransmit and Fast Recovery, etc.) focus on detecting whether a packet loss is due to congestion. However, the throughput of the network continues to be low during the modified congestion control mechanism operation specifically in satellite networks due to large propagation delay and bulk data transfers. In this paper, we propose a convex optimization based congestion control (COCC) algorithm that uses convex optimization to reduce congestion and achieve a maximal network throughput.

Three important parameters that contribute to congestion in a satellite network are the input buffer size, incoming and outgoing data rates of each satellite. The input buffer size and the incoming data rates determine the effectiveness of receiving data. The outgoing data rate determines the effectiveness of processing the received transmission and relaying it to the next satellite in the chain of communication links. An imbalance in the parameters can result in a satellite receiving more data than it can process, leading to congestion. The proposed algorithm consists of formulating the input buffer utilization and the incoming data rate as a convex function. Convex optimization is used to solve this convex function with associated constraints to determine the maximal possible throughput of each satellite and thereby reduce network congestion.

The paper is organized as follows: In section 2, we discuss the related work on congestion control in multi-layered satellite networks. Section 3 presents the multi-layered satellite network architecture. Section 4 provides a brief discussion of the parameters that influence congestion. In section 5, we present the traditional TCP modeling that is used for comparison. Section 6 presents the formulation of congestion control as a convex function. Section 7 presents an introduction to convex optimization and its application to congestion control. Simulation and performance evaluation of the proposed algorithm is presented in Section 8 by comparing the performance with traditional TCP-CCM. Section 9 concludes with discussion on performance issues of the COCC algorithm.

2. RELATED WORK

A QoS oriented congestion control algorithm is proposed for satellite networks in [16]. A satellite node utilizes an equation to compute the sending rate for each data flow, while the intermediate satellite nodes continuously detect real-time package-loss rates for timely adjustments. Simulation results indicate that the algorithm can provide superior congestion control performance, and raise network throughputs without reducing the QoS. However, the equation used to compute the sending rate for each data flow does not optimize the network throughput. Neither does it provide any flexible control mechanism to control source or intermediate satellite nodes to modulate sending rates. Moreover, effects of the algorithm for a multi-layered satellite network are not presented.

Congestion control using an optimized load-balancing traffic distribution algorithm for two-layered satellite network is proposed in [17]. The load-balancing scheme of the proposed method is developed by adopting a traffic distribution model, which is based upon network capacity estimation and theoretical analysis of the congestion rate in each layer. When congestion is

detected, the routing tables of satellites are modified to avoid the congested nodes. The performance of this method is effective in terms of improved throughput and lower packet drops. Congestion control for a multi-layered satellite network in [18] is based on the probability of packet drop. Queuing ratios of satellites are varied based on the probability of packet drops at the given instance of time. This determines the traffic reduction ratio. New transmission rates are computed using the ratio that reduces congestion.

A congestion control algorithm based on sudden start and rapid recovery algorithm is introduced in [19]. The sudden start increases the transmission window size rapidly. Probe packets are transmitted periodically to check for congestion. On congestion, the rapid recovery phase algorithm cuts the window size by half for every lost packet. The performance shows higher network throughput and better fairness in sharing network resources in comparison to TCP-CCM. The limitation of the algorithm is the additional data overhead due to the probe packets.

Multilayer multicast congestion control algorithm is introduced in [20]. The satellites are grouped to retrieve session information from the ongoing traffic. The routing is computed based on the session information. Additionally, every packet is marked with priorities by every layer. Packets of lower priority are blocked during congestion and released after recovery. The algorithm has the advantage of being reliable in case of link failures, long and variable delays, limited control overhead and fair sharing of network resources.

Congestion control algorithm for lower earth orbit satellites is introduced in [21]. The round trip time (RTT) for any transmission is estimated. For a given route, the satellites are grouped based on the same number of hops and RTT. A feedback window is multicast once for every RTT to avoid congestion. The algorithm requires no modifications to a router or end-user. The performance indicates better load balancing and link utilization than traditional congestion control algorithms.

A fuzzy logic based congestion control algorithm is introduced in [22]. The algorithm formulates congestion as a function of queuing and weather characteristics. The history of weather changes and queuing for every satellite is maintained. The algorithm then computes fuzzy logic table providing the probable values of these variables. This helps in tuning of Random Early Detection (RED) algorithm. The performance of the algorithm is shown to be better than the traditional RED algorithm.

A congestion controller using data-driven switching control theory is introduced in [23, 24]. A control scheme of proportional integral-derivative structure is used to represent the congestion in networks. The controller monitors the network for any congestion. A cost function is designed to evaluate control parameters for the controller. The parameters deduced show that the algorithm is computationally less intensive than most common algorithms making it suitable for real time applications.

A study on the set of guidelines governing satellite queuing system is provided in [25]. It provides a fair routing algorithm that selectively drops packets to reduce congestion. The algorithm discriminates packets that impose bandwidth more than their allocation. This discrimination enables the satellite to drop the right packets during congestion. The performance is shown to be better than traditional congestion control algorithms through simulations. However, Huang *et al* state in [25] that the implementation on a satellite network may not be feasible.

3. MOTIVATION

As mentioned before, SSA using MLSN involves a large number of nano-satellites, with each satellite involving dense data transmissions. Furthermore, a real-time SSA using MLSN would require to have maximum feasible network throughput, even during congestion phase.

In all of the previous work discussed, the congestion is reduced by reducing the transmission rate either linearly or exponentially without any consideration to the network throughput. The review of congestion control algorithms in [26] shows the same. Our proposed algorithm differs significantly by adopting a different goal for congestion control. The goal is to clear congestion while maintaining maximal network throughput. To achieve this goal, congestion control is formulated as a convex function with incoming data rates of each satellite as the variable of optimization. It reduces congestion and optimizes the data flow simultaneously, providing an efficient network throughput.

4. ARCHITECTURE

A novel multi-layered satellite routing algorithm is proposed in [27]. The proposed routing algorithm performance is demonstrated on a satellite network consisting of satellites distributed over multiple layers with an individual layer situated either at lower earth orbit (LEO) or middle earth orbit (MEO) or geosynchronous earth orbit (GEO). The performance of the network in [27] is shown to have low communication overhead and better throughput than other fewer-layered satellite networks. However, the focus of this work is only on optimal routing and does not address the issues with congestion and maximal network throughput. In this work, we demonstrate our convex optimization based congestion control algorithm on the satellite network test bed, which is a modified version of the layered satellite network architecture proposed in [27]. The modifications are the LEO and the MEO layers, are referred to as layer-1 and layer-2 respectively, comprising of only nano-satellites. Layer-1 and layer-2 are not expected to be situated at the low and medium earth orbits. The GEO layer is referred as layer-3 consisting of GEO satellites capable of communicating with the ground stations. The communication (transmission and reception rates) capabilities of satellites are assumed to increase from layer-1 through layer-3. Satellites are assumed to communicate within and between layers via intra-orbital and inter-orbital links respectively. It is assumed that every satellite knows its position via geographic coordinate system. The hierarchy of the satellites is shown in Fig 1.

Let the number of GEO satellites be N_G, number of layer-2 satellites be N_M and number of layer-1 satellites be N_L. The satellites are represented by

$$G = \{g_i \mid i = 1,2,...,N_G\} \tag{1}$$

$$M = \{m_j \mid j = 1,2,...,N_M\} \tag{2}$$

$$L = \{l_k \mid k = 1,2,...,N_L\} \tag{3}$$

where, g_i, m_j, l_k represent the individual layer-3, layer-2 and layer-1 satellites respectively. As seen in Fig. 1, layer-1 has two sub-layers deviating from the architecture proposed in [27]. In order to efficiently maintain data flow between satellites, manager or cluster head (CH) satellites are introduced.

The individual satellite naming convention used in identifying the data flow or links is discussed below:

- For layer-1, satellite links have two representations, $l_{k,h}$ and $l^{h}_{k,j}$, where $l_{k,h}$ is the link between k^{th} non-cluster head satellite in layer-1 and CH satellite h of layer-1. $l^{h}_{k,j}$ is the satellite link between k^{th} CH satellite in layer-1 to the j^{th} satellite in layer-2.
- Satellites ($m_{j,i}$) in layer-2 are arranged in a single orbit, where j is the identifier of a satellite in layer-2 and i is the identifier of a satellite in layer-3.
- Layer-3 will have satellites that may or may not have ground connectivity. The satellites having connectivity to a ground station are selected as cluster heads. The two identifiers of satellite links in this layer are $g_{i,h}$ and g^{h}_{i}. $g_{i,h}$ is the link between i^{th} satellite and CH satellite of layer-3. g^{h}_{i} is the link between the ith CH in layer-3 to the ground station.

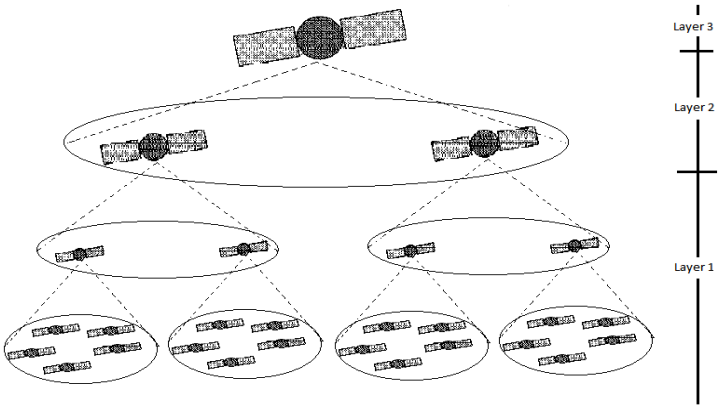

Fig. 1. Hierarchy of the Multi-layered Satellite Network

The data collected by $l_{k,h}$ is transmitted to $l^{h}_{k,j}$. Each $l^{h}_{k,j}$ routes this data to $m_{j,i}$, which further routes it to either $g_{i,h}$ or g^{h}_{i}. The $g_{i,h}$ relays their data to g^{h}_{i}, and eventually data to the ground stations.

5. CONGESTION CONTROL PARAMETERS

Due to the dynamic topology of a satellite network, the parameters like propagation delay, maximum possible data rates, etc., change within a well-defined bandwidth. However, these parameters can be assumed to be constant within a snapshot. A snapshot is defined as a brief period of time and in which the network topology change is minimal. A snapshot approach is useful in analyzing the current state of a dynamic network, and determines the operational parameters of the network for the next state. At the beginning of every snapshot, every satellite g_i, m_j and l_k based on their current position, will compute the following three parameters:

- Line of sight with other satellites,
- Maximum data transmission rates
- Data recipients

5.1. Line of Sight

The inter-orbital and intra-orbital links being wireless require a LOS for transmission. The satellites using the geographical coordinate system will determine the LOS satellites as discussed in [28, 29]. To determine LOS, position vectors of a satellite and difference vectors are used. A position vector of a satellite is the Euclidean vector representing the position of the satellite with the center of the earth as its origin. A difference vector is the Euclidean vector obtained by the subtraction of two Euclidean vectors. Using these vectors, LOS is computed as follows:

- Let θ_1 represents the angle between satellite A's position vector and the difference vector (difference between A and B satellites' position vector).
- Let θ_2 represents the angle between satellite B's position vector and the difference vector.
- A LOS exists between A and B if any of the following conditions is satisfied:
  - $\theta_1 > 90^\circ$
  - $\theta_1 \leq 90^\circ$ and $\theta_2 < 90^\circ$
  - $\theta_1 \leq 90^\circ$, $\theta_2 \geq 90^\circ$ and the orthogonal from the center of the earth to the line joining the two satellites is greater than the radius of the earth.

5.2. Maximum Data Transmission Rates

Once the LOS between two satellites is determined, the satellites are considered as neighbors. Laser transmission is assumed as the mode of communication in this work to achieve high transmission rates. Laser transmission rate is dependent on a number of parameters [30] like transmission power, area of transmitter antenna, distance between satellites, etc. For a given laser communication configuration, the relationship between maximum data transmission rate and the distance between two satellites can be expressed as

$$R_{\max} \alpha \frac{1}{D^2} \tag{4}$$

where,

D is the distance between the two satellites.

D varies between satellites in different layers constantly due to their orbital locations. The transmission rate of a transmitting satellite is the arrival rate at the receiving satellite. Even though, $R_{\max}$ is the maximum possible transmission rate of a satellite in a snapshot, the actual transmission rate will be dictated by the underlying TCP.

5.3. Data Recipients

A top down approach is adopted to select the data recipients at each layer. The notations and data flow for the network is as shown in Fig. 2. CH satellites are primarily chosen based on LOS. Satellites that do not have a LOS with a CH in a snapshot, do not participate in any transmission activity. Satellites having LOS to multiple CHs can choose to transmit to any or all of them.

CH g_i^h is chosen based on its connectivity to a ground station. CH $l_{k,j}^h$ is chosen based on greedy algorithm of maximum neighboring l_k satellites. From a set of l_k satellites having a $m_{j,i}$ neighbor, a satellite in the set with maximum number of neighboring l_k is chosen as a CH.

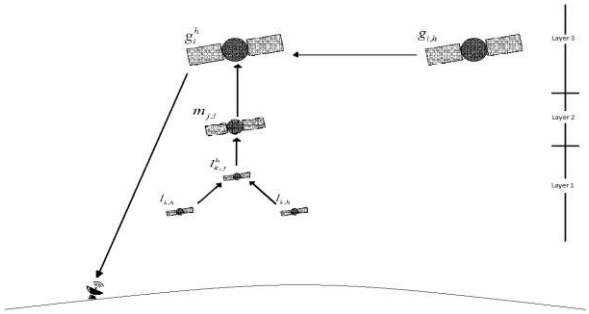

Fig. 2. Data flow in the Multi-Layered Satellite Network

6. TCP MODELLING

In this work, the TCP flavor described in [31] has been adopted for comparison with the convex optimization based congestion control algorithm.

At the beginning of every snapshot, the satellites resume transmission activity based on the computed hierarchy of transmission. The allocated rate of transmission R_{alloc}, governed by TCP, will be a fraction of $R_{\max}$ as given in Eq. 5

$$R_{alloc} = T_{tcp} R_{\max} \tag{5}$$

where, T_{tcp} is the a threshold satisfying Eq. 6

$$0 \le T_{tcp} \le 1 \tag{6}$$

The threshold T_{tcp} varies based on the success or failure of every transmission. In every snapshot, the satellites follow the TCP principles i.e., slow start or exponential growth phase below a preset TCP transmission rate and a linear growth thereafter. The linear growth is continued till congestion is detected or T_{tcp} reaches unity. If congestion is detected, the transmission is subjected to the TCP-CCM where the slow start window is cut by half and slow start is restarted. Once the congestion is cleared, the TCP resumes back its transmission with linear growth. If no congestion is detected, the transmission rate is maintained at $R_{\max}$. Furthermore, the satellites are allowed to transmit data in bursts. The amount of data a satellite can transmit in bursts is limited by the bandwidth-delay product [32].

7. FORMULATION OF CONGESTION CONTROL AS CONVEX FUNCTION

Let the service rate of packets of a satellite be μ. Let the maximum arrival rate of packets on an i^{th} input link of a satellite be λ_i. In order to empty the buffer, and thus reduce congestion, the service rate and the arrival rates must satisfy the relation:

$$\mu > \sum_{i=1}^{n} \lambda_i \tag{7}$$

where, n indicates the number of satellites transmitting. At $\mu = \sum_{i=1}^{n} \lambda_i$, the network is said to be at a critical state indicating that the buffer is always empty. For any satellite with buffer capacity B, Eq. 7 can be re-written as:

$$\mu > \sum_{i=1}^{n} \lambda_i + \left(B_{util} \times B\right) \tag{8}$$

where,

$0 \le B_{util} \le 1$.

The product $B_{util}B$ represents buffer utilization. If the data rates in Eq. 8 are optimized, a network will operate with minimal congestion and maximal throughput.
Let $R_{\max}^{n} \in R^{n}$ be maximum transmission rates of all satellites transmitting to a single CH satellite:

$$R_{\max}^{n} = \begin{bmatrix} \lambda_1 & \lambda_2 & \dots & \lambda_n \end{bmatrix} \tag{9}$$

where, n is the number of incoming links of a CH satellite. In order to find an effective data rate satisfying the condition of minimum queuing delay, a scalar multiple for each λ_i has to be considered. The collection of scalar multiples is represented as $W = \begin{bmatrix} w_1 & w_2 & \dots & w_n \end{bmatrix}$, where $0 \le w_i \le 1$, such that:

$$\left(R_{\max}^{n}\right)^{T} W < \mu - \left(B_{util} \times B\right) \tag{10}$$

Eq. 10 is a linear equation of $W \in R^{n}$. Next, we will show Eq. 10 to be a convex function.

8. CONVEX OPTIMIZATION AND APPLICATION TO CONGESTION CONTROL

A set S, is defined as convex if and only if it satisfies the condition [33] described in Eq. 11.

$$\theta x_1 + (1-\theta) x_2 \in S \tag{11}$$

where,

$x_1, x_2 \in S$,

$x_1 \neq x_2$,

$\theta \in R$, and

$0 \le \theta \le 1$.

A function $f(X): R^{n} \to R$ is considered convex [33] if and only if for all $X_1, X_2 \in domain(f)$ satisfies Eq. 12.

$$f\left(\theta X_1 + (1-\theta) X_2\right) \le \theta f\left(X_1\right) + (1-\theta) f\left(X_2\right) \tag{12}$$

Consider the inequality,

$$a^{T} X \le b \tag{13}$$

where,

$a \in R^{n}$,

$b \in R$, and

$X \in R^n$ is the unknown to be determined.

Eq. 13 represents a linear inequality in n-dimensional half-space with multiple solutions. X is a convex set since it satisfies Eq. 11 and therefore is a solution of Eq. 13 for a given a, b. S. Boyd and L. Vanderberghe have shown linear functions to be convex functions [33].Comparing Eq. 10 and Eq. 13, it can be seen that $\left(R^n_{\max}\right)^T$ and $\mu - \left(B_{util} \times B\right)$ are a^T and b respectively, thereby Eq. 10 is a convex function and a linear inequality.

Eq. 10 or Eq. 13 can also be solved using a simplex algorithm. Simplex algorithms are infeasible for large data [34]. For SSA using MLSR, a large number of nano-satellites are involved. Hence, in Eq. 10, as n grows large, simplex algorithm becomes infeasible. Furthermore, simplex algorithm optimizes linear functions only. Convex optimization can be applied on a convex function which can be linear, quadratic or geometric. Hence, optimizing congestion control formulated as a convex function allows future work to add additional parameter or constraints to congestion control for different or complex networks.

Any standard convex optimization toolkit can be used to solve Eq. 10. To obtain the global minima and in this work, the CVX toolkit [33] developed by S. Boyd and L. Vanderberghe for implementing convex optimization in Matlab is used. To solve a convex function, this toolkit requires the convex function to be specified in a particular format. The toolkit requires objective variable and convex constraints to solve the optimization problem. The objective in the congestion control problem is optimizing W which is n-dimensional. However, the toolkit allows the objective to be only a single dimension variable. Therefore, a variable γ is introduced which will be maximized for each satellite as shown in Eq. 14.

$$
\begin{aligned}
&\text{maximize} \gamma \\
&\text{subject to} \\
&\quad \left(R^n_{\max}\right)^T W < \mu - \left(B_{util} \times B\right) \\
&\quad 0 \le w_i \le 1 \\
&\quad w_i \lambda_i \ge \alpha_i \\
&\quad w_i \lambda_i \le \beta_i \\
&\quad \gamma < w_i
\end{aligned}
\tag{14}
$$

where,

α_i, β_i are the lower and upper limits of the i[th] incoming link rate.

Since γ faces the constraint $\gamma < w_i$, in-turn, all elements of w_i are maximized. The constraint $0 \le w_i \le 1$ forces w_i to be a convex set. The other two constraints are to enforce the effective incoming link rate is maintained within a bandwidth. The advantage of convex optimization is observed in these two constraints. It facilitates to optimize transmission rates within the desired bandwidth which would not be possible if least squares technique was used.

The COCC algorithm on a CH satellite is triggered when the effective buffer utilization is within the bounds defined by $[\, B_{lower}, B_{upper} \,]$. Therefore, the COCC algorithm is activated at

$B_{util}B > B_{upper}$ and deactivated at $B_{util}B < B_{lower}$. Once the COCC phase ends, TCP-CCM regains control of the transmission.

A CH after computing the optimal transmission rates $(\lambda_i w_i)$ for its incoming links, relays these desired rates to all of its neighboring satellites and this process is repeated on all congested CH satellites.

9. SIMULATIONS AND ANALYSIS

The simulations are tailored to evaluate performance of COCC in comparison to TCP. The comparison is performed by considering two parameters namely:

- Average Buffer utilization of a Layer: Average Buffer Utilization is defined as the average of the buffer utilization of each CH satellite in a layer for a snapshot.
- Average Link utilization of a Layer: Average Link Utilization is defined as the average of the link utilization of each satellite in a layer for a snapshot.

Simulations are performed with 135 satellites distributed across the three layers in the ratio of 1:4:40. Layer-1 contains 120 satellites distributed in orbits with altitude ranging from 28,000 km to 32,500 km. Layer-2 contains 12 satellites distributed in orbits with altitude ranging from 33,000 km to 35,000 km. Layer-3 contains 3 satellites in the geosynchronous orbit. Based on the above satellite distribution, the average theoretical data rates for a CH satellite in layer-1, layer-2 and layer-3 was 1 Mbps, 10 Mbps and 8 Mbps respectively. The layer-1 theoretical data rate is significantly less compared to layer-2 theoretical data rate due to a smaller antenna with lower transmission capability. Layer-3 theoretical data rate is also lower compared to layer-2 theoretical data rate due to the large distance between geosynchronous satellites and ground stations and the effect of earth's atmosphere on laser transmission. The buffer size of each satellite in layer-1, layer-2 and layer-3 were set to 1 MB, 1 GB and 10MB respectively. The buffer size on a geosynchronous satellite was set to a lower value to increase the effect of congestion. Initially, simulations were performed with a 30 second snapshot intervals. Since our proposed algorithm works only on network layer, the network flow for duration of 30 minutes was simulated using the CVX toolkit on Matlab and Satellite ToolKit (STK). The simulation results presented are based on 10 trials. The standard deviation from the 10 trials for average buffer utilization and average link utilization vary from 3.7% to 6.7% across the layers.

In Figs. 3, 4 and 5 the average buffer utilization for layers 3, 2 and 1 are shown respectively. In Figs. 6, 7 and 9 the corresponding average link utilization for layers 3, 2 and 1 are shown respectively.

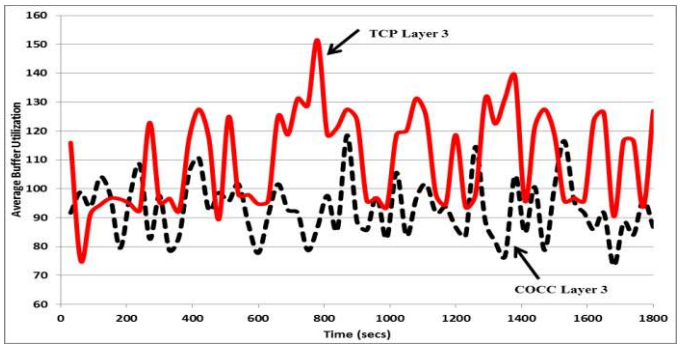

Fig. 3. Layer-3 Average Buffer Utilization for TCP-CCM and COCC

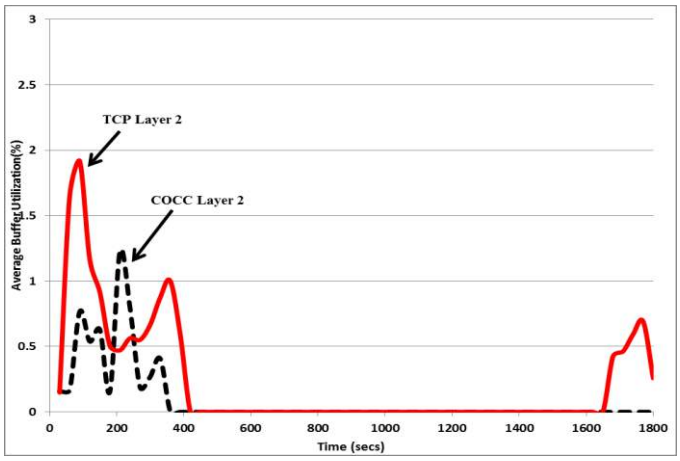

Fig. 4. Layer-2 Average Buffer Utilization for TCP-CCM and COCC

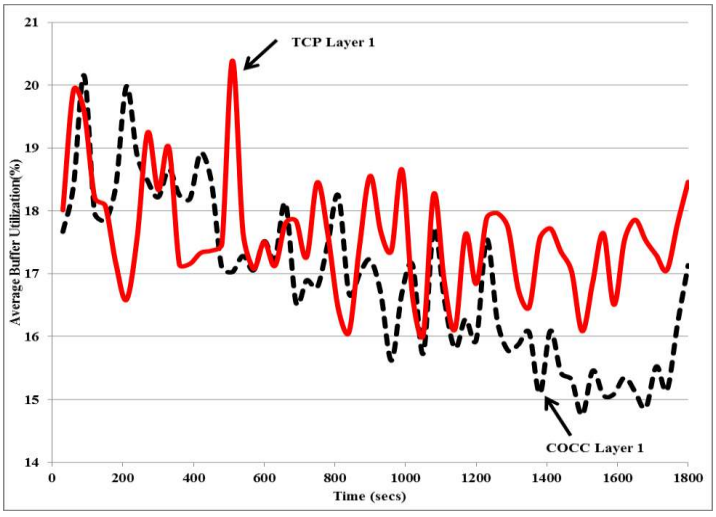

Fig. 5. Layer-1 Average Buffer Utilization for TCP-CCM and COCC

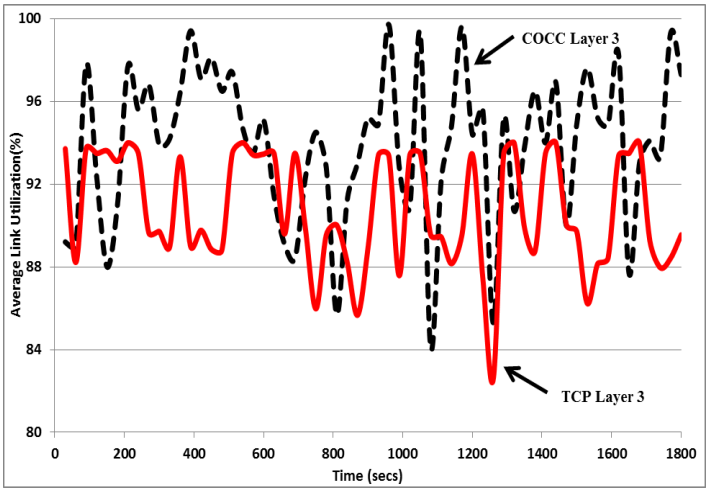

Fig. 6. Layer-3 Average Link Utilization for TCP-CCM and COCC

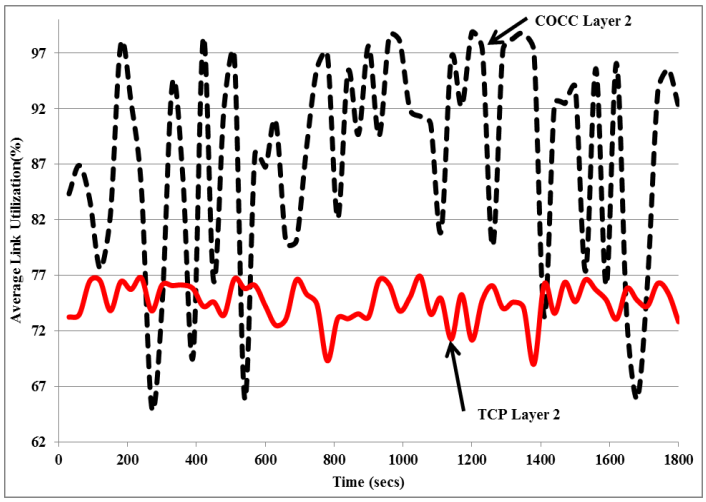

Fig. 7. Layer-2 Average Link Utilization for TCP-CCM and COCC

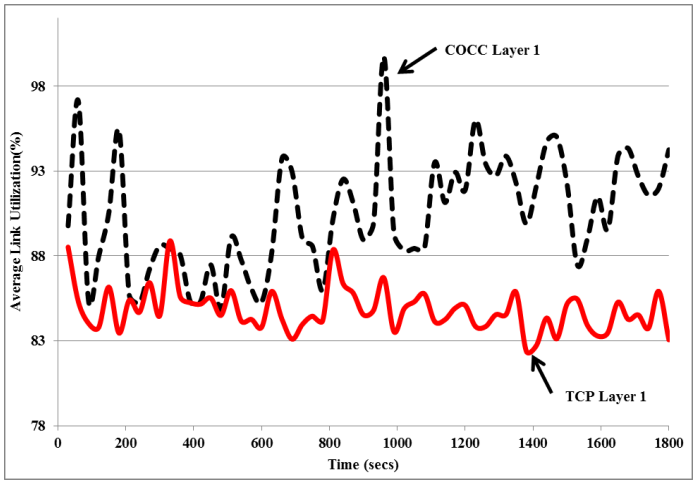

Fig. 8. Layer-1 Average Link Utilization for TCP-CCM and COCC

In Fig. 3 the average buffer utilization of satellites in layer-3 with traditional TCP-CCM is above 100% on an average for the entire simulation. This indicates significant number of packets being dropped. However, with the COCC algorithm on an average, the buffer utilization is around 100%. Since the buffer utilization at layer-3 with TCP-CMM is above 100%, the corresponding average link utilization is less than 80% for satellites in layer-2 as seen in Fig. 7. However, with COCC algorithm, the average link utilization for the same satellites in layer-2 is close to 90% due to buffer utilization reduction in layer-3. In Fig. 4, the buffer utilization with TCP-CCM or COCC is negligible compared to other layers. This is due to the satellites in this layer having higher theoretical transmission rate, larger buffer size and experiencing a lower input data rate from CHs in layer-1. It was observed due to the layer-2 and layer-1 orbit altitudes, in any given snapshot, a total of 30 satellites among the 120 satellites in layer-1 were chosen as CHs. Hence each CH in layer-1 is servicing a maximum of 3 non-CH satellites. Therefore the average buffer utilization of the CHs in layer-1 is only around 20% for both TCP-CCM and COCC as seen in Fig. 5. Since the ground stations do not experience any congestion in our simulations, the link utilization in layer-3 is high as seen in Fig. 6. The link utilization of layer-1 satellites is not affected by the buffer utilization in layer-2. The link utilization with TCP-CCM in layer-1 is less

compared to that with COCC as seen in Fig. 8. This is due to the use of slow start and congestion avoidance by TCP-CCM at the start of a new snapshot.

Even though COCC performs better congestion control it still has some limitations. One of the limitation is the lethargic congestion control at activation of COCC. When COCC is activated on a congested CH satellite, the new transmission rates to reduce congestion is computed and transmitted on all its incoming links with a delay. Due to this delay, the buffer utilization is still shooting above 100% in Fig. 3. This limitation can be overcome by allowing COCC a continuous control over congestion control mechanism. However, allowing COCC to perform continuous congestion control imposes a large computational burden as shown in Fig. 11. To avoid this computational burden, instead of allowing COCC to perform continuous congestion control we have explored varying the duration of a snapshot. In Fig. 9, the buffer utilization with snapshot durations of 30 and 15 seconds are shown. It can be seen the buffer utilization not exceeding 100% with 15 seconds snapshot and thereby no packets are dropped resulting in high link utilization as seen in Fig. 10.

As previously mentioned, the other limitation is the computational burden of COCC. The computation time of COCC is dependent on parameters such as number of neighboring satellites, snapshot interval, data transmission rates, iterations involved in convex optimization etc. For a 30s snapshot interval executed on a Quad-core desktop, an average computation time was 3.25 minutes with 50 satellites as shown in Fig. 11. It can also be noticed that the computational time increases linearly with increasing number of satellites. At this stage due to the computational burden COCC is not suitable for real-time application.

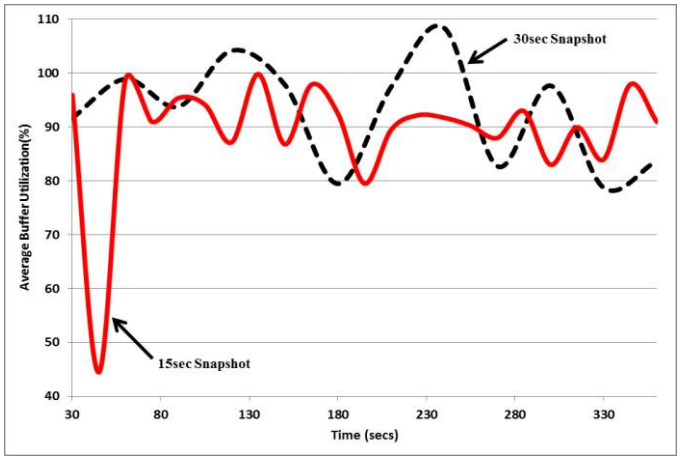

Fig. 9. Layer-3 Average Buffer Utilization for varied Snapshot Interval

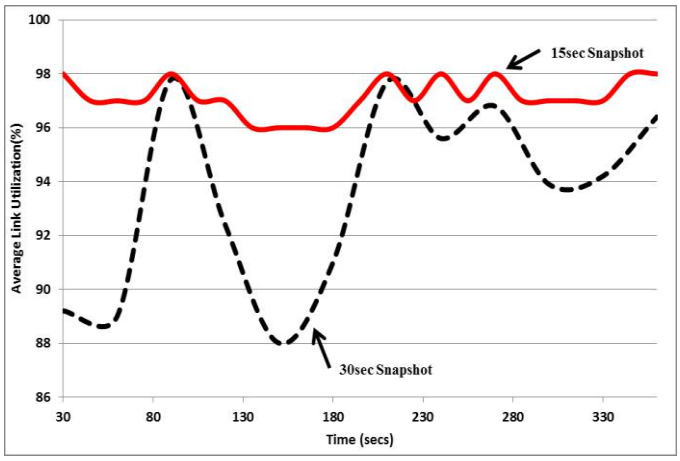

Fig. 10. Layer-3 Average Link Utilization for varied Snapshot Interval

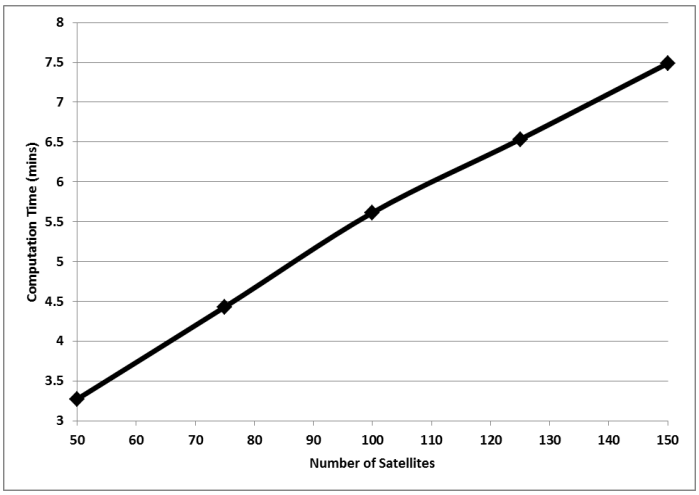

Fig. 11. New Data Rates Computation Time with COCC

10. CONCLUSIONS

The paper proposes a new congestion control algorithm for layered satellite networks. The approach is to formulate congestion control as a convex optimization problem. The convex function is optimized using convex optimization approach at discrete intervals of time to determine optimal transmission rate of each satellite such that the network congestion is reduced while maintaining optimal network throughput. The performance of COCC was compared with TCP-CCM and the performance of COCC is better. It was observed that the satellites transmitted higher transmission rates with COCC algorithm. Furthermore, the performance of COCC is improved when the snapshot duration is reduced. Currently, a constant control by COCC is not feasible due to large computational burden.

To use COCC algorithm in real-time, the COCC algorithm needs to be executed in parallel for each satellite necessitating parallelization of the CVX toolkit.

ACKNOWLEDGEMENTS

We would like to thank National Center for Atmospheric Research, Boulder, for providing resources.

REFERENCES

[1] Werner, Markus, Cecilia Delucchi, Hans-Jörg Vögel, Gerard Maral, & Jean-Jacques De Ridder, (1997) "ATM-based routing in LEO/MEO satellite networks with intersatellite links", IEEE Journal on Selected Areas in Communications, Vol. 15, No. 1, pp. 69-82.

[2] Lee, Jaeook, & Sun Kang, (2000) "Satellite over Satellite (SOS) Network: A Novel Architecture for Satellite Network", Nineteenth Annual Joint Conference of the IEEE Computer and Communications Societies, Vol. 1, pp. 392–399.

[3] Nishiyama, Hiroki, Daigo Kudoh, Nei Kato, & Naoto Kadowaki, (2011) "Load Balancing and QoS Provisioning Based on Congestion Prediction for GEO/LEO Hybrid Satellite Networks", Proceedings of the IEEE, Vol. 99, No. 11, pp. 1998–2007.

[4] Wang, Ruhai, Tarik Taleb, Abbas Jamalipour, & Bo Sun, (2009) "Protocols for reliable data transport in space internet", IEEE Communications Surveys Tutorials, Vol. 11, No. 2, pp. 21-32.

[5] Lakshman, T. V., & Upamanyu Madhow, (1997) "The performance of TCP/IP for networks with high bandwidth-delay products and random loss", IEEE/ACM Transactions on Networking, Vol. 5, No. 3, pp. 336-350.

[6] Metz, Christopher, (1999) "TCP over satellite… The final frontier", IEEE Internet Computing, Vol. 3, No. 1, pp. 76–80.

[7] Partridge, Craig, & Shepard, Timothy, (1997) "TCP/IP performance over satellite links", IEEE Network Mag., pp. 44–49.

[8] Bakre, Ajay, and B. R. Badrinath, (1995) "I-TCP: Indirect TCP for mobile hosts", International Conference on Distributed Computing Systems (ICDCS), pp. 136–143.

[9] Oueslati-Boulahia, Sara, Ahmed Serhrouchni, Samir Tohmé, S. Baier, & Marouane Berrada, (2000) "TCP over satellite links: Problems and solutions", Telecommunication Systems, Vol. 13, pp. 199-212.

[10] Keshav, Srinivasan, & Samuel P. Morgan, (1997) "SMART retransmission: performance with overload and random losses", IEEE Infocom, Vol. 3, pp.1131–1138.

[11] Balakrishnan, Hari, Venkata N. Padmanabhan, Srinivasan Seshan, & Randy H. Katz, (1997) "A comparison of mechanisms for improving TCP performance over wireless links", IEEE/ACM Transactions on Networking, Vol. 5, No. 6, pp. 756-769.

[12] Padmanabhan, Venkata N., & Randy H. Katz, (1998) "TCP Fast Start: A technique for speeding up web transfer", IEEE Globecom.

[13] Akyildiz, Ian F., Giacomo Morabito, & Sergio Palazzo, (2001) "TCP-Peach: A New Congestion Control Scheme for Satellite IP Networks", IEEE/ACM Transactions on Networking, Vol. 9, No. 3, pp. 307-321.

[14] Utsumi, Satoshi, Salahuddin Muhammad Salim Zabir, & Shiratori, Norio (2008) "TCP-Cherry: A new approach for TCP congestion control over satellite IP networks", Computer Communications, Vol. 31, No. 10, pp. 2541-2561.

[15] Kim, Jaehyun, Choo, Hyunseung & Kim, Dongsoo (2012) "TCP CAE: an improved congestion control using comparative ACK-based estimator", The Journal of Supercomputing, Vol. 59, No. 2, pp. 1019-1034.

[16] Liu, Heyu, & Sun, Fuchun, (2014) "A QoS-Oriented Congestion Control Mechanism for Satellite Networks", Mathematical Problems in Engineering.

[17] Nishiyama, Hiroki, Tada, Yasunori, Nei Kato, Yoshimura, Naoko, Morio Toyoshima, & Kadowaki, Naoto, (2013) "Toward optimized traffic distribution for efficient network capacity utilization in two-layered satellite networks", Vehicular Technology IEEE Transactions, Issue 62, No. 3, pp. 1303-1313.

[18] Taleb, Tarik, Mashimo, Daisuke, Jamalipour, Abbas, Hashimoto, Kazuo, Yoshiaki Nemoto, & Nei Kato, (2006) "SAT04-3: ELB: An Explicit Load Balancing Routing Protocol for Multi-Hop NGEO Satellite Constellations", Global Telecommunications Conference, pp. 1-5.

[19] Akyildiz, Ian F., Morabito, Giacomo, & Palazzo, Sergio, (2001) "TCP-Peach: a new congestion control scheme for satellite IP networks", IEEE/ACM Transactions on Networking, Vol. 9, No. 3, pp. 307-321.

[20] Peng, Jun, & Sikdar, Biplab, (2004) "Multilayer multicast congestion control in satellite environments", IEEE Journal on Selected Areas in Communications, Vol. 22, No. 3, pp. 449-461.

[21] Taleb, Tarik, Kato, Nei & Nemoto, Yoshiaki, (2006) "REFWA: An Efficient and Fair Congestion Control Scheme for LEO Satellite Networks", IEEE/ACM Transactions on Networking, Vol. 14, No. 5, pp. 1031-1044.

[22] Vallamsundar, Banupriya, Zhu, Jiesheng, K. Ponnambalam, Huang, Changcheng, Srinivasan, Anand & Cheng, Brian , (2007) "Congestion Control for Adaptive Satellite Communication Systems Using Intelligent Systems", International Symposium on Signals, Systems and Electronics, pp. 415-418.

[23] Cao, Jinhua, & Stefanovic, Margareta, (2009) "Switching congestion control for satellite TCP/AQM networks," American Control Conference, pp. 4842–4847, June 2009.

[24] Cao, Jinhua, & Stefanovic, Margareta, (2010) "New results in stable switching congestion control for satellite TCP/AQM networks", 49th IEEE Conference on Decision and Control (CDC), pp.5643-5648.

[25] Huang, Xiao, & Jiao, Chengbo, (2008) "Congestion Control in Satellite Networks", 4th International Conference on Wireless Communications, Networking and Mobile Computing, pp.1-4.

[26] Kushwaha, Vandana, (2013) "A review of router based congestion control algorithms", International Journal of Computer Network and Information Security (IJCNIS), Vol. 6, No. 1,pp. 1.

[27] Akyildiz, Ian F., Ekici, Eylem & Bender, Michael D., (2002) "MLSR: a novel routing algorithm for multilayered satellite IP networks", IEEE/ACM Transactions on Networking, Vol. 10, No. 3, pp. 411-424.

[28] Gerdan, George P., & Deakin, Rodney E., (1999) "Transforming Cartesian Coordinates X, Y, Z to Geographical Coordinates ", Australian Surveyor, Vol. 44, No. 1, pp. 55-63.

[29] Shamos, Michael Ian, & Hoey, Dan, (1975) "Closest-point problems", 16th Annual Symposium on Foundations of Computer Science, pp. 151-162.

[30] Majumdar, Arun K, (2005) "Free-space laser communication performance in the atmospheric channel", Journal of Optical and Fiber Communications Reports, Vol. 2, No. 4, pp. 345-396.

[31] Ghani, Nasir, & Dixit, Sudhir, (1999) "TCP/IP enhancements for satellite networks", IEEE Communications Magazine, Vol. 37, No. 7, pp. 64-72.

[32] Chen, Kai, Xue, Yuan, Shah, Samarth H., & Nahrstedt, Klara, (2004) "Understanding Bandwidth-delay Product in Mobile Ad Hoc Networks", Computer Communications, Vol. 27, No. 10, pp. 923-934.

[33] Boyd, Stephen, & Vandenberghe, Lieven , (2004) "Convex Optimization", Cambridge University Press.

[34] Beasley, John E., & Beasley, John E. eds, (1996) "Advances in linear and integer programming", Oxford: Clarendon Press.

EFFICIENT APPROACH FOR DESIGNING A PROTOCOL FOR IMPROVING THE CAPACITY OF ADHOC NETWORK

Suresh Kurumbanshi[1] and Dr. Shubhangi Rathkanthiwar [2]

[1]Department of Electronics & Telecommunication Engineering, Y.C.C.E, Nagpur, Maharashtra-India
[2]Department of Electronics Engineering, Y.C.C.E, Nagpur, Maharashtra-India

ABSTRACT

In Adhoc Network, prime issues which affects the deployment, design and performance of an Adhoc Wireless System are Routing, MAC Scheme, TCP, Multicasting, Energy management, Pricing Scheme & self-organization, Security & Deployment consideration. Routing protocols are designed in such a way that it should have improvement of throughput and minimum loss of packets. Another aspect is efficient management of energy and the requirement of protracted connectivity of the network. The routing algorithm designed for this network should monitor the energy of the node and route the packet accordingly. Adhoc Network in general has many limitations such as bandwidth, memory and computational power. In Adhoc Network there are frequent path break due to mobility. Also time synchronization is difficult & consumes more Bandwidth. Bandwidth reservations requires complex Medium Access Control protocol. In this field the work of quantitative and qualitative metrics analysis has been done. The analysis of protocol performance for improving the capacity of adhoc network using probabilistic approaches of the network is yet to be proposed. Our probabilistic approach will cover analysis of various computational parameters for different mobility structures. In our proposed method we have distributed mobile nodes using Pareto distribution & formulated various energy models using regression statistic.

KEYWORDS

Manet, Seed, Pareto, Regression

1. INTRODUCTION

A mobile communication has seen a rapid exponential growth. Mobile devices are preferred mode of communication for accessing the internet through Smartphones, Tablets etc. Mobile adhoc networks has no lasting network infrastructure. It establishes the transmission of new path in order to renovate the network route. There is the need for efficient management, optimization & operation for improving the quality of signal, coverage & service. The node mobility and multiple hop characteristics of adhoc networks makes the fixed network routing protocol ineffectual to meet demands of adhoc network. Realization of different kind of mobile Ad hoc network routing protocols [1] has been done till now.An important aspect is the mathematical analysis & modelling in which how much percent the capacity can be enhanced using probabilistic approaches & its role in routing the protocol for efficient energy management.

1.1. Related Work & Novelty

There are many challenges in wireless adhoc networks such as Routing, Mobility, Bandwidth constraint, Error prone & shared channel, quick route reconfiguration [2]. Moreover, impact of distribution of mobile nodes using Pareto distribution on network performance for improving the capacity of adhoc network is a vital issue which has been discussed in this paper.

1.1.1. Routing Protocols

Routing Protocol Proactive

In proactive routing table, a node preserves routing information about other nodes in the network through one or more routing tables. This protocol requires a significant messaging overhead to maintain an ordered and updated routing table consuming more power, bandwidth and decreases the throughput.

Reactive Routing Protocol -On Demand

It is a on demand routing protocol. When idle, it does not maintain any routing Table. If a node wish to send a packet to another node then the protocol searches the path and tries to establish the connectivity for subsequent transmission & reception of packets.

AODV

AODV is mainly developed for Mobile Ad hoc networks, used in technologies like ZigBee. It is the algorithm which works on demand & discovers route between nodes as per the requirement of the source node. This protocol uses route request messages (RREQ) which are swamped to the network for finding the path which is required by a source node [3].

1.1.2. Energy Management

Energy Management

Energy management [4] is the important process which utilizes the sources & consumers of energy in a node or in the network as a whole for improving the lifetime of the network. Energy management will be useful for enhancing the battery life which is achieved by changing the node pattern using Pareto distribution ; By using distributed scheduling schemes and handling the process and interface device for the minimization of power consumption.

Transmission Power Management

Design of hardware of Radio Frequency module should have minimum consumption of power in all three states of operations i.e. transmit, receive & sleep. Going to the sleep mode when not transmitting or receiving can be done by additional hardware that can wake up on reception of control signal. The use of variable MAC protocol can lead to several advantage that includes energy saving at the nodes, increase in bandwidth reuse and reduction in interference. The network layer routing protocol can consider battery life & relaying node of the intermediate nodes while selecting a path so that load can be balanced across the network. Performance analysis is also carried out using various Routing Protocols [5]. Routing protocol always tries to minimize energy consumption & find out the most efficient approach [6]. Minimizing energy consumption using Meta Heuristic is elaborated in [7]. Various performance analysis of Routing protocols in wireless adhoc network for different mobility structures are covered in [8] & [9].

1.1.3. Probabilistic Approaches

Random variables with different distributions will be created in Network Simulator. It has important role in traffic modelling and network simulation [10].

Generator & Seeds

In insertion to its distribution, there will be other aspects too, to formulate random variables. The generation of random variables should be independent of each other. The generation of random variable is done using origin i.e. seed.

Creating Random Variables

We have created a new generator and assigned a seed value 2 using NS2 commands .When we actually create a random variable, we have to define its distribution type and its parameters. We create RVs with Pareto, Constant, Uniform and Hyper exponential distribution [11].

Pareto Distribution

A Pareto distribution RV, is constructed by specifying its expectation and its shape parameter.

$$F(x) = 1 - (1 / x^{a}); \quad a > 0 \quad \& \quad 1 \leq x < \infty$$

Constant**:** A deteriorated random variable is the constant which equals to its values.
Uniform Distribution: It is defined across the smallest and largest point in its support.

2. FINDINGS & DISCUSSION

For checking various computational parameters, no. of nodes & its maximum number of replies, wireless adhoc network is simulated with various simulation parameters & routing protocols as below. Energy model is also added in NS2 in order to find out various energy levels for different routing Protocol. Energy analysis of wireless nodes will help in deciding the network lifetime & ensures energy saving capability of the node.

Table 1. Simulation Parameters

Simulation Parameter	Type / Value
Channel	wireless
Propagation	Radio Propagation model
Area	1500 x 1500
No.of nodes	20
Routing Protocol	AODV
Initial energy	5
TX power	0.9
Rx-Power	0.8
Idle Power	0.0

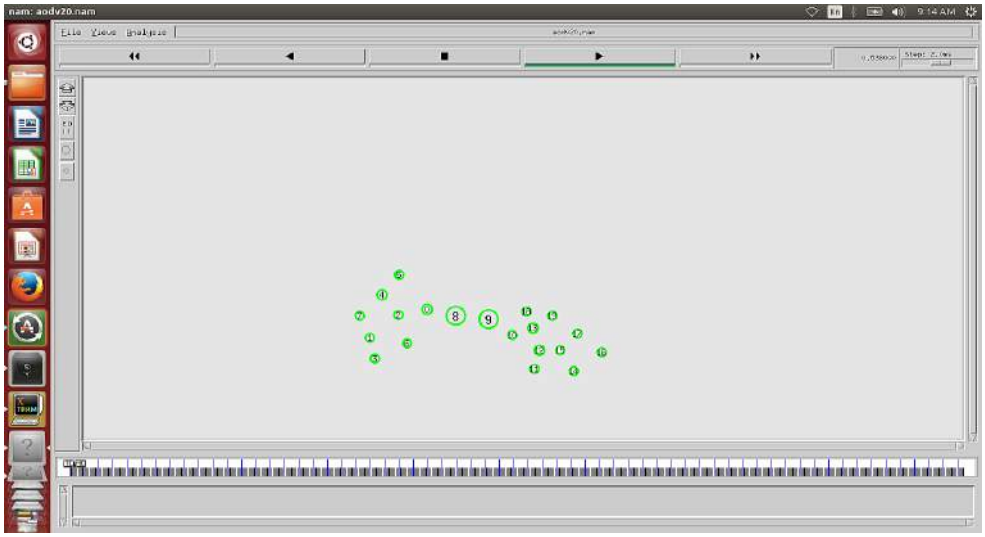

Fig. 1. NAM output for 20 mobile nodes using AODV Protocol

In figure 1, simulation results using NS2 are shown for wireless adhoc network using AODV routing protocol for 20 mobile nodes.

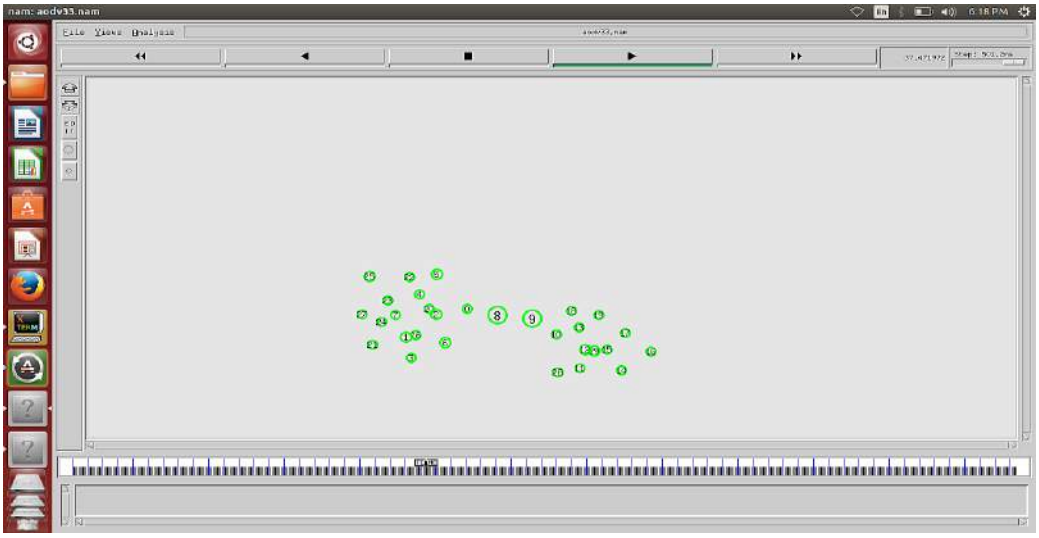

Fig.2. NAM output for 30 mobile nodes using AODV Protocol

In figure 2, simulation results are shown for wireless adhoc network using AODV routing protocol for 30 mobile nodes with the simulation parameters as indicated in Table-1.Table 2 lists values of computational parameters i.e. throughput, packet delivery ratio and residual energy after simulating various no.of mobile nodes.

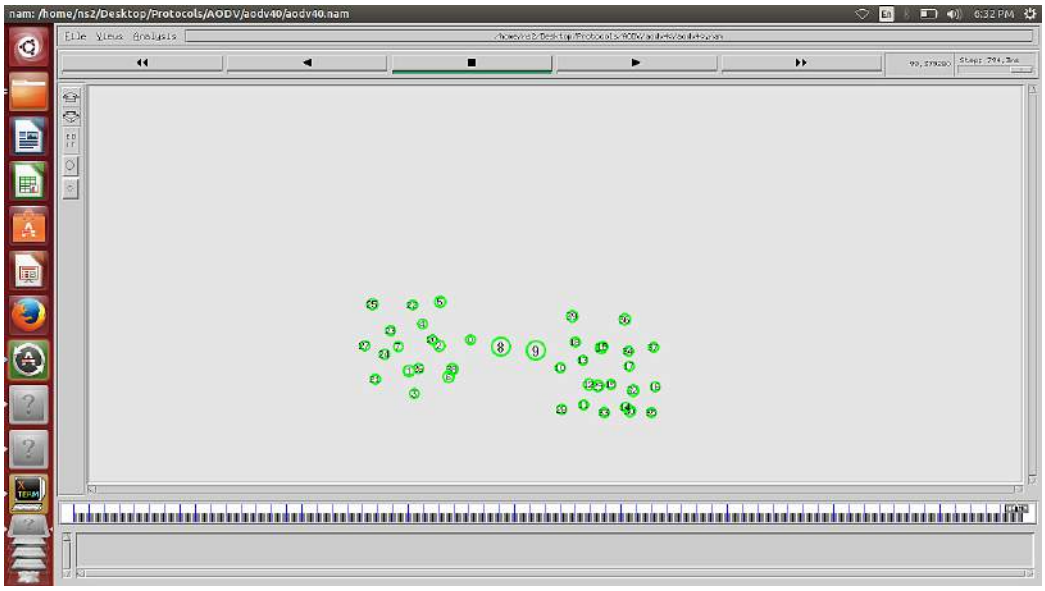

Fig.3. NAM output for 40 mobile nodes using AODV Protocol

Figure 3 shows NAM simulation for wireless adhoc network using AODV routing protocol for 40 mobile nodes.

From the table 2, it is clear that packet delivery ratio is better using DSDV protocol for low mobility network but energy level goes down after active communication is over.From the data of various computational parameters of above tables, we have run the regression and found following regression model for each table.

Table 2: Comparative analysis of various computational parameters i.e. Throughput, Packet delivery ratio and residual energy using DSDV Protocol.

No. of nodes(n)	Throughput T(kbps)	Packet delivery PDR (%)	Residual Energy in(Er) (J)
10	87.31	92.5	0.0017
20	213.53	93.13	1.025
30	408.89	86.8	1.005
40	274.85	87.72	0.12
50	289.9	82.0	0.52

Table 3: Summary Output

Sr.No	Regression statistic	
1	Multiple R	0.746143826
2	R Square	0.556730609
3	Adjusted R Square	-0.773077562
4	Standard Error	0.637854047
5	observation	5

Energy model computed using above regression is
$Er = -4.57 - 0.0046*n + 0.0039*T + 0.048*PDR$

Table 4: Comparative analysis of various computational parameters i.e. throughput, packet delivery ratio and residual energy using AODV protocol

No. of nodes(n)	Throughput T(kbps)	Packet delivery ratio (PDR) (%)	Residual energy Er(J)
10	38.32	86.00	0.23
20	83.66	90.61	4.27
30	67.09	79.85	0.43
40	23.96	61.36	3.93
50	26.10	70.47	2.01

From the table 4, it is clear that packet delivery ratio is better using AODV protocol for low mobility network as well as residual energy level is also better after active communication. Regression model derived for the data of table 4 is as follows:

Table 5: Summary Output

Sr.No	Regression statistic	
1	Multiple R	1
2	R Square	1
3	Adjusted R Square	65535
4	Standard Error	0
5	observation	4

Energy model computed using above regression is
$Er = 5.82 - 0.55*n - 0.42*T + 0.49*PDR$

Table 6: Comparative analysis of various computational parameters i.e. Throughput, Packet delivery ratio and residual energy using AOMDV Protocol

No. of nodes (n)	Throughput T(kbps)	Packet Delivery Ratio PDR (%)	Residual energy Er(J)
10	132.47	78	0.21
20	48.46	23.3	0.24
30	68.38	23.2	1.76
40	33.71	9	0.003
50	82.42	23	0.79

From the table 6, it is clear that packet delivery ratio & residual energy level is not satisfactory using AOMDV protocol for low mobility network. Also the level of residual energy is not promising after active communication is over.

Regression model for the above table 6 is as follows:

Table 7: Summary Output

Sr.No	Regression statistic	
1	Multiple R	1
2	R Square	1
3	Adjusted R Square	65535
4	Standard Error	0
5	observation	4

Energy model computed using above regression is
Er = 5.82 – 0.55*n – 0.42*T+0.49*PDR

In addition to above results, simulations are also carried out for wireless adhoc network using Pareto distribution for calculation of throughput, packet delivery ratio and residual energy & values of these computational parameters are found to be same as if the same network simulated without Pareto distribution .The complete simulation results are shown below.

Table 8: Comparative analysis of various computational parameters i.e. Throughput, Packet delivery ratio and residual energy for Pareto distribution using AODV protocol

No. of nodes(n)	Throughput T(kbps)	Packet delivery ratio PDR (%)	Residual energy Er(J)
10	66.83	90.57	1.056
20	83.66	94.0	1.77
30	67.09	79.85	0.43
40	23.96	61.36	3.93
50	26.10	70.47	2.01

Regression model for the above table 8 is as follows:

Table 9: Summary Output

Sr.No	Regression statistic	
1	Multiple R	1
2	R Square	1
3	Adjusted R Square	65535
4	Standard Error	0
5	observation	4

Energy model computed using above regression is
Er = 11.28 – 0.28*n – 0.2*T+0.14*PDR

Table 10: Comparative analysis of various computational parameters i.e. Throughput, Packet delivery ratio and residual energy for Pareto distribution using DSDV Protocol

No. of nodes	Throughput (kbps)	Packet Delivery Ratio (%)	Residual Energy Er(J)
10	87.31	92.53	0.0017
20	213.53	92.53	1.025
30	408.89	86.80	1.005
40	250.96	84.80	0.15
50	289.90	82.00	0.52

Table 11: Summary Output

Sr.No	Regression statistic	
1	Multiple R	1
2	R Square	1
3	Adjusted R Square	65535
4	Standard Error	0
5	observation	4

Energy model computed using above regression is

$$Er = -59.19+0.17*n+0.009*T+0.59*PDR$$

Table 12: Comparative analysis of various computational parameters i.e. Throughput, Packet delivery ratio and residual energy for Pareto distribution using AOMDV protocol

No. of nodes	Throughput (kbps)	Packet Delivary Ratio (%)	Residual Energy (J)
10	132.47	72.78	0.21
20	48.46	23	0.24
30	68.38	23	1.76
40	33.71	0.9	0.003
50	82.42	23	0.79

From the above table it is clear that packet delivery ratio is not promising using AOMDV protocol as well as residual energy is less after active communication.
Regression model for the above table 12 is as follows:

Table 13: Summary Output

Sr.No	Regression statistic	
1	Multiple R	1
2	R Square	1
3	Adjusted R Square	65535
4	Standard Error	0
5	observation	4

Energy model computed using above regression is

$$Er = 1.28 - 0.16*n+0.16*T - 0.24* PDR$$

3. CONCLUSION

The research work carried out debriefs new dimensions in the analysis of computational parameters of wireless adhoc network with & without application of Pareto distribution for changing node placement in wireless adhoc network. Energy of a node gradually reduces along with time. It is basically a proactive routing table in which each and every node has to maintain its own routing table to forward packet to its destination. But at the end of a simulation, energy of the node varies due to addition of new node in a path because MANET do not have fixed infrastructure. Residual energy of a node is retained more with the node even after active communication with AODV protocol as compared to DSDV for low mobility network scenario. The proposed method demonstrates the simulation of wireless adhoc network up to 50 mobile nodes using Pareto distribution & its comparison is carried out for its computational parameters i.e. throughput, packet delivery ratio & residual energy with and without applying pareto distribution . It is concluded that, even if we simulate the network by changing the node placement using Pareto distribution, it does not affect the computational parameters of the network for low mobility network and linear models for each results shows that $R^2 > 0.5$ which indicates that independent variables explains good amount of variation for predicting future values of energy for given input.

REFERENCE

[1] Zulfiqar Ali, Waseem Shahzad , "Analysis of Routing Protocols in Adhoc and Sensor Wireless Networks based on swarm intelligence,"International Journal of Networks and Communications, ISSN: 2168- 4936.

[2] Sofia Hamad, Hadi Noureddine and hamed AL Raeshidy, "Link Stability and Energy Aware for efficient Routing in Mobile Adhoc Network," 14th international symposium on wireless network, 2011.

[3] YANG Yin-jun, "Improvement and Analysis of Multipath Routing Protocol AOMDV based on CMMBCR," 2011 IEEE

[4] Md. Nafees Rahman, M. A. Matin, "Efficient Algorithm for Prolonging Network Lifetime of Wireless Sensor Networks," pp 561- 568 Volumes 16, Number 6, December 2011

[5] S. Mohapatra, P.Kanungo, "Performance analysis of AODV, DSR, OLSR and DSDV routing protocol using NS2 Simulator", international Conference on Communication Technology and System Design 2011, Elsevier, March 13, 2012.

[6] A Review on Energy Efficient Approaches for AODV Protocol, "International Journal of Engineering,sciences and researchTechnology, ISSN: 2277- 9655, May 2013 .

[7] Ibukunola.A.Modupe, Oludayo.O.Olugbara, Minimizing energy consumption in Wireless Adhoc Networks with Meta Heuristics," the fourth International conference in Wireless Adhoc Networks with Meta heuristics, Procedia Computer Science 19 (2013), 106- 115

[8] Geethu Mohandas, Dr.Salaja Silas & Shini Sam, "Servey on Routing Protocols on Mobile Adhoc Networks", Automation, Computing, "Communication, Control and Compressed Sensing, 2013 Conference.

[9] B. Nancharaiah, B. Chandra Moan, "The performance of hybrid Routing Intelligent algorithm in mobile Adhoc Networks," Elsevier, May 2014.

[10] Hui zhang Sheng Chen,Ä universal Approach for coverage probability & Throughput analysis for cellular Networks", IEEE Transactions on vehicular vehicular Technolgy, Vol 64, No.9, Sept 2015.

[11] David Gonzalez and Jyri Hamalainer,"Topology and irreguarityin cellular Networks"2015 IEEE Wireless communication and Network Conference(WNNC):-Track 3: Mobile & Wireless networks

AUTHORS

Mr. Suresh Kurumbanshi is B.E. and M.Tech in Electronics Engineering from RTM Nagpur University, Nagpur. He is Pursuing Ph.D. in Electronics Engineering from Department of Electronics & Telecommunication Engineering, Yeshwantrao Chavan College of Engineering, Nagpur. He has an industrial experience in Finolex Cables ltd, Pune & was working as a Sr. Lecturer in Electronics Department of G.H.Raisoni college of Engineering Nagpur. Later on he was handling responsibility of Head of Electronics Engineering Department at Rajiv Gandhi College of Engineering, Nagpur. Recently he was Head of Applied Sciences & Humanities Department in NMIMS University, Mumbai, Shirpur off Campus. He is currently working as Assistant Professor in the Department of Electronics & Telecommunication Engineering and In-charge of ISTE Chapter in MPSTME, NMIMS University, Shirpur Campus. His research area includes Adhoc Network, Mobile communication using stratospheric platforms.

Dr. Shubhangi Vikas Rathkanthiwar is presently working as Professor and Head of Department of Electronics Engineering, Yeshwantrao Chavan College of Engineering, Nagpur, India and as Deputy Director, International relations office, Meghe Group of Institutions, India. Her area of expertise is Wireless Communications and Soft Computing. She has 72 research papers in her credit. Her book 'An intelligent Wireless LAN system: Performance evaluation in fading multipath environment' is published in Germany. She is recognized reviewer of Journal of Applied Soft Computing, Elsevier, IEEE transactions on Vehicular Technology and IEEE transactions on Industrial Electronics. She is reviewer and Technical program committee member of several IEEE conferences. She is editorial member of several International Journals. She has filed two patent applications and one of her patent is published by Government of India. She is recipient of Best research paper award, Best Teacher award and 'Shikshak Ratna award'.

GENERATION OF SYNTHETIC POPULATION USING MARKOV CHAIN MONTE CARLO SIMULATION METHOD

Anu P. Alex[1], Prinsha T[2] and Manju V. S[3]

[1]Department of Civil Engineering, College of Engineering Trivandrum
[2]Department of Civil Engineering, Malabar Institute of Technology, Anjarakandy
[3]Department of Civil Engineering, College of Engineering Trivandrum

ABSTRACT

Activity based travel demand models are widely used in transportation planning to predict future demand of transportation. Disaggregate level data for the entire population is required as input to these models, which included household level and person level attributes for the entire study area. These data are usually collected by the population census, but are rarely available due to confidentiality reasons. Hence as a viable alternative, population synthesis techniques are used to supplement the microdata. An attempt has been made in this study to generate synthetic population using Markov Chain Monte Carlo Simulation method and to compare this with conventional method. Thiruvananthapuram Corporation in Kerala was selected as the study area and sample data were collected by household survey. The algorithm for population synthesis was coded in C++. The methodology was validated using 16 percentage of the collected data. Prediction accuracy of the method was compared with conventional method and was found better.

KEYWORDS

Microsimulation, Synthetic population, Beckman's method, MCMC method.

1. INTRODUCTION

Microsimulation is a mechanism for forecasting the state of a dynamic, complex system by simulating the behavior of the individuals in the system. The fundamental data required for microsimulation model are the details of individual and household attributes for the entire population of the study area. These details are usually collected in a population census but is not been made available to the public due to privacy and confidentiality reasons. Population synthesis techniques are commonly used as viable alternative to supplement the lack of availability of microdata. The process of population synthesis involves expanding a sample drawn from a population to a full set of synthetic population. These are algorithms that apply to sample data and its aggregated population data, in order to generate a synthetic population which is statistically representative of the actual population data. Different algorithms used for the process may generate synthetic population with different quality [1]. Since synthetic population is the input to activity based travel demand models, there had been a tremendous increase in the research works related to generation of synthetic population over the last fifteen years.

The conventional approach to synthesize base year population is based on a methodology originally developed by Beckman et al. [1]. This approach involves integrating aggregate data

DOI: 10.5121/ijci.2016.5117

from one source with disaggregate data from another source. Beckman's population synthesis approach uses the disaggregate data as "seeds" to create individual population records that are collectively consistent with the cross tabulations provided by the aggregate data. A new algorithm was proposed by Guo and Bhat [1] and they discussed about its data structure, operation and the step by step procedure. They generated synthetic population for Dallas /Fort-Worth area and census block groups were used as the aggregate data. Ryan et al. [2] discussed the synthetic reconstruction method based on Iterative Proportional Fitting (IPF) and Combinatorial Optimization method (CO) and the algorithms were tested. Programs to execute the CO and IPF methods were written in C++. Auld et al. [3] explained the population synthesis using Iterative Proportional Fitting Procedure. They used category reduction as a control for zero cell issue. The algorithm was designed to be used for any geographic area. The methodology was validated by generating the synthetic population for Southwestern Cook County. Ye et al. [4] tested the generation of synthetic population using Iterative Proportional Updating algorithm and matching the distributions of both household and person attributes in it. The algorithm involved iteratively adjusting and reallocating household weight. They included an example to illustrate the algorithm and its geometric interpretation. Ma [5] discussed about disaggregate travel demand models and activity based transportation planning models. Conceptual overview of the generation of synthetic population was described by the author.

Another method to population synthesis is Markov Chain Monte Carlo (MCMC) simulation based approach, which will overcome the limitations of IPFP [6]. Farooq et al. [6] described population synthesis using Markov chain Monte Carlo simulation. They have also explained about the simulation based approach and preparation of conditionals. The real population from Swiss census was used to compare the performance of simulation based synthesis with the standard IPF. Finally they have obtained better result for Monte Carlo Simulation method. Performance of synthesis procedures has been assessed using the Standardized Root Mean Square Error (SRMSE). The proposed methodology was implemented by Farooq et al. [7] for a real case study, where a synthetic population was generated for the base year of an integrated land use and transport model for the region of Brussels.

Anu et al. [8] conducted a study on generation of synthetic population for Thiruvananthapuram city by Beckman's method which is the conventional method. They have checked the prediction accuracy at both aggregate level and disaggregate level. They found that the prediction accuracy is above 90 percentage in the case of total number of households and total number of females and it is above 80 percentage in the case of total population and total number of males. The present paper attempts to develop synthetic population using MCMC method for Thiruvananthapuram city and to compare the results with conventional method.

2. MARKOV CHAIN MONTE CARLO METHOD FOR SYNTHETIC POPULATION

The methodology involved in Markov Chain Monte Carlo (MCMC) simulation is to draw agents (households) directly from the joint distribution. For example, joint probability distribution of X, Y… etc. is a probability distribution that gives the probability that each of X, Y… etc. falls in any particular range or discrete set of values. Gibbs sampler is used to simulate the draw. Instead of joint distribution conditional distributions are used as input for Gibbs sampler. This method is applicable when joint distribution is unknown, but conditional distributions are known. The only information that is required to generate the next agent is the previous agents synthesized and the input conditionals. Conditional distribution of one variable is the distribution of one variable conditioned on all other variables. For example, X and Y are two jointly distributed random variables then the conditional distribution of Y given X is the probability distribution of Y when X is known to be a particular value. Gibbs sampler generates a Markov chain of samples each of

which is correlated with the nearby samples. Steps involved in development of synthetic population using Monte Carlo simulation are shown in figure 1.

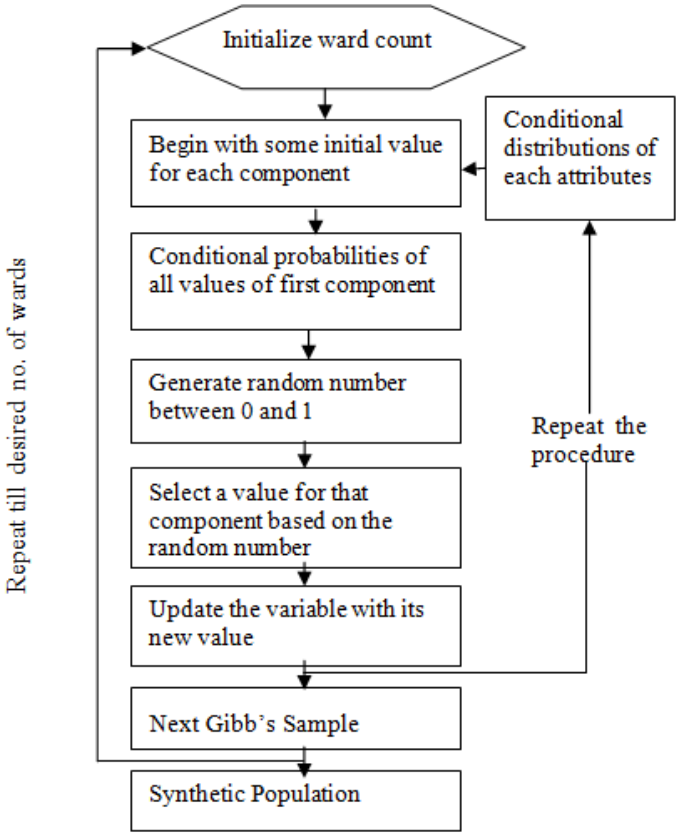

Figure 1. Steps involved in Monte Carlo simulation

The method starts with inputting the conditional distributions of each attributes. First some initial value is chosen for each attributes of first household, which is the first Gibbs sample. Conditional probabilities for all possible values of the first attribute are determined. Next step is generation of random numbers between 0 and 1. Based on the range in which the random number falls, the attribute value is selected. This step is repeated for all the other attributes to get the next Gibbs sample. This whole procedure is repeated for required number of times to get synthetic households in a ward. Similarly synthetic population is generated for all the 87 wards of Thiruvananthapuram Corporation.

2.1. Development of Algorithm

An algorithm for developing synthetic population based on MCMC method was coded in C++. 84 percentage of the collected data were used as input for the program and remaining 16 percentage of the data were used for validation.

2.1.1. Pseudo Coding

Pre Processor Directives
{
Variable declaration;

```
Read conditional probability distribution files of all attributes, household file, person file, ward total file;
For no. of wards
{
Read total no. of households from ward total file;
For total no. of households
{
For no. of attributes
{
Generate random number;
Check the range of conditional probability where the random no. falls;
Choose the attribute value;
Assign persons from person file;
List Household and person attributes;
}
End
}
```

3. OUTCOME OF THE STUDY

Outcome of the study is synthetic population for 87 wards of Thiruvananthapuram Corporation, which included the household level and person level attributes of each household. The number of households as per 2011census is191446 for Thiruvananthapuram Corporation and number of households predicted in the study are 213051 and 191466 by Beckman's method [8] and by MCMC method respectively. This shows that synthetic households were predicted with an accuracy of 100 percentage in MCMC method and 89 percentage in Beckman's method. Total population as per 2011 census is 762535.The synthesized data are 705036 by Beckman's method and 785352 by MCMC method respectively. The population was predicted with an accuracy of 92 percentage in Beckman's method and 97 percentage in MCMC method.

4. VALIDATION

Validation of the method was done by generating synthetic population for ward 18 (Kannammoola). This comprises 16 percentage of the total data collected. Synthetic population was generated for Kannammoola ward and the results were compared with data obtained from survey and conventional method [8]. Prediction accuracy in aggregate level results are shown in Table 1. Synthetic population of Thiruvananthapuram Corporation generated using Monte Carlo simulation technique was found better in prediction accuracy than Beckman's method.

Both household level and person level attributes were also compared. Household level validation results are shown in figures 3 to 6. It shows that the actual and synthesized population is almost equal when compared with household level attributes like number of males, number of females, vehicle ownership and number of workers in case of MCMC method compared to Beckman's method. Percentage accuracy obtained for each case is shown in Table 2.

Table 1. Results of Validation at Aggregate Level

Attributes	Actual population from census data	Synthesized population by Beckman's method	Prediction accuracy (%)	Synthesized population by MCMC method	Prediction accuracy (%)
Total number of households	191446	213051	88.71	191446	100
Total population	762535	705036	92.46	785352	97
Total number of males	371037	343714	92.63	356550	95.93
Total number of females	391498	361322	92.29	428802	90.47

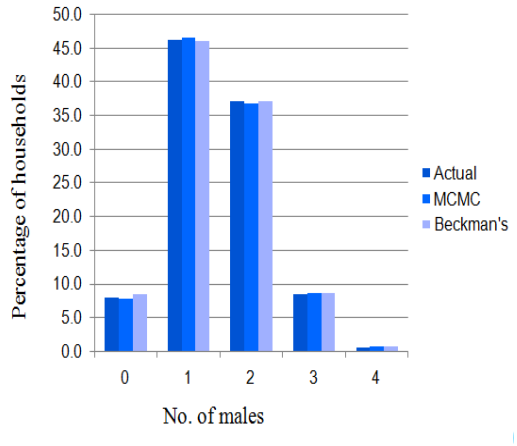

Figure 2. Comparison of HH based on no. of males

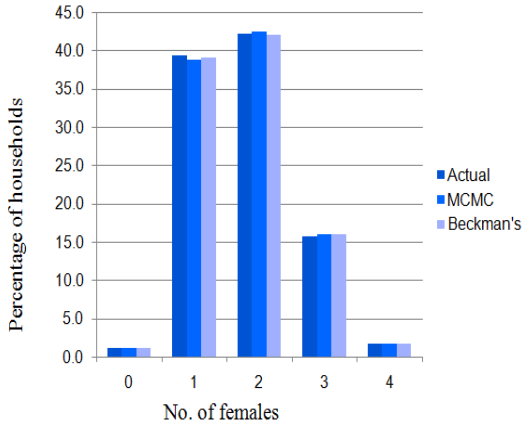

Figure 3. Comparison of HH based on no.of females

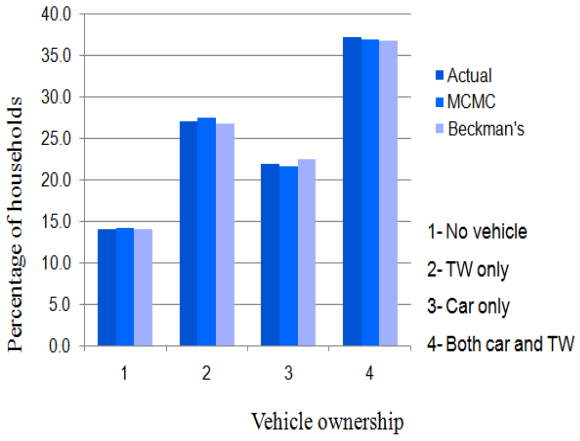

Figure 4. Comparison of HH based on Vehicle ownership

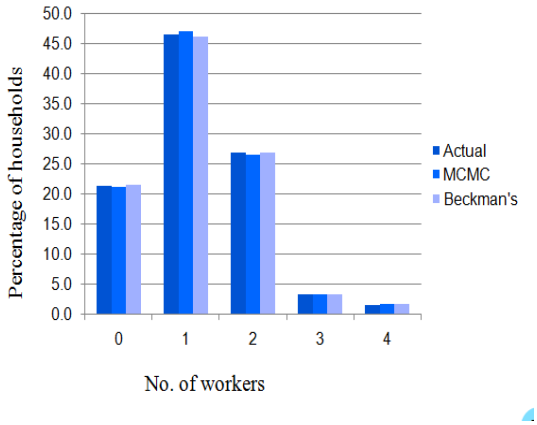

Figure 5. Comparison of HH based on number workers

Table 2. Summary of results HH level

Sl. No.	HH level Attributes	Accuracy (%) Beckman's	Accuracy (%) MCMC
1	Number of males	97.04	98.77
2	Number of females	98.57	99.09
3	Vehicle ownership	98.97	99.02
4	Number of workers	98.48	99.38

It is found that household level attributes like number of males, number of females, vehicle ownership and number of workers have an accuracy above 97 percentage in Beckman's method and about 99 percentage in MCMC method Person level validation results are shown in figure 7 to 11, which gives the comparison of percentage of individuals based on gender, age group, marital status, education level and employment status. It can be inferred that actual and synthesized population are closer in the case of gender and marital status. Percentage accuracy obtained for each case is shown in Table 3.

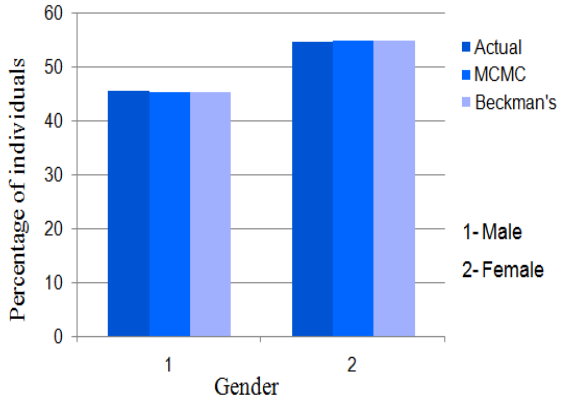

Figure 6. Comparison of persons based on gender

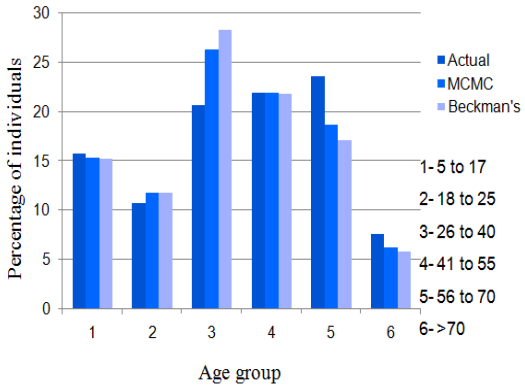

Figure 7. Comparison of persons based on age group

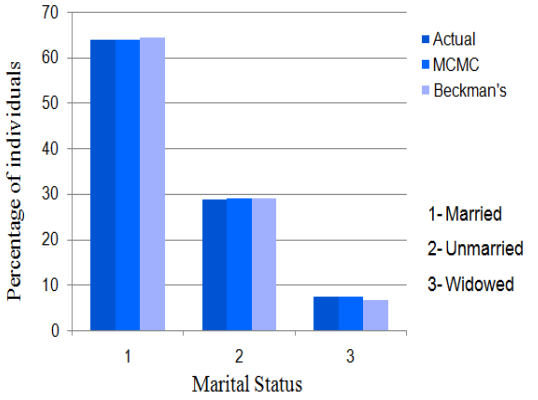

Figure 8. Comparison of persons based on marital status

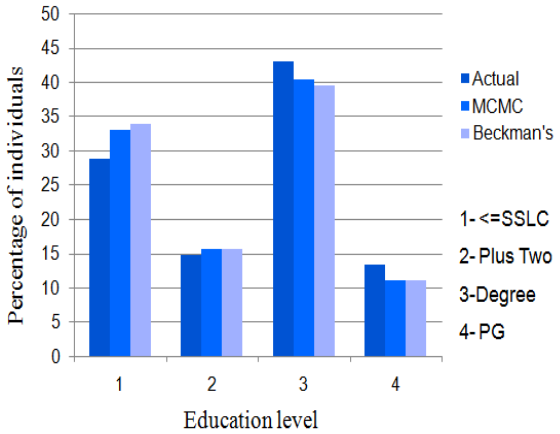

Figure 9. Comparison of persons based on education level

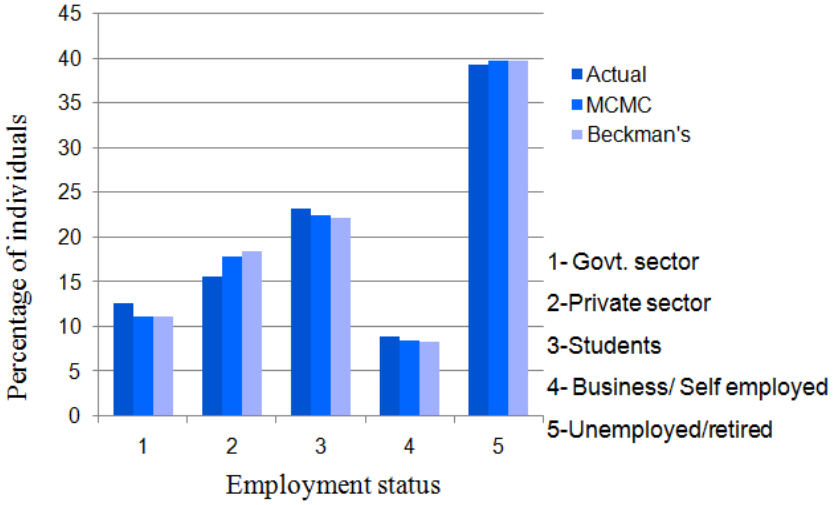

Figure 10. Comparison of persons based on employment level

Table 3. Summary of results person level

Sl. No.	Person level attributes	Accuracy (%) Beckman's	Accuracy (%) MCMC
1	Gender	99.67	99.79
2	Age group	83.5	87.11
3	Marital status	96.32	99.27
4	Employment	91.4	93.26
5	Education level	87.87	89.72

It is found that accuracy level is above 90 percentage in the case of gender, marital status and employment status and above 80 percentage in the case of age group and education level in Beckman's method. The accuracy level is above 99 percentage in gender and marital status and above 87 percentage in marital status, employment level and education level in MCMC method.

5. CONCLUSION

Travel demand models are essential tool in transportation planning for predicting the future demand of transportation. There are two approaches, trip based and activity based modeling out of which, activity based models provide more realistic representation of travel behavior. Hence now a day's activity based models are widely used. Disaggregate level population data are essential for activity based models which are usually collected by population census. But due to confidentiality reasons these data are not available for the public. Hence population synthesis techniques are used to generate synthetic population as input to activity based travel demand models. An attempt has been made in this paper to generate synthetic population for Thiruvananthapuram city which can be used as an input for activity based travel demand model for the city. An algorithm to generate synthetic population based on MCMC method has been presented in this paper.

Algorithm for the development of synthetic population was coded in C++. 84 percentage of the collected data were used as input for the program. The method was validated in the disaggregate level by applying it to ward number 18 of Thiruvananthapuram Corporation, which included 16

percentage of the collected data. Validation at aggregate level was done using census data. The following conclusions were made from the study;

- The prediction accuracy is more in the case of Markov Chain Monte Carlo simulation method compared to the Beckman's method both in household level and person level attributes
- Prediction accuracy of synthetic households was greater for MCMC method than Beckman's method by 12%
- Prediction accuracy of total population was greater for MCMC method than Beckman's method by 5%.
- Prediction accuracy of total number of males was greater for MCMC than Beckman's method by 14%.

Prediction accuracy of total number of females was greater for MCMC than Beckman's method by 2%.

ACKNOWLEDGEMENT

Authors express their gratitude to Kerala State Council for Science, Technology and Environment (KSCSTE) for funding the project.

REFERENCES

[1] J.Y. Guo, and C. R. Bhat, (2007). "Population synthesis for microsimulating travel behaviour", *Transportation Research Record*, 2014 (12) 92–101.

[2] J. Ryan, H. Maoh, and P. Kanaroglou, (2007), "Population synthesis: comparing major techniques using a small complete population of firms" working paper of *Mc Master university*

[3] J. Auld, A.K Mohammadian, and K. Wies, (2008). "Population synthesis with control category optimization", paper presented at the 10th *International Conference on Application of Advanced Technologies in Transportation*, Athens, Greece, May 2008.

[4] X. K. Ye, K.C. Pendyala, B. Sana, and P. Waddell, (2009) "Methodology to Match Distributions of Both Household and Person Attributes in Generation of Synthetic Populations". The 88th *Annual Meeting of the Transportation Research Board,* Washington, D.C.

[5] Lu Ma., (2011) "Generating disaggregate population characteristics for input to Travel-demand models" A dissertation presented to the *University of Florida*

[6] B. Farooq, M. Bierlaire, and G. Flotterod, (2013), "Simulation based population synthesis", *Transportation research board*

[7] B. Farooq, M. Bierlaire, and G. Flotterod, (2013), "Simulation based generation of synthetic population for Brussels case study", *Transportation research board*

[8] P. A. Anu, T. Prinsha, and V.S. Manju, (2015) "Generation of synthetic population using Beckman's method" The 16th *National Conference on Technological Trends*, Trivandrum, September 2015

AUTHORS

Mrs. Anu P. Alex, is working as Assistant Professor in Civil Engineering, College of Engineering Trivandrum, Kerala. She obtained B.Tech in Civil Engineering from Kerala University and M.E. in Transportation Engineering and Management from NIT, Trichy. She has more than 15 research papers in National and International Journals and Conferences.

Prinsha T., is working as Assistant Professor in Civil Engineering Malabar Institute Of Technology, Kannur, Kerala. She obtained B.Tech in Civil Engineering from CUSAT and M.Tech (Traffic and Transportation Engineering) from College of Engineering, Trivandrum.

Dr. Manju V. S., is working as Associate Professor in Civil Engineering at College of Engineering, Trivandrum. She graduated in B.Tech (Civil Engineering) under University of Kerala and M. Tech (Transportation Planning) from National Institute of Technology, Calicut. She did her doctoral programme under University of Kerala. She has published more than 20 research papers in National and International Journals and Conferences.

INTENTIONAL BLANK

POSTERIOR RESOLUTION AND STRUCTURAL MODIFICATION FOR PARAMETER DETERMINATION IN BAYESIAN MODEL UPDATING

Kanta Prajapat[1] and Samit Ray-Chaudhuri[2]

[1]Department of Civil Engineering, IIT Kanpur, Kanpur, UP-208016, India
[2]Department of Civil Engineering, IIT Kanpur, Kanpur, UP-208016, India

ABSTRACT

When only a few lower modes data are available to evaluate a large number of unknown parameters, it is difficult to acquire information about all unknown parameters. The challenge in this kind of updation problem is first to get confidence about the parameters that are evaluated correctly using the available data and second to get information about the remaining parameters. In this work, the first issue is resolved employing the sensitivity of the modal data used for updation. Once it is fixed that which parameters are evaluated satisfactorily using the available modal data the remaining parameters are evaluated employing modal data of a virtual structure. This virtual structure is created by adding or removing some known stiffness to or from some of the stories of the original structure. A 12-story shear building is considered for the numerical illustration of the approach. Results of the study show that the present approach is an effective tool in system identification problem when only a few data is available for updation.

KEYWORDS

Bayesian statistics, Modal parameters, Eigen sensitivity, Structural modification, MCMC

1. INTRODUCTION

The non-uniqueness issue associated with the inverse problem's solution makes the probabilistic approach more reliable over the deterministic approach for system identification problems. In last few decades, Bayesian model updating has rapidly arisen as a reliable and effective approach for system identification problems probabilistically. The efficiency of Bayesian model updating depends on various issues like the efficiency of simulation algorithm, data used for updation, prior distributions, likelihood function etc. Many of these issues have been successfully resolved in recent years [1-13]. Bayesian probabilistic approach is applied to localize and quantified the amount of damage in [24] employing incomplete and noisy modal data. A novel approach for online health monitoring and damage assessment of structures using Bayesian probabilistic measures is presented in [25]. In this approach at first identification of the system is done in its undamaged state and then continuous monitoring cycles are run to detect the damage in the structure. Appropriate model class selection using response measurements of structural system by showing examples of some linear and non-linear structural systems is shown in [6]. Bayesian approach for updation and model class selection for Masing hysteretic structural models is employed in [26]. A damage localization technique in structures under Bayesian inference using vibration measurements (modal data) on a steel cantilever beam is presented [27]. Damage detection in plate type structures is studied in [28]. Damage assessment of a slice of 7-story RC building using Bayesian uncertainty quantification technique is studied in [29].

DOI: 10.5121/ijci.2016.5118

Many times in Bayeisan updation problems the available data for updation falls short to give complete information about the all unknown parameters. The reason behind this is that the available data is not sensitive to all of the unknown structural parameters. Therefore, information about only those parameters can be acquired accurately for which the used data for updation is sensitive.

When modal data is used as evidence to update the structural model many researches have suggested different ways to take variance for prediction error model of frequency and mode shape data types [14-18]. Most of these studies consider only two variances one for frequencies of all modes and other for mode shape components of all modes. Only a few studies consider separate variances for data of different modes. However, depending on various conditions all frequencies and mode shape components of all modes may require separate variances for their prediction error models for an efficient information extraction from these data points. This study employs a sensitivity based approach recently given by the authors [24] to derive the variances for prediction error models of different data points to efficiently extract the information from these data points.
In this work, a novel Bayesian approach is presented to determine those parameters for which the available data for updation is not sensitive. The first thing in this kind of problem is to first get those parameters that can be successfully resolved using the available data. For this purpose a data sensitivity based term named as parameter impact is introduced in this work. It is shown that this newly introduced term successfully separate those parameters which can be resolved using available data from those which cannot be resolved. After this separation the resolved parameters are considered as known parameters. To resolve the remaining parameters a virtual structure is created by adding some high stiffness to those stories whose stiffness is successfully determined previously. It is observed that the modal data of this virtual structure is capable to give information about previously unresolved parameters. Ideally the approach is only effective when the modal data of this virtual structure can be determined using modal data of the original structure. A current research is in progress by the authors for this purpose, however, present study assumes that modal data of this virtual structure is known (using eigenvalue analysis).

Since a shear building approximation represents most of the civil engineering structures appropriately, a 12-stoery numerical shear building model is used for the illustration of the approach. Only fundamental mode data is used for updating the stiffness parameters of the shear building model. Markov chain Monte Carlo simulation technique is employed using Metropolis-Hasting algorithm to simulate the samples from the posterior distribution. The mean of the posterior distribution is taken as the parameter estimation of distribution to represent the unknown stiffness parameters. Results of this study show that the present approach is very efficient to resolve all unknown parameters even when the data available is not sensitive to the unknown parameters.

2. BAYESIAN MODEL UPDATING WITH MODAL DATA

The need to predict the response of a physical system due to a future excitation involves the requirement of a correct mathematical model for that system. This is done so that proper retrofitting measures can be taken if requires based on the response of the mathematical model. Bayesian modal updating involves parameter updation of an initially assumed crude mathematical model based on the response of the physical system. The process of updation is assumed to be satisfactory when the response of the mathematical model matches with the response of the physical system for a given input.

This updation of model parameters is done using Bayes' theorem as given below:

$$p(\theta \mid D) = \frac{p(D \mid \theta)\, p(\theta)}{p(D)} \tag{1}$$

where, $\theta \in R^n$ is the parameter vector which need to be updated and D is the available evidence from the system. Expression $p(\theta)$ is known as the prior distribution of θ and $p(D \mid \theta)$ represents the probability of the evidence D when a belief of θ is taken as true and called as the likelihood of the evidence for that belief. The total probability of the evidence D for the model is a constant and can be given by the sum of the likelihood of the evidence for each and every belief of θ which is represented as $p(D)$. The expression $p(\theta \mid D)$ is known as the posterior distribution of the parameter vector θ. When the evidence D consists of modal data of the system it can be shown that likelihood for frequency and mode shape components can be expressed as:

$$p(\omega_i / \boldsymbol{\theta}, \sigma_{\omega_i}) = \frac{1}{\sigma_{\omega_i}\sqrt{2\pi}} e^{-\frac{(\omega_i - \hat{\omega}_i(\boldsymbol{\theta}))^2}{2\sigma_{\omega_i}^2}} \tag{2}$$

$$p(\boldsymbol{\varphi}_i / \boldsymbol{\theta}, \mathbf{V}_{\boldsymbol{\varphi}_i}) = \frac{1}{(2\pi)^{n/2}\mathbf{V}_{\boldsymbol{\varphi}_i}^{1/2}} \exp\left(-\frac{1}{2}\left(\boldsymbol{\varphi}_i - \hat{\boldsymbol{\varphi}}_i(\boldsymbol{\theta})\right)^T \mathbf{V}_{\boldsymbol{\varphi}_i}^{-1}\left(\boldsymbol{\varphi}_i - \hat{\boldsymbol{\varphi}}_i(\boldsymbol{\theta})\right)\right) \tag{3}$$

Here, ω_i and $\boldsymbol{\varphi}_i$ represent the observed frequency and the mode shape vector of the i^{th} mode of the system $i = 1...m$ and $\hat{\omega}_i(\boldsymbol{\theta})$ and $\hat{\boldsymbol{\varphi}}_i(\boldsymbol{\theta})$ represent the frequency and mode shape of the model for the i^{th} mode respectively. In achieving (2) and (3) it is considered that the difference in model and system response is normally distributed with zero mean. Standard deviation of the deviation in frequency of the i^{th} mode is taken as σ_{ω_i} and $\mathbf{V}_{\boldsymbol{\varphi}_i}$ represents the covariance matrix of the deviation in i^{th} mode shape vector components. Now, if it is assumed that the frequency and mode shape of an energy mode are statically independent informatively. Further, if each mode is independent to other mode then for m modes the likelihood of the evidence D can be given as:

$$p(D / \boldsymbol{\theta}) = \prod_{i=1}^{m} p\left(\omega_i \mid \boldsymbol{\theta}, \sigma_{\omega_i}\right).p\left(\boldsymbol{\varphi}_i \mid \boldsymbol{\theta}, \mathbf{V}_{\boldsymbol{\varphi}_i}\right) \tag{4}$$

Now, to evaluate the covariance matrix $\mathbf{V}_{\boldsymbol{\varphi}_i}$, mode shape components are taken as uncorrelated to each other, resulting $\mathbf{V}_{\boldsymbol{\varphi}_i}$ to a diagonal matrix. Therefore, if, d is the length of the parameter vector θ, then the total unknown parameters in updation problem are increased to $d + m(n+1)$, where, n is the number of observed degrees of freedom and can be expressed as:

$$\bar{\boldsymbol{\theta}} = \left\{ \boldsymbol{\theta}^T, \left\{ \sigma_{\omega_i}^2, \mathbf{V}_{\boldsymbol{\varphi}_i 11} ... \mathbf{V}_{\boldsymbol{\varphi}_i nn} \right\}_{i=1}^{m} \right\}^T \tag{5}$$

Equation (4) now can be rewritten as:

$$p(D / \bar{\boldsymbol{\theta}}) = \prod_{i=1}^{m} p\left(\omega_i \mid \bar{\boldsymbol{\theta}}\right) \prod_{j=1}^{n} p\left(\boldsymbol{\varphi}_{ij} \mid \bar{\boldsymbol{\theta}}\right) \tag{6}$$

In a recent study [24] by authors it is shown that modal data sensitivity towards structural parameters can be used to evaluate the ratio of variance of error models for frequency and mode shape components of different modes. In this way exhaustive information from the data used for the updation can be obtained without increasing the number of unknown parameters (unknown

variances for each data point) in the updation algorithm. The present study uses this approach to evaluate the unknown variances.

3. PROBLEM STATEMENT

Many times in a model updation problem the data used for updation falls short to acquire information about all unknown parameters of the problem. Bayesian model updation algorithm works on the error minimization concept to get information about unknown parameters. In most of the Bayesian updation algorithms it is assumed that the unknown parameters are statistically independent. This fact makes each and every individual unknown parameter solely responsible to get any informatio about that parameter. Now, if there are some unknown parameters that are incapable to produce a change in the modal data used for updation with a change in that parameter for the adopted updation scheme then information for these parameters cannot be achieved in updation process. This work presents a novel approach to get information about these relatively hard to achieve unknown parameters with limited available data for updation. In order to acquire information about these parameters it is required to make the data used for updation sensitive towards the change in these parameters. Therefore, in the first stage of updation process information about those unknown parameters can be achieved for which the used modal data is sensitive. Next step of updation process involves the separation of accurately acquired and not acquired unknown parameters in the first stage. In this work modal data sensitivity towards unknown parameters is first used for an efficient posterior resolution of the parameters. Then, a virtual structural modification based approach is used to make the available modal data sensitive for the parameters which are not acquired accurately in the first stage of updation.

4. PROPOSED APPROACH

If modal data is considered for updation of unknown parameters k_i, $i = 1...t$ here, t is the total number of unknown parameters. Now, for square of frequency ω_I^2 of I^{th} mode, its derivative with respect to a parameter k_i is given by [19-23].

$$\frac{\partial \omega_I^2}{\partial k_i} = \frac{1}{C_I} \boldsymbol{\varphi}_I^T . \left[\frac{\partial \mathbf{K}}{\partial k_i} - \omega_I^2 \frac{\partial \mathbf{M}}{\partial k_i} \right] \boldsymbol{\varphi}_I \tag{7}$$

where,

$$C_I = \boldsymbol{\varphi}_I^T . \mathbf{M} \boldsymbol{\varphi}_I \tag{8}$$

and, if for mode shape $\boldsymbol{\varphi}_I$ of I^{th} mode, its derivative can be found using below expression [19-23].

$$\left[\mathbf{K} - \omega_I^2 \mathbf{M} \right] \frac{\partial \boldsymbol{\varphi}_I}{\partial k_i} = - \left[\frac{\partial \mathbf{K}}{\partial k_i} - \frac{\partial \omega_I^2}{\partial k_i} \mathbf{M} - \omega_I^2 \frac{\partial \mathbf{M}}{\partial k_i} \right] \boldsymbol{\varphi}_I \tag{9}$$

In Equations (7) and (9) $\mathbf{K}$ and $\mathbf{M}$ are the stiffness and mass matrix of the structure respectively. After getting the first stage value of unknown parameters these derivatives can be obtained for different unknown parameters. It is to be noted that to evaluate these derivatives the unknown stiffness matrix (assuming mass matrix is known) is constructed using first stage result of unknown parameters. In this approach a novel term is introduced for the posterior resolution of unknown parameters. Since Bayesian model updating algorithm is based on the error minimization between response of the system and the response of the mathematical model defined with some parameters. The uncertainty in the value of an unknown parameter can be assumed to be inversely proportional to the ability of that parameter to change the response of the

model with a change in the parameter itself for the adopted updation scheme. Now if a term 'parameter impact' (μ_k) is defined as the absolute sum of first order derivative of each and every modal data used for updation with respect to that parameter then it can be expressed as:

$$\mu_{k_i} = \left|\frac{\partial \omega_I^2}{\partial k_i}\right| + \left|\frac{\partial \varphi_{Ij}}{\partial k_i}\right|; \qquad \begin{Bmatrix} I = 1...m \\ j = 1...n \\ i = 1...t \end{Bmatrix} \tag{10}$$

where, m is the number of considered modes, n is the number of observed degrees of freedom and t is the total number of unknown parameters. Therefore, if ψ_{k_i} represents the uncertainty in parameter k_i after first stage of updation it can be given as:

$$\psi_{k_i} \propto \frac{1}{\mu_{k_i}} \tag{11}$$

The above relation is used for the meaningful posterior resolution of the unknown parameters and to get most uncertain parameters after first stage in this approach. After knowing the most uncertain parameters after first stage a local damage based approach is utilized to improve the parameter impact μ_k of these parameter so that uncertainty in the value of these parameters can be reduced in the second stage of updation. It is to be noted here that those parameters which has a relatively higher impact are already determined in the first stage and can be taken as known parameters. In the second stage a virtual structural modification is done by adding high stiffness to those stories of the structure for which the stiffness parameters are already determined in the first stage. It is seen that this virtual structure has a higher parameter impact than the original structure for those parameter which are determined as the most uncertain parameter in the first stage. Therefore, the modal data of the original structure along with the modal data of the virtual structure can be utilized to know the remaining unknown structural parameters. The approach can be repeated for more stages using different virtual structure till all the uncertain parameters are achieved.

The most challenging task in this approach is to evaluate the modal data of the virtual structure employing the modal data of the original structure. Although some techniques are available in literature to evaluate the modal data of the virtual structure but accuracy of these techniques depend on the number of available modes of the original structure and also most of these techniques are applicable for small modifications only. In case when only a few lower modes data are available these techniques are hard to rely for large modifications. However, practically only a few lower mode data are available from the original structure and also in many cases a large modification is required to improve the parameter impact. Authors' are currently trying to get an effective approach to obtain the modal data of the virtual structure, however, in this work the modal data for the virtual structure is simply obtained by the eigenvalue analysis and not using modal data of original structure. Further work is needed for the practical implementation of this approach.

5. ILLUSTRATIVE EXAMPLE

A numerically simulated 12-storey shear building frame is adopted to illustrate the approach (Figure 1). Stiffness parameter for a story is defined as the multiplier of assumed nominal stiffness of that story (4×10^8 N/mm for each story). Mass of each story is assumed to be known (1×10^5 kg) whether all stiffness parameters are assumed to be unknown for updation algorithm. These unknown stiffness parameters are found out employing present approach by taking only first mode data (frequency and mode shape). This data is generated by taking a known value of all

unknown parameters $k_i, i = 1...12$. Mode shape data are normalized with respect to the response of bottom story. To simulate the practical scenario this data is contaminated by a noise of coefficient of variation 5%. A total of 15 such contaminated data sets are then taken to find out the unknown stiffness parameters. To avoid any biasness in the algorithm exponential prior with mean value of 2 is adopted for the choice of prior distribution of all unknown stiffness parameters. The total unknown parameters in the algorithm are the unknown stiffness parameters, multiplication factor of normalized variances and shape parameter of proposal distribution of this multiplication factor. Prior distribution of these additional two unknown parameters are taken as uniform in a range 0.00001 to 10 for multiplication factor and 1 to 1000000 for shape parameter. For proposal distribution for all the unknown parameters Gamma distribution is adopted. Metropolis-Hasting Markov Chain Monte Carlo (MCMC) algorithm is employed to draw samples from the high dimensional posterior distribution.

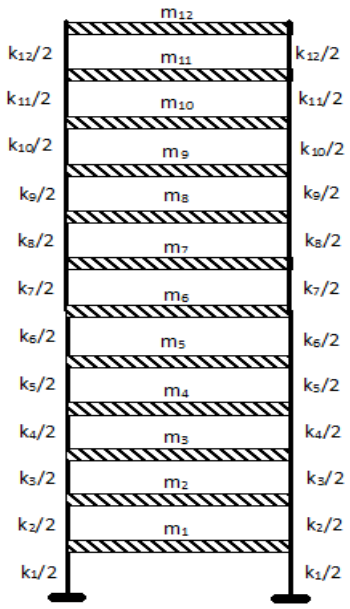

Figure 1: Schematic diagram of adopted shear building frame

Table 1 shows the result of the first stage for all unknown parameters in terms of posterior mean and variance and percentage deviation from the actual value. First stage is defined as the updation using the modal data of original structure. The subsequent stages are updation using the modal data of original as well as the modified structure. The modified structure is the structure with stiffness modification of some of the stories where a known stiffness is added to those stories. Table 1 also shows the parameter impact (μ_k) for different parameters normalized with respect to μ_{k_1}. It can be observed from Table 1 that those parameters which have higher μ_k are successfully determined in the first stage, however, parameters with lower μ_k cannot be resolved successfully in first stage. It can also be observed that the posterior variance is also a good measure of parameter certainty. However, in case of highly noisy data (not presented here) it is observed by the authors that posterior variance may give a false depiction of parameter accuracy. Therefore, based on μ_k parameters $k_i, i = 6...12$ are determined as the most uncertain unknown parameters after first stage that cannot be resolved using modal data of original structure. Figure 2 shows the Markov chain for different parameters and it can be observed form this figure that chain is not seen to be converged for parameters $k_i, i = 6...12$. Therefore, to improve the parameter impact of these parameters the original structure is virtually modified by adding stiffness to those stories whose stiffness parameters are successfully found in the first stage.

These stories stiffness is increased to two times of its current stiffness. Now modal data of this modified structure along with the original structure is used to determine the remaining unknown parameters which are not resolved successfully from first stage. In this work the modal data of virtual structure is not obtained using the modal data of the original structure but is obtained directly from eigenvalue analysis and contaminated with noise.

Table 1: Posterior statistics at first stage (original structure)

Unknown parameters with	Mean	Variance	Deviation (%)	Normalized parameter impact (μ_{k_i})
k_1=1.0	0.9697	0.0006	3.03	1.0
k_2=1.0	1.0406	0.0011	4.06	0.45
k_3=1.0	0.8991	0.0024	10.09	0.44
k_4=1.0	1.0322	0.0084	3.22	0.35
k_5=1.0	0.8587	0.0094	14.13	0.37
k_6=1.0	1.2045	0.0758	20.45	0.22
k_7=1.0	0.839	0.0236	16.10	0.27
k_8=1.0	1.5538	0.3277	55.38	0.12
k_9=1.0	0.937	0.0573	6.30	0.15
k_{10}=1.0	1.3531	0.3951	35.31	0.08
k_{11}=1.0	1.1558	0.3537	15.58	0.06
k_{12}=1.0	2.4023	0.8146	140.23	0.01

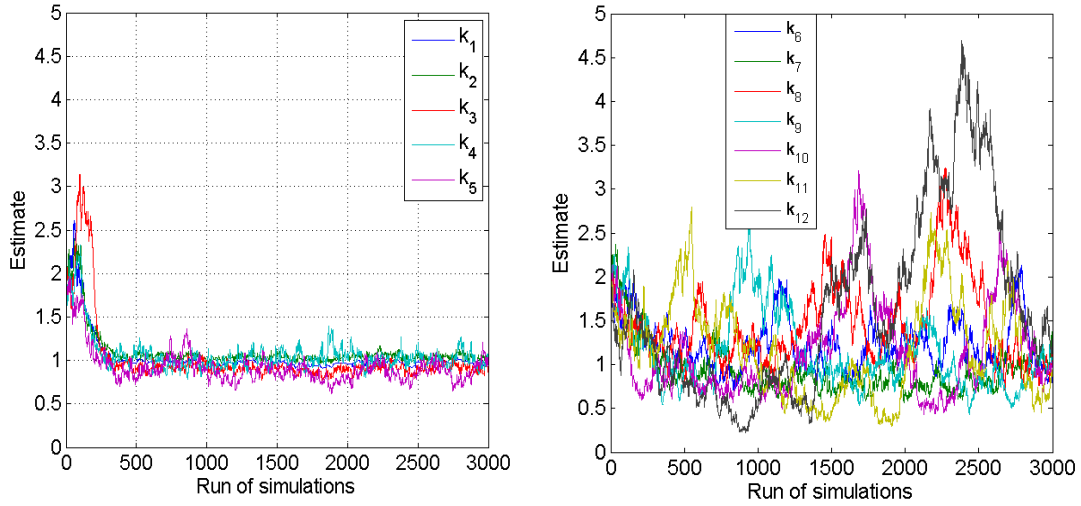

a. Well determined parameters b. Undetermined parameters

Figure 2: Markov Chain for different parameters in first stage

Results for stage 2 is shown in Table 2. It can be observed from this table that parameters $k_i, i = 6...9$ are successfully resolved in this stage which has higher μ_k in this stage than the previous stage. It is to be noted that in all stages μ_k is normalized with respect to μ_{k_1} only. Figure 3 shows the Morkov chain and posterior distribution of some of the parameters for stage 2. Results after two more modifications are shown in Table 3. Therefore, it can be concluded that the present approach is quite efficient to determine the unknown parameters using data of only first mode.

Table 2: Posterior statistics at second stage (modified structure)

Unknown parameters with	Mean	Variance	Deviation (%)	Normalized parameter
k_6=1.0	1.0126	0.0042	1.26	0.45
k_7=1.0	0.9810	0.0156	1.90	0.40
k_8=1.0	1.0469	0.0306	4.69	0.31
k_9=1.0	1.0691	0.0567	6.91	0.24
k_{10}=1.0	1.4114	0.4685	41.14	0.14
k_{11}=1.0	0.8308	0.1343	16.92	0.15
k_{12}=1.0	3.5123	14.2292	251.23	0.02

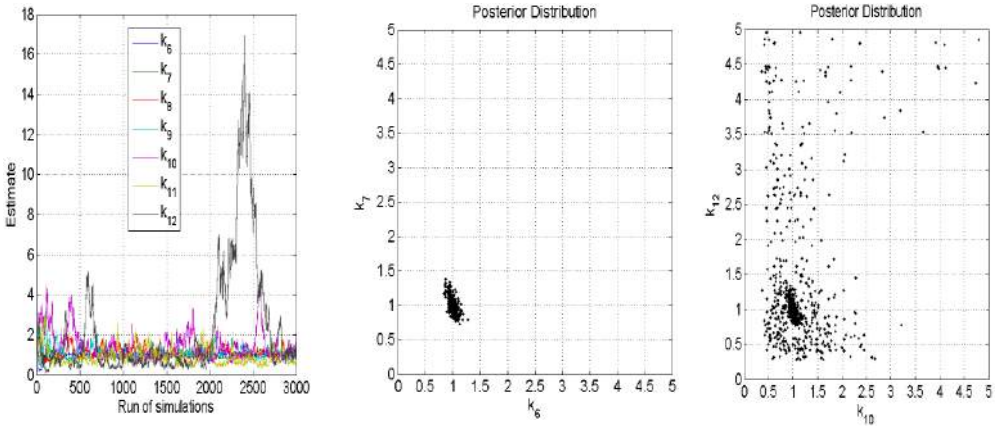

a. Markov chain b. Well determined parameters c. Ill determined parameters

Figure 3: Second stage statistics

Table 3: Posterior statistics at final stage

Unknown parameters with	Mean	Deviation (%)
k_1=1.0	0.9697	3.03
k_2=1.0	1.0406	4.06
k_3=1.0	0.8991	10.09
k_4=1.0	1.0322	3.22
k_5=1.0	0.8587	14.13
k_6=1.0	1.0126	1.26
k_7=1.0	0.981	1.90
k_8=1.0	1.0469	4.69
k_9=1.0	1.0691	6.91
k_{10}=1.0	1.037	3.70
k_{11}=1.0	1.044	4.40
k_{12}=1.0	1.1912	19.12

6. CONCLUSIONS

A sensitivity based novel term is introduced for the posterior resolution of unknown parameters. It is observed that the present approach is highly effective and efficient to resolve the unknown parameters under Bayesian inference. The result of the study shows that using the present approach those parameters of a system can also be found for which the data available for the updation is not very sensitive. However, the current approach is yet to be tested for the practical scenario. Future research is needed for the complete implementation of the present approach on real structures. In civil engineering structures the approach can be a useful tool for system identification or damage detection when not much data is available for updation. It is also observed that the posterior variance can also be used as a good measure of parameter accuracy. However, in case of highly noisy data the reliability of variance based accuracy suffers.

REFERENCES

[1] Beck, J. L. and Katafygiotis, L. S. (1991) "Updating of a model and its uncertainties utilizing dynamic test data." *Computational Stochastic Mechanics*, Springer, pp125–136.

[2] Beck, J. L. and Katafygiotis, L. S. (1998) "Updating models and their uncertainties. i: Bayesian statistical framework." *Journal of Engineering Mechanics*, Vol. 124, No. 4, pp455–461.

[3] Chen, L., Qin, Z., and Liu, J. S. (2001) "Exploring hybrid monte carlo in bayesian computation." *sigma*, Vol. 2, pp2–5.

[4] Papadimitriou, C., Beck, J. L., and Katafygiotis, L. S. (2001) "Updating robust reliability using structural test data." *Probabilistic Engineering Mechanics*, Vol. 16, No. 2, pp103–113.

[5] Beck, J. L. and Au, S. K. (2002) "Bayesian updating of structural models and reliability using markov chain monte carlo simulation." *Journal of Engineering Mechanics*, Vol. 128, No. 4, pp380–391.

[6] Beck, J. L. and Yuena, K. V. (2004) "Model selection using response measurements: Bayesian probabilistic approach." *Journal of Engineering Mechanics*, Vol. 130, No. 2, pp192–203.

[7] Ching, J., Muto, M., and Beck, J. L. (2005) "Bayesian linear structural model updating using gibbs sampler with modal data." *Proceedings of the 9th International Conference on Structural Safety and Reliability*, Millpress, pp2609–2616.

[8] Marwala, T. and Sibisi, S. (2005) "Finite element model updating using bayesian approach." *In Proceedings of the International Modal Analysis Conference, Orlando, Florida, USA*.

[9] Ching, J. and Chen, Y. C. (2007) "Transitional markov chain monte carlo method for bayesian model updating, model class selection, and model averaging." *Journal of Engineering Mechanics*, Vol. 133, No. 7, pp816–832.

[10] Mthembu, L., Marwala, T., Friswell, M. I., and Adhikari, S. (2008) "Bayesian evidence for finite element model updating." *arXiv preprint arXiv:0810.2643*.

[11] Cheung, S. H. and Beck, J. L. (2009) "Bayesian model updating using hybrid monte carlo simulation with application to structural dynamic models with many uncertain parameters." *Journal of Engineering Mechanics*, Vol. 135, No. 4, pp234–255.

[12] Cheung, S. H. and Beck, J. L. (2010) "Calculation of posterior probabilities for bayesian model class assessment and averaging from posterior samples based on dynamic system data." *Computer-Aided Civil and Infrastructure Engineering*, Vol. 25, No. 5, pp304–321.

[13] Boulkaibet, I., Marwala, T., Mthembu, L., Friswell, M. I., and Adhikari, S. (2011) "Sampling techniques in bayesian finite element model updating." *arXiv preprint arXiv:1110.3382*.

[14] Christodoulou, K. and Papadimitriou, C. (2007) "Structural identification based on optimally weighted modal residuals" *Mechanical Systems and Signal Processing*, Vol. 21, No. 1, pp4–23.

[15] Goller, B., and Schueller, G.I. (2011) "Investigation of model uncertainties in bayesian structural model updating," *Journal of sound and vibration*, Vol. 330, No. 25, pp6122–6136.

[16] Papadimitriou, C., Argyris, C., Papadioti, D. C., and Panetsos, P. (2014) "Uncertainty calibration of large-order models of bridges using ambient vibration measurements," in *Proc. EWSHM-7th European Workshop on Structural Health Monitoring*.

[17] Behmanesh, I., Moaveni, B., Lombaert, G., and Papadimitriou, C. (2015) "Hierarchical bayesian model updating for structural identification," *Mechanical Systems and Signal Processing*.

[18] Fox, R. L., and Kapoor, M. P. (1968) "Rates of change of eigenvalues and eigenvectors," *AIAA journal*, Vol. 6, No. 12, pp2426–2429.
[19] Rogers, Lynn C. (1970) "Derivatives of eigenvalues and eigenvectors," *AIAA journal*, Vol. 8, No. 5, pp943–944.
[20] Nelson, R. B. (1976) "Simplified calculation of eigenvector derivatives" *AIAA journal*, Vol. 14, No. 9, pp1201–1205.
[21] Adhikari S. (1999) "Rates of change of eigenvalues and eigenvectors in damped dynamic system" *AIAA journal*, Vol. 37, No. 11, pp1452–1458.
[22] Smith, D. E., and Siddhi, V. (2006) "A generalized approach for computing eigenvector design sensitivities" in *Proc. SEM annual conference and exposition on experimental and applied mechanics*.
[23] Prajapat, K., and Ray-Chaudhuri S. "Prediction Error Variances in Bayesian Model Updating Employing Data Sensitivity" *Journal of Engineering Mechanics*, (under review).
[24] Sohn, H. and Law, K. H. (1997) "A bayesian probabilistic approach for structure damage detection." *Earthquake engineering and structural dynamics*, Vol. 26, No. 12, pp1259–1281.
[25] Vanik, M. W., Beck, J. L., and Au, S. K. (2000) "Bayesian probabilistic approach to structural health monitoring." *Journal of Engineering Mechanics*, Vol. 126, No. 7, pp738–745.
[26] Muto, M. and Beck, J. L. (2008) "Bayesian updating and model class selection for hysteretic structural models using stochastic simulation." *Journal of Vibration and Control*, Vol. 14 (1-2), 7–34.
[27] Huhtala, A. and Bossuyt, S. (2011) "A bayesian approach to vibration based structural health monitoring with experimental verification." *Journal of Structural Mechanics*, Vol. 44, No. 4, 330–344.
[28] Kurata, M., Lynch, J. P., Law, K. H., and Salvino, L. W. (2012) Bayesian Model Updating Approach for Systematic Damage Detection of Plate-Type Structures. Springer.
[29] Simoen, E., Moaveni, B., Conte, J. P., and Lombaert, G. (2013) "Uncertainty quantification in the assessment of progressive damage in a 7-story full-scale building slice." *Journal of Engineering Mechanics*, Vol. 139, No. 12, pp1818–1830.

AUTHORS

Kanta Prajapat is a research scholar at the department Civil Engineering, Indian Institute of Technology Kanpur and working with Dr. Samit Ray-Chaudhuri. She received her Master of Technology degree from the same institute in 2011, and Bachelor of Engineering degree from M.B.M. Engineering College Jodhpur in 2009.

Dr. Samit Ray-Chaudhuri is a professor at the department of Civil Engineering, Indian Institute of Technology Kanpur. Prior to joining IITK, he was working as a postdoctoral researcher with Professor Masanobu Shinozuka, in the department of Civil and Environmental Engineering at the University of California, Irvine. He received his Doctor of Philosophy degree from the University of California at Irvine, Master of Technology degree from the Indian Institute of Technology Kanpur (IITK), and Bachelor of Engineering degree from Bengal Engineering College, currently known as Bengal Engineering and Science University, all majored in civil engineering.

FREQUENCY RESPONSE ANALYSIS OF 3-DOF HUMAN LOWER LIMBS

Keyur Hirpara[1], Hemant Nagarsheth[2] and V M Daiya[3]

[1]Department of Mechanical Engineering, Institute of Technology,Nirma UniversityAhmedabad, Gujarat
[2] Mechanical Engineering Department, SVNIT, Surat, Gujarat
[3] Mechanical Engineering Department, SVNIT, Surat, Gujarat

ABSTRACT

Frequent and prolonged expose of human body to vibrations can induce back pain and physical disorder and degeneration of tissue. The biomechanical model of human lower limbs are modeled as a three degree of freedom linear spring-mass-damper system to estimate forces and frequencies. Then three degree of freedom system was analysed using state space method to find natural frequency and mode shape. A program was develop to solve simplified equations and results were plotted and discussed in detail. The mass, stiffness and damping coefficient of various segments are taken from references. The optimal values of the damping ratios of the body segments are estimated, for the three degrees of freedom model. At last resonance frequencies are found to avoid expose of lower limbs to such environment for optimum comfort.

KEYWORDS

Frequency Response Analysis, Biomechanics, Human Limbs, Dynamics

1. INTRODUCTION

Most of the time vibrations are undesirable and when people are exposed to vibration it may causing back pain, fatigue stresses and disorder. So it is very much essential to know frequency at various joints of lower limbs at particularly frequencies near the principal resonance. Several models capable of undergoing vibratory motion have been described in the literature. The model, consisting of a mass, spring and damper, was developed by Y. Matsumoto and M.J. Griffin [1]. They simulated the standing subjects exposed to vertical whole-body vibration. A model with two-degree of freedom discrete system was analysed for damped vibration analysis by Z. Oniszczuk [2]. More details of the human body were imitated in the three-dimensional biomechanical model for simulating the response of the human body to vibration stress was developed by M. Fritz [3]. In the study carried out by Tae-Hyeong Kim at. el. [4], vibration transmissibility in the vertical direction was measured for a biomechanical model of the human body in a sitting posture. S. Kitazaki and M. J. Griffin [5] analysed a whole-body vertical vibration, using a finite element model of the human body.

2. DEVELOPMENT OF THE EQUATION OF MOTION

In all literature mentioned before no extensive study of human lower limbs were found. Using basic theory of vibration [6], a three-degree of freedom model consists of masses, springs and dampers is developed simulating the lower limb in preceding work presented by K P Hirpara [7].

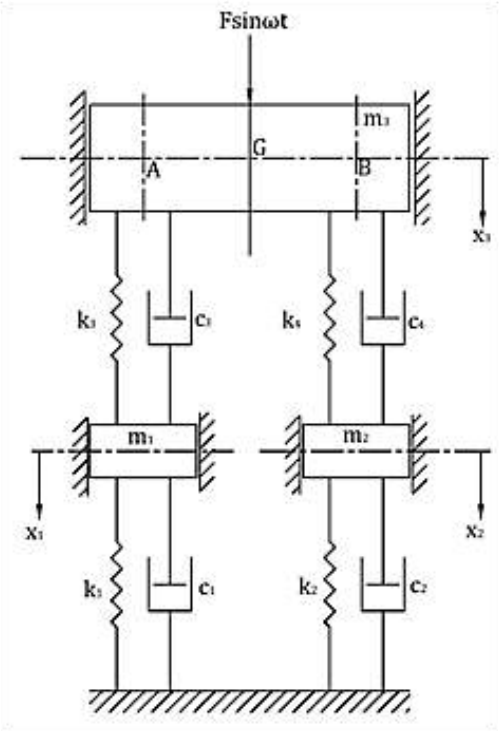

Figure 1. 3-dof linear vibration model under consideration

Figure 1 shows a three degree of freedom with three masses m_1, m_2 andm_3. m_1 and m_2 tied to ground through spring k_1 and k_2 and damper c_1 and c_2 similarly both are connected to mass m_3 through spring k_3 and k_4 and damper c_3 and c_4. The system is assumed to be free in executing oscillations in the vertical direction only, also clearance between mass and guide is negligible, the springs and dampers are assumed mass less and deformation of spring and damper is linear.Measuring the displacement, velocity and acceleration quantities (downwards positive), and applying Lagrangian equation to this system,

$$m_1\ddot{x_1} + (c_1 + c_3)\dot{x_1} + (k_1 + k_3)x_1 - c_3\dot{x_3} - k_3x_3 = F1$$
$$m_2\ddot{x_2} + (c_2 + c_4)\dot{x_2} + (k_2 + k_4)x_2 - c_4\dot{x_3} - k_4x_3 = F2$$
$$m_3\ddot{x_3} + (c_3 + c_4)\dot{x_3} + (k_3 + k_4)x_3 - c_3\dot{x_1} - k_3x_1 - c_4\dot{x_2} - k_4x_2 = F3$$

In order to solve time domain problems using a computer, it is desirable to change the form of the equations for the 3-dof system with three second order differential equations to six first order differential equations which is known as state space form.

Considering forces are acting on each masses are F1, F2 and F3 respectively. Equations of motion for 3-dof model can be written in state space form as,

$$\dot{z_1} = z_2$$
$$\dot{z_2} = [F_1 - (c_1 + c_3)z_2 - (k_1 + k_3)z_1 + c_3z_6 + k_3z_5]/m_1$$
$$\dot{z_3} = z_4$$
$$\dot{z_4} = [F_2 - (c_2 + c_4)z_4 - (k_2 + k_4)z_3 + c_4z_6 + k_4z_5]/m_2$$
$$\dot{z_5} = z_6$$
$$\dot{z_6} = [F_3 - (c_3 + c_4)z_6 - (k_3 + k_4)z_5 + c_3z_2 + k_3z_1 + c_4z_4 + k_4z_3]/m_3$$

Eiganvalue can be written in state space form,

$$(\lambda I - A)$$

$$= \lambda I - \begin{bmatrix} 0 & 1 & 0 & 0 & 0 & 0 \\ \frac{-(k_1+k_3)}{m_1} & \frac{-(c_1+c_3)}{m_1} & 0 & 0 & \frac{k_3}{m_1} & \frac{c_3}{m_1} \\ 0 & 0 & 0 & 1 & 0 & 0 \\ 0 & 0 & \frac{-(k_2+k_4)}{m_2} & \frac{-(c_2+c_4)}{m_2} & \frac{k_4}{m_2} & \frac{c_4}{m_2} \\ 0 & 0 & 0 & 0 & 0 & 1 \\ \frac{k_3}{m_3} & \frac{c_3}{m_3} & \frac{k_4}{m_3} & \frac{c_4}{m_3} & \frac{-(k_3+k_4)}{m_3} & \frac{-(c_3+c_4)}{m_3} \end{bmatrix}$$

3. DYNAMIC ANALYSIS OF THE 3-DOF MODEL

To solve original damped system equation for complex Eigenvalues and Eigenvectors it is Normalize to unity. Than magnitude and phase angle of each of the Eigenvector entries are calculated. Also the percentage of critical damping (damping ratio) for each mode and the motions of the three masses for all three modes are calculated. Results were plotted the real and imaginary displacements of each of the degrees of freedom separately.

For the 3-dof damped system matrix, taking the closed form determinant is far too complicated, so MATLAB was used to solve the Eigenvalue problem numerically. MATLAB code was develop to determine eigenvalue, eigenvector, magnitude and phase angle, critical damping ratio and frequency response using specific values of m, c and k and which are taken from research paper published by Devendra P. Garg et al and T. C. Gupta [8,9].

Table 1: Values of Mass, Damping coefficients stiffness and force at each joints

Mass (kg)	Stiffness (N m^{-1})	Damping coefficient (N sm^{-1})	Force (N)
m1= 8.26	k_1= 3.590 X 10^5	c_1= 963.2	F_1= 100
m2= 8.26	k_2= 3.590 X 10^5	c_2= 963.2	F_2= 100
m3= 59.10	k_3= 3.590 X 10^5	c_3= 963.2	F_3= 100
--	k_4= 3.590 X 10^5	c_4= 963.2	--

4. RESULT AND DISCUSSIONS

4.1. Eigen values and Eigenvectors

The six Frequencies derived from the program are listed below,

Table 2: Natural frequencies at each joints

	Eigenvalues in complex form	Natural frequency (rad/sec)
Mass 1	-1.2901 + 2.8200i -1.2901 - 2.8200i	3.101
Mass 2	-1.1661 + 2.7079i -1.1661 - 2.7079i	2.948
Mass 3	-0.1022 + 0.8670i -0.1022 - 0.8670i	0.873

Note that the two Eigenvalues which correspond to each of the three modes are complex conjugates of each other, and that the real parts of the all third mode Eigenvalues are negative. Here it shows that mode 1 takes highest time to reach at equilibrium stage as compare to mode 2, and mode 3 having highest damping ratio so it will take lesser time to reach on equilibrium stage.

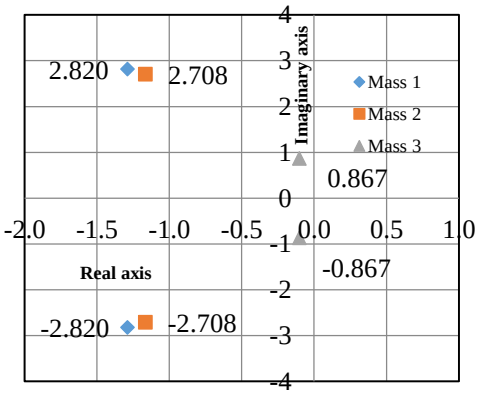

Figure 2: Eigenvalues in complex form

The Eigenvectors than normalizes from low to high frequency by dividing each Eigenvector by its position state for mass 1, the first term in each Eigenvector.

Table 3: Eigenvectors

	Displacement states	Velocity states	Displacement states	Velocity states	Displacement states	Velocity states
Mode 1	0.0100 -0.1022 +0.8670i	0.0100 -0.1022 -0.8670i	0.0100 -1.1661 +2.7079i	0.0100 -1.1661 -2.7079i	0.0100 -1.2901 +2.8200i	0.0100 -1.2901 -2.8200i
Mode 2	0.0100 + 0.0000i -0.1022 + 0.8670i	0.0100 - 0.0000i -0.1022 - 0.8670i	-0.0100 + 0.0000i 1.1661 - 2.7079i	-0.0100 - 0.0000i 1.1661 + 2.7079i	0.0100 - 0.0000i -1.2901 + 2.8200i	0.0100 + 0.0000i -1.2901 - 2.8200i
Mode 3	0.0182 + 0.0000i -0.1865 + 1.5820i	0.0182 - 0.0000i -0.1865 - 1.5820i	-0.0000 - 0.0000i 0.0000 - 0.0000i	-0.0000 + 0.0000i 0.0000 + 0.0000i	-0.0021 + 0.0000i 0.2743 - 0.5996i	-0.0021 - 0.0000i 0.2743 + 0.5996i

The six rows of each Eigenvector (mode shapes) are related to the six states, where even rows are the displacement states and odd rows are the velocity states. Each velocity row is equal to the displacement row associated with it times.

The first two columns of the Eigenvector matrix define mode 1, the third and fourth define mode 2 and the fifth and sixth columns define mode 3. Like the two complex conjugate Eigenvalues for each mode, the two Eigenvector columns for each of the modes are complex conjugates of each other.

The percentage of critical damping for each of the three modes is than calculated,

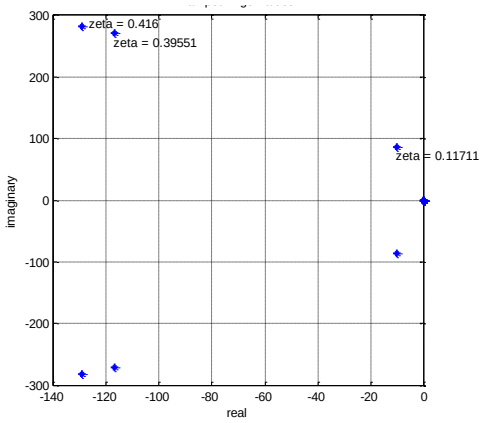

Figure 3: Damped Natural frequencies

Note that the damping ratios are 0.1171, 0.3955 and 0.416 for modes 1 and 2 and 3 respectively which is shown in the figure 3.

4.2Initial Condition Responses

The motion in that mode is defined as the sum of the motions due to the two conjugate Eigenvalues/Eigenvectors for that mode. Initial condition transient responses for the three modes, illustrating the cancelling of the imaginary components and the doubling of the real components are plotted

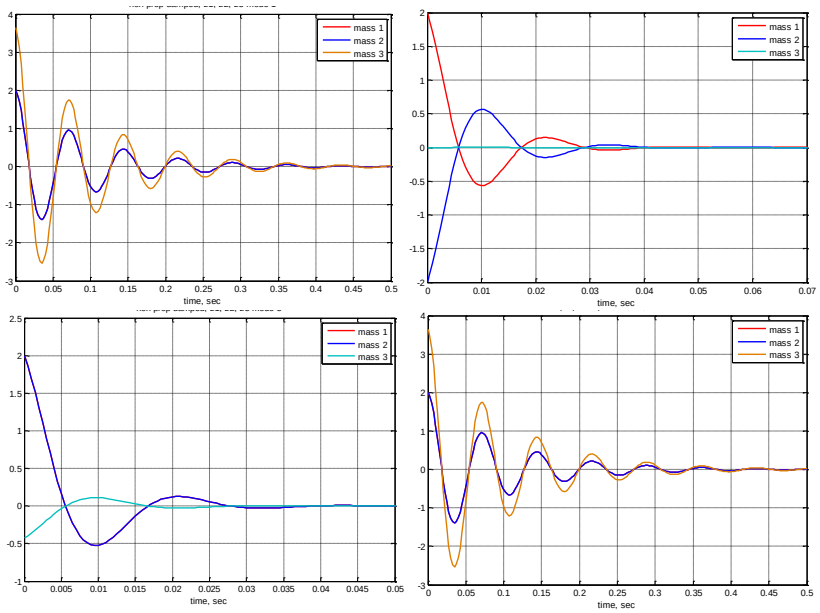

Figure 4: Non proportional damped vibration for mode 1; (a) real and imaginary for m1 (a) real and imaginary for m2 (a) real and imaginary for m3 (d) combined for m1, m2 and m3

The figure 4 show the motions of the masses decreasing due to the damping. The imaginary components are out of phase and cancel each other, leaving only twice the real component as the final motion. Unlike the undamped case, the three masses do not reach their maximum or minimum positions at the same time. Since the damping is quite small, it is hard to see on the

plots the small differences in times at which the maxima and minima are reached. Also it can be seen from the Figure 4(d), mass 1 and mass 2 are moving in a same phase and mass 3 is in different phase. Response time for this mode is 0.5 seconds.

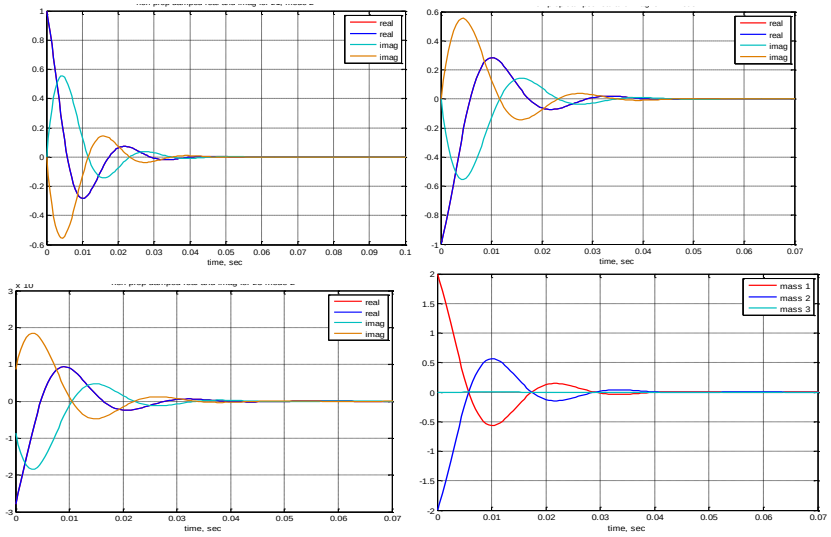

Figure 1: Non proportional damped vibration for mode 2; (a) real and imaginary for m1 (a) real and imaginary for m2 (a) real and imaginary for m3 (d) combined for m1, m2 and m3

Compared to the responses for the mode 1 in Figure 5, the response for mode 2 damps out faster for two reasons, first, it has higher damping. Secondly, even if zeta were the same for the two modes, the higher frequency of mode 2 will create higher velocities, hence higher damping from the velocity-dependent damping term. Note that the equal damping values for the dampers make the center mass have a small motion. Response time for this mode is 0.07 seconds. Also from Figure 5(d) mass 1 and 2 are in opposite phase and having almost same magnitude but mass 3 is almost in steady condition.

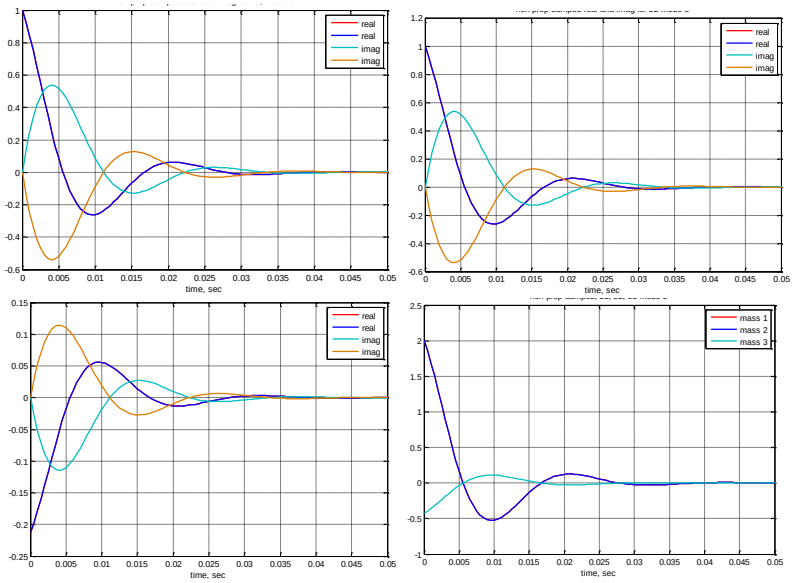

Figure 6: Non proportional damped vibration for mode 3; (a) real and imaginary for m1 (a) real and imaginary for m2 (a) real and imaginary for m3 (d) combined for m1, m2 and m3

Compared to the responses for the mode 2 in Figure6, the response for mode 3 damps out faster because it has higher damping as mode 2 has 0.3955 damping ratio and mode 3 has 0.416 damping ratio. Also, if zeta were the same for the two modes, the higher frequency of mode 3 will create higher velocities, hence higher damping from the velocity-dependent damping term. Response time for this mode is 0.05 seconds. Also from Figure 6(d) we can see that mass 1 and 2 are in same phase but mass 3 is in different phase.

4.3Frequency response

The four distinct transfer functions for the default values of m, k and c are plotted using MATLAB. Frequency response curves are also determined from analysis and plots are displayed in Figure 7.

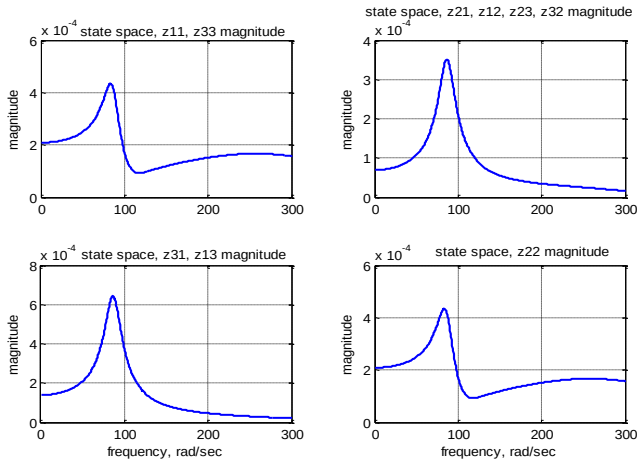

Figure 7: Frequency response curves, magnitude v/s frequency

From the above graph it can be written that at frequency 83 rad/sec magnitude reaches maximum at 0.434 mm in state Z11 and Z33. In state Z21, Z12, Z23, Z32 at 86.5 rad/sec frequency, maximum magnitude reached was 0.335 mm. In third graph at same frequency max magnitude reached was 0.665 mm. From forth graph it is predicted that 85 rad/sec frequency magnitude reaches at 0.434 mm and get down.

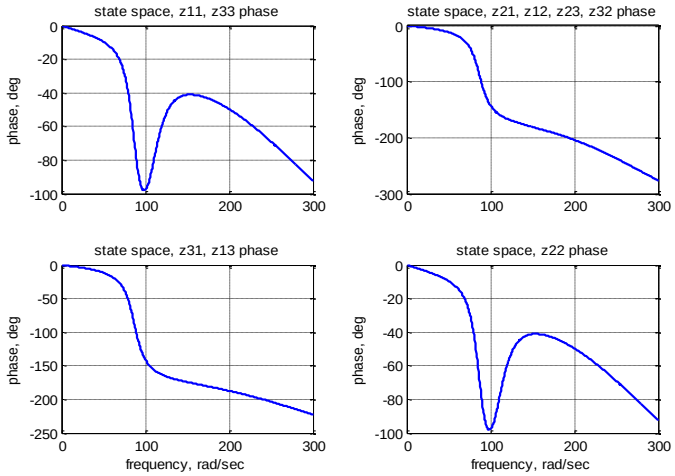

Figure 8: Frequency response curves, magnitude v/s frequency

Phase difference at frequency 98 rad/sec is -98.05 in first graph, -138 in second graph and -136.3 in third graph. In last graph having same behaviour as first graph. Also from graph it can be easily predicted that with the increase in frequency phase angle is decreases from 0 to up to 300.

5. CONCLUSIONS

Initially 3-dof model is developed using Lagrange's considering three linear motions. Three Eigenvalues was found in complex form using MATLAB and natural frequencies obtained, which are 3.101, 2.948 and 0.873 rad/sec. Also different mode shapes are found. The damping ratio obtained for mode 1 is 0.117, for mode 2 is 0.3955 and for mode 3 is 0.416. Initial condition response graphs were plotted for each mode in Figure 4, Figure 5 and Figure 6. Further frequency response curves were depicted in the study. At frequency of 85 rad/sec each state variables were having highest magnitude.

With the aid of the model it is possible to hypothesize the causes of various resonance peaks. It is seen from the result that at joint of one knee joint resonant frequency is approximately 0.49 Hz for both legs and the mass of the whole body on the stiffness of the legs results in a resonance near 0.13 Hz.

REFERENCES

[1] Y. Matsumoto and M.J. Griffin, Mathematical models for the apparent masses of standing subjects exposed to vertical whole-body vibration, Journal of Sound and Vibration 260 (2003) 431–451.

[2] Z. ONISZCZUK, damped vibration analysis of a two-degree-of-freedom discrete system, Journal of Sound and vibration (2002) 257(2), 391-403

[3] M. Fritz, Three-dimensional biomechanical model for simulating the response of the human body to vibration stress , Med. Biol. Eng. Comput., 1998, 36, 686-692

[4] Tae-Hyeong Kim, Development of a biomechanical model of the human body in a sitting posture with vibration transmissibility in the vertical direction, International Journal of Industrial Ergonomics 35 (2005) 817–829

[5] S KITAZAKI and M J GRIFFIN, a modal analysis of whole-body vertical vibration, using a finite, element model of the human body, Journal of Sound and Vibration(1997) 200(1), 83-103.

[6] M.J. Griffin, Handbook of Human Vibration, Academic Press, London, 1990.

[7] Keyur P Hirpara, Dr.Hemant J Nagarsheth, V M Daiya, Development of Four Degree of Freedom Vibratory Model of Human Lower Limbs, International Conference on Multidisciplinary Research & Practice, ISSN 2321-2705, Volume I Issue VIII.

[8] DEVENDRA P. GARG AND MICHAEL A. ROSS, Vertical Mode Human Body Vibration Transmissibility, IEEE transactions on systems, man, and cybernetics, vol. Smc-6, no. 2.

[9] T. C. Gupta, Identification and Experimental Validation of Damping Ratios of Different Human Body Segments Through Anthropometric Vibratory Model in Standing Posture, ASME Vol. 129, AUGUST 2007.

AUTHORS

KeyurHirpara is currently working as an assistant professor at Mechanical engineering department, Institute of technology, Nirma University, Ahmedabad. He is having 10 years of experience in academics and industry.

DEVELOPMENT AND TESTING OF AN ENERGY HARVESTING TILE

Ganesh Sevagamoorthy[1] and Jayabal K[2]

[1]Indian Institute of Information Technology Design and Manufacturing, Kancheepuram, India.
[2]Indian Institute of Information Technology Design and Manufacturing, Kancheepuram, India.

ABSTRACT

This paper presents development and experimental analysis of a piezoelectric mounted flexible beam attached with an oscillating tile that can be used to scavenge energy from footsteps in crowded places. The energy harvesting system consists of a piezoelectric bimorph cantilever beam inside a hollow box which connects to the ground with the help of springs. Multiple piezoelectric patches are pasted on the beam. When the foot is placed on the tile and removed, the hollow box displaces in turn causing the beam to oscillate harvesting electrical power. A prototype is developed and the performance of the piezoelectric energy scavenging tile is tested. The variations of power output for different load resistances are obtained and the optimal load resistance is suggested.

KEYWORDS

Energy harvesting, Piezoelectric material, Bi-morph cantilever beam.

1. INTRODUCTION

The world energy production sector is in transition and is nowadays called to face great challenges in a context in which the fossil fuel reserves are running out, while the energy demand steadily increases. On the other hand, the rising cost and the related environmental issues make the use of conventional energy resources more and more difficult [1]. There are an estimated 1.3 trillion barrels of proven oil reserve left in the world's major fields, which at present rates of consumption will be sufficient to last 40 years. By 2040, production levels may be down to 15 million barrels per day – around 20% of what we currently consume. It is likely by then that the world's population will be twice as large, and more of it industrialised and therefore oil dependent [2]. Energy harvesting has been of interest to many researchers for decades. Researchers have put much effort into energy conversion and it is recently suggested that piezoelectric materials are one of the best options in energy conversion from mechanical into electrical [3]. Piezoelectric materials produce electrical charges when subjected to dynamic strain. These materials can be used to capture and store vibrational energy. The Energy storage characteristics of Piezo-generator and the effect of the capacitance of the capacitor and the initial voltage are discussed by Umeda et al [4]. The various piezoelectric devices available have been discussed in detail by Sodano et al [5]. There are two methods to accumulate the charge produced by the piezoelectric harvester. The first one uses capacitors and the second one nickel metal hydride batteries. The rechargeable batteries are found to have more desirable qualities than the capacitor [6].

A lot of energy is being spent by pedestrian traffic while walking in crowded places like malls, train stations, airports, etc. Here, energy expended when the foot is placed on the ground results in vibration which can be converted into electrical energy. This can be done, among others, with the help of multiple piezoelectric patches placed on either side of the cantilever beam. The energy from the footstep can be transferred to the beam through a box. An improved design based on aforementioned idea was discussed and a numerical analysis was also reported in a recent work [7]. The main idea of the present work is to design a simple and cheap energy harvesting device to scavenge the energy expended while some one walks over the energy scavenging tile.

2. DESIGN

The design of the energy scavenging tile consists of a box which is placed in a cavity connected with the base through springs. This box has a cantilever beam inside and several piezoelectric patches are pasted on either side of the beam as shown in Figure 1. As it can be seen, when the foot is placed on the box, the box displaces down and as the person removes his or her foot, it comes back to its original position due to spring action. Inertia causes the beam within the box to vibrate thereby producing electric power. Figure 2 displays the schematic sketch of the energy harvesting tile and various parts.

Figure 1. Energy scavenging tile with the piezo mounted beam

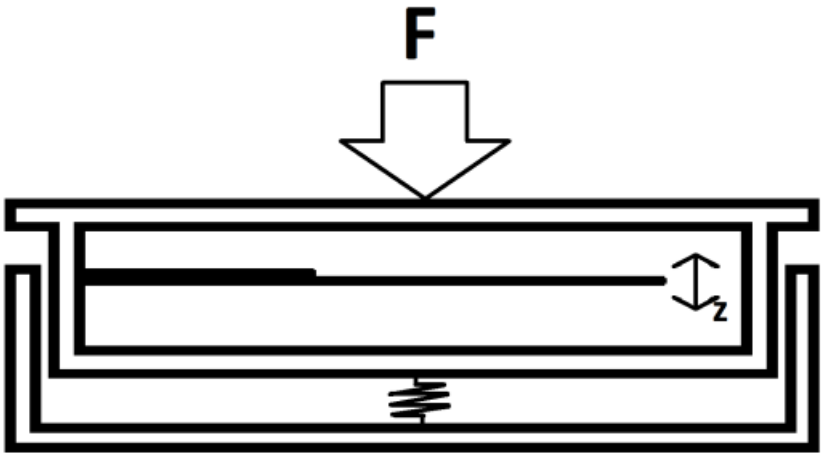

Figure 2. Schematic view of the Energy harvesting tile and its working

The prototype consists of a wooden box and a wooden platform with inner dimensions 34cm x 34cm x 10cm. The box can displace up and down on the platform as it is supported by eight compression springs. One side of the box has a slot to accommodate the beam. Two L-shaped hinges are attached on either side of the slot to tightly hold the beam in place. The inside box has outer dimensions of 33.5cm x 33.5cm x 10cm. The cantilever beam is a steel ruler of length 27.5cm, made of stainless steel and has six piezoelectric patches pasted on it (three on either side of the beam) and these piezoelectric patches are connected in series. The piezoelectric material used is a piezo buzzer element, each having a radius of 2.5cm. Due to the restriction arising out of the comfort of pedestrian, the vertical displacement of the box is constrained to 1 cm.

3. EXPERIMENT

The output from the piezoelectric element is connected onto a breadboard across a load resistance. The voltage across the load resistance is measured and plotted with the help of an oscilloscope. For characterizing the prototype, a force of 200 N is applied on the top of the hollow box so it has a deflection of 10 mm and resulting output voltage is plotted on the oscilloscope. The system described here is designed to utilize the *z*-axis vibration as the only vibration source for the device. The output voltage is measured for various values of load resistances. The complete experimental setup with the oscillating box and necessary measuring devices is shown in Figure 3.

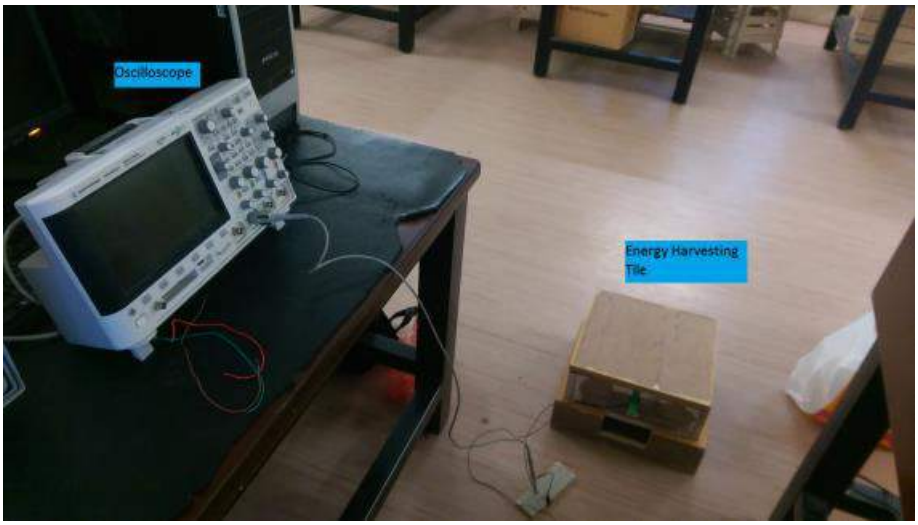

Figure 3. Experimental Setup

4. RESULTS AND DISCUSSION

The energy scavenging was subjected to a constant transverse load and its power output was measured with the help of an oscilloscope. The values of voltage obtained are used to find the power developed by the device and check the performance of the energy harvesting device. Two cases have been studied with an open circuit and with a load resistance.

4.1. Open Circuit

The output voltage obtained from the experiment performed on the energy scavenging tile are shown in the Figure 4. The experimental results show that the tile produces a peak AC Voltage of 56.8 Volts in the open circuit condition.

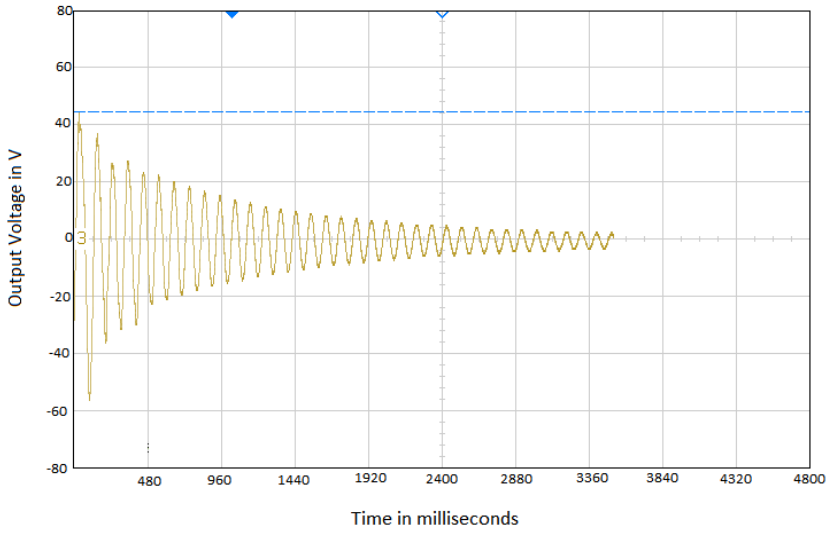

Figure 4. Output voltage for open circuit

4.2. Circuit with resistive load

The voltage across the circuit has been measured for eleven different resistances. The output voltage waveform for 180 kilo ohm resistance is shown in Figure 5. It has a peak voltage of 4.7 volts. The output voltages for different resistances has been plotted in Figure 6. It can be seen that the output voltages increase with load resistances. In Figure 7, a plot between the current and load resistances shows that the current decreases with increase in load resistance. The piezoelectric energy harvester produces a max power of around 122.72μW at a load resistance near to 180 kilo ohms. This is shown in a graph between the max power output and load resistance in Figure 8.

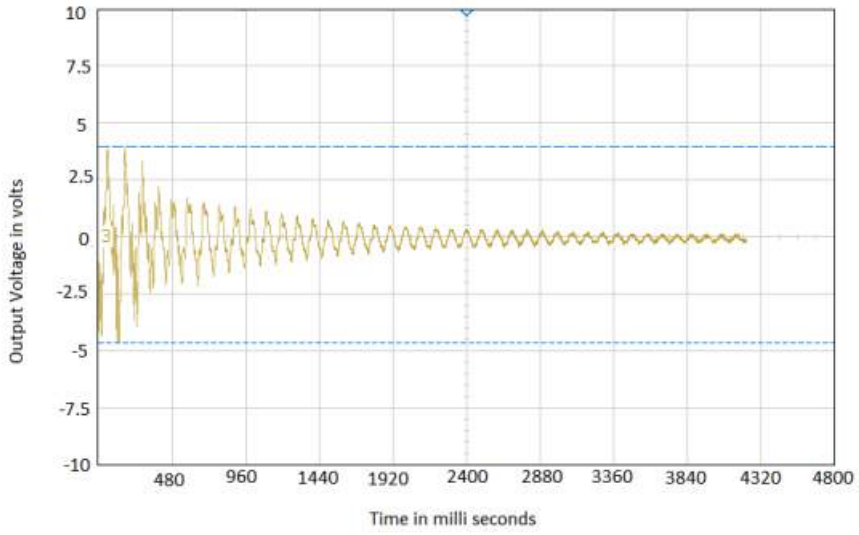

Figure 5. Output voltage for 180 kilo-ohms load resistance

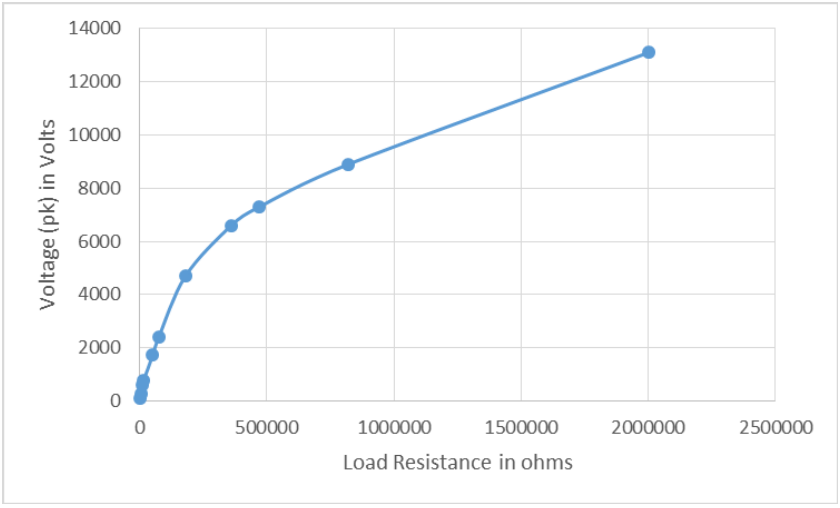

Figure 6. Voltage peak vs Load resistance

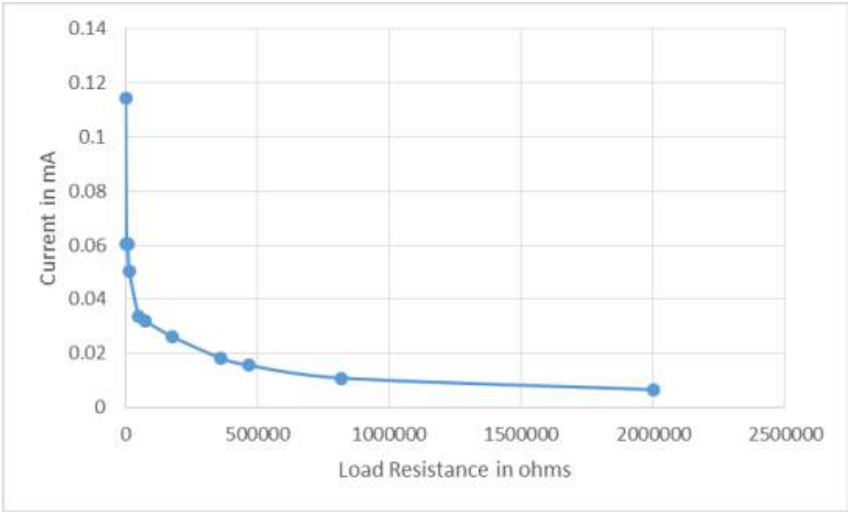

Figure 7. Current peak vs Load resistance

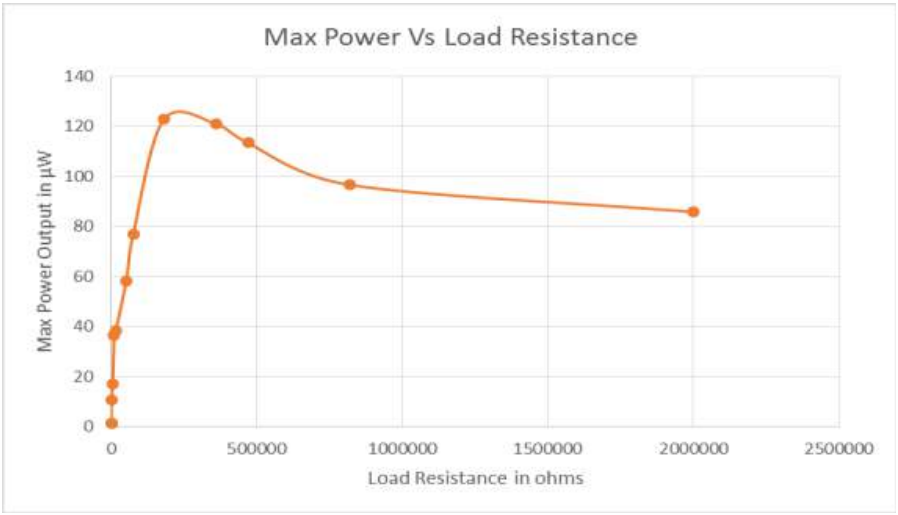

Figure 8. Max power output vs Load resistance

5. CONCLUSION

In this work, it is attempted to develop a simplified energy harvesting tile and its performance was tested for different load resistances. It is found that a force of 20 kilo-grams resulted in producing a peak AC power of around 122 micro-Watts. This design can further be extended with more beams placed inside the hollow box to produce more power which can be harvested while someone walking on the tile. In addition, the platform base may be pasted with piezo stacks, as is conventionally done, which will enhance the power output. This tile can also be used to get statistical data in shops and also for security system as a part of an intruder detecting system owing to its ability to detect small change in pressure.

REFERENCES

[1] A. Messineo, G. Panno (2011) "LNG cold energy use in agro-food industry: a case study in Sicily", Journal of Natural Gas Science and Engineering, 3: 356-363.
[2] http://www.imeche.org.
[3] S.R. Anton, H.A. Sodano (2007) "A review of power harvesting using piezoelectric materials (2003–2006)", Smart Materials & Structures, 16:R1-R21.
[4] M. Umeda, K. Nakamura, S. Ueha (1997) "Energy Storage Characteristics of a Piezo-Generator Using Impact Induced Vibration." Japanese Journal of Applied Physics, Vol. 35, Part 1, No. 5B, pp. 3146-3151.
[5] H.A. Sodano, G. Park, D.J. Inman (2005) "Comparison of Piezoelectric Energy Harvesting Devices for Recharging Batteries", Journal of Intelligent Material Systems and Structures, 16(10), 799-807.
[6] H.A. Sodano, G. Park, D.J. Inman (2005) "Generation and Storage of Electricity from Power Harvesting Devices", Journal of Intelligent Material Systems and Structures, 16(1), 67-75.
[7] A. Messineo (2012) "Piezoelectric bender transducers for energy harvesting applications", Energy Procedia 14.39 – 44.

BUCKLING CHARACTERISTICS STUDY OF ISOTRUSS STRUCTURE WITH DIFFERENT POSITIONS OF LONGITUDINAL MEMBERS

M. Gavade [1] and S. Roy [2]

[2]R&DE (E), Defence Research & Development Organisation, Pune-411015, India

ABSTRACT

The present paper illustrates a light weight composite IsoTruss structure and its characteristics in buckling through finite element modelling and simulations. IsoTruss provides excellent opportunities to enhance the strength to weight ratio of a structural element. The paper presents the comparative study of compressive buckling load carrying capacity with respect to bay length of IsoTruss under placement of longitudinal members at different location along the axis of IsoTruss. The study concludes that the IsoTruss exhibits global as well as local buckling characteristics for progressive bay length of IsoTruss. The IsoTruss with longitudinal members placed away from axis has better compressive buckling load carrying ability than the IsoTruss with longitudinal members nearer to the axis of the IsoTruss.

KEYWORDS

IsoTruss, critical load, longitudinal members, helical members, Bay length, buckling analysis, global buckling, local buckling, Carbon fibre, tensile test.

1. INTRODUCTION

The IsoTruss structure classified as an open lattice structure. Open lattice structure is a regular, periodic configuration of points, particles or objects throughout an area or a space, especially the arrangement of ions or molecules in a crystalline solid. It could be made of strips of metal, wood, or similar material overlapped or overlaid in a regular, usually crisscross pattern. Compare to convectional beam, column and tubular structural member load carrying capacity of IsoTruss structure is more, very precisely its strength to weight ratio is more due to its unique lattice structural configuration. Figure 2b shows a typically eight nodded IsoTruss structure. It has a longitudinal member as well as helical member. Longitudinal members could be design to carry bending and compressive load and helical member for torsion loads. Therefore its performance is better than the conventional structural member for the load combination of bending, compression and torsion load. The bay length is the distance between the successive repeating structures of the IsoTruss. The axis of IsoTruss is the profile passing through the centres of the geometry of the cross section. The helical members are which spirals about the axis of IsoTruss along the profile decided by the number of nodes as shown in Figure 1. The longitudinal members are positioned along the axis of the IsoTruss through the intersection of helical members of IsoTruss. Outside diameter is the diameter of the circle encircling the extremes of the cross section of the IsoTruss. The tetrahedrons are at the outermost region of the cross section of IsoTruss. The helical members while spiralling about the axis of IsoTruss give rise to a tetrahedron structure at the outermost part of the cross section of IsoTruss. The helical members which spirals around the longitudinal members stretched along the length of IsoTruss provide torsion strength, while the longitudinal members placed along the length provides tensile, compressive and as well as

DOI: 10.5121/ijci.2016.5121

bending strength. Number of nodes represents the geometry of the cross section of IsoTruss. Number of nodes decides the profile of the helical members. A six node IsoTruss represents a cross section of IsoTruss with two triangles 180 degree with respect to each other as shown in Figure 2a. An eight node configuration has two squares as shown in Figure 2b. A 10 node configuration will have two pentagons as shown in Figure 2c. IsoTruss structures have been manufactured using several different methods [1–6]. In the present study material used for IsoTruss is 24K carbon fibre cordage impregnated with epoxy resin. The local and global compressive buckling behaviour of 8-noded IsoTruss has been studied by Rackliffe et. al.[7]. It has observed that local buckling depends on bay length, for shorter bay lengths higher the buckling loads. Global buckling, on the other hand, is independent of bay length. In the present study longitudinal members of the IsoTruss placed at the different intersection of helical members along the IsoTruss axis. The position of these longitudinal members on the IsoTruss affects the buckling characteristics of the IsoTruss, which is examined in the following study.

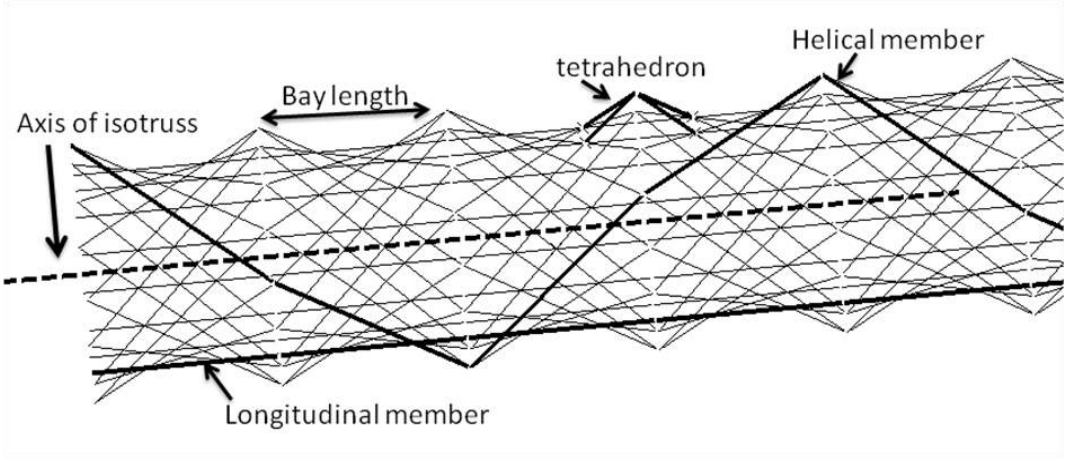

Figure 1. IsoTruss of eight node configuration

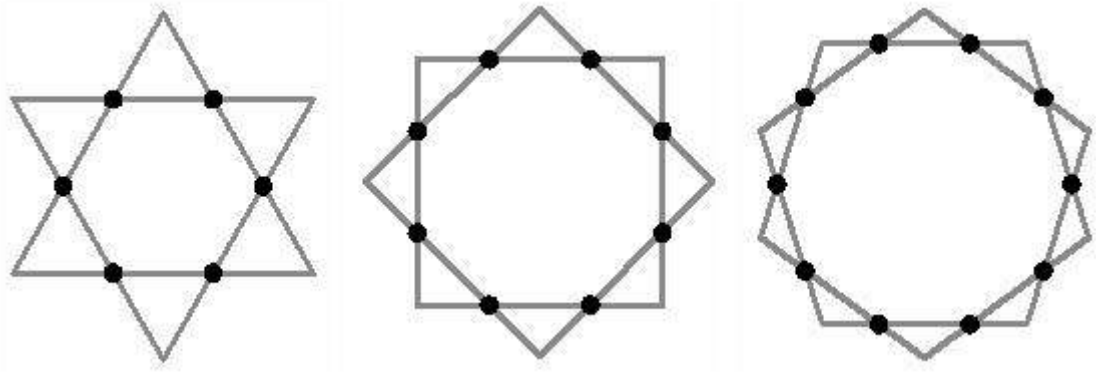

2a 2b 2c

Figure 2. IsoTruss cross section having different node

2. MATERIAL CHARACTERIZATION

In the present study material used for IsoTruss is 24K carbon fibre cordage impregnated with epoxy resin. To investigate the material properties of resin impregnated carbon cordages, tensile specimens has been prepared and tested. Photograph 3 shows a typical specimen used for tensile

test. Specimens are prepared using Rein Film Infusion (RFI) process with a curing temp of 80^0 C for 1 hr. Diameter of the each carbon cordage specimen becomes 2 mm and density is 0.0024 gms/cubic meter after infusion. Specimens are tested in universal testing machine (UTM) as shown in Photograph 2. Figure 3 shows stress-strain graph from which the Modulus of elasticity is determined as 250 GPa. Table 1 shows the material properties of the carbon cordages used in FE analysis.

Photograph 1. Tensile test specimen

Photograph 2. Specimen on UTM for testing

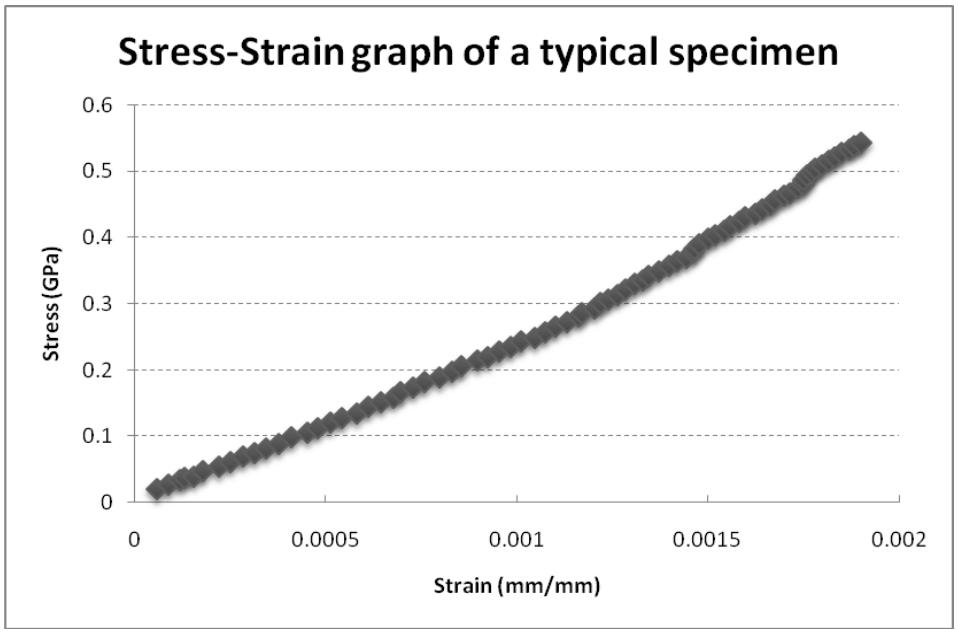

Figure 3. Stress-strain graph of a typical specimen

Table 1. Material Properties of 24k carbon cordage with impregnated resin

Modulus of Elasticity (GPa)	250
Density (gms/cubic meter)	0.0024
Diameter of carbon fibre thread(mm)	2

3. FINITE ELEMENT MODELLING AND BUCKLING ANALYSIS

Three different types of eight nodded IsoTruss have been considered for FE analysis as follows

Type 1: IsoTruss with longitudinal members at the base of the tetrahedron abbreviated as IL (i.e. Internal longitudinal member), as shown in Figure 4a.
Type 2: IsoTruss with longitudinal members at the uppermost point or vertex of the tetrahedron abbreviated as EL (i.e. External longitudinal member), as shown in Figure 4b.
Type 3: IsoTruss with longitudinal members at vertex and base points of the tetrahedron abbreviated as IEL (i.e. Internal & External Longitudinal members), as shown in Figure 4c.

Figure 5a, 5b and 5c shows the cross-section of the IL, EL and Type IEL IsoTruss respectively.

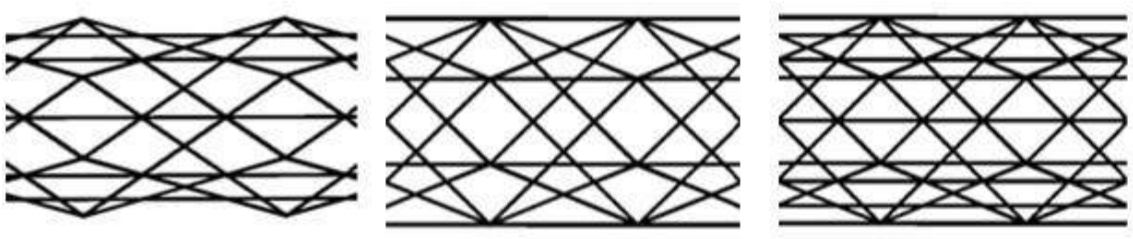

4(a) 4(b) 4(c)

Figure 4. IsoTruss having longitudinal member at different location

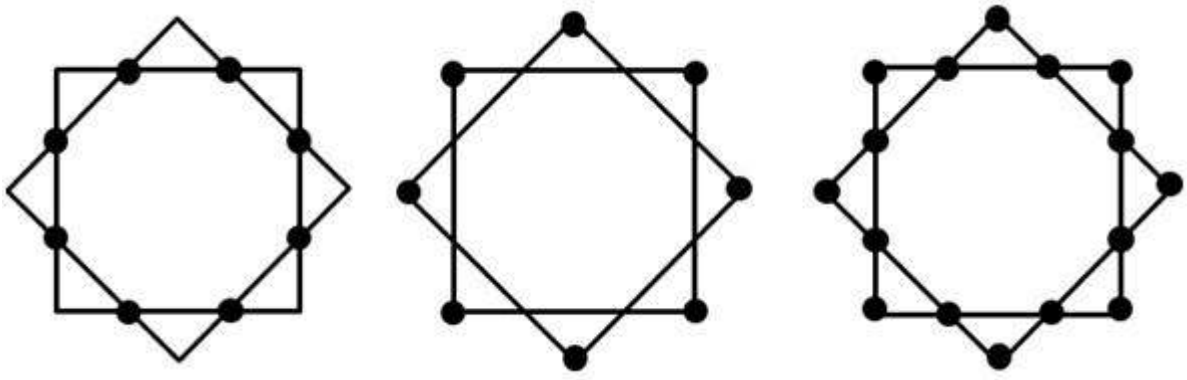

5(a) 5(b) 5(c)

Figure 5. IsoTruss having longitudinal member at different location(cross sectional view)

In the present study IsoTruss considered for the buckling analysis is of eight node configuration. The outer diameter of the truss is 106 mm and total length is 1.5 meters. Finite element (FE) model of the IsoTruss has been prepared using ABAQUS 6.10 FE software. IsoTruss is modelled using 2 node linear beam element.

The compressive load carrying capacity can be determined considering Euler's buckling formulation of columns. The compressive load carrying capacity of a column with one end fixed and one end free is given by the critical load $P_{cr.}$

$$P_{cr} = \frac{\pi^2 EI}{4L^2} \quad (1)$$

Where, E is modulus of elasticity of the material, n is number of mode, I is Moment of Inertia, L is the Length of the column.

As per the Equation 1 the critical load is proportional to moment of inertia. The moment of inertia is directly proportional to the distribution of the mass along the neutral axis. Thus Moment of inertia will increase if the longitudinal members are placed away from the neutral axis which passes from the centre point the IsoTruss (as IsoTruss is a symmetric structure in cross section).Thus the IsoTruss-EL and IsoTruss-IEL are expected to have better compressive handling capacity than IsoTruss-IL.

In the present study buckling characteristics study has been done using ABAQUS 6.10 FE software. During analysis one end of the IsoTruss is constrained for all degrees of freedom and on the other end a reference load of 1N is applied. FE analysis gives the load factor (Eigen value) for the IsoTruss and using Equation 2, the load carrying capacity of the IsoTruss is determined.

$$P = P_r + (\lambda \times P_r) \quad (2)$$

Where P_r is the reference load, λ is the load factor and P is the critical buckling load the truss can carry safely.

4. RESULTS & DISCUSSION

The Figure 6 illustrates the compressive buckling load carrying capacity for IsoTruss IL, EL and IEL as a function of bay length of the IsoTruss. From the Figure 6 it can be observe that the critical buckling load decreases as the bay length increases for all three types of IsoTruss. For IL and IEL IsoTruss from 50 to 150 mm bay length buckling load is all most constant. All three types of IsoTruss exhibit a global buckling for a range of bay lengths from 50mm to 200mm. From 200 to 300 mm bay length there is a transition zone of global to local deformation. IsoTruss with bay length greater than 300m shows local buckling behaviour and also exhibit a very small compressive buckling load carrying capacity before buckling. IsoTruss IEL shows maximum buckling load carrying capacity than IsoTruss IL & EL as expected.

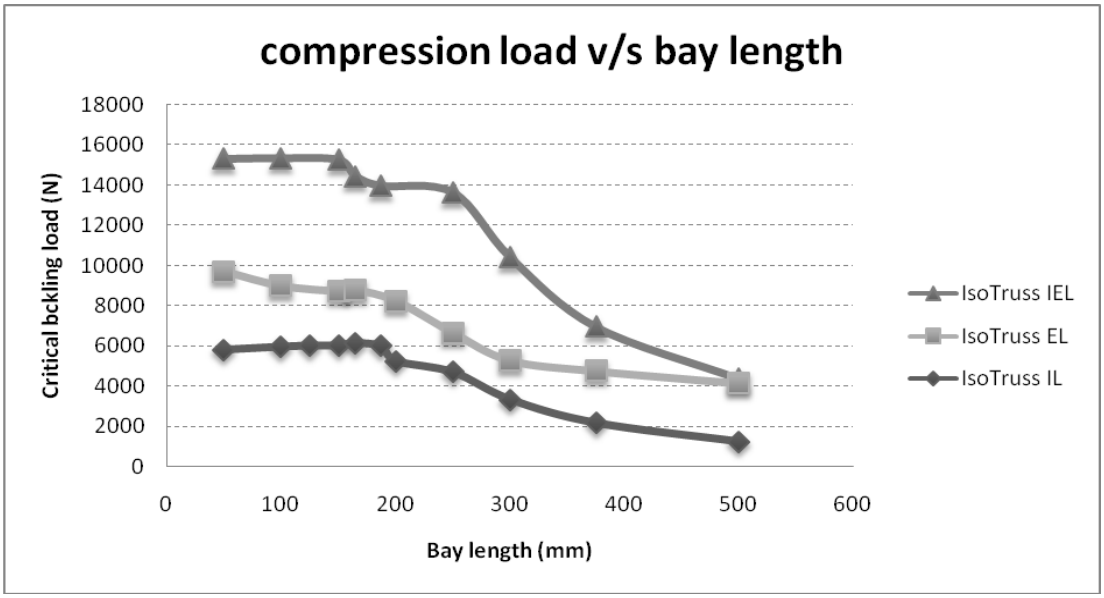

Figure 6. Compressive Load vs. bay length of IsoTruss

Figure 7 shows the deformed shape for the first mode of buckling of IsoTruss IL, EL and IEL with 100 mm bay length. The shape indicates a global buckling behaviour.

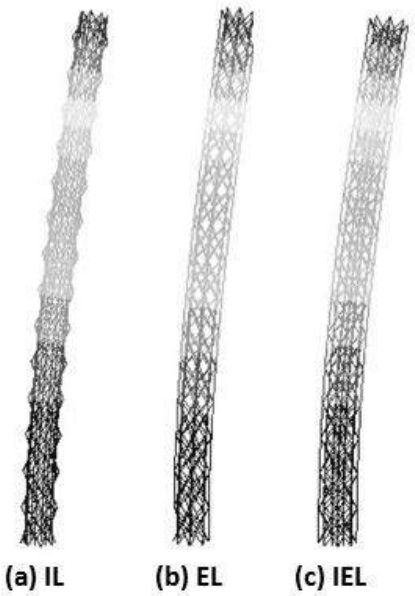

100mm Bay Length IsoTruss Type	Critical Buckling Load (N)
(a) IL	5967.0
(b) EL	8989.2
(c) IEL	15357.0

Figure 7. First buckling mode shapes for 100 mm bay length

Figure 8 shows deformed shape of IsoTruss IL, EL and IEL with bay length 200 mm for the first mode of buckling. IsoTruss IL, EL shows the local buckling and IEL shows the global buckling behaviour. Figure 9 shows deformed shape of IsoTruss IL, EL and IEL with bay length 300 mm for the first mode of buckling. It indicates localization of deformation in the IsoTruss.

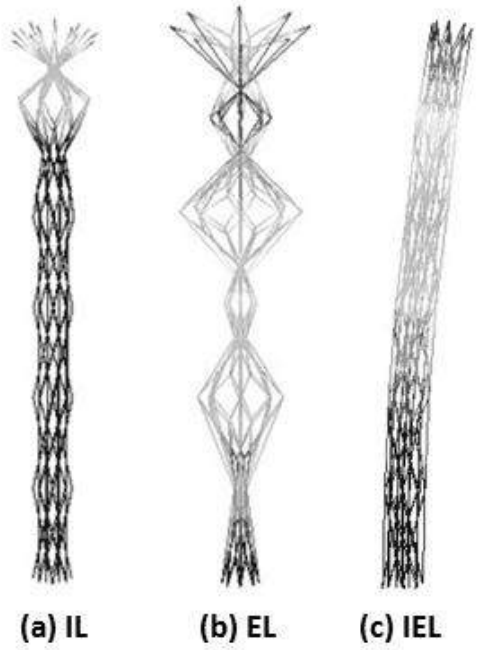

250 mm Bay Length IsoTruss Type	Critical Buckling Load (N)
(a) IL	4699.2
(b) EL	6663.9
(c) IEL	6663.9

Figure 8. First buckling mode shapes for 250 mm bay length

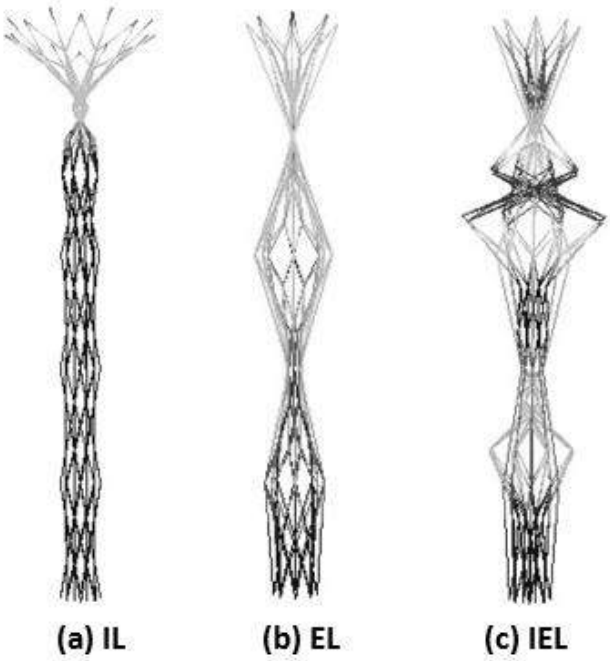

300mm Bay Length IsoTruss Type	Critical Buckling Load (N)
(a) IL	3338.7
(b) EL	5284.7
(c) IEL	10425.0

Figure 9. First buckling mode shapes for 300 mm bay length

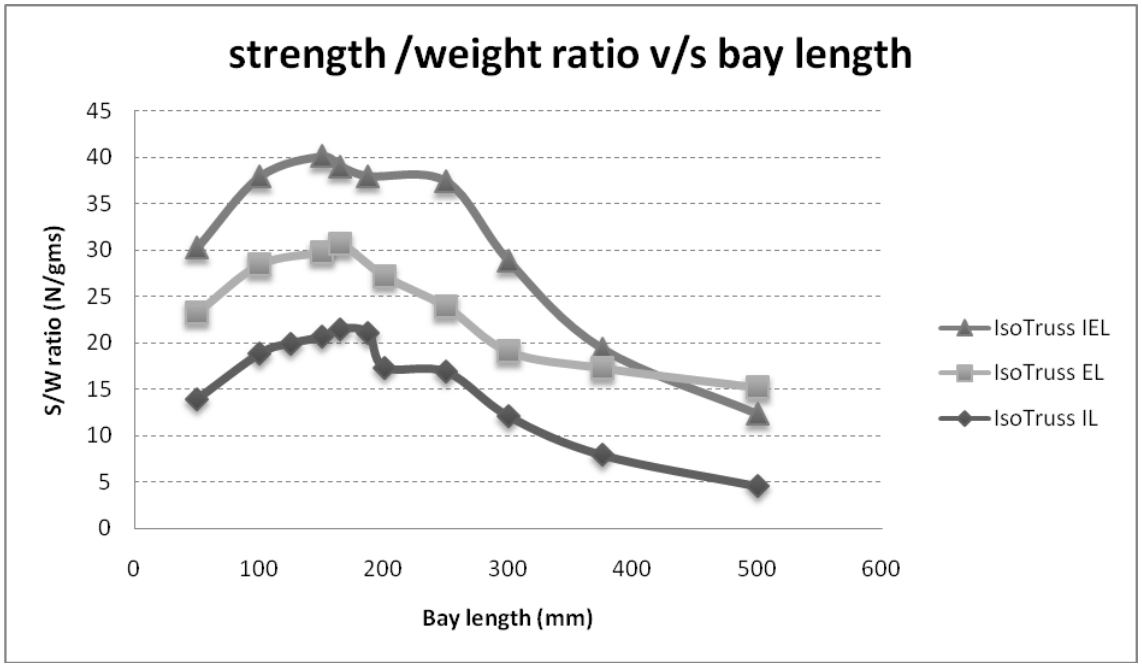

Figure 10. Strength to Weight ratio vs. Bay length of IsoTruss

The Figure 10 shows the strength to weight ratio as a function of bay length. The IsoTruss IL and IsoTruss EL have same weight as they have eight longitudinal members each which are just placed at different distance from axis of IsoTruss. But IsoTruss IEL have a slightly greater weight than the IL & EL because it has 16 longitudinal members. This greater number of longitudinal member of IsoTruss IEL gives it the unique strength. Hence it has a higher strength to weight ratio than the remaining type even though being the heaviest among the types considered. From the Figure 11 it could also be observed that all the three types of IsoTruss considered in the analysis exhibits a higher strength to weight ratio roughly at 170 mm bay lengths.

5. CONCLUSION

Material used in the present study is 24K carbon fibre cordage impregnated with epoxy resin. Material property used in the FE analysis is obtained by tensile test of several specimens in UTM machine. Comparative compressive buckling load carrying capacity of three different types of 8-noded IsoTruss namely IsoTruss-IL, IsoTruss-El, and IsoTruss IEL is examined with progressive bay length. In the IsoTruss-IL longitudinal members positioned at the base of the tetrahedron, in the IsoTruss-EL longitudinal members positioned at the vertex of the tetrahedron abbreviated as EL, where as in the IsoTruss-IEL longitudinal members positioned at the base as well as vertex of the tetrahedron. It is observe for 50 to 150 mm bay length buckling load is all most constant for all three types of IsoTruss. All three types of IsoTruss exhibit a global buckling for a range of bay lengths from 50mm to 200mm. From 200 to 300 mm bay lengths there is a transition zone of global to local deformation. IsoTruss's with bay lengths greater than 300m shows local buckling behaviour and also exhibit a very small compressive buckling load carrying capacity before buckling. It is also observe that IsoTruss-IEL have better compressive buckling load carrying capacity and better strength to weight ration compare to other two type of IsoTruss.

REFERENCES

[1] Weaver Thomas J., (1999) "Mechanical characterization of a graphite/epoxy IsoTruss subject to simple and biaxial loads", M.S. Thesis, Brigham Young University, Provo, Utah.
[2] Yoder Jacob A., (2000) "IsoTruss to IsoTruss connections and small scale IsoTruss design for mountain bike frames", S. Thesis, Brigham Young University, Provo, Utah.
[3] Jones Layne S., (2000) "Flexural behaviour of spirally consolidated double IsoTruss reinforced concrete beams", M.S. Thesis, Brigham Young University, Provo, Utah.
[4] Jarvis David, (2001) "Development of a rectangular IsoTruss for reinforced concrete beams", M.S. Thesis, Brigham Young University, Provo, Utah.
[5] Phillips Joseph K, (2001) "IsoTruss bicycle frame design using beam theory and shear flow analysis", M.S. Thesis, Brigham Young University, Provo, Utah.
[6] Rackliffe Mary E, (2002) "Development of ultra-lightweight IsoTruss grid structures", M.S. Thesis, Brigham Young University, Provo, Utah.
[7] Mary E. Racliffe, David W. Jesen, Warren K. Lucas, (2005) "Local and global buckling of ultra-light weight IsoTruss structures", Composites Science and Technology, Vol. 66, No. 5, pp. 282-288.

.

AUTHOR INDEX